

ADVERTIMENT. L'accés als continguts d'aquesta tesi queda condicionat a l'acceptació de les condicions d'ús establertes per la següent llicència Creative Commons:  <https://creativecommons.org/licenses/?lang=ca>

ADVERTENCIA. El acceso a los contenidos de esta tesis queda condicionado a la aceptación de las condiciones de uso establecidas por la siguiente licencia Creative Commons:  <https://creativecommons.org/licenses/?lang=es>

WARNING. The access to the contents of this doctoral thesis it is limited to the acceptance of the use conditions set by the following Creative Commons license:  <https://creativecommons.org/licenses/?lang=en>



Studies of viral and host biomarkers in hepatitis C virus infected patients

Meritxell Llorens Revull

Thesis submitted for the Degree of Doctor in Biochemistry, Molecular Biology and Biomedicine

Laboratory of Viral Hepatitis

Unit of Liver disease

Vall d'Hebron Research Institute

Department of Biochemistry and Molecular Biology

Faculty of Biosciences

Autonomous University of Barcelona

Barcelona, 2023

Thesis directors

Dr. Josep Quer Sivila Dra. Marta Bes Maijó Dra. Celia Perales Viejo

Thesis tutor

Dr. Jaume Farrés Vicén

Thesis candidate

Meritxell Llorens Revull

This Doctoral Thesis has been accepted by the Academic Commission of the Doctoral Program (CAPD) to be presented as a compendium of publications, listed below, in accordance with UAB Academic regulations applicable to university studies regulated in accordance with RD 1393/2007-RD 861/2010.

- Meritxell Llorens-Revull, Josep Gregori, Cristina Dopazo, Francisco Rodríguez-Frías, Damir Garcia-Cehic, Maria Eugenia Soria, Qian Chen, Ariadna Rando, Celia Perales, Juan Ignacio Esteban, Josep Quer and Itxarone Bilbao. Study of Quasispecies Complexity and Liver Damage Progression after Liver Transplantation in Hepatitis C Virus Infected Patients. *Genes* (2021) 12, 1731. <https://doi.org/10.3390/genes12111731>

- Meritxell Llorens-Revull, Maria Isabel Costafreda, Angie Rico, Mercedes Guerrero-Murillo, Maria Eugenia Soria, Sofía Píriz-Ruzo, Elena Vargas-Accarino, Pablo Gabriel-Medina, Francisco Rodríguez-Frías, Mar Riveiro-Barciela, Celia Perales, Josep Quer, Silvia Sauleda, Juan Ignacio Esteban, Marta Bes. Partial restoration of immune response in Hepatitis C patients after viral clearance by direct-acting antiviral therapy. *PLoS ONE* 16(7): e0254243. <https://doi.org/10.1371/journal.pone.0254243>

- The third article presented in this Doctoral Thesis has been included after CAPD evaluation.

This thesis and the articles derived have been financial supported by Instituto de Salud Carlos III cofinanced by the European Regional Development Fund (ERDF), by grants: PI16/00337, PI18/00210, PI19/00301 and PI19/00533; Clinical Trial Gov. Identifier: NCT0170784; Gilead GLD00006; and from Centro para el Desarrollo Tecnológico Industrial-CDTI of the Spanish Ministry of Economics and Competitiveness (MINECO) grant number: IDI-20200297 and IDI-20151125.

Meritxell Llorens Revull has received financial support from Instituto de Salud Carlos III by a predoctoral fellowship (FI20/00313), cofinanced by the European Regional Development Fund (ERDF).

I. ACKNOWLEDGMENTS

Pues no, al final no me jubilo aquí! Després de tants moments, tantes històries, tants records només em queda agrair a totes les persones que heu format part d'aquesta etapa tant important a la meua vida.

Primer de tot agrair-vos Josep, Marta i Celia haver-me donat la oportunitat de fer el doctorat sota la vostra direcció. Gràcies Josep per ser tant pròxim i estar sempre disposat a ajudar. Tenies raó, al final la feina de formigueta dona el seus fruits i t'estic molt agraïda per haver confiat i apostat per mi. Gràcies Marta per estar sempre apunt per tot el que convingués, ajudar-me, preocupar-te i ser tant resolutiva. Gracias Celia por ser siempre tan cercana, apoyarme y combinar profesionalidad y buen rollo. I a tu Mari que ni que oficialment no siguis la meua directora de tesis per mi és com si ho haguessis sigut. Volia agrair-te tota l'ajuda per tirar endavant els projectes, les dificultats, la infinitat d'hores que m'has dedicat, la perfecció en cada detall i tot el que he après de la teua forma de treballar. Al Jaume Farrés, per la seva eficiència, amabilitat i disponibilitat.

Poder haver format part d'aquest equip també és gràcies a la Sílvia i al Nyanyo. Sílvia gràcies per la teua professionalitat i dedicació a la feina i a tu Nyanyo, per ser un gran metge, científic i persona. Sempre recordaré amb carinyo les reunions que començaven amb exosomes i hepatitis C i acabaven amb la formació dels forats negres, USA i el Kovu.

A las casa Lopez crushes; Sofi, Mer y Elena. El mejor equipo del mundo! Gracias por todos los momentos que hemos vivido en el VHIR y fuera, por todas las tardes de risas y desahogos, gracias por la cantidad de veces que me habéis escuchado, aconsejado y arropado. Dicen que las penas compartidas son menos pena y yo no puedo estar más agradecida por la piña tan necesaria durante estos años! Como siempre decíamos es curioso lo distintas que somos pero lo bien que nos entendemos!

I | ACKNOWLEDGMENTS

Gracias Mar y Aurora por las cervezas en Montbau y las torradas de tres quesos, las comidas NASH&Co, el soporte moral durante estos años pero sobre todo durante estos últimos meses de escritura simultánea de las tesis doctorales. Gracias Manu, por todos los ratitos de despacho, por saber ver más allá, apoyarme y animarme. Gràcies Moni per totes les estonetes de despatx, per escoltar-nos sempre i per els innumerables consells. Gràcies Imma per preocupar-te per tots i ajudar-nos sempre. Gracias Maria por ser tan cercana y accesible y haberme adoptado como una NASH girl más.

También a todos los compis con quien he tenido el placer de compartir un trocito de mi paso en el VHIR-BST; Miren, Qian, Sarai, Federico, Teresa, Carla, Diana, Laia, Carmen, Maria, etc. Gracias por los cafés terapia, todo el apoyo y consejos recibidos durante estos años.

Y como no Angie, gracias por tu grandísimo trabajo y organización que nos facilita la vida a todos. Por todas las conversaciones en el zulo, las risas y sobretodo por la cantidad de veces que te has quedado conmigo hasta las tantas de la madrugada ayudándome en el labo. Estoy segura que a partir de ahora los días infinitos de curro recordaré el salami ;)

Gràcies a tot l'equip d'hepatitis virals entre ells al George, Irati, Sergi, Carolina, Marta, Damir, etc... Al Biopep per la seva iniciativa, pulcritud i ajuda en la part bioinformàtica y a Paco por su cortesía y por contagiarme su entusiasmo por la ciencia. Hago extensivo el agradecimiento a todo su equipo, a Bea por la conexión que tuvimos desde el primer momento, por preocuparte e impulsarme hacia arriba cuando lo necesité, y con especial cariño a Selene, Sara, Francesca, Chari, David, Irene, Gerard, Unai, Adrián, Marçal, Cris, Ari y Marta.

Agrair també a tot l'equip de materno en especial a la "travel manager" Adriana y a todo el equipo de Madrid por el trabajo en miRNAs, un placer haber podido compartir proyectos con vosotros. Y entre ellos destacarte tí Mariu, gracias por

la ayuda, dedicación, profesionalidad y ganas de hacer las cosas bien. Sin ti las decoraciones de navidad no fueron las mismas! :P Y a Esteban Domingo por su sabiduría, sus aportaciones y consejos en los proyectos compartidos.

Gràcies a tot el personal de la UAT, la meva segona casa jeje però en especial a la Irene, al Joan i al Norbert per ajudar-me amb tot ni que anéssiu a tope de feina, tenir una paciència increïble i tot el bon rotllo durant aquests anys. Gracies també a tots els celadors, segurates de nit, i personal de neteja per ser sempre tant amables i tenir bones paraules; Jesus, Pablo, Tao, Rai, Montse, etc. Gracies també a tot el personal del servei d'hepatologia, bioquímica, core, microbiologia i a tots els col·laboradors dels articles per haver contribuït a que aquesta tesis sigui possible.

A tots els amics, la família que un escull; els micros, la colla de Cornu, los vecinos del barrio, la Celi, la Cris, l'Oscar, al pandemic team, als amics del pallars i terrassa, gràcies a tots per la vostra amistat, per fer-me sentir estimada i amb una xarxa de suport brutal en els moments que més ho he necessitat.

A tots els que heu sigut els meus compis de pis durant tots aquests anys. Gràcies per la paciència, per les converses a la cuina, les desputricamentes, pels consells, els ànims, els sopars improvisats, por los almuerzos colombianos y las confiancias, las noches de cine, los domingos de balcón, disfraces y cuarentena.

Gràcies a tota la família Heras, la família Vives i la família Cairilla per haver-me fet sentir una més i per tot el suport i estima rebuda durant aquests anys.

Gràcies a la meva família; tiets, cosins, parents... Llorens, Tous, Revull, Anguera, Currius, Sibina, Pont, Formentí. Sou un pilar essencial per a mi, gràcies per fer-me sempre costat. Us estimo molt!

I als 4 de casa, gracias per ser refugi a on acudir quan tot trontolla... A qui he d'agrair gran part del que sóc avui. Us estimo moltíssim!

I | ACKNOWLEDGMENTS

Als meus avis Andreu i Maria, gràcies per ser exemple de treball, esforç, dedicació, perseverança i ensenyar-me el significat d'un ofici i uns valors.

A la meva tieta Josefina, gràcies per haver-me fet sempre costat incondicionalment, per ensenyar-me a entendre i acceptar les persones tal com son i perdonar. Ets un exemple de superació.

Al padrí Domènec i l'àvia Rosa, els meus segons pares. Gràcies per haver-me cuidat sempre, per tota l'atenció i estima rebuda, per haver estat sempre presents, sempre al peu de canó. Em feu i fareu sempre molta falta.

A la meva germana Mònica, gràcies perquè al teu costat sempre m'he sentit protegida i estimada. Sempre has procurat cuidar-me, recolzar-me, animar-me i donar-me suport. Tinc moltíssima sort de poder comptar amb un llurdim de germana com tu. Sempre ens quedarà Malmö!

Also to Simon, thanks to support me, advise me and be part of the family.

Als meus pares Maite i Andreu, us ho he d'agrair tot perquè sense el vostre esforç i treball per donar-nos-ho tot res d'això hauria estat possible. Sou exemple d'amor incondicional i bondat. Gràcies per ser-hi sempre, ajudar-me, aconsellar-me i cuidar-me. No puc estar més agraïda de tenir-vos com a pares perquè per mi sou els millors.

I per últim, gràcies a tu monmonet que ho has patit de primera mà jeje. Per estar sempre al meu costat, per la infinita paciència, escoltar-me, donar-me consells, pels massatges de cap, pel suport i suportar-me :P, per donar-me impuls per tirar endavant i creure en mi quan fins i tot jo havia deixat de creure-hi. Gràcies per compartir amb mi la vida!

II. TABLE OF CONTENTS

III. ABBREVIATIONS.....	15
IV. GLOBAL SUMMARY	21
1. INTRODUCTION	25
1.1 Hepatitis C Virus	27
1.1.1 HCV discovery.....	27
1.1.2 Natural history of HCV disease.....	27
1.1.3 HCV acquisition routes	29
1.1.4 HCV structure	29
1.1.4.1 Viral particle	29
1.1.4.2 Genome	30
1.1.5 Quasispecies.....	32
1.1.6 Prevalence and distribution	34
1.1.7 Treatment timeline.....	36
1.1.8 Vaccination and future perspectives for HCV elimination	37
Summary 1.1.....	38
1.2 Immune response in HCV infection.....	38
1.2.1 Innate immune responses.....	39
1.2.1.1 HCV mechanisms to evade the innate immune system.....	40
1.2.2 Adaptive immune responses.....	42
1.2.2.1 HCV mechanisms to evade the adaptive immune system.....	43
1.2.3 Immune response after DAAs-mediated infection resolution	46
Summary 1.2.....	46

II | TABLE OF CONTENTS

1.3 Extracellular vesicles	47
1.3.1 Extracellular vesicles discovery	47
1.3.2 Brief overview	47
1.3.3 EVs types	48
1.3.4 EVs isolation methods.....	49
1.3.5 Exosome biogenesis	50
1.3.6 Cargo composition	51
1.3.6.1 Lipids	51
1.3.6.2 Proteins	52
1.3.6.3 Nucleic acids.....	52
1.3.7 Cargo Sorting.....	54
1.3.8 Biomarkers	55
1.3.9 EVs role in immune response.....	56
1.3.9.1 Exosomes as antigen-presenting platforms.....	58
1.3.9.2 Exosomes and T cell exhaustion	58
1.3.10 EVs and HCV infection.....	59
Summary 1.3	61
2. HYPOTHESIS	63
3. OBJECTIVES	67
3.1 Primary objectives.....	69
3.2 Secondary objectives	69
4. COMPENDIUM OF ARTICLES	71
4.1 Study 1	73

Study of quasispecies complexity and liver damage progression after liver transplantation in hepatitis C infected patients.....	73
4.1.1 Article 1 summary	75
4.1.1.1 Introduction.....	75
4.1.1.2 Hypothesis	75
4.1.1.3 Objectives	75
4.1.1.4 Study design	76
4.1.1.5 Results according to objectives	77
4.1.1.6 Conclusions.....	80
4.1.2 Article 1	81
4.1.3 Article 1 Supplementary material	99
4.2 Study 2.....	115
Partial restoration of immune response in hepatitis C patients after viral clearance by direct-acting antiviral therapy.....	115
4.2.1 Article 2 summary	117
4.2.1.1 Introduction.....	117
4.2.1.2 Hypothesis	117
4.2.1.3 Objectives	117
4.2.1.4 Study design	118
4.2.1.5 Results according to objectives	119
4.2.1.6 Conclusions.....	123
4.2.2 Article 2	125
4.3 Study 3.....	145

Comparison of extracellular vesicle isolation methods for miRNAs sequencing	145
4.3.1 Article 3 summary	147
4.3.1.1 Introduction	147
4.3.1.2 Hypothesis.....	147
4.3.1.3 Objectives.....	148
4.3.1.4 Study design.....	148
4.3.1.5 Results according to objectives.....	149
4.3.1.6 Conclusions	153
4.3.2 Article 3	155
4.3.3 Article 3 Supplementary material	181
5. DISCUSSION.....	207
5.1 Quasispecies dynamics before and after LT, and parameters that would be predictive of fibrosis progression at one year after LT	209
5.2 Relevance of cellular immune response, liver inflammation and fibrosis regression, after HCV elimination mediated by DAAs	213
5.3 Development of new strategies for biomarker-discovery to predict advanced liver diseases in patients after HCV infection.....	218
6. CONCLUSIONS.....	223
6.1 Principal conclusions.....	225
6.2 Secondary conclusions.....	225
V. FUTURE PERSPECTIVES	227
V.I Multi-centric studies.....	227
V.II Epigenetic studies	227

V.III EV's effect in immune response.....	228
V.IV EVs-miRNAs to monitor HCV-patients follow-up.....	230
7. REFERENCES.....	231
VI. ANNEX	267
VI.I Isolation methods.....	267
VI.I.I Lipid nanoprobe.....	267
VI.I.II Precipitation-based method	268
VI.I.III Magnetic bead-based method	268
VI.II Articles in which the thesis candidate has collaborated.....	270

II. LIST OF FIGURES

Figure 1 Representation of the HCV genome organization30

Figure 2 Viral quasispecies population33

Figure 3 Global HCV seroprevalence distribution of genotypes.....35

Figure 4. Different DAA combinations currently available for treatment of HCV, and its HCV protein targets.....37

Figure 5. Evasion of innate immunity by HCV viral proteins.....41

Figure 6 Success and failure of adaptive immune response.....44

Figure 7 Exosome biogenesis50

Figure 8 EVs composition.....51

Figure 9. Functional properties of immune cell-derived EVs in cancer57

Figure 10. Boxplots with diversity indices showing differences between the pre-LT and post-LT quasispecies.....78

Figure 11. Viral load differences between pre and post-LT samples.....80

Figure 12. CD4+ T cell exhaustion markers expression.....120

Figure 13. Proliferation responses of CD4+ and CD8+ HCV-specific Tcells.....122

Figure 14. Liver inflammation and fibrosis markers123

Figure 15. Diagram of EVs isolation methods used for the comparison.....148

Figure 16. Characterization of three EVs isolation methods151

Figure 17. miRNAs detected by the three miRNAs sequencing protocols.....152

Figure 18. miRNAs detected with the three EV isolation methods153

Figure 19. TEM images of EV’s concentrate extracted by precipitation-based method.....268

Figure 20. TEM images of EV’s concentrate extracted by magnetic beads-based method.....269

III. ABBREVIATIONS**A**

AB	Apoptotic Bodies
ADAR1	Adenosine Deaminase Acting on RNA-1
AFP	Alfa-Fetoprotein
AFP	Alfa-Fetoprotein
Ago-2	Argonaute-2
Alix	ALG-2-Interacting protein X/PDCD6IP
ANOVA	Analysis of Variance
APC	Antigen Presenting Cell
Apo	Apolipoproteins
APRI	AST-to-Platelet Ratio Index
APRI	AST-to-Platelet Ratio

C

CAMs	Cell Adhesion Molecules
CfDNA	Cell-free DNA
CFSE	Carboxyfluorescein Succinimidyl Ester
CircRNAs	Circular RNAs

D

DAA	Direct-Acting Antivirals
DC	Dendritic Cell
DNA	Deoxyribonucleic Acid
DsDNA	Double-stranded DNA

E

EOT	End Of Treatment
-----	------------------

III | ABBREVIATIONS

ESCRT Endosomal Sorting Complex Required for Transport
EVs Extracellular Vesicles

F

FDA Food and Drug Administration
FIB-4 Fibrosis-4
FUW12 12 weeks Follow-Up

G

GRAD Isopycnic ultracentrifugation using iodixanol gradients

H

HCC Hepatocellular Carcinoma
HCV Hepatitis C Virus
HLA Human Leukocyte Antigen
HnRNPs Heterogeneous nuclear Ribonucleoproteins
Hsc Heat shock cognate
HSCs Hepatic Stellate Cells
Hsp Heat shock proteins

I

ICTV International Committee of Taxonomy of Viruses
IDL Intermediate-Density Lipoprotein
IFN Interferon
IFN- α Interferon-alfa
IFN- γ Interferon-gamma
IL Interleukin
ILVs Intraluminal Vesicles
IRES Internal Ribosome Entry Site
IRF-3 Regulatory Factor-3

IS	Immunological Synapse
ISGs	IFN-Stimulated Genes
J	
JAK	Janus Kinase
K	
Kb	Kilobases
KCs	Kupffer Cells
L	
LAG-3	Lymphocyte-Activation Gene 3
LDL	Low-Density Lipoprotein
lncRNAs	Long non-coding RNAs
Lp(a)	Lipoprotein (a)
LT	Liver Transplant
LUBAC	Linear Ubiquitin Chain Assembly Complex
M	
MAMs	Mitochondria-Associated Membranes
MAVS	Mitochondrial Antiviral-Signaling
MDA5	Melanoma Differentiation-Associated 5
Mf	Mutation frequency
MHC	Major Histocompatibility Complex
MiRISC	miRNA Induced Silencing Complex
MiRNAs	MicroRNA
MRNA	Messenger RNA
MtDNA	Mitochondrial DNA
MtRNA	Mitochondrial RNAs
MVBs	Multivesicular Bodies

III | ABBREVIATIONS

MVs Microvesicles

µm Micrometers

N

NANB Non-A, Non-B hepatitis

NAP1L1 Nucleosome Assembly Protein 1-Like 1

NCR Non-Coding Regions

NcRNA Non-coding RNAs

NEB NEBNext Multiplex Small RNA Library Prep Set for Illumina

NEMO NF-κB Essential Modulator

NEXT NEXTFlex Small RNA-Seq Kit v3

NF-κB Nuclear Factor Kappa B

NK Natural Killer

Nm Nanometer

NS Non-Structural

NSMase2 Neural Sphingomyelinase 2

NTA Nanoparticle Tracking Analysis

O

ORF Open Reading Frame

P

PAMPs Pathogen-Associated Molecular Patterns

PBMC Peripheral Blood Mononuclear Cell

PCA Principal Component Analysis

PD-1 Programmed cell Death protein 1

PDCs Plasmacytoid Dendritic Cells

PD-L1 Programmed cell Death protein 1 ligand

PEG Pegylated

PiRNAs PIWI-interacting RNAs

PKR	Protein Kinase R
PRRs	Pathogen Recognition Receptors
PS	Phosphatidylserine
PTMs	Post-Translational Modifications
π	Nucleotide diversity
Q	
qD	Hill numbers
R	
Rab	Ras-associated binding
RBPs	RNA Binding Proteins
RBV	Ribavirin
RdRp	RNA-dependent RNA-polymerase
RIG-I	Retinoic acid-Inducible Gene-I
RLRs	RIG-I-Like Receptors
RNA	Ribonucleic Acid
RRNAs	Ribosomal RNAs
S	
SEC	Size Exclusion Chromatography
SFC	Spots Forming Cells
SMARTer	SMARTer smRNA-seq kit
SnoRNAs	Small nucleolar RNAs
SnRNAs	Small nuclear RNAs
SsDNA	Single-stranded DNA
STAT	Signal Transducer and Activator of Transcription
SVR	Sustained Virological Response
T	

III | ABBREVIATIONS

TBK1	TANK-Binding Kinase 1
TCR	T-Cell Receptor
TEM	Transmission Electron Microscopy
TGF- β	Transforming Growth Factor β
Th	T helper
TIM-3	T cell Immunoglobulin and Mucin domain-containing protein 3
TLRs	Toll-Like Receptors
TNF	Tumor Necrosis Factor
Treg	T Regulatory
TRIF	TIR-domain-containing adapter-inducing interferon- β
TRNAs	Transfer RNA
Tsg	Tumor susceptibility gene

V

VL	Viral Load
VLDL	Very-Low-Density Lipoprotein
VtRNAs	Vault-RNAs

W

W4	Week 4 during treatment
WHO	World Health Organization

IV. GLOBAL SUMMARY

L'hepatitis C crònica és una de les principals causes de malaltia hepàtica en fase terminal i principal indicació de transplantament hepàtic (TH). El tractament amb antivirals d'acció directa (DAAs) permet l'eliminació viral en el 98% dels casos, però no evita l'evolució de la malaltia, principalment en pacients amb fases avançades. En aquest sentit, tant els factors virals com els de l'hoste juguen un paper clau en l'evolució de la malaltia i per això, aquesta tesi pretén abordar alguns d'aquests aspectes.

L'objectiu del primer estudi va ser analitzar el paper de factors virals, tals com la càrrega viral i la complexitat de les quasiespècies com a índexs predictius de progressió de dany hepàtic després del TH en pacients no tractats, per determinar quin seria el moment òptim per administrar els DAAs post-TH. Els resultats van demostrar que la composició de les quasiespècies difereix entre pacients i que els índexs de diversitat viral no mostren capacitat predictiva de progressió de fibrosis. Ara bé, l'augment de càrrega viral als 15 dies del TH respecte a la carga viral abans del TH, si que és un factor predictiu de progressió de dany hepàtic a l'any del TH.

L'objectiu del segon estudi es centra en factors de l'hoste, en estudiar l'eficàcia de la resposta immune adaptativa com a factor clau en l'evolució de la malaltia. L'exposició constant a antígens virals junt amb altres factors immunològics durant la infecció crònica, dona lloc a un deteriorament funcional de les cèl·lules T. La discussió actual, es centra en què ocorre a la resposta immune adaptativa un cop s'elimina el virus, si es produeix una restauració total, parcial o no es recupera. Per això en el segon estudi es van analitzar els canvis fenotípics i funcionals de les cèl·lules T CD4+ i CD8+ abans, durant i després del tractament. Abans dels DAAs, es va observar que les cèl·lules CD4+ presentaven un fenotip d'esgotament caracteritzat per

una forta expressió de PD-1. L'anàlisi de la resposta de les cèl·lules T després d'eliminar el virus, va mostrar una reducció de l'expressió de PD-1 de les cèl·lules T CD4+ en pacients no cirròtics, sense tractament previ i menors de 55 anys no tractats prèviament, així com una restauració de la capacitat de proliferació de les cèl·lules T específiques del VHC en la majoria dels pacients. Contràriament, els perfils de citocines del tipus T-helper 1 (IFN- γ i IL-2), continuaven deteriorats després de 12 setmanes de l'eliminació del VHC. Així doncs els resultats mostren una restauració parcial de la resposta immune adaptativa. En quant al dany hepàtic, l'eliminació del virus en tots els casos va suposar una reducció de la inflamació hepàtica i una regressió de la fibrosis, indicant-ne l'efecte positiu dels DAAs que porta a la regeneració hepàtica generalitzada, malgrat l'evolució d'alguns pacients cap a l'hepatocarcinoma. Amb aquesta premissa cal buscar noves eines que permetin la detecció precoç de malalties hepàtiques avançades.

En aquest sentit, els miRNAs encapsulats en vesícules extracel·lulars (EVs) són potencials biomarcadors de diagnòstic i pronòstic, ja que proporcionen informació rellevant de l'estat del pacient, mitjançant mètodes no invasius. No obstant, la manca d'un mètode estandarditzat per descobrir nous biomarcadors dificulta l'aplicació d'aquestes eines. Per la qual cosa, l'objectiu del tercer estudi ha estat comparar diferents mètodes d'aïllament d'EVs i d'anàlisi de miRNAs per l'aplicació clínica. Els resultats han mostrat que els gradients de iodixanol per separar EVs i la preparació de llibreries amb el kit NEBNext Multiplex Small RNA Library per seqüenciació massiva, són els mètodes més reproduïbles i precisos per detectar miRNAs i utilitzar-los com a biomarcadors per la detecció precoç de malalties derivades de la infecció per VHC.

Chronic hepatitis C infection is one of the major causes of end-stage liver disease and an indication for liver transplantation (LT). Treatment with direct acting antivirals (DAAs) achieve viral elimination in 98% of cases, but does not prevent disease's evolution, mainly in patients with advanced stages. In this sense, both viral and host factors play a key role in disease's evolution, therefore this thesis aims to address some of these aspects.

The objective of the first study was to analyse the role of viral factors, such as viral load and quasispecies complexity, as predictive indices of liver damage progression after LT in untreated patients, to determine which would be the optimal timing to administer DAAs after LT. Results demonstrated that HCV kinetics differ between patients, and that none of the diversity measures have shown predictive capacity of fibrosis progression. However, the increase in viral load at 15th day post-LT compared to the viral load pre-LT, is indeed a predictive factor of liver damage progression after one year of the LT.

The objective of the second study focuses on host factors, on study the effectiveness of adaptive immune response as a key factor in the evolution of the disease. During chronic HCV infection, constant exposure to viral antigens along with immunological factors results in functional impairment of T-cell functions. The current discussion focuses on what happens to the adaptive immune response once the virus is eliminated, whether there is a full, partial restoration or no recovery. Therefore, in the second study, the phenotypic and functional changes of CD4+ and CD8+ T cells were analysed before, during and after treatment. Before DAAs, CD4+T cells were observed to exhibit an exhaustion phenotype characterized by a strong PD-1 expression. Analysis of T-cell response after eliminating the virus showed a reduction in PD-1 expression of CD4+ T cells in non-cirrhotic, naïve and patients-naïve younger than 55 years, as well as a restoration of the proliferative capacity of HCV-specific T cells in most patients. Conversely, T-helper 1-type cytokine profiles (IFN- γ and IL-2)

remained impaired upon 12 weeks of HCV elimination. Hence, results point to a partial restoration of the adaptive immune response. Regarding liver damage, the elimination of the virus in all cases resulted in a reduction of liver inflammation and a regression of fibrosis stage, indicating a positive effect of DAAs, leading to a generalized liver regeneration despite the evolution of some patients towards hepatocarcinoma. With this premise, it is necessary to look for new tools that allow the early detection of advanced liver diseases.

In this sense, miRNAs encapsulated in extracellular vesicles (EVs) are potential diagnostic and prognostic biomarkers, as they provide relevant information of the current state of the patient by using non-invasive methods. However, the lack of a standardized method to discover new biomarkers hinders the application of these tools. Therefore, the objective of the third study was to compare different methods of EVs isolation and miRNA analysis for clinical application. Results showed that iodixanol gradients to isolate EVs and the preparation of libraries with NEBNext Multiplex Small RNA Library kit for next generation sequencing are the most reproducible and accurate methods to detect miRNAs and use it as biomarkers for early detection of diseases resulting from HCV infection.

1. INTRODUCTION

1.1 Hepatitis C Virus

1.1.1 HCV discovery

In 1975, a transfusion-associated hepatitis unrelated to hepatitis A and B virus infections was identified, naming the disease non-A, non-B hepatitis (NANB)¹. In the mid-1980s, it was demonstrated that the disease was caused by a small and enveloped virus related to *Flaviviridae* or *Togaviridae* viruses². Later on, it was observed that chronic NANB hepatitis leads to liver cirrhosis in 10% to 20% of infected patients³. For decades, extensive research was performed to isolate the causal agent of NANB disease. It was not until 1989 that Choo et al., after 8 years of screening on the bacteriophage lambda expression library confronted to serum samples, that they identified a clone that expressed a protein recognized by antibodies of the positive samples. The first clone expressing NS3 protease derived from the genome of that agent, was termed as Hepatitis C Virus (HCV)⁴. Since the identification of the complete sequence of HCV genome, noteworthy progress had been made in elucidating the genetic organization of the virus, facilitating the production of recombinant infectious virus in cell culture and in developing drug testing and screening⁵. HCV has become a model virus defining new paradigms in virology, immunology and biology and a unique model to study long-term side effects of persistent infection evolved into a chronic disease, after removing the causal agent.

In 2020, Michael Houghton, Harvey J. Alter, and Charles M. Rice, were awarded the Nobel Prize in Medicine for their contribution in the discovery and characterization of HCV⁶.

1.1.2 Natural history of HCV disease

Hepatitis C is an infectious disease caused by HCV. When HCV enters the human body, starts an acute infection where the virus mostly replicates in hepatocytes,

establishing an intrahepatic infection that generally results in liver inflammation. When inflammation and hepatocellular injury persists along the years, is commonly associated with significant liver-related morbidity and mortality.

Approximately, 15–45% of infected people spontaneously clear the virus, but the vast majority of infections course asymptotically and become chronic⁷. The outcome of HCV infection depends on viral/host factors, and the effectiveness of the host immune response^{8,9}. Of those with chronic HCV infection, 10–20% will silently develop advanced liver fibrosis/cirrhosis within 20–30 years¹⁰, 3–6% will develop hepatic decompensation¹¹, and 2–4% will develop liver cancer or liver failure¹².

Liver transplant (LT) is the main indication for patients with hepatic decompensation. For those patients that did not received direct acting antiviral (DAA) – based regimens before LT, the reinfection of the engrafted liver is universal within the next hours after surgical intervention and fast progression to cirrhosis is observed in 10%-30% of patients within 5 years^{13,14}. Furthermore, over 40% of graft recipients show decompensation within 12 months after the diagnosis of recurrent cirrhosis, and up to 60% experience a decompensation episode 3 years later¹⁵. The factors that accelerate the post-LT progression of liver damage in HCV patients are uncertain and seem to depend on the characteristics of the virus and the patient¹⁶.

Although infection rates have decreased globally over the last decades, HCV infection is still a public threat. According to World Health Organization (WHO), 58 million people worldwide still have chronic HCV infection. Around 399.000 people died of chronic HCV infection in 2016 and approximately 290.000 in 2019. Moreover, it is estimated about 1.5 million new infections every year.

Additionally, chronic HCV infections are frequently associated with extrahepatic manifestations such as B-cell non-Hodgkin's lymphoma, type II diabetes, autoimmune diseases and cardiovascular pathologies¹⁷⁻²⁰.

1.1.3 HCV acquisition routes

HCV is a blood-borne virus. Before the implementation of a blood screening process in 1991, HCV-infected blood components were considered the main route of HCV acquisition, leading to persistent infection which commonly progresses into chronic liver diseases^{1,21,22}. Nowadays the highest risk group for HCV infection are people who inject drugs after sharing infected needles²³. However, it can also be spread through parenteral transmission, unregulated tattoos or body piercings, accidental needle sticks, unsafe health care practices as inadequate sterilization of medical equipment, and less often through sexual contact, especially among people with HIV coinfection^{11,24}.

1.1.4 HCV structure

1.1.4.1 Viral particle

HCV is an enveloped virus with a spherical capsid typically ranging 40-100 nanometers (nm) in diameter. The HCV lipid membrane contains lipid ratios slightly different from those of the host cell membranes, and is mainly composed of cholesterol, cholesteryl esters, sphingomyelin and phosphatidylcholine. Moreover, HCV particles have been described to be associated with apolipoproteins (Apo), especially ApoB and ApoE, as lipoproteins are closely related to HCV assembly and release^{25,26}.

1.1.4.2 Genome

HCV genome is composed by a positive single-stranded ribonucleic acid (RNA) molecule of 9.6 kilobases (Kb) that contains one open reading frame (ORF) flanked by two noncoding regions (NCR), 5' NCR and 3' NCR, respectively, which are essential for RNA translation and replication^{27,28}.

The 5' region includes an internal ribosome entry site (IRES) responsible for ORF translation. ORF codifies for one polyprotein of 3011 aa that is co- and post-translationally processed into structural and non-structural (NS) proteins by proteolysis using cellular and viral proteases as shown in Figure 1^{29,30}.

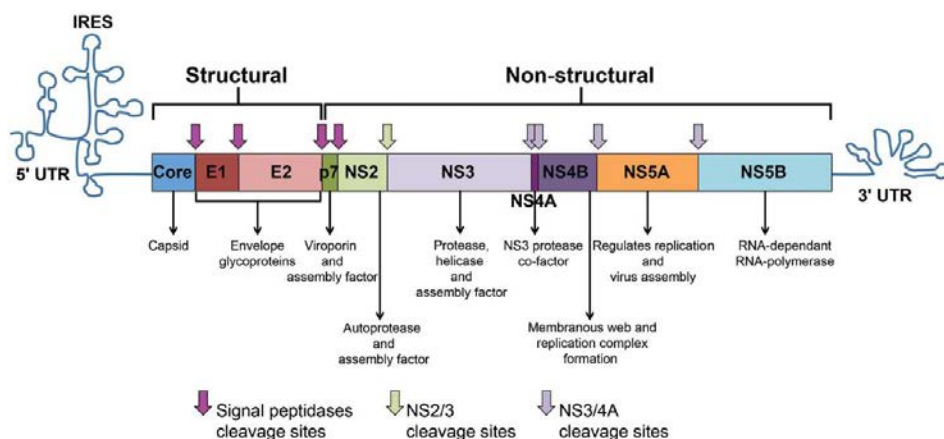


Figure 1 Representation of the HCV genome organization³¹. The single long hepatitis C virus (HCV) ORF encoding the polyprotein, and the predicted secondary structures of the flanking 5' and 3' non-translated regions (NTRs) are depicted. The 5' NTR contains an internal ribosome entry site (IRES). Polyprotein cleavage by cellular signal peptidases is indicated by dark purple arrows at the corresponding ORF position. Green and light purple arrows refer to cleavage by the viral proteases. Major functions of the HCV polyprotein cleavage products are indicated.

The 5' coding region codes for the structural proteins: C protein, widely used for serological diagnosis as it is one of the most conserved regions. Moreover, it is essential for nucleocapsid formation and it interacts with proteins involved in

cellular signaling, apoptosis, carcinogenesis and lipid metabolism. E1 and E2 proteins are involved in envelope constitution and are essential for virus entry. Envelope glycoprotein is the most hypervariable region^{32,33}.

P7 polypeptide, located between the structural and non-structural proteins, has an ion channel activity and it is involved in viral assembly, secretion and infectivity^{32,33}.

The 3' coding region codes for the NS or enzymatic proteins: Protein NS2 is a cysteine-protease involved in NS2-NS3 cleavage, virus assembly and release. Protein NS3 is a serine-protease responsible for cleavage between NS3 and NS4A and also NS4B/NS5A, and NS5A/NS5B. Protein NS3 also has a helicase activity necessary for viral RNA replication and NTPase activity. NS3-helicase domain, together with core protein, accumulate most of the antigenic sites, and this protein has been widely used for serological diagnosis. Protein NS4 is composed of two subunits: NS4A that binds to the serine-protease domain of the NS3 protein to form the NS3/4A protease and NS4B that is involved in the modulation of NS5B, carcinogenesis processes, impairment of endoplasmic reticulum function and the formation of intracellular membrane structures called membranous web, essential for viral replication. Finally, protein NS5 is also composed by two subunits; NS5A related with viral pathogenesis, assembly, secretion and replication, and NS5B that is an RNA-dependent RNA-polymerase (RdRp), which act as the catalytic enzyme of the replication machinery^{32,33}. Since, HCV RdRp lack of proof-reading activity, HCV has a very high mutation rate. The consequence of this high variability is the continuous production of variants that generates a complex mixture of different but closely related genomes known as viral quasispecies^{34,35}. Another consequence is the classification, at present, of HCV into 8 genotypes with 30-35% of divergence, and 93 subtypes of 20-25% of divergence³⁶.

1.1.5 Quasispecies

HCV does not infect patients as a virus with a defined genomic nucleotide sequence but as a complex and dynamic viral population made of many viral variants that may have some phenotypic differences between them. Those viral variants form a viral population, called quasispecies, subjected to constant genetic variation, competition and selection^{37,38}.

As previously mentioned, this great genetic variability is due to the lack of proofreading activity of the RdRp that leads to substantial sequence variations in the HCV genome, which displays mutation rates in the range of 10^{-3} - 10^{-4} substitutions per site and per replication cycle and a fixation rate of 1.5×10^{-3} base substitutions per site, per year^{39,40}. This high genomic variability added to an elevated virion production, with an average rate of 1.3×10^{12} virions/day and a half-life of 2.7 hours/virion, evokes to an extremely dynamic and highly adaptable viral population⁴¹.

Therefore, the dynamics of a quasispecies is reflected by changes in the frequencies of the haplotypes (defined as all different sequences) that conform it, caused by changes in their fitness, conditioned by inter- and intra-mutant spectrum interactions and environmental fluctuations⁴². In a constant environment, virions that coexist may exhibit different characteristics, and usually have lower fitness than the dominant genome, which is the best adapted to replicate under those specific conditions. However, if suddenly an abrupt environmental change occurs, some of the mutants generated may be favoured by granting a selective advantage making them to gain fitness in the new environment thus acquiring dominance, resulting in modification of the consensus sequence, as represented in Figure 2⁴³.

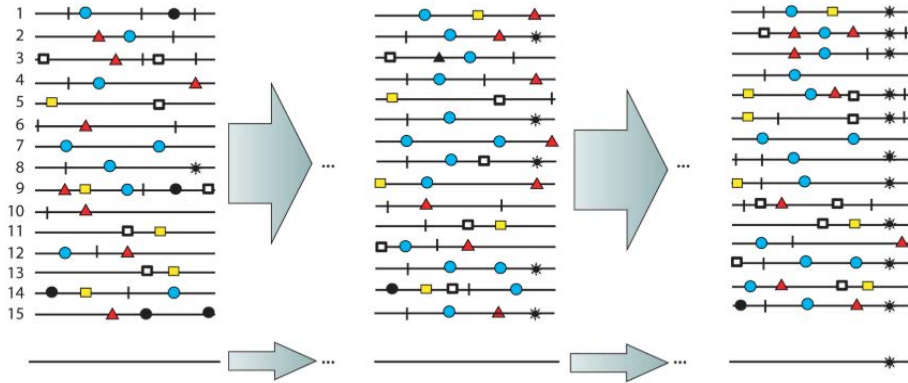


Figure 2 Viral quasispecies population. Each line represents a different genome with several mutations represented as coloured symbols. The consensus sequence is represented as the bottom line. A beneficial mutation is generated in genome 8 represented as a black asterisk. Figure adapted from⁴³.

In this way, the so-called bottleneck phenomenon can be defined when some genomes from a large quasispecies infect an individual. When such genomes increase their fitness, they may become the new dominant genome (master) of the quasispecies. It has been described that repeated genetic bottleneck events, influenced by parental population fitness, result in a decrease of complexity of mutant spectra and a decrease of the fitness, followed by a stationary phase of fitness values^{44,45}.

Viral quasispecies complexity has been defined as the “intrinsic property that quantifies the diversity and frequency of haplotypes, independently of the population size that contains them”. The relevance of the viral complexity has been evidenced by the lower adaptability of viruses whose polymerase shows a higher or lower copying fidelity than the wild type with a comparable population size in the same biological context⁴⁶.

High variability rates and a continuous natural selection of viral variants are partly responsible of viral persistence and the lack of protective immunity against reinfection⁴⁷. Some defective virions that are generated from non-

neutral mutations can be eliminated by the immune system. Other genomes are eliminated when they exceed the maximum mutation rate, named error threshold, entering into error catastrophe and losing its genetic information⁴⁸. Those variants that survive can affect the pathogenesis, induce immune tolerance, develop resistance to antivirals or to neutralizing antibodies and thus contribute to chronic infection⁴⁹.

Therefore, when studying an infection, it is important to be aware that some members of the quasispecies may be relevant for establishing chronic infection in HCV infected patients, and approaches based on studying the diversity and complexity of the entire viral population should be considered.

1.1.6 Prevalence and distribution

HCV is a host-specific and pathogenic virus that belongs to the *Flaviviridae* family within the *Hepacivirus* genus⁵⁰.

According to the latest update of the International Committee of Taxonomy of Viruses (ICTV), eight genotypes and ninety-three confirmed subtypes of hepatitis C have been described³⁶.

HCV infection remains spread all over the world, and its prevalence differs within regions as shown in Figure 3. According to latest data provided by WHO, the highest incidence of HCV is in the East of the Mediterranean Region and in Europe, with around 12 million people chronically infected in each region. In the South-East Asia and the Western Pacific, it is estimated around 10 million people. About nine million people are chronically infected in Africa and 5 million in America.

HCV genotype distribution varies according to the geographic origin and transmission risk as represented in Figure 3. Genotype 1 is the most prevalent globally and represents 46% of all HCV cases, with the majority of cases located

in East Asia, Europe and America. Genotype 2 is responsible of 9% of HCV cases, generally distributed around East Asia and Africa. Genotype 3 represents the 30% and is primarily distributed in South Asia. Genotype 4 represents the 8% and is mainly found in Africa and the Middle East. Genotype 5 is responsible of <1% of all HCV cases and is spread around Southern Africa. Genotype 6 is responsible for approximately 5% of cases and predominate in East Asia. Genotypes 7 and 8 are the newest and fewer represented subtypes, originally described from Central Africa and East Asia respectively, although are not represented on Figure 3^{51,52}.

Moreover, it has been described a correlation between HCV genotypes and disease severity. HCV genotypes 1 and 3 have been associated with faster liver damage progression and the possibility of hepatocellular carcinoma (HCC) development, which may result in poor survival in patients with HCV-related HCC^{53–55}.

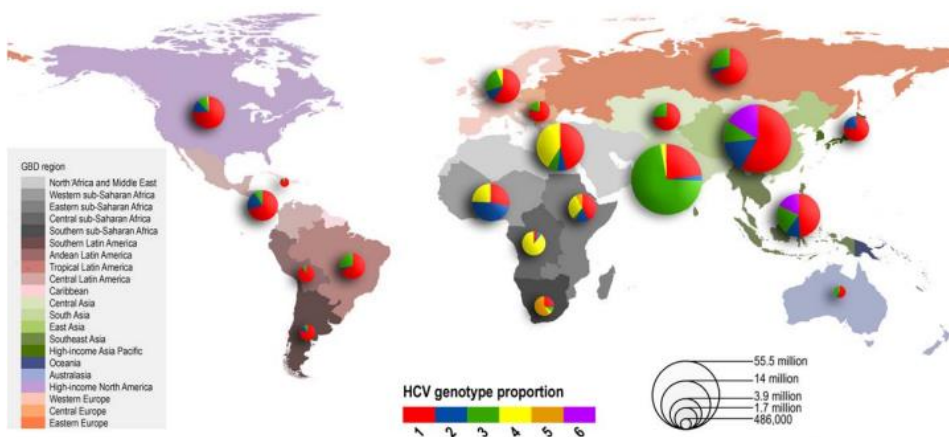


Figure 3. Global HCV seroprevalence distribution of genotypes. Size of pie charts is proportional to the number of seroprevalent⁵².

1.1.7 Treatment timeline

In 1991, the Food and Drug Administration (FDA) approved interferon-alfa (IFN- α) for hepatitis C infection treatment. Low sustained virological response (SVR) (16-20%), as well as frequent clinically adverse events, were observed with the administration of IFN- α alone^{56,57}.

In the late 1990s, IFN- α combined with Ribavirin (RBV) for the treatment of hepatitis C infection was approved. This combined regimen managed to double SVR rates in all patients compared to IFN monotherapy, but still frequent clinically adverse events were observed among the majority of patients⁵⁸⁻⁶⁰.

In the early 2000s, pegylated interferon (pegIFN) therapy and later on the administration of pegIFN alfa-2a plus RBV were approved for hepatitis C treatment. It was demonstrated a higher SVR in those patients receiving peginterferon alfa-2a plus RBV (56%) than those receiving interferon alfa-2b plus RBV without polyethylenglicol (44%) or peginterferon alfa-2a without RBV (29%)⁶¹.

In 2011, the first-generation of DAAs was approved by the FDA. Since then, HCV treatment-guidelines have changed drastically due to their increased efficacy, safety, and tolerability compared with previously HCV treatments. At the first beginning, those DAAs needed to be administered with pegIFN alfa-2a plus RBV in order to avoid relapses after the end of treatment and to achieve up to 75% of SVR. Short after, several IFN-free oral therapies were developed and suitable for all patients, including those previously intolerant of or ineligible for IFN therapy. With the onset of new generation DAAs and the possibility to combine different DAAs in a single pill (Figure 4) treatment regimens and treatment adherence have been improved leading to a SVR in more than 98% of patients regardless of viral genotype and with minimal side effects⁶²⁻⁶⁴.

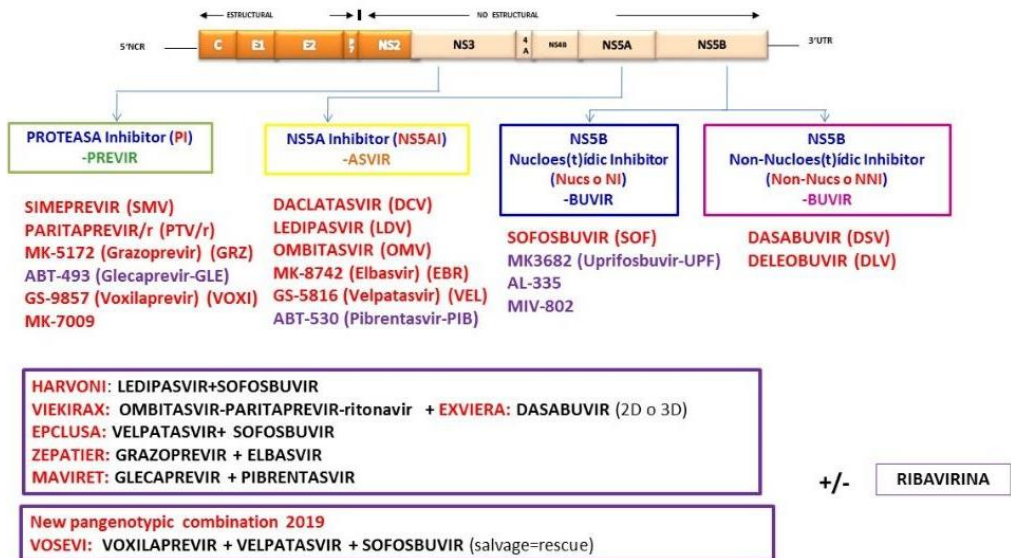


Figure 4. Different DAA combinations currently available for treatment of HCV, and its HCV protein targets. Inhibitors target the NS3/4A protease, the non-structural protein NS5A, and the viral polymerase NS5B.

1.1.8 Vaccination and future perspectives for HCV elimination

Global eradication of HCV infection will not be achieved in the absence of an effective vaccine. Unfortunately, no vaccine exists for HCV infection and although current investigation is underway, further studies based on HCV genetic diversity, immune response and other mechanisms of viral persistence are needed^{65,66}.

Although preventive measures notably help to reduce the incidence of HCV infection nowadays, a global control is still a public health concern because of the low diagnosis and treatment access worldwide. By 2030, the WHO set a common global goal of HCV elimination by planning to reach a 90% of diagnosis of all HCV cases, an 80% of treatment coverage and a 65% reduction in HCV-related deaths⁶⁷.

Summary 1.1

Chronic HCV liver infection is still a global health problem, and liver transplant (LT) is the main indication for patients with hepatic decompensation. As pointed out before, reinfection of the engrafted liver is universal within the next hours after surgical intervention in untreated patients, and host/viral factors causing fast or low progression to cirrhosis are uncertain. Therefore, finding a predictive index of liver damage progression is a requirement for decision making related to which would be the optimal timing to administer DAAs after LT.

1.2 Immune response in HCV infection

The relationship between HCV and the host is dynamic; the virus tries to be undetected by the immune system in order to coexist, while the immune system tries to clear the virus without harming itself. The balance between these two biological forces depends on the viral replication kinetics as well as on the quality and quantity of the immune system response. Robust innate and adaptive immune responses are necessary for viral clearance.

The first host defence barrier against HCV is the innate immunity. It is activated when specific pathogen recognition receptors (PRRs) of the host cell recognize and bind to pathogen-associated molecular patterns (PAMPs) and, consequently, antiviral signals to clear the virus are induced. Afterwards, adaptive immune response is triggered. Activation of lymphocytes is mediated through three signals; the first is signalling through T-cell receptor (TCR), the second is induced by antigen receptors when an antigen is recognized through costimulatory signals induced by molecules provided by professional antigen presenting cells (APC), and the third is via cytokines⁶⁸.

1.2.1 Innate immune responses

Upon HCV infection, HCV acts as PAMPs and is detected by two PRRs, the retinoic acid-inducible gene-I (RIG-I) like RIG-I-like receptors (RLRs) and the Toll-like receptors (TLRs). RIG-I recognizes HCV RNA as a foreign antigen and interacts with mitochondrial antiviral-signalling proteins (MAVS) on mitochondria-associated membranes (MAMs). The binding of RIG-I to MAVS trigger downstream activation of interferon (IFN) regulatory factor-3 (IRF-3) and nuclear factor kappa B (NF- κ B) that induce type I and III IFN expression signalling in the liver⁶⁹. Secreted IFNs bind to their cognate IFN receptor and activates the Janus Kinase/Signal Transducer and Activator of Transcription (JAK/STAT) pathway, which induce the IFN-stimulated genes (ISGs) expression that results in the degradation of viral RNA and death of infected hepatocytes^{70,71}. IFN also activates the Adenosine deaminase acting on RNA-1 (ADAR1), which has an antiviral role by inducing mutations in HCV dsRNA strands that destabilize the secondary viral RNA structures, and through suppressing IFN and ISGs expression^{72,73}.

In addition to the hepatocytes, type I IFNs are also secreted by non-parenchymal cells, especially by plasmacytoid dendritic cells (pDCs). During HCV infection, it is observed a diminished pDCs frequency in the blood and increased pDC homing to the liver as well as a diminished IFN- α production⁷⁴. Moreover, the activation of resident hepatic cells, such as stellate cells and liver macrophages called Kupffer cells (KCs), enhance the production of inflammatory mediators like pro-inflammatory cytokines and chemokines that also helps to sustain an inflammatory state⁶⁹.

1.2.1.1 HCV mechanisms to evade the innate immune system

HCV uses different strategies to evade the innate immune system and persist within the host. To do so, HCV proteins interact with relevant host proteins inactivating essential pathways for HCV clearance, early during acute infection as represented on Figure 5 and briefly explained below.

HCV core induces degradation of STAT1, and consequently suppress the expression of IFN⁷⁵. Furthermore, HCV core suppress Nuclear Factor Kappa B (NFkB) activation and related inflammatory responses being involved in anti-apoptotic processes that protect infected hepatocytes from cell death^{76,77}.

HCV E2 interacts with PKR, inactivating its kinase activity and blocking its inhibitory effect on protein synthesis and cell growth⁷⁸.

It was reported that HCV p7 suppresses the antiviral function of exogenous IFN⁷⁹.

HCV NS3/4A proteins cleaves to MAVS⁸⁰ and/or TIR-domain-containing adapter-inducing interferon- β (TRIF) protein disrupting RLR pathway⁸¹. It also inactivates Riplet and consequently inhibit RIG-I and IRF-3 activation⁸². Moreover, through competitive binding, NS3 blocks the interaction between the adaptor protein NF- κ B essential modulator (NEMO) and the linear ubiquitin chain assembly complex (LUBAC), that consequently inhibit NF- κ B activation⁸³. HCV NS3 protein binds to TANK-Binding Kinase 1 (TBK1) and therefore inhibit IRF-3 activation⁸⁴.

HCV NS4B inhibit RIG-I-mediated IFN- β production signalling and downregulate TLR3-mediated interferon signalling^{85,86}.

Moreover, HCV core and NS3 proteins modulate monocytes activity to secrete Interleukin (IL)-10 and Tumor Necrosis Factor (TNF- α) that inhibit IFN- α production⁷⁴.

HCV NS5A interacts and represses PKR to avoid the antiviral effects of IFN⁸⁷, downregulates IFNs expression induced by RIG-I- and Melanoma Differentiation-Associated 5 (MDA5)⁸⁸, and interacts with nucleosome assembly protein 1-like 1 (NAP1L1) blocking its nuclear translocation and leading to inefficient RIG-I and TLR3 responses⁸⁹.

HCV inhibits IFN- α production by pDCs through direct interaction, in a way that is independent of infection and replication inside the pDCs⁷⁴.

Apart from the mechanisms related to viral proteins, HCV had developed other strategies to evade the innate immune system such as modulation of host miRNAs directly related to HCV infection outcome⁹⁰ and/or through extracellular vesicles (EVs) containing viral RNA, which reduces the chances to be detected by host defenses⁹¹.

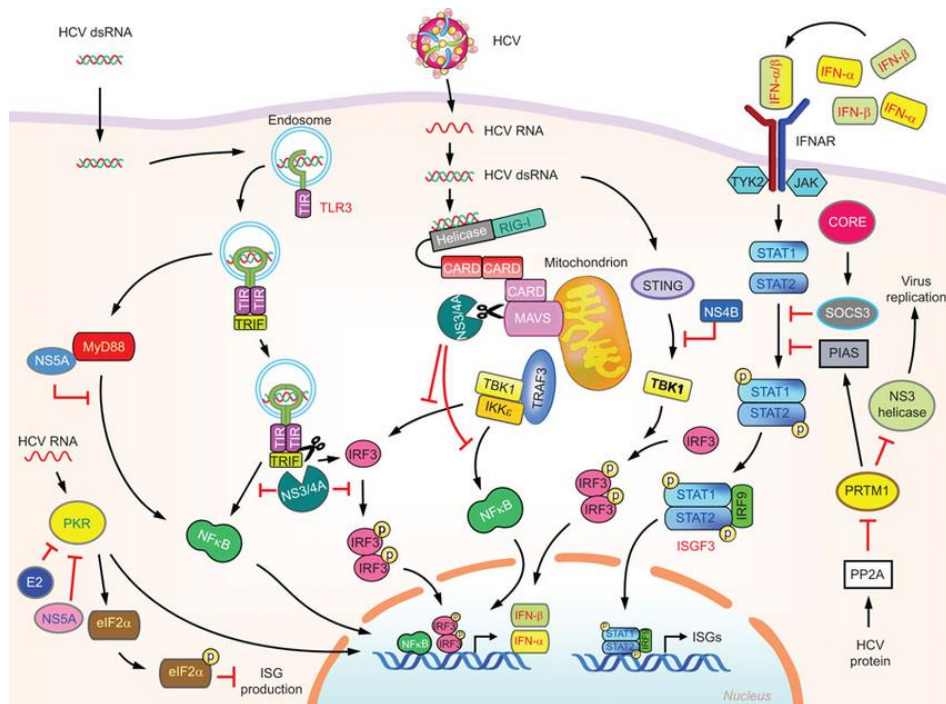


Figure 5. Evasion of innate immunity by HCV viral proteins⁹².

1.2.2 Adaptive immune responses

HCV-specific T cell immune responses are required for viral control.

CD8⁺ T cells play an essential role in HCV control since they recognize viral peptides in Human Leukocyte Antigen (HLA) class I molecules present in infected cells. Once specific antigen recognition occurs, several mechanisms get activated and HCV-specific CD8 T cells may be involved not only in the elimination of infected hepatocytes by cytolytic mechanisms but also by non-cytolytic effector mechanisms^{93,94}.

On the other hand, CD4⁺ T cells recognize viral peptides in HLA class II molecules present in antigen-presenting cells (APCs). Once recognition, HCV-specific CD4⁺ T cells start a process of expansion and clonal differentiation towards CD4⁺ T helper cells (Th). Two types of Th cells can be generated; Th1 which produce cytokines, like IL-2, IFN- γ and TNF- α , essentials for CD8⁺ T cell cytotoxic responses, and Th2 which produce cytokines, like IL-4, IL-5, IL-6 and IL-10, that stimulate antibody production by B cells^{95,96}.

HCV-specific antibodies are detected 8–20 weeks after infection, and decline to undetectable levels within 10-20 years of recovery from infection^{97,98}.

- During acute HCV infection, viral replication is detected from the first week of infection and have the highest peak at week 4. CD8 cytotoxic response coincides with the peak of transaminase levels at week 7-8 of infection, but it is not enough to control and clear the virus. Thus, CD4⁺ T cells have important helper functions, contributing to maintain CD8⁺ T cell response and preventing viral escape from T cell response. Specifically, CD4⁺ T cell response help to reduce the viral load, normalize transaminases levels and induce a phenotypic and functional change of CD8⁺ T cells⁹⁹.

Accordingly, self-limiting HCV infections are associated with expansion of virus-

specific CD8+ T cells, a broad CD4+ T cell responses, and a strong cytotoxic T lymphocyte response as represented on Figure 6A¹⁰⁰⁻¹⁰³.

- During chronic HCV infection, constant exposure to viral antigens along with immunological factors results in varying degrees of functional impairment of HCV-specific T-cell effector functions, contributing to viral persistence¹⁰⁴⁻¹⁰⁶. Thereby, persistent infection is characterized by intrahepatic compartmentalization of anergic and exhausted CD8+ T cells, characterized by their inability to produce IFN- γ and IL-2, and HCV-specific CD8+ T cells with regulatory and inhibitory functions. In peripheral blood and liver, also coexist CD4+ T cells with an exhausted or anergic phenotype while regulatory T cells (Tregs) are overrepresented¹⁰⁷⁻¹¹⁰. Lack or loss of helper functions by CD4+ T cells can result in a dysfunctional CD8+ T cell response and an immune response failure against the virus^{111,112}. Furthermore, a dysregulation of cytokine milieu occur during chronic infection, promoting activation-induced apoptosis of CD4+ and CD8+ T-cells in the liver¹¹³.

1.2.2.1 HCV mechanisms to evade the adaptive immune system

HCV uses several mechanisms to evade the adaptive immune system and persist within the host as it is represented in Figure 6B. Among them, highlight mutational escape mechanisms and the induction of phenotypic and functional changes in the immune cells.

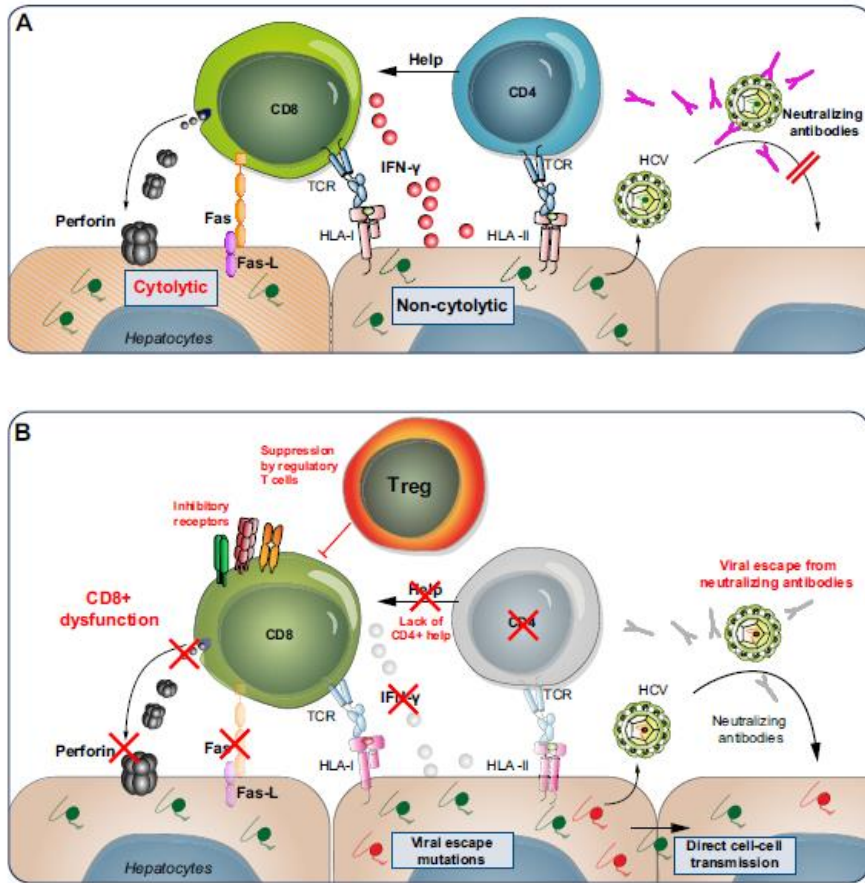


Figure 6 Success and failure of adaptive immune response. (A) Effective CD8+ and CD4+ T cell responses as in self-limiting HCV infections. (B) Mechanisms that contribute to HCV persistence and consequently adaptive immune response failure, such as viral escape, T cell exhaustion, lack of CD4+ T cell help or the action of regulatory T cells¹¹⁴.

Firstly, viral escape mutations on epitope recognized by B and T cells cause reduced recognition from T cells and antibodies, and consequently the virus cannot be neutralized^{115,116}. Moreover, HCV can impair T cell activation through inhibition of cytokine production, antigen presentation by dendritic cells (DCs) and macrophages^{117–119}.

Secondly, HCV proteins can directly interact with the complement system by binding to C1 receptor on T cells, and decrease its proliferative capacity and cytokine production¹²⁰.

Thirdly, T cell anergy is a tolerance mechanism, that contribute to viral persistence, in which T cells fail to suppress viral replication because they are in a hypo responsive state. After antigenic stimulation, CD8+ T cells present reversible alterations in the proliferative, cytotoxic, and antiviral cytokines secretion capacity. This dysfunction is already observed from the first stages of acute infection regardless the outcome of the disease. However, in patients with a self-limited course of the infection, the recovery of CD8+ T cell functions is associated with a decrease of viremia and disease resolution. In contrast, patients who evolve towards chronicity does not ameliorate CD8+ T cell functions and those remain persistently suppressed^{121,122}. Additionally to antigenic stimulation, it has been described that CD4+ and CD8+ Tregs may also contribute to disrupt T cell effector functions and consequently maintain a persistent infection^{108,110}.

In addition, a prolonged antigen stimulation can induce exhaustion in previously activated and functional T cells. T cell exhaustion is defined by a lack of effector functions and overexpression of inhibitory receptors like Programmed cell Death protein 1 (PD-1), T cell Immunoglobulin and Mucin domain-containing protein 3 (TIM-3) and Lymphocyte-Activation Gene 3 (LAG-3), resulting in ineffective T cell responses¹²³. In this line, PD-1 upregulated expression together with low costimulatory signals and/or limited cytokine milieu triggers inhibitory PD-1 signals that impair T-cell responses. At the same time, high expression of PD-1 marker have been correlated with high levels of HCV-specific CD8+ apoptosis in blood during acute infection and in liver during chronic infection¹²⁴.

Lastly, as it was previously mentioned, a vigorous CD8+ T cell response require an effective CD4+ T cell help response. CD4+ T cell response failure can occur due to an excess of antigenic stimulation, antigen presentation by non-professional cells or immature APCs in suboptimal costimulatory conditions¹²⁵⁻¹²⁷.

1.2.3 Immune response after DAAs-mediated infection resolution

Several groups have investigated whether DAAs treatment, and the subsequent elimination of HCV, can restore the HCV-specific immune responses, although controversial results have been reported. For instance, it has been demonstrated that HCV-specific T cell functions does not completely ameliorate after SVR¹²⁸. In contrast, other studies have documented an increase in T-cell functionality after DAA treatment¹²⁹. It is known that an early impairment of proliferation may contribute to loss of T cell response and chronic HCV persistence¹³⁰. Although there is not yet a solid evidence that T cell proliferation is fully recovered after HCV cure, several studies have seen an increase in the proliferative profile of CD8+ T cells in chronic HCV-infected patients after DAA treatment^{129,131,132}. In contrast, in other studies a partial or inexistent proliferative capacity recovery has been documented^{133,134}. Likewise, few and contradictory information have been reported about CD4+ T cell proliferative capacity after DAAs^{134,135}.

Summary 1.2

HCV-specific immune response is essential in HCV infection outcome. As mentioned before, during chronic infections the immune response remains impaired but there is still an open question on whether the elimination of HCV by DAAs results in a full, partial or inexistent restoration of the immune response. Characterizing the immunological status of patients after resolving

HCV infection would help to understand disease's evolution and the associated sequelae of the infection.

1.3 Extracellular vesicles

1.3.1 Extracellular vesicles discovery

In 1946, EVs were first observed as pro-coagulant platelet-derived particles in plasma samples¹³⁶. After that, several groups pointed the presence of vesicles in multiple and diverse samples, but their function and uses were still unknown. In the late 1980s, EVs were first described as small vesicles released by exocytosis when multivesicular bodies (MVBs) fused with the plasma membrane in reticulocytes^{137,138}. For so long, EVs were considered garbage that cells get rid of it. A decade later, the discovery of the function of EVs as activators of the immune system made them gain prominence in the scientific community¹³⁶. With the discovery that EVs contain RNA, acquired substantially renewed interest as mediators of cell-to-cell communication, and since then EVs have been extensively studied as potential biomarkers and therapeutic tools.

1.3.2 Brief overview

EVs are lipid membrane vesicles secreted by hematopoietic and non-hematopoietic cells into the extracellular space. From the extracellular space, EVs can travel through body fluids, including blood, urine, saliva, amniotic fluid, bile, ascites, breast milk, etc. and reach distant cells¹³⁹. EVs serve as functional vehicles of intercellular communication as they carry a complex cargo of lipids, proteins, sugars, and nucleic acids, that when delivered to the target cells are capable to modulate and reprogram recipient cells¹⁴⁰. Furthermore, the contents, size and membrane composition of EVs are highly variable as directly depend on the cell of origin, the state of the donor cell (differentiated, stressed,

stimulated, etc.), and environmental conditions¹⁴¹. For that reason, EVs give relevant information of the current state of the patient and may offer prognostic information in a huge range of diseases. Moreover, EVs play a significant role not only in pathological but also in physiological processes as well as maintaining the homeostasis, both in eukaryote and prokaryote organisms¹⁴².

1.3.3 EVs types

It has been described three main subtypes of EVs, apoptotic bodies (AB), microvesicles (MVs) and exosomes, which differ between them by its origin, size, content and function.

- AB range in size from 50 nm up to 5 micrometers (μm) in diameter and are generated as a result of plasma membrane blebbing during apoptotic processes¹⁴³. AB content is similar to cell lysates, composed by intact organelles, chromatin, glycosylated proteins and proteins related to the nucleus, mitochondria, golgi apparatus and endoplasmic reticulum^{144,145}.

- MVs range in size from 100 nm up to 1 μm in diameter and are shed from the plasma membrane. Within its content, it is found cytosolic and plasma membrane associated proteins, heat shock proteins, cytoskeletal proteins, integrins, and proteins containing post-translational modifications (PTMs) such as glycosylated and phosphorylated proteins, nucleic acids, etc^{144,146}.

- Exosomes range in size from 30 up to 150 nm and are originated by inward budding of intraluminal vesicles (ILVs) into MVBs, which fuse with the plasma membrane releasing ILVs to the extracellular milieu. When ILVs are in the extracellular milieu are called exosomes¹³⁹. Due to their biogenesis, exosomes contain proteins from endosomes, plasma membrane and the cytosol as well as nucleic acids, lipids and metabolites¹⁴⁷ (detailed information is summarized below). Exosomes 'float' to a density range of 1.08-1.19 g/cm^3 , since density

may vary from cell to cell depending on the exosome protein content¹⁴⁸. Thus, exosomes are likely to protect their cargo thanks to their lipid bilayer membrane and their small size that helps to prolong their circulation half-life and enhance their biological activity¹⁴⁹.

Amongst EVs, exosomes have generated greater interest due to their biogenesis and specific cargo that makes these vesicles as the main target for therapeutic, diagnostic and prognostic biomarkers in many different clinical situations, as described below.

1.3.4 EVs isolation methods

Since many years, ultracentrifugation has been used as the gold standard method for EVs isolation, as it allows the sedimentation of a wide range of vesicles; however, this is a time consuming procedure that requires expensive equipment and yields low-purity EVs; this is why an increasing number of laboratories are currently using other methodologies¹⁵⁰. Precipitation-based methods also result in high EVs recovery, without specific infrastructures requirements, but the low purity of isolated EVs is a major problem¹⁵¹. Isopycnic ultracentrifugation using iodixanol gradients has the same requirements than ultracentrifugation in terms of time and equipment, but it provides higher EV purity because it discriminates vesicles subtypes according to their density¹⁵². Finally, size exclusion chromatography (SEC) is widely used for size-based particle isolation, and leads to large EV batches that are well separated from smaller particles and proteins¹⁵³.

1.3.5 Exosome biogenesis

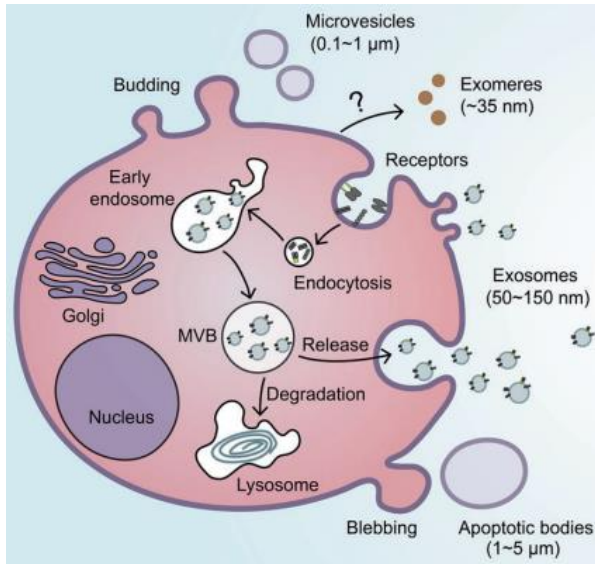


Figure 7 Exosome biogenesis¹⁵⁴.

Exosomes are formed by inward budding of early endosome membranes, which then mature into late endosomes or also called MVBs. During this process, MVBs accumulate ILVs in their lumen that carry specific sorted proteins,

lipids, and cytosol. Then, those MVBs fuse with the plasma membrane releasing their content into the extracellular environment or fuse with lysosomes to be degraded as represented in Figure 7¹³⁹. The fate of that vesicles depends on ILV's and thus of the MVB's content, on the presence or absence of cholesterol in MVB's membranes, as well as on the presence of endogenous and exogenous stimuli^{155,156}. MVBs, ILVs formation and consequently exosomes biogenesis can be due to Endosomal Sorting Complex Required for Transport (ESCRT)-dependent and -independent mechanisms, depending of the cargo that is sorted within a given cell.

1.3.6 Cargo composition

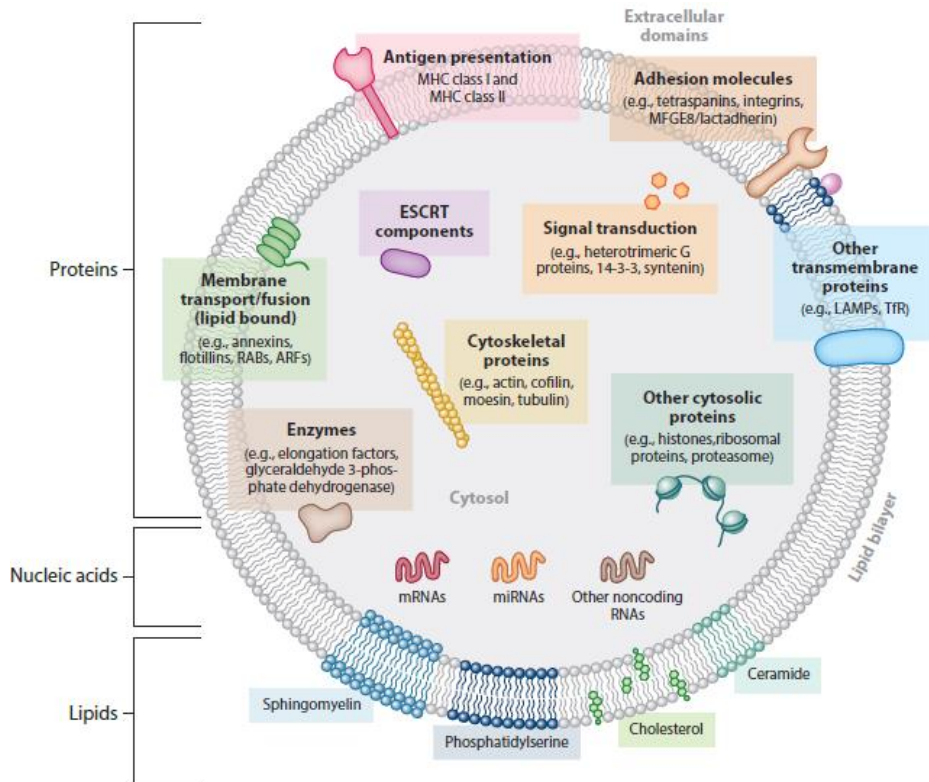


Figure 8 EVs composition¹³⁹.

Databases like vesiclepedia and evpedia include data of EVs content as well as on the purification procedures that helps scientists to be updated, and to better understand the complexity and functionality of these vesicles.

1.3.6.1 Lipids

Exosomes carry certain type of lipids, which are essential for maintaining their biological activity, and that together with membrane-bound proteins determine the structure and function of the exosomes membrane. Due to their biogenesis, a similar distribution of lipids in the inner and outer membrane of the exosomes and the plasma membrane is expected. Although, differences in lipid

composition between exosomes and their secreting cells, point to specific mechanisms of cargo sorting. Exosomes are mainly enriched in sphingomyelin, phosphatidylserine (PS), cholesterol and ceramide as represented in Figure 8¹⁵⁷.

1.3.6.2 Proteins

It has been described a heterogeneous protein composition within exosomes as shown in Figure 8. Some of the cellular proteins present in exosomes depend on the cell of origin, whereas others are constitutively present in exosomes regardless of cell type¹³⁹. The presence of coat-proteins like clathrin, adhesion molecules such as integrins, cell adhesion molecules (CAMs), and tetraspanins like CD63, CD9, and CD81 has been described. Moreover, heat-shock proteins like Heat shock cognate (Hsc) 70 and Heat shock proteins (Hsp) 90, cytoskeletal proteins like actin, tubulin, cofilin, and moesin and antigen presentation molecules like Major Histocompatibility Complex (MHC) class II and class I have been observed in exosomes. In addition, there are also proteins related to cell signalling, such as subunits of trimeric G proteins, proteins involved in membrane transport and fusion such as Ras-associated binding (Rabs) and Annexins, Raft-associated proteins, enzymes and elongation factors, as well as, ESCRT proteins like Tumor susceptibility gene (Tsg) 101 and ALG-2-interacting protein X/PDCD6IP (Alix)¹⁵⁸.

1.3.6.3 Nucleic acids

Deoxyribonucleic Acid (DNA)

Although the biological functions of DNA inside exosomes are still largely unknown, it may have relevant functions in the maintenance of cellular homeostasis, intracellular communication, and immune response modulation. Furthermore, DNA inside EVs either entirely or in fragments, recently gained

interest as it reflects the mutational status of parental cancer cells, which suggests that its role in pathological processes is also relevant¹⁵⁹.

Exosomes content includes cell-free DNA (cfDNA), single-stranded DNA (ssDNA), double-stranded DNA (dsDNA), mitochondrial DNA (mtDNA), transposons, and even viral DNA¹⁶⁰.

RNA

Relevant differences in a transcriptomic level have been observed from exosomes versus donor cells, as a selective incorporation of certain RNAs into exosomes is carried out¹⁶¹. Moreover, the RNA cargo of exosomes varies between cell types and can be affected by exogenous stimuli^{162,163}.

Various types of RNA molecules are found in exosomes, with a selective enrichment towards smaller RNAs as compared to the cell transcriptome¹⁶⁴. Beyond protein-coding transcripts like messenger RNA (mRNA), exosomes contain various non-coding RNAs (ncRNA). These include microRNA (miRNAs), transfer RNA (tRNAs), long ncRNAs (lncRNAs), circular RNAs (circRNAs), mitochondrial RNAs (mtRNA), ribosomal RNAs (rRNAs), as well as, Y RNAs, PIWI-interacting RNAs (piRNAs), small nucleolar RNAs (snoRNAs), small nuclear RNAs (snRNAs), and vault-RNAs(vtRNAs)^{165,166}.

miRNAs are small and highly conserved ncRNAs, of about 20-30 nt length, that play a critical role as posttranscriptional regulators of gene expression¹⁶⁷. They can modulate gene transcription by influencing chromatin structure, chromosome segregation, RNA processing, and by eliciting gene silencing through repressing mRNAs translation and/or through reducing mRNAs stability and consequently enhancing mRNAs degradation¹⁶⁸.

Thereby, they are involved in biological processes like development, cell proliferation and differentiation, apoptosis, immune regulation and metabolism¹⁶⁹.

In addition, they are also involved in pathological processes, having a significant function in regulating cancer progression. Exosomes derived from tumor cells deliver miRNAs to neighbouring or distant cells altering its phenotype. Subsequently, those miRNAs interfere with tumor immunity and the microenvironment, facilitating primary tumor growth, angiogenesis, metastatic cell migration, pre-metastatic niche formation and drug resistance¹⁷⁰. Furthermore, in a pathological process, injured cells secrete much more exosomes than healthy cells, and those exosomes are enriched with miRNAs linked to the pathogenesis¹⁷¹.

To avoid nucleolytic degradation, miRNAs are present in many body fluids associated with RNA binding proteins (RBPs), with high and low density lipoproteins or encapsulated in EVs, mostly exosomes (EVs-miRNAs)¹⁷²⁻¹⁷⁴. Thus, the majority of miRNAs that are circulating freely are concentrated when encapsulated in exosomes¹⁷⁵.

1.3.7 Cargo Sorting

Exosomal cargo sorting is mediated by ESCRT-dependent and independent mechanisms and can be influenced by external stimuli like the stress.

ESCRT-dependent sorting mechanism; ESCRT complex helps proteins to be loaded into exosomes. It recognizes ubiquitylated cargoes and prevents them from degradation by sorting them into exosomes. In addition to ubiquitination, acetylation is also implicated in the sorting of proteins into exosomes¹⁷⁶.

ESCRT-independent sorting mechanism; PTMs can regulate the protein cargo sorting and promote the enrichments of some proteins in exosomes. Besides

ubiquitination and acetylation, ISGylation, SUMOylation, glycosylation, oxidation, phosphorylation, citrullination and myristoylation can control exosome cargo loading and interact between various PTMs¹⁷⁶.

Additionally, lipid raft, tetraspanins and ceramide-mediated mechanisms are also involved on lipid, protein and RNA sorting¹⁷⁶.

Moreover, miRNAs and RNA loading in exosomes can be modulated by different mechanisms such as sumoylated heterogeneous nuclear ribonucleoproteins (hnRNPs)-dependent mechanism, neural sphingomyelinase 2 (nSMase2)-dependent mechanism, the 3'-end of the miRNA sequence-dependent pathway, the miRNA induced silencing complex (miRISC)-related pathway, membrane proteins and RNA-binding proteins related pathway as well as raft-based microdomains¹⁷⁶.

1.3.8 Biomarkers

Studying miRNAs encapsulated in EVs, mostly exosomes, and not total miRNAs present in plasma samples have several advantages. Firstly, exosomes give relevant information of the current state of the patient and may offer prognostic information in a huge range of diseases¹⁷⁷. Secondly, as many diseases have heterogeneous clinical presentations, exosome monitoring may permit compiling real-time information coming directly from the different players involved in the pathological process, which would include injured cells, immune cells, metastatic cells, etc.^{178,179}. Thirdly, the easy access and stability of EV-miRNAs in biological fluids make them an attractive alternative as minimally invasive test, known as liquid biopsies¹⁸⁰. And lastly, the fact that exosomes transfer miRNAs between cells during cell-cell communication and that those miRNAs regulate gene expression locally and distantly during physiological and

pathological processes, converts them not only in potential therapeutics but also in diagnostic and prognostic biomarkers^{181,182}.

Even though in the last few years, the scientific community have gained interest on EV-miRNAs as biomarker sources because of the reasons pointed above, discrepancies on miRNA patterns and its validation are still frequent between research groups. It would be due to the use of different EV isolation methods, the use of different miRNA extraction, library preparation and sequencing kits or the differences on sample procedure and origin¹⁸³⁻¹⁸⁵. Moreover, the separation of EVs from particles like lipoproteins that also contain miRNAs, is extremely difficult depending on the isolation method used¹⁸⁶.

1.3.9 EVs role in immune response

Over a decade after the discovery of EVs, the first studies revealing the role of EVs in the immune system were published. In 1996, Raposo et al. demonstrated that exosomes derived from B lymphocytes induced antigen-specific MHC class II-restricted T cell responses, suggesting that they may be responsible for maintenance of long-term T cell memory or T cell tolerance¹³⁶.

Nowadays, it is widely accepted that exosomes can be secreted by all types of immune cells, have specific cargo crucial for their immunomodulatory properties and are potential therapeutic agents. In this line, exosomes not only have a pivotal role in immune stimulation, but also in immune suppression and maintenance of peripheral tolerance by inducing T cell anergy or activation-induced cell death¹⁸⁷.

In a tumour microenvironment, EVs derived from tumour cells may serve as homeostatic mediators for tumour niche maintenance, and exhibit positive or negative effects on antitumor immune responses. To achieve so, EVs use several mechanisms, some of them summarized in Figure 9, as can be the inactivation

of cytotoxic responses such as those induced by Natural Killer (NK) cells, the induction of activated T cell apoptosis, and the impairment of dendritic cell differentiation¹⁸⁸. In addition, immune derived-EVs may modulate B and T cell differentiation and proliferation, T cell migration and expansion, as well as, DC maturity.

Therefore, EVs derived from immune cells contain cytokines, chemokines, cytolytic and cytotoxic proteins that can modulate effector functions and induce cytotoxic cell lysis and elimination of target cell^{187,189}.

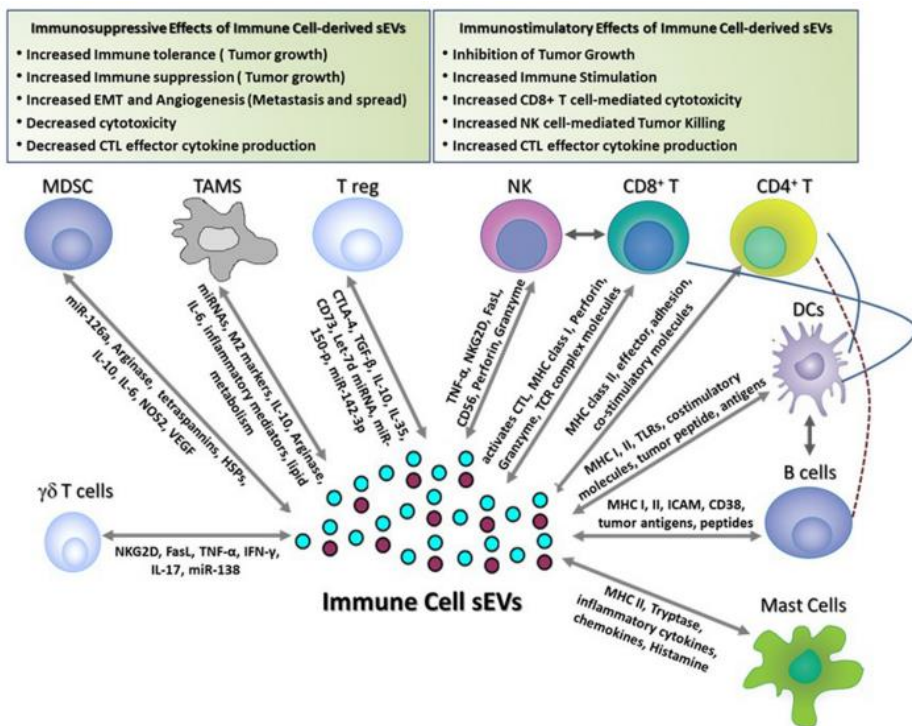


Figure 9. Functional properties of immune cell-derived EVs in cancer ¹⁸⁹

1.3.9.1 Exosomes as antigen-presenting platforms

An effective immune response is possible due to a specific communication network between different cell types and exosomes, distantly or through cell synapses.

Exosomes derived from immune cells present MHC and T cell costimulatory molecules on their surface as a mechanism of antigen presentation. The mechanism by which exosomes mediate antigen delivery to T cells is still unclear.

One mechanism is based on the presentation of antigenic peptide–MHC complex to T cells by DCs after capturing exosomes¹⁹⁰. Moreover, DC can activate T cells by capturing exosomes and presenting exosome's antigenic molecules to their endogenous MHC complex¹⁹¹. In addition, immunological synapse (IS) formation has been described to promote exosomal transfer between T cells and APCs. Transferred exosomes containing miRNAs, regulate gene expression on the APCs, driven by the presence of antigens. So, this antigen-specific T cell cross-priming with unidirectional miRNA transfer also contribute to regulate the final outcome of T cell activation¹⁹². Finally, exosomes by their own have the potential to directly activate T cells¹⁹³.

1.3.9.2 Exosomes and T cell exhaustion

T cell exhaustion is one of the major mechanisms of chronic infections and cancer immune evasion.

It has been found that exosomes from activated DCs presented more antigenic molecules than exosomes from immature DCs, suggesting that the state of the cell of origin may influence the ability to stimulate T cells. Accordingly, it has been observed that exosomes-derived from immature DCs promote T-cell

energy and the activation of Treg cells¹⁹⁴. In addition, HCC-derived exosomes have shown the ability to remodel macrophages, inhibit the expression of inflammatory cytokines, induce pro-inflammatory factors, upregulate the expression of inhibitory receptors in T cells and promote T cell exhaustion, accelerating HCC progression¹⁹⁵. Moreover, it has been described that HCC-derived exosomes contain proteins such as 14-3-3 ζ that when transferred to T cells affects its activity. Overexpression of that protein decrease the activation and proliferation of naive T cells correlating with an exhausted phenotype, decrease the excretion of cytotoxic cytokines and potentiate the differentiation of effector T cells to Treg¹⁹⁶.

Likewise, other mechanisms that enhance T cell exhaustion have been found. Exosomes derived from cancer cells contain circRNAs, like circRNA-002178, that modulate PD-1 and PD-L1 expression in tumor and T cells and induce CD8+ T cell exhaustion¹⁹⁷. Furthermore, exosomes secreted by exhausted CD8+ T cells could be uptaken by non-exhausted CD8+ T cells, and consequently impaired their functions. It has been observed that proliferation, cell activity and cytokines production of non-exhausted CD8+ T cells are decreased in contact with exosomes derived from exhausted CD8+ T cells, while the number of exhausted CD8+ T cells is increased, indicating that exosomes can promote the exhaustion of non-exhausted CD8+ T cells¹⁹⁸.

1.3.10 EVs and HCV infection

In a hepatitis C context, an active infection and/or liver damage induce a dysregulation of the endogenous EV-miRNAs that can be used as biomarkers for diagnosis. Besides, EVs composition may reflects different liver damage stages, the outcome of antiviral treatment or liver transplantation as well as monitoring of minimal residual disease or relapse after HCC resection, being a good tool for prognosis and surveillance studies in HCV positive patients.

During HCV infection, EVs content promote an efficient viral replication and liver damage progression. As briefly explained in the sections above, miRNAs are key regulators of gene expression and function of target cells. Likewise, those are some examples of EV-miRNAs impact on HCV infection.

Exosomes derived from infected hepatocytes contain miRNA-192 that enhance the production of transforming growth factor β (TGF- β), which results in the activation and transdifferentiation of hepatic stellate cells (HSCs) into myofibroblasts and upregulation of fibrogenic markers that lead to the development of liver tissue fibrogenesis¹⁹⁹. In the same line, exosomes derived from HCV-infected hepatocytes carry miR-19a that activate HSCs and triggers fibrogenic pathways in the cells, increasing the expression of pro-fibrogenic markers and pro-fibrogenic cytokines that participate in liver fibrosis progression²⁰⁰. Moreover, exosomes of HCV infected patients containing the complex Argonaute-2 (Ago2)-miR122-HSP90 potentially increase HCV replication²⁰¹.

In addition to the EV's role as mediators of immune responses, they can act as vehicles that promote viral transmission, replication and progression of the pathogenesis.

In the context of HCV infection, EVs derived from HCV-infected cells might be a vehicle to transfer miRNAs, viral genomes, entire viral particles, defective particles or vesicles containing proteins like envelope proteins, Ago2 etc, from infected to naïve cells, leading and establishing a productive infection similar to that produced by the HCV itself. In this way, EVs might help HCV components to do not be recognized by the immune system and entry target cells. Accordingly, EVs packaging might hide and protect viral particles from immune system, suggesting that they may also represent an advantage for the evolution of HCV quasispecies²⁰². Moreover, it is possible that EVs derived from HCV infected hepatocytes play a role in stabilizing and maintaining persistence of viral

infection by inducing peripheral immune tolerance, highlighting the need to develop highly accurate methodologies to isolate and characterize EVs from HCV chronically infected patients and from the same patient after eradicating HCV infection.

Summary 1.3

EVs miRNAs have recently gained interest as potential diagnostic and prognostic biomarkers, as they provide relevant information of the current state of the patient by using non-invasive methods. Nevertheless, discrepancies on miRNA patterns and their validation are still frequent between research groups. Hence, methods that result in minimal contamination are necessary to enable the precise characterization of miRNA content within EVs. Selecting appropriate isolation methods is therefore a critical step for miRNA-based biomarker discovery.

2. HYPOTHESIS

Identification of viral and host biomarkers as indicators of liver fibrosis progression or other related-comorbidities would help in patient management. It may anticipate disease progression, and assist in improving the quality of life of HCV-positive patients irrespectively of their having resolved the infection.

Characterizing the immunological status of patients after resolving HCV infection by DAAs would help to understand whether patients will evolve to a reversion of impaired liver functions and an improvement of health's status or towards a worsening of related or derived liver diseases.

Improving the isolation and characterization of EVs using a suitable method of purification together with accurate miRNA sequencing methodology, would facilitate the discovery of miRNA as biomarkers of disease progression.

3. OBJECTIVES

3.1 Primary objectives

1. To seek a parameter that would be predictive of fibrosis progression at 1 year after LT, which could be useful to decide the time to start a DAA therapy.
2. To investigate whether HCV cure by DAAs could reverse the impaired immune response due to HCV infection.
3. To establish the most suitable EVs isolation method to assess circulating miRNAs profiles for clinical applications.

3.2 Secondary objectives

1. To analyse HCV quasispecies composition before and after LT, and possible changes occurring in the quasispecies complexity soon after LT.
2. To evaluate diversity indices as predictors of fast liver fibrosis progression.
3. To study viral factors like viral load as predictors of fast liver fibrosis progression.
4. To investigate phenotypical changes in CD4+ T cells towards T cell exhaustion after HCV elimination by DAAs.
5. To evaluate functional changes in HCV-specific T cells by studying cytokines (IFN- γ and IL-2) secretion and proliferation capacity of both CD4+ and CD8+ T cells after HCV elimination by DAAs.
6. To determine if liver inflammation and fibrosis stage regression occurred after HCV elimination.
7. To compare EVs isolated by different methods
8. To analyse the yield, abundance and diversity of miRNAs obtained from different library preparation protocols.
9. To analyse the yield, abundance and diversity of miRNAs obtained using different EV isolation methods

4. COMPENDIUM OF ARTICLES

4.1 Study 1

Study of quasispecies complexity and liver damage progression after liver transplantation in hepatitis C infected patients

4.1.1 Article 1 summary

4.1.1.1 Introduction

Cirrhosis derived from chronic HCV infection is still a common indication for liver transplantation. Reinfection of the engrafted liver is universal in untreated patients at the time of transplant, and causes fast progression of cirrhosis in around one-third of these patients. The factors that accelerate the post-LT progression of liver damage in HCV patients are uncertain and seem to depend on the characteristics of the virus and the patient. To prevent damage to the liver graft after LT, effective DAAs-therapy is required as soon as possible. However, because of post-LT clinical instability, it is difficult to determine the optimal time to start DAAs with a low risk of complications.

4.1.1.2 Hypothesis

Identification of a viral indices or biomarkers as indicators of liver fibrosis progression or other related-comorbidities would help to anticipate fatal outcomes and improve the quality of life of HCV positive patients, whether or not they resolved the infection.

4.1.1.3 Objectives

1. To analyze HCV quasispecies composition before and after LT, and changes occurring in the quasispecies complexity soon after LT.
2. To evaluate diversity indices as predictors of fast liver fibrosis progression.
3. To study viral factors like viral load as predictors of fast liver fibrosis progression.

4.1.1.4 Study design

- Ten chronic HCV-infected patients who underwent orthotopic LT were included in the study.
- The histological grade of liver fibrosis was evaluated according to the ISHAK fibrosis score in liver biopsy specimens 1 year after transplantation.
- RNA was extracted from serum samples collected 6 weeks before LT (pre-LT) and 15 days after LT (post-LT). Amplification products were quantified and analysed for quality prior to sequencing. Purified DNA from each sample was mixed forming equimolar pools, and HCV genomes isolated from pre-LT and post-LT samples were sequenced using a next-generation sequencing platform. Then, sequences obtained were pairwise-aligned with respect to the dominant haplotype and filtered.
- HCV quasispecies composition were studied by phylogenetic analysis. Haplotypes from the pre- and post-LT quasispecies were clustered by UPGMA on the matrix of Kimura-80 genetic distances.

Diversity analyses were carried out to define the viral quasispecies complexity at the molecular level. Mutation frequency (Mfmax), Hill numbers (qD of order 0, 1, 2, infinity), and nucleotide diversity (π), were the diversity indices used. Quasispecies complexity changes before and after LT were studied using the Mann-Whitney U test on each diversity index. Moreover, whether the diversity changes showed a general trend from pre-LT to post-LT, considering all indices, was examined by a multivariate analysis. Associations between the liver damage level (high vs. low) at 1-year post-LT and each diversity index in both the pre- and post-LT samples were studied by fitting a linear model of a single factor with two levels, high and low fibrosis. The adjusted R^2 was assessed as a measure of prediction accuracy.

- Viral loads (VL) were measured using the Cobas 6800 system. Associations between the differences in VLs (log VL post-LT minus log VL pre-LT) and liver damage level (high vs. low) at 1-year post-LT was carried out using a single fixed factor analysis of variance (ANOVA).

4.1.1.5 Results according to objectives

4.1.1.5.1 Objective 1: To analyze HCV quasispecies kinetics before and after LT, and changes occurring in the quasispecies complexity soon after LT

Three different patterns of reinfection were observed in the comparison of the phylogenetic analyses of pre- and post-LT samples.

The first pattern represented in the majority of patients showed mixed populations where the master sequence remained invariant before and after LT, and most of the individual haplotypes were not common among populations; instead, some specifically shared haplotypes had successfully developed new subpopulations after LT.

The second pattern showed a viral bottlenecking effect. The pre-LT master sequence is different after LT, and two clearly separate quasispecies with no or only one shared haplotype can be differentiated between pre and post-LT populations.

In the third pattern, the master sequence was highly conserved in both the pre- and post-LT quasispecies and the vast majority of haplotypes were also conserved in the two populations.

Moreover, the study of changes occurring in the quasispecies complexity comparing the sample from pre-LT and the one 15 days after LT using unidimensional and principal components analysis, point that no changes were observed towards an increase or decrease in viral complexity after LT. Hence, on Figure 10, patients represented near 0 would be explained by random changes of the quasispecies diversity after LT, while patients represented above

0 would explain a diversity reduction due to homogenization of the quasispecies.

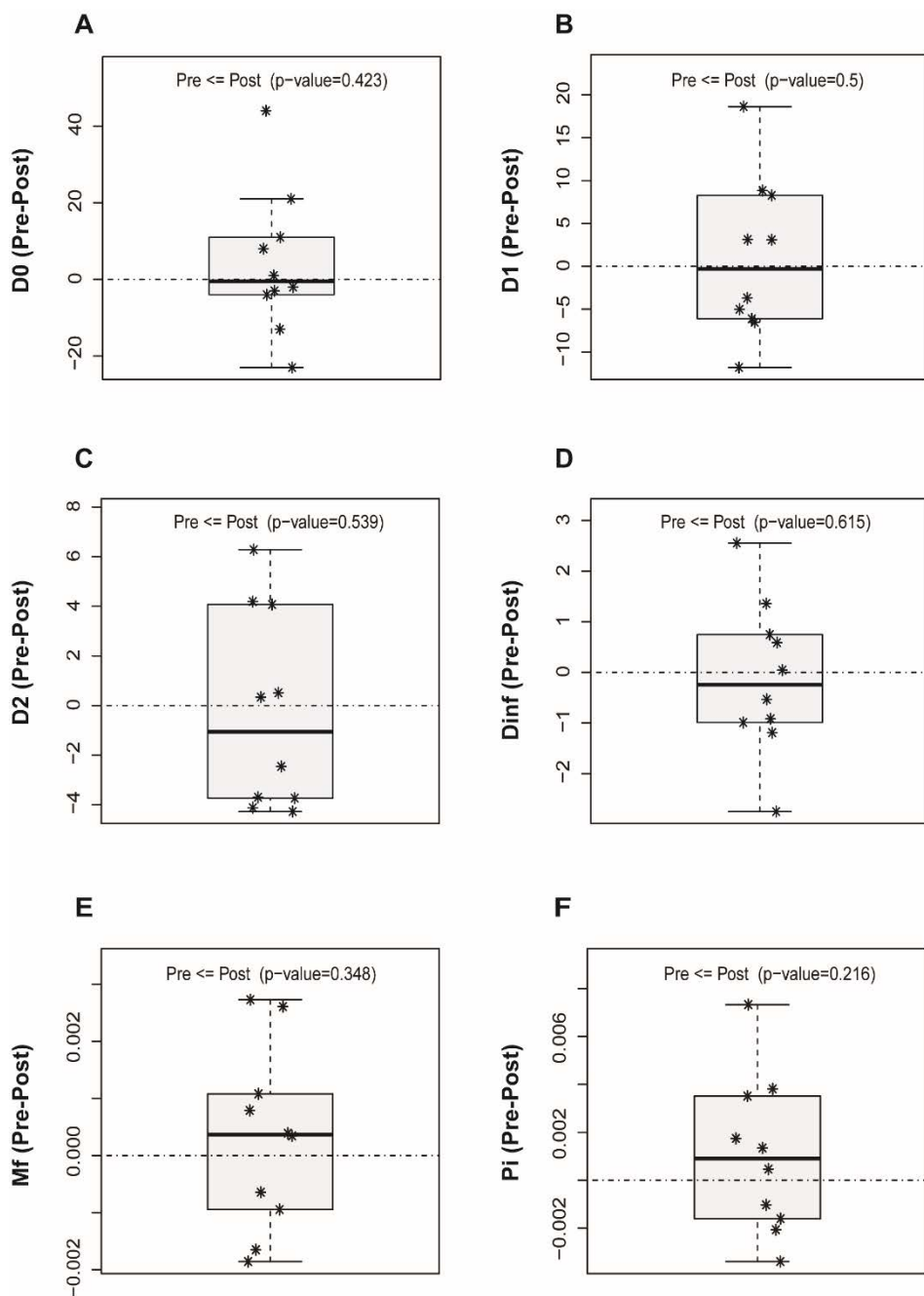


Figure 10. Boxplots with diversity indices showing differences between the pre-LT and post-LT quasispecies. (A) D0: hill number of order 0, (B) D1: hill number of order 1, (C)

D2: hill number of order 2, (D) Dinf: Hill number of order infinity, (E) Mfmax: mutation frequency, (F) π : nucleotide diversity. Each patient is represented as *. The p-value resulting from the Mann-Whitney U-test is included.

4.1.1.5.2 Objective 2: To evaluate diversity indices as predictors of fast liver fibrosis progression.

The adjusted R^2 was very low for all of the diversity indices, indicating that they lacked predictive capability in both samples as shown in Table 1. Therefore, complexity indexes cannot be used as predictors of future liver damage degree evolution.

	Diversity Measures					
	Adjusted R^2 (D0)	Adjusted R^2 (D1)	Adjusted R^2 (D2)	Adjusted R^2 (Dinf)	Adjusted R^2 (Mf)	Adjusted R^2 (π)
Pre-LT	0.086	0.064	0.118	0.111	0.021	0.027
Post-LT	0.060	0.026	0.019	0.025	0.063	0.051

Table 1. Ability of diversity measurements (qD of order 0, 1, 2, infinity, Mfmax, and π) to predict high or low fibrosis degree at 1 year post-LT using both pre-LT and 15 day post-LT samples. Prediction accuracy of each diversity measure is represented as adjusted R^2 .

4.1.1.5.3 Objective 3: To study viral factors like viral load as predictors of fast liver fibrosis progression.

A significant association between viral load (VL) and progression of liver damage was found. Patients showing a VL increase at 15 days post-LT (relative to pre-LT VL), developed advanced fibrosis at 1-year post-LT, whereas the decrease in VL was associated with minimal liver fibrosis changes (Figure 11). It suggests that an increase in VL after LT compared with the pre-LT sample, can be used as a

prognostic value for decision making on prescribing an HCV DAA-based treatment to minimize disease progression.

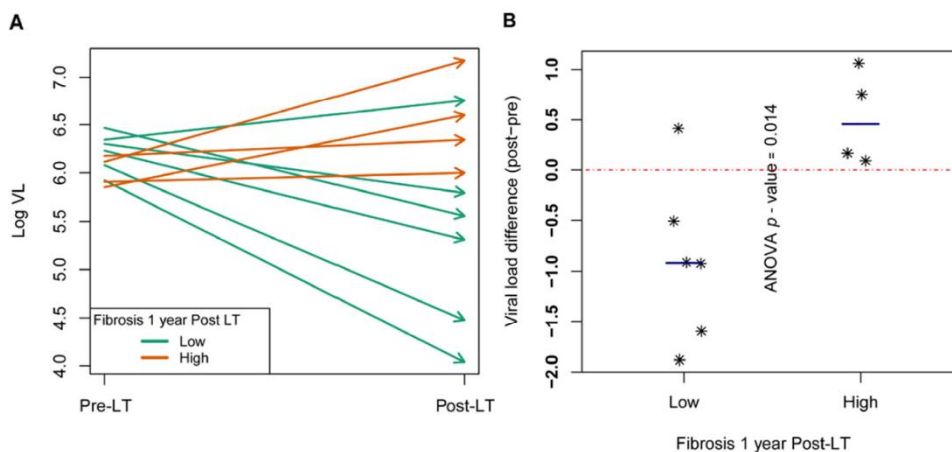


Figure 11. Viral load differences between pre and post-LT samples. (A) Arrows showing the evolution of log VL from pre-LT (arrow tails on the left) to 15-day post-LT (arrow heads on the right side of the box). At one year post-LT, patients with high fibrosis (F3–F4) in orange, patients with low fibrosis (F0–F2) in green. (B) Scatterplot with differences in log VL at 15 days post-LT minus pre-LT. The ANOVA p-value in the comparison of the two levels of liver damage is included. Each patient is represented as *.

4.1.1.6 Conclusions

1. HCV quasispecies composition pre- and post-LT differ between patients, suggesting that homogenization of the composition of the viral population after liver graft reinfection is not a general effect..
2. HCV quasispecies complexity measured by several diversity indices does not correlate with the fibrosis progression at 1-year post-LT.
3. Higher VL at day 15 post-LT as compared to the pre-LT VL values, may predict fast liver fibrosis progression.

4.1.2 Article 1

Study of quasispecies complexity and liver damage progression after liver transplantation in hepatitis C infected patients

Meritxell Llorens-Revull, Josep Gregori, Cristina Dopazo, Francisco Rodriguez-Frías, Damir Garcia-Cehic, Maria Eugenia Soria, Qian Chen, Ariadna Rando, Celia Perales, Juan Ignacio Esteban, Josep Quer* and Itxarone Bilbao

Genes 2021, 12, 1731. <https://doi.org/10.3390/genes12111731>

Article

Study of Quasispecies Complexity and Liver Damage Progression after Liver Transplantation in Hepatitis C Virus Infected Patients

Meritxell Llorens-Revull ^{1,2,3} , Josep Gregori ^{1,2,4} , Cristina Dopazo ^{2,5}, Francisco Rodriguez-Frías ^{2,3,6} , Damir Garcia-Cehic ^{1,2}, Maria Eugenia Soria ¹, Qian Chen ¹, Ariadna Rando ⁶, Celia Perales ^{1,2} , Juan Ignacio Esteban ^{1,2,7}, Josep Quer ^{1,2,3,*}  and Itxarone Bilbao ^{2,5,8} 

- ¹ Liver Diseases-Viral Hepatitis, Liver Unit, Vall d'Hebron Institut de Recerca (VHIR), Vall d'Hebron Hospital Universitari, Vall d'Hebron Barcelona Hospital Campus, Passeig Vall d'Hebron 119-129, 08035 Barcelona, Spain; meritxell.llorens@vhir.org (M.L.-R.); josep.gregori@gmail.com (J.G.); damir.garcia@vhir.org (D.G.-C.); maria.soria@vhir.org (M.E.S.); qian.chen@vhir.org (Q.C.); cperales@cbm.csic.es (C.P.); jiesteban@vhebron.net (J.I.E.)
- ² Centro de Investigación Biomédica en Red de Enfermedades Hepáticas y Digestivas (CIBERehd), Instituto de Salud Carlos III, Av. Monforte de Lemos, 3-5, 28029 Madrid, Spain; cdopazo@vhebron.net (C.D.); frarodri@gmail.com (F.R.-F.); ibilbao@vhebron.net (I.B.)
- ³ Biochemistry, Molecular Biology, Universitat Autònoma de Barcelona (UAB), Campus de la UAB, Plaça Cívica, 08193 Bellaterra, Spain
- ⁴ Roche Diagnostics SL, Avinguda de la Generalitat, 171-173, 08174 Sant Cugat del Vallès, Spain
- ⁵ Hepatobiliopancreatic Surgery and Transplant Unit, Vall d'Hebron Institut de Recerca (VHIR), Vall d'Hebron Hospital Universitari, Vall d'Hebron Barcelona Hospital Campus, Passeig Vall d'Hebron 119-129, 08035 Barcelona, Spain
- ⁶ Biochemistry and Microbiology Departments, Vall d'Hebron Institut de Recerca (VHIR), Vall d'Hebron Hospital Universitari, Vall d'Hebron Barcelona Hospital Campus, Passeig Vall d'Hebron 119-129, 08035 Barcelona, Spain; ariadna.rando@vhir.org
- ⁷ Medicine, Universitat Autònoma de Barcelona (UAB), Campus de la UAB, Plaça Cívica, 08193 Bellaterra, Spain
- ⁸ Surgery, Universitat Autònoma de Barcelona (UAB), Campus de la UAB, Plaça Cívica, 08193 Bellaterra, Spain
- * Correspondence: josep.quer@vhir.org or josep.quer@ciberehd.org



Citation: Llorens-Revull, M.; Gregori, J.; Dopazo, C.; Rodriguez-Frías, F.; Garcia-Cehic, D.; Soria, M.E.; Chen, Q.; Rando, A.; Perales, C.; Esteban, J.I.; et al. Study of Quasispecies Complexity and Liver Damage Progression after Liver Transplantation in Hepatitis C Virus Infected Patients. *Genes* **2021**, *12*, 1731. <https://doi.org/10.3390/genes12111731>

Academic Editor: Salvador F. Aliño

Received: 29 September 2021

Accepted: 26 October 2021

Published: 28 October 2021

Publisher's Note: MDPI stays neutral with regard to jurisdictional claims in published maps and institutional affiliations.



Copyright: © 2021 by the authors. Licensee MDPI, Basel, Switzerland. This article is an open access article distributed under the terms and conditions of the Creative Commons Attribution (CC BY) license (<https://creativecommons.org/licenses/by/4.0/>).

Abstract: Cirrhosis derived from chronic hepatitis C virus (HCV) infection is still a common indication for liver transplantation (LT). Reinfection of the engrafted liver is universal in patients with detectable viral RNA at the time of transplant and causes fast progression of cirrhosis (within 5 years) in around one-third of these patients. To prevent damage to the liver graft, effective direct-acting antiviral (DAA) therapy is required as soon as possible. However, because of post-LT clinical instability, it is difficult to determine the optimal time to start DAAs with a low risk of complications. Evaluate changes in quasispecies complexity following LT and seek a predictive index of fast liver damage progression to determine the timing of DAA initiation. HCV genomes isolated from pre-LT and 15-day post-LT serum samples of ten patients, who underwent orthotopic LT, were quantified and sequenced using a next-generation sequencing platform. Sequence alignments, phylogenetic trees, quasispecies complexity measures, biostatistics analyses, adjusted R2 values, and analysis of variance (ANOVA) were carried out. Three different patterns of reinfection were observed (viral bottlenecks, conserved pre-LT population, and mixed populations), suggesting that bottlenecks or homogenization of the viral population is not a generalized effect after liver graft reinfection. None of the quasispecies complexity measures predicted the future degree of liver damage. Higher and more uniform viral load (VL) values were observed in all pre-LT samples, but values were more dispersed in post-LT samples. However, VL increased significantly from the pre-LT to 15-day post-LT samples in patients with advanced fibrosis at 1-year post-LT, suggesting that a VL increase on day 15 may be a predictor of fast liver fibrosis progression. HCV kinetics after LT differ between patients and are not fibrosis-dependent. Higher VL at day 15 post-LT versus pre-LT samples may predict fast liver fibrosis progression.

Keywords: hepatitis C virus; liver transplantation; fibrosis; variability; complexity measures; viral load

1. Introduction

Hepatitis C virus (HCV) infection is a cause of end-stage liver disease and an indication for liver transplantation (LT). The reinfection of the engrafted liver is universal in patients with detectable viral RNA during the first days, and even the first hours, after transplantation [1,2]. Symptomatic HCV hepatitis then develops in 1 to 4 months, although the clinical pattern varies. Within 5 years after LT occurs, there is a fast progression to cirrhosis in 10% to 30% of patients [3–6]. Before the introduction of interferon-free regimens, only 30% of non-transplant patients with HCV-related cirrhosis had liver decompensation at 10 years, whereas more than 40% of graft recipients showed decompensation within 12 months after the diagnosis of recurrent cirrhosis, and up to 60% experienced a decompensation episode 3 years later [4,7–10].

The factors that accelerate the post-LT progression of liver damage in HCV patients are uncertain and seem to depend on the characteristics of the virus and the patient [11,12]. Reports have shown that some amino acid signatures in the NS5B region of HCV are specific to patients developing cholestatic fibrosis hepatitis, which is a severe variant of HCV infection recurrence after liver transplantation [13]. However, there is little information on the diversity index and other viral factors that could help predict the accelerated progression of liver damage.

The advent of safe and highly effective direct-acting antiviral agents (DAAs) has profoundly changed the management of patients with advanced liver damage and those undergoing LT. Although DAA treatment before LT would be the best option, drug-to-drug interactions between some DAAs and various immunosuppressive agents may jeopardize this approach. Furthermore, some DAAs should be avoided in patients with severely impaired liver function and renal dysfunction because of complications, the most common being renal failure, which is not unusual after LT. An alternative is treatment soon after the procedure or when the risk of chronic rejection has decreased and immunosuppressive rejection medication is stable [14]. Hence, the question arises as to when would be the best time to start DAA treatment. The ELITA consensus statements [9] summarize the factors that should be considered to determine whether pre- and post-LT DAA therapy is justified in patients listed for decompensated cirrhosis without hepatocellular carcinoma (HCC). In general, patients who will progress faster to cirrhosis (fast progressors) should be treated earlier after LT than those with slower progression (slow progressors), who can be treated later, after the patient's health status has improved. Therefore, finding a predictive index of fast liver damage progression to determine the timing of DAA initiation is of great interest, and quasispecies composition has been related to viral persistence, disease progression, and response to antiviral agents [15–17].

HCV is an enveloped, positive-sense, single-stranded RNA virus of the genus Hepacivirus in the Flaviviridae family [18]. The lack of proofreading activity of the nonstructural protein 5B (NS5B) RNA-dependent RNA polymerase leads to substantial sequence variation in the HCV genome, which displays mutation rates in the range of 10⁻³–10⁻⁵ mutations per nucleotide copied [19]. Hence, HCV does not exist as a single genome, even in a single infected individual; instead, it is a complex and dynamic distribution of non-identical but related genomes known as a viral quasispecies that undergoes a continuous process of genetic variation, competition, and selection [20–25]. The viral quasispecies complexity has been defined as the “intrinsic property that quantifies the diversity and frequency of haplotypes, independently of the population size that contains them” [26]. The relevance of the viral complexity level has been evidenced by the lower adaptability of viruses whose polymerase shows a higher or lower copying fidelity than the wild type with a comparable population size in the same biological context [27–30]. Therefore, when studying an infection, it is important to be aware that all members of the quasispecies

may be relevant for establishing chronic infection, and an approach based on studying the diversity and complexity of the entire viral population should be considered.

The aim of this study was to evaluate changes occurring in the complexity of the HCV quasispecies soon after LT, seeking a parameter that would be predictive of fibrosis progression at 1 year following the procedure, which could be useful for guiding the timing of the start of DAA therapy.

2. Materials and Methods

This study consisted of ten HCV patients who underwent orthotopic LT, fulfilled the inclusion criteria, and had none of the exclusion criteria, as shown in the Supplementary Material.

This study was approved by the local institutional review board for clinical research, and all patients gave written informed consent in accordance with the 1975 Declaration of Helsinki.

Ten patients were included in the study, five being infected with HCV genotype 1 subtype a (G1a), four with G1b, and one with G3a [31]. Serum samples were collected 6 weeks before LT at the time they were included in the waiting list and 15 days after LT at the moment of hospital discharge.

The histological grade of liver fibrosis was evaluated according to the ISHAK fibrosis score [32] in liver biopsy specimens 1 year after transplantation. Viral load (VL) before LT (6 weeks) and 15 days after LT were measured using the Cobas 6800 system (Roche Applied Science, Basel, Switzerland; lower limit of detection, 10 IU/mL).

2.1. RNA Extraction, RT-PCR, Heminested-PCR Amplification and Quantification

A 30 µL amount of total RNA was obtained by extracting between 140 and 280 µL of the 6 weeks pre-LT and 15 days post-LT serum sample (depending on the VL of each) using the QIAamp Viral RNA Mini Kit 250 (Qiagen, Hilden, Germany) and following the manufacturer's instructions. Samples P03 and P05 with the lowest VL required a double serum volume for RNA extraction to avoid bias occurring in the sequencing studies.

Reverse transcription polymerase chain reaction (RT-PCR) was performed as previously described [31]. Briefly, the reverse transcription of the NS5B region (nucleotides (nt) 8254–8707) was carried out using the Transcriptor One-Step reverse RT-PCR kit (Roche Applied Science, Basel, Switzerland). HCV RNA was reverse-transcribed into complementary deoxyribonucleic acid (cDNA) (30 min at 50 °C) and PCR-amplified for 35 cycles (10 s at 94 °C, 30 s at 53 °C, and 30 s at 68 °C) with specific oligonucleotides (5Bu8254: CNTAYGAYACCMGNTGYTTTGACTC; 5Bd8707: TTNGADGAGCADGATGTWATBAGCTC). A final product of 454 nt was obtained. Nucleotide positions were marked according to isolate H77 accession number AF009606 [33]. The reaction mixture for RT-PCR was prepared as follows: 28.5 µL H₂O-PCR 1×, 10 µL buffer 5×, 2.5 µL DMSO, 1.5 µL upstream primer (20 pmol), 1.5 µL downstream primer (20 pmol), 1 µL polymerase, and 5 µL RNA.

Heminested PCR was then performed with 5 µL of DNA from the above PCR using the FastStart High Fidelity PCR System dNTPack kit (Roche Applied Science Basel, Switzerland) with 20 pmol of the labeled upstream primer (13N5Bo8254: GTTGTAACGACGCCAGTCNTAYGAYACCMGNTGYTTTGACTC) and 20 pmol of the labeled downstream primer (13N5Bo8641: CACAGGAAACAGCTATGACCGARTAYCTGGTCATAGCNTCCGTGAA), both of which included a complementary universal M13 primer at the 5' end. HCV DNA was amplified in a 35-cycle PCR (30 s at 94 °C, 30 s at 56 °C, and 30 s at 72 °C) with a reaction mixture comprised of 33 µL H₂O-PCR 1×, 5 µL buffer 10×, 1 µL dNTP, 2.5 µL DMSO, 1.5 µL of 20 pmol upstream primer, 1.5 µL of 20 pmol downstream primer, 0.5 µL polymerase, and 5 µL DNA. A final product of 428 nt (including primers) was obtained.

PCR products from different isolates were pooled together before deep sequencing. Each isolate was tagged with a different multiplex identifier (MID) by performing a short (15 cycles) PCR. The final product was 498 nt in length (including primers, MID, and adaptors for GS-Junior sequencing), spanning nucleotides 8254–8641.

Amplification products were analyzed using 2% agarose gel electrophoresis with the QIAquick gel extraction kit (Qiagen, Valencia, CA, USA), quantified using the PicoGreen assay (Invitrogen, Carlsbad, CA, USA), and quality-analyzed using a BioAnalyzer DNA 1000 LabChip (Agilent, Santa Clara, CA, USA) prior to sequencing.

2.2. Ultradeep Pyrosequencing (UDPS)

Purified DNA from each sample was mixed, forming equimolar pools. Each pool was sequenced by UDPS-based next-generation sequencing (NGS) on the GS-Junior platform (454 Life Sciences, Roche, Branford, CT, USA), following the manufacturers' protocol.

2.3. Nucleotide Haplotypes and Diversity Analyses

Sequencing data analysis was performed as previously reported [34,35]. Briefly, sequences were demultiplexed by the MID and specific primer and pairwise-aligned with respect to the dominant haplotype, excluding reads that did not cover the full amplicon or harbored more than 2 indeterminations or 3 gaps. Accepted indeterminations and gaps were repaired as per the dominant haplotype. Reads were collapsed to haplotypes and their corresponding frequencies. Only those with abundances above 0.1% and common to the forward and reverse strands were kept. All computations were made in the R language and platform [36] with in-house-developed scripts and with the help of the Biostrings [37], ape [38], seqinr [39], and ade4 [40] packages.

Diversity analyses were carried out on sequences that passed the filters, standardizing to the lowest coverage with a down-sampling and fringe-trimming approach [35]. The following diversity indices were used to define the viral quasispecies complexity at the molecular level [26]: mutation frequency (Mfmax), Hill numbers (qD) [41,42], and nucleotide diversity (π) [43,44].

2.4. Phylogenetic Analysis

For the phylogenetic analysis, read alignments were further filtered, discarding all haplotypes below 0.5% [35]. Haplotypes from the pre- and post-LT quasispecies were clustered by UPGMA (Unweighted Pair Group Method with Arithmetic mean) on the matrix of Kimura-80 genetic distances [45].

2.5. Biostatistic Analyses

Quasispecies complexity changes before and after LT were studied using the Mann-Whitney U test on each diversity index, with the null hypothesis of equal population means and the alternate hypothesis of greater diversity in pre-LT samples. Diversity indices were computed in the pre-LT and 15 day post-LT sample.

A principal component analysis was performed on the matrix of diversity measures, allowing the representation of samples characterized by variables that could be strongly correlated on orthogonal axes. The aim of this multidimensional exploratory analysis was to determine whether the diversity changes showed a general trend from pre-LT to post-LT when all indices were included in a multivariate analysis.

Associations between the liver damage level at 1 year post-LT and each diversity index in both the pre-LT and 15-day post-LT samples were studied by fitting a linear model of a single factor with two levels, high fibrosis (F3–F4) and low fibrosis (F0, F1, F2). The adjusted R² was assessed as a measure of prediction accuracy.

Associations between the differences in VLs (log VL at 15 days post-LT minus log VL pre-LT) and liver damage level (high vs. low) at 1 year post-LT was carried out using a single fixed factor analysis of variance (ANOVA) with a significance level of 0.05.

The statistical methods used in this study were reviewed by Josep Gregori from Liver Diseases-Viral Hepatitis, Liver Unit, Vall d'Hebron Institut de Recerca (VHIR), Vall d'Hebron Hospital Universitari, Vall d'Hebron Barcelona Hospital Campus, Universitat Autònoma de Barcelona, Passeig Vall d'Hebron 119-129, Barcelona, Spain; Centro de Investigación Biomédica en Red de Enfermedades Hepáticas y Digestivas (CIBERehd),

Instituto de Salud Carlos III, Madrid, Spain; Roche Diagnostics SL, Sant Cugat del Vallès, Barcelona, Spain.

3. Results

Patient data, viral load, and complexity measures are reported in Supplementary Table S1.

3.1. Viral Kinetics and Histological Grade

HCV RNA was detected in all patient samples: mean and standard deviation (SD) 1.52×10^6 (SD 703492.881) at pre-LT and 2.91×10^6 (SD 4655095.8) at 15 days post-LT. The following histological diagnoses according to the ISHAK classification were established in liver biopsies acquired at 1 year: F0 in 3 patients, F1 in 1, F2 in 2, F3 in 2, and F4 in 2 others. One of the two patients with F4 fibrosis grade (P10) developed cholestatic fibrosis hepatitis 6 months after liver transplantation.

3.2. Phylogenetic Studies

Three different patterns were obtained in the comparison of the phylogenetic analyses of pre- and post-LT samples (Figure 1). In the first pattern, observed in 7 of the 10 patients (70%), the master sequence (sequence with the highest percentage of reads) remained before and after LT. In this group, five of the patients were subtype 1a and two were subtype 1b. Interestingly, the master sequence was present in a higher percentage before than after LT in 4 of the 7 patients, remarking that 3 patients were HCV subtype 1a, while only 1 was 1b. In patient P10 who had a cholestatic event at six months after LT, the master sequence remained dominant after LT. In the analysis of the quasispecies in these patients, we found that most of the individual haplotypes were not common to both (pre- and post-LT) populations; instead, some specifically shared haplotypes had successfully developed new subpopulations (Figure 1A and Supplementary Figures S1–S6).

The second pattern, seen in 2 of the 10 patients, showed a clear viral “bottleneck” effect. The pre-LT master sequence had changed after LT, and two clearly separate quasispecies with no or only one shared haplotype were observed (Figure 1B and Supplementary Figures S1–S7). Both patients were HCV subtype 1b.

Finally, in the third pattern, observed in 1 of the 10 patients, the master sequence was highly conserved in both the pre- and post-LT quasispecies, with greater representation in the pre-LT samples. The vast majority of haplotypes were also conserved in the two populations and present in similar percentages (Figure 1C). The patient showed that the unique pattern corresponded with genotype 3a.

3.3. Unidimensional Analyses

For each diversity measure, a Mann–Whitney *U*-test was carried out, in which the null hypothesis was that diversity changes were random after transplantation, and, therefore, the average difference was 0. The alternative hypothesis was that diversity was reduced after transplantation due to the homogenization of the quasispecies, and the average difference was greater than 0.

The differences (pre/post-LT) for each diversity measure with the resulting *p*-value from the Mann–Whitney *U*-test are shown in Figure 2A–F. In all cases, the 0 was well inside the observed distribution of differences and the *p*-values obtained were well above 0.05.

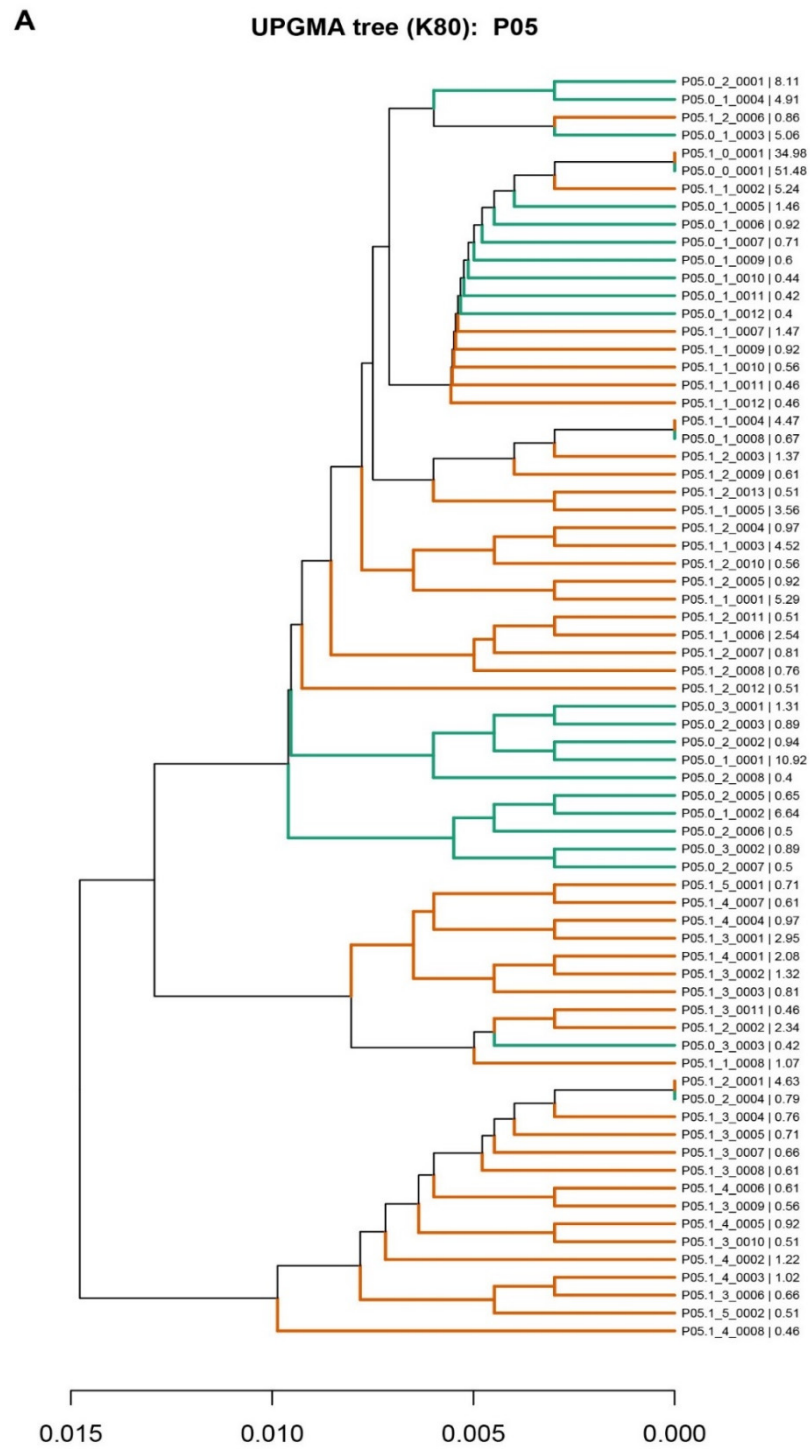


Figure 1. Cont.

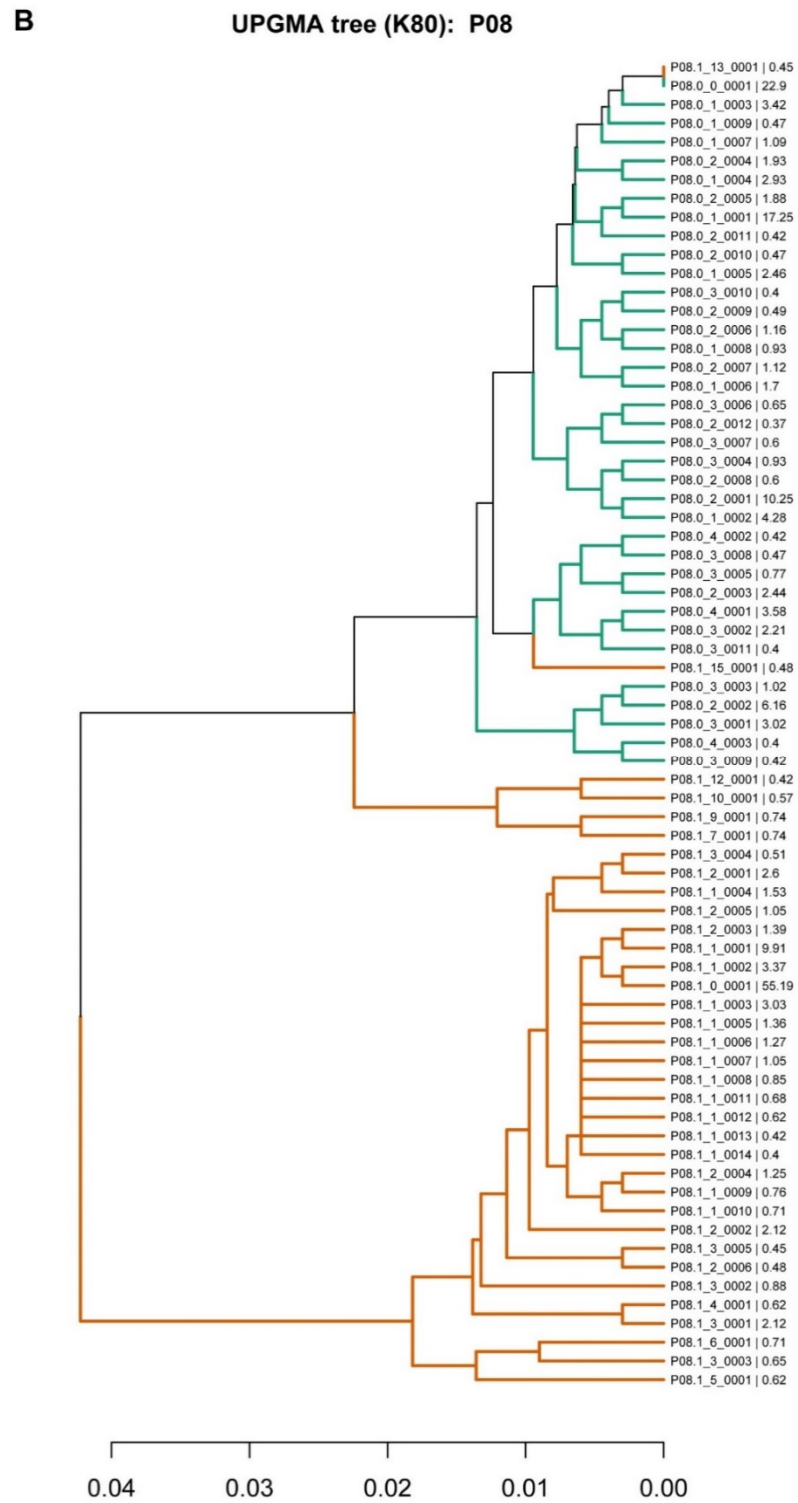


Figure 1. Cont.

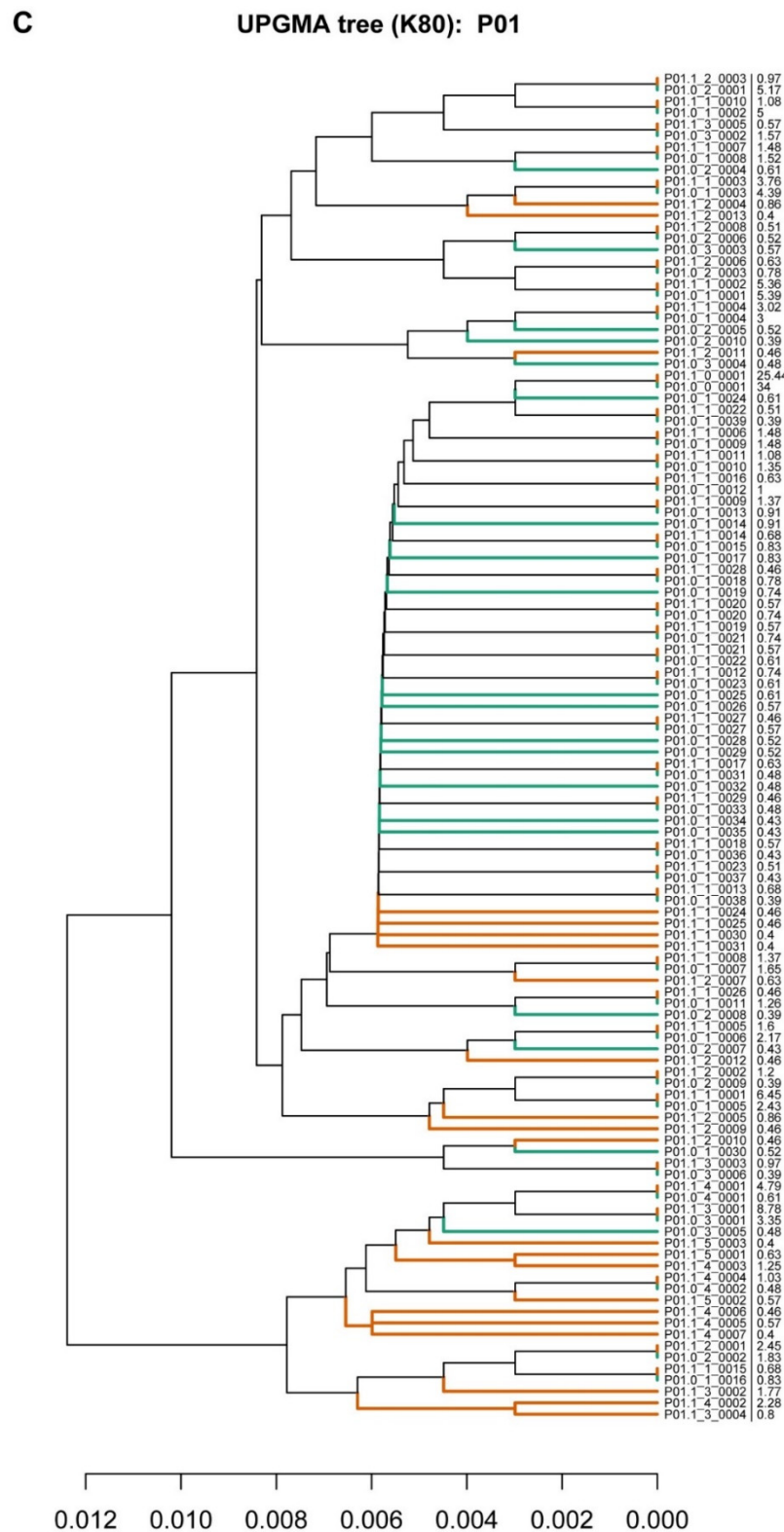


Figure 1. Phylogenetic trees representing the evolution of pre-LT and post-LT quasispecies and their relationship to the pre-LT and post-LT quasispecies. Haplotypes (from the pre-LT and post-LT quasispecies) are represented in orange, and haplotypes from the pre-LT and post-LT quasispecies are in green. The nomenclature used was Pxx.y.z.vvvv, where xx is the patient identifier (P01, P02 etc), y is the sample identifier (0 for pre-LT, 1 for post-LT), z is the number of differences between the haplotype and the master sequence, and vvvv is an identifier for haplotypes with the same number of mutations in the quasispecies. The last percent number represents the frequency at which each haplotype is represented in the quasispecies.

Figure 2. Boxplots with diversity indices showing differences between the pre-LT and post-LT quasispecies. The alternative hypothesis was that diversity was reduced after transplantation due to the homogenization of the quasispecies, and the average difference was greater than 0.

The differences (pre/post-LT) for each diversity measure with the resulting p -value from the Mann–Whitney U -test are shown in Figure 2A–F. In all cases, the 0 was well inside the observed distribution of differences and the p -values obtained were well above 0.05.

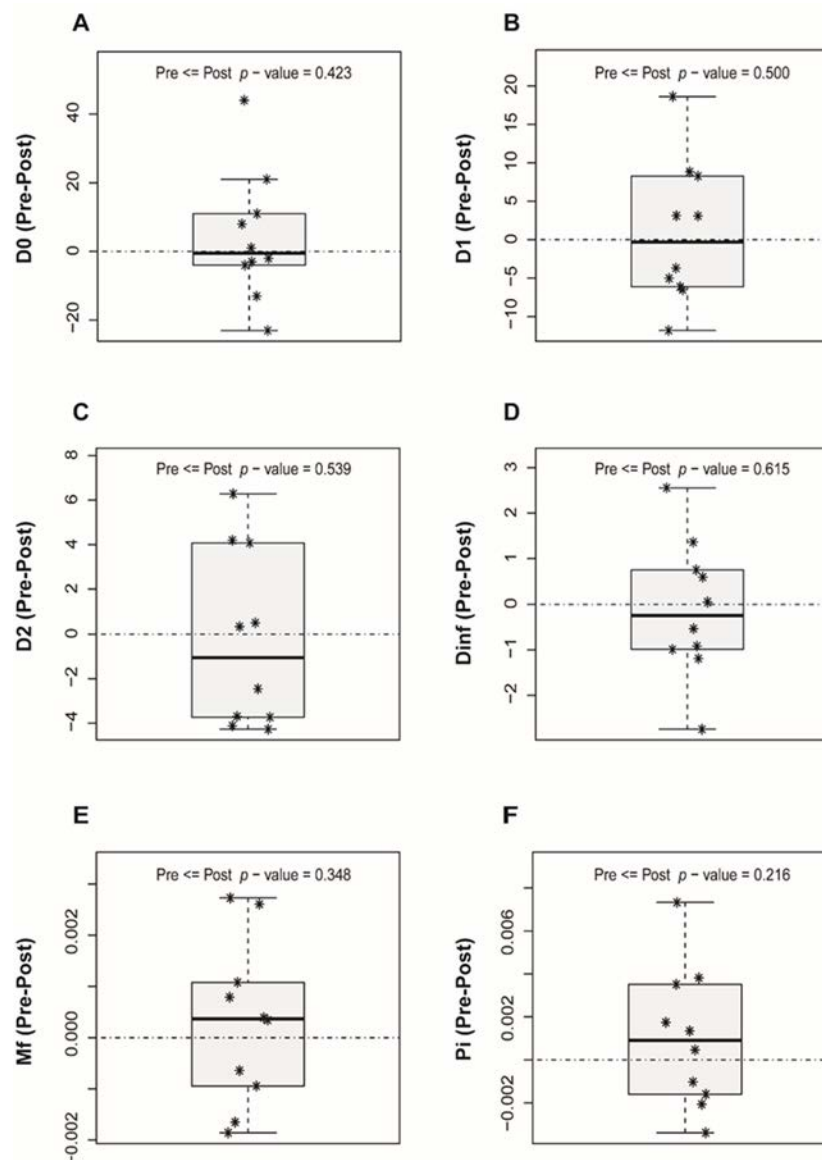


Figure 2. Boxplots with diversity indices showing differences between the pre-LT and post-LT quasispecies. (A) D0: hill number of order 0, (B) D1: hill number of order 1, (C) D2: hill number of order 2, (D) Dinf: hill number of order infinity, (E) Mfmax: mutation frequency, (F) π : nucleotide diversity. Each patient is represented as *. The p -value resulting from the Mann–Whitney U -test is included.

3.4. Principal Components Analysis

Principal Components Analysis analyses, changes towards lower viral complexity after transplantation were not confirmed. In Figure 3A–C, a significant multivariate association between LT and the diversity measures would result in a consistent pattern of arrows pointing in approximately the same direction, which is not the case.

3.5. Associations between Diversity Measures and Fibrosis at 1 Year Post-LT

Liver fibrosis as a measure of liver damage was dichotomized into low (F0, F1) and high (F3, F4) values. The distribution of values for the various diversity indices in each liver damage group and in pre-LT and 15 days post-LT samples is shown in Table 1. Here, the adjusted R2 value acts as an assessment of the prediction accuracy. Of note, the adjusted R2 was very low for all of the diversity measures, indicating that they lacked predictive capability in both samples.

between LT and the diversity measures would result in a consistent pattern of arrows pointing in approximately the same direction, which is not the case.

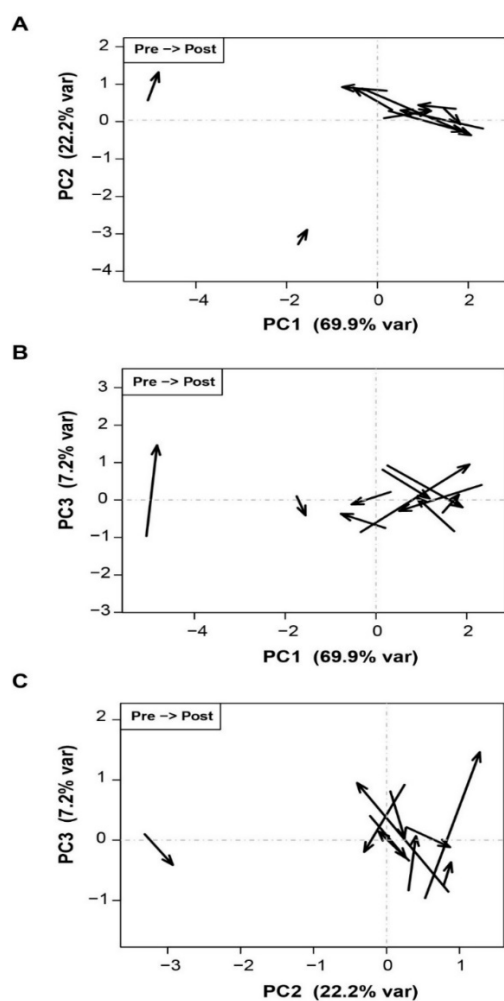


Figure 3. Samples represented on the planes of the first three principal components. Each pair of samples is represented as an arrow, with pre-LT at the tail and post-LT at the head. (A) PC2 vs. PC1; (B) PC3 vs. PC1; (C) PC3 vs. PC2.

3.5. Associations between Diversity Measures and Fibrosis at 1 Year Post-LT

Table 1. Ability of diversity measures (qD of order 0, 1, 2, infinity, Mfmax, and π) to predict high or low fibrosis degree at 1 year post-LT using both pre-LT and 15 day post-LT samples. Prediction accuracy of each diversity measure is represented as adjusted R². The distribution of values for the various diversity indices in each liver damage group and in pre-LT and 15 days post-LT samples is shown in Table 1. Here, the adjusted R² value acts as an assessment of the prediction accuracy. Of note, the adjusted R² was adjusted for the diversity measure used in the prediction. They adjusted predictive capability (R²) of both samples.

	Adjusted R ² (D0)	Adjusted R ² (D1)	Adjusted R ² (D2)	Adjusted R ² (Dinf)	Adjusted R ² (Mf)	Adjusted R ² (π)
Pre-LT	0.086	0.064	0.118	0.111	0.021	0.027
15 day post-LT	0.025	0.025	0.025	0.025	0.025	0.025

Table 1. Ability of diversity measures (qD of order 0, 1, 2, infinity, Mfmax, and π) to predict high or low fibrosis degree at 1 year post-LT using both pre-LT and 15 day post-LT samples. Prediction accuracy of each diversity measure is represented as adjusted R².

3.6. Associations between VL and Fibrosis at 1 Year Post-LT

Patients showing a VL increase at 15 days post-LT relative to the pre-LT value developed a high degree of fibrosis (F3, F4) and were considered fast progressors. In contrast, patients showing a VL decrease after LT could be considered slow progressors, as they showed minimal liver fibrosis changes (F0, F1) at 1 year after transplantation. The VL values were high and uniform in all pre-LT samples but were more dispersed in the post-LT samples (Figure 4A). In the ANOVA, a statistically significant association between VL and the progression of liver damage was found ($p = 0.0144$) (Figure 4B).

oped a higher degree of fibrosis (F3, F4) at 1 year post-LT; therefore, they could be considered fast progressors. In contrast, patients showing a VL decrease after LT could be considered slow progressors, as all showed minimal liver fibrosis changes (F0, F1) at 1 year after transplantation. The VL values were high and uniform in all pre-LT samples but were more dispersed in the post-LT samples (Figure 4A). In the ANOVA, a statistically significant association between VL and the progression of liver damage was found ($p = 0.0144$) (Figure 4B).

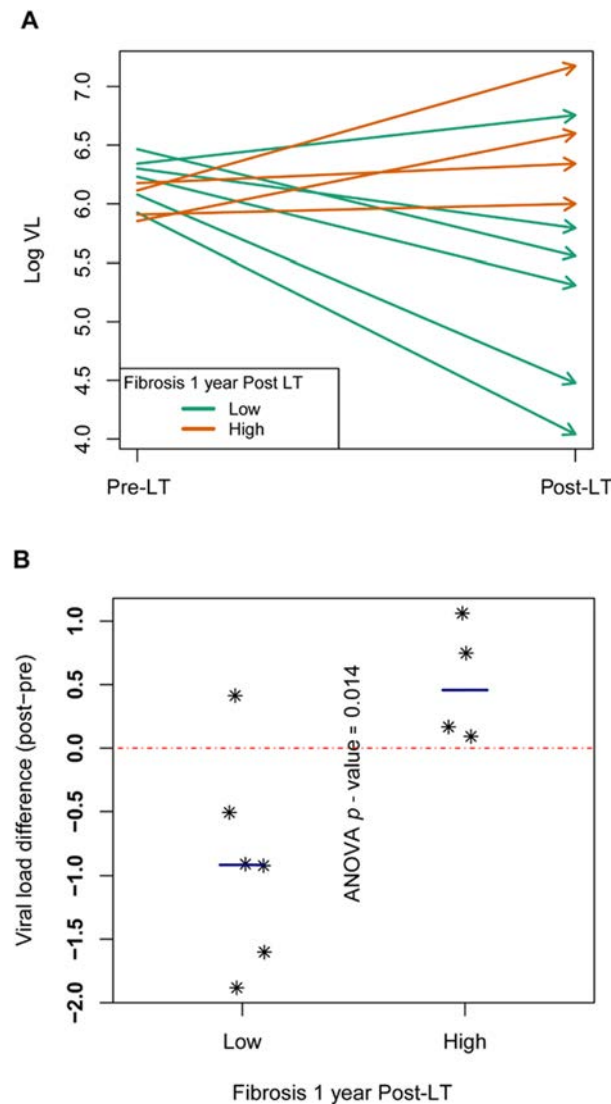


Figure 4. Viral load differences between pre and post-LT samples. (A) Arrows showing the distribution of Log VL from pre-LT (arrows on the left) to 15 days post-LT (arrows on the right side of the box). At one year post-LT, patients with high fibrosis (F3–F4) in orange, patients with low fibrosis (F0–F2) in green. (B) Scatterplot with differences in log VL at 15 days post-LT minus pre-LT. The ANOVA p -value in the comparison of the two levels of liver damage is included. Each patient is represented as *.

4. Discussion

Liver replacement causes a drastic change in the environment in which the virus had adapted to proliferate; therefore, changes would be expected to occur in the composition of the quasispecies following LT. After the primary HCV target organ is removed, there is a substantial reduction in the overall VL, and the viral populations remaining in the bloodstream and extra-hepatic reservoirs initiate infection of the new liver graft [1,46]. The number of viral particles (population size) starting the reinfection, together with differences in the liver graft, state of immunosuppression, and patient characteristics, may influence the evolutionary outcome and affect the quasispecies composition [22,47,48].

In this scenario, during graft reinfection, a genetic phenomenon known as “bottlenecking” is expected [49] in which the fittest virions are selected in the absence of an effective immune response, thereby increasing their frequency in serum with still limited variability [50]. In this sense, our phylogenetic studies have revealed three different patterns of viral behavior after liver graft infection. In the first pattern, observed in most patients

(70%), the master sequence was conserved, but the mutant spectra differed. Only some sequences were the same as the pre-LT ones, suggesting that the reinfection of the liver was caused by the master and the most prevalent pre-LT sequences. In the two patients with the second pattern, the master sequence differed from the pre-LT one, and the mutant spectra were completely different, suggesting that reinfection of the liver graft was caused by a minor mutant from the pre-LT quasispecies. Finally, in the third pattern (one patient), the pre-LT quasispecies was maintained after liver transplantation, suggesting massive reinfection of the liver graft by most of the pre-LT virions. Despite pattern 2 and 3 only include patients with subtypes 1b and 3 respectively, the small sample size (two for pattern 2 and one for pattern 3), do not allow us to extract conclusions on the effect of the subtype in the viral quasispecies behavior after LT. However, pattern 1 has been found in patients with subtype 1a and 1b, suggesting that in most of the cases, and independently of the liver damage progression, HCV reinfection follows this particular pattern master sequence, which remains after LT but with different mutant spectra. Interestingly, in the patient that had a cholestatic fibrosis hepatitis (P10) master sequence, it remained dominant after LT as previously reported by Gambato et al. in which 62% of cholestatic patients showed the remaining of master sequence compared with the 11% in the patients with mild recurrence [13]. The main limitation of this study is the small sample size. The main reason for the low number of patients included is that most of the patients are efficiently treated with DAAs before and soon after LT, thus limiting the number of samples fulfilling inclusion criteria for our study in which we require patients with at least one year of untreated follow-up.

It is widely recognized that liver fibrosis rapidly progresses in some patients, leading to cirrhosis at 1 year post-LT (fast-progressors), whereas others show minimal changes in the transplanted graft at the same time point (slow-progressors). In this situation, we hypothesized that the viral complexity indices might predict the fast or slow progression of liver damage. However, after conducting an exhaustive analysis of changes in the HCV quasispecies complexity measures (qD , M_{fmax} , and π) obtained before LT and 15 days following LT, none of the measures studied were significantly associated with progression to more aggressive liver damage at 1 year following the procedure. This may be because the viral quasispecies is a highly variable and dynamic population that fluctuates greatly over time, and the results may vary according to the moment at which the sample is collected and analyzed. Hence, we cannot exclude that the analysis of samples taken at a later point after LT might have led to the identification of a complexity index predictive of fast liver damage progression.

Interestingly, we observed a significant increase in VL values from pre-LT to 15 days post-LT in all patients who had an advanced stage of fibrosis 1 year after the procedure, in accordance with previous findings [51]. Our results support the notion that the difference in VL before and after LT may be of value in predicting fibrosis progression. Thus, VL changes may be a useful criterion to determine whether to administer DAA treatment as soon as possible post-LT or delay it until the patient is clinically stable.

5. Conclusions

To sum up, none of the viral complexity measures studied at 15 days after liver transplantation were significantly associated with liver damage progression at 1 year following the procedure. Three different patterns of liver graft reinfection were observed based on phylogenetic analyses. VL values were high and uniform in all pre-LT samples but were more dispersed in the post-LT samples. An increase in viral load after liver transplantation was associated with fast progression to liver fibrosis and could be an indicator that effective antiviral treatment should be started as soon as possible in these particular patients.

Supplementary Materials: The following are available online at <https://www.mdpi.com/article/10.3390/genes12111731/s1>, Figures S1–S7: Phylogenetic trees representing the liver quasispecies

population before (pre-LT) and after (post-LT) liver transplantation. Table S1. Clinical data, viral load, and pre/post-LT viral complexity measures. Inclusion and exclusion criteria.

Author Contributions: M.L.-R. designed the study, performed the experiments, acquired, analyzed, and interpreted the data, wrote the manuscript and approved the version of the article to be published; J.G. made essential contributions to the study concept and design, developed software tools and helped perform the analysis and interpretation of the data, reviewed the manuscript and approved the version of the article to be published; C.D. substantially contributed to collecting the patient samples, the study concept and design, writing and reviewing the manuscript, and approving the version of the article to be published; F.R.-F. and C.P. critically reviewed the study for intellectual content and approved the manuscript; D.G.-C., M.E.S., Q.C., and A.R. participated equally in performing the research and contributed to the sample collection and storage; J.I.E. directed the study, corrected the manuscript and approved the final version; J.Q. and I.B. played essential roles in the development of this study. Both authors made large contributions to the concept and design of the study, added intellectual content in the interpretation of the data, and participated in writing the manuscript and approving the final version. All authors have read and agreed to the published version of the manuscript.

Funding: This study was supported by grants from Instituto de Salud Carlos III cofinanced by the European Regional Development Fund (ERDF) with grant numbers PI19/00533, PI19/00301, Clinical Trial Gov. Identifier: NCT01707849, and from Centro para el Desarrollo Tecnológico Industrial-CDTI of the Spanish Ministry of Economics and Competitiveness (MINECO) grant number, IDI-20200297. C.P. is supported by the Miguel Servet program of Instituto de Salud Carlos III, grant CP14/00121, cofinanced by the ERDF. Astellas Pharma Inc and Novartis Pharma also provided funding for the study, but these companies had had no role in the study design, data collection or analysis, decision to publish, or preparation of the manuscript.

Institutional Review Board Statement: The study was conducted according to the guidelines of the Declaration of Helsinki, and approved by the Institutional Review Board of Hospital Universitari Vall d'Hebrón, de Barcelona, EVL-VHC-HVH.12 / EudraCTn^o: 2012-002105-22.

Informed Consent Statement: Informed consent was obtained from all subjects involved in the study.

Data Availability Statement: The data presented in this study are available on request from the corresponding author.

Acknowledgments: The authors thank the Department of Hepatobiliarypancreatic Surgery and Transplantation for performing sample collection, Judit Carbonell Segura for her expert technical assistance, and Celine Cavallo for English language support and helpful editing suggestions.

Conflicts of Interest: Josep Gregori works in Roche Diagnostics. This fact did not change.

References

1. Garcia-Retortillo, M.; Xavier, F.; Feliu, A.; Eduardo, M.; Josep, C.; Miquel, N.; Antoni, R.; Rodes, J. Hepatitis C virus kinetics during and immediately after liver transplantation. *Hepatology* **2002**, *35*, 680–687. [[CrossRef](#)]
2. Wright, T.L.; Donegan, E.; Hsu, H.H.; Ferrell, L.; Lake, J.R.; Kim, M.; Combs, C.; Fennessy, S.; Roberts, J.P.; Ascher, N.L.; et al. Recurrent and acquired hepatitis C viral infection in liver transplant recipients. *Gastroenterology* **1992**, *103*, 317–322. [[CrossRef](#)]
3. Gane, E.J.; Portmann, B.C.; Naoumov, N.V.; Smith, H.M.; Underhill, J.A.; Donaldson, P.T.; Maertens, G.; Williams, R. Long-term outcome of hepatitis C infection after liver transplantation. *N. Engl. J. Med.* **1996**, *334*, 815–820. [[CrossRef](#)] [[PubMed](#)]
4. Berenguer, M.; Prieto, M.; Rayón, J.M.; Mora, J.; Pastor, M.; Ortiz, V.; Carrasco, D.; San Juan, F.; Burgueño, M.-J.; Mir, J.; et al. Natural History of Clinically Compensated Hepatitis C Virus-Related Graft Cirrhosis After Liver Transplantation. *Hepatology* **2000**, *32*, 852–858. [[CrossRef](#)] [[PubMed](#)]
5. Prieto, M.; Berenguer, M.; Rayón, J.M.; Córdoba, J.; Argüello, L.; Carrasco, D.; García-Herola, A.; Olaso, V.; De Juan, M.; Gobernado, M.; et al. High incidence of allograft cirrhosis in hepatitis C virus genotype 1b infection following transplantation: Relationship with rejection episodes. *Hepatology* **1999**, *29*, 250–256. [[CrossRef](#)] [[PubMed](#)]
6. Thein, H.H.; Yi, Q.; Dore, G.J.; Krahn, M.D. Estimation of stage-specific fibrosis progression rates in chronic hepatitis C virus infection: A meta-analysis and meta-regression. *Hepatology* **2008**, *48*, 418–431. [[CrossRef](#)] [[PubMed](#)]
7. Samuel, D.; Forns, X.; Berenguer, M.; Trautwein, C.; Burroughs, A.; Rizzetto, M.; Trepo, C. Report of the Monothematic EASL Conference on Liver Transplantation for Viral Hepatitis. (Paris, France, January 12–14, 2006). *J. Hepatol.* **2006**, *45*, 127–143. [[CrossRef](#)] [[PubMed](#)]

8. Gallegos-Orozco, J.F.; Yosephy, A.; Noble, B.; Aqel, B.A.; Byrne, T.J.; Carey, E.J.; Douglas, D.D.; Mulligan, D.; Moss, A.; de Petris, G.; et al. Natural history of post-liver transplantation hepatitis C: A review of factors that may influence its course. *Liver Transplant.* **2009**, *15*, 1872–1881. [[CrossRef](#)] [[PubMed](#)]
9. Belli, L.S.; Duvoux, C.; Berenguer, M.; Berg, T.; Coilly, A.; Colle, I.; Fagioli, S.; Saye, K.; Georges, P.P.; Massimo, P.; et al. ELITA consensus statements on the use of DAAs in liver transplant candidates and recipients. *J. Hepatol.* **2017**, *67*, 585–602. [[CrossRef](#)]
10. Berenguer, M.; Ferrell, L.; Watson, J.; Prieto, M.; Kim, M.; Rayón, M.; Córdoba, J.; Herola, A.; Ascher, N.; Mir, J.; et al. HCV-related fibrosis progression following liver transplantation: Increase in recent years. *J. Hepatol.* **2000**, *32*, 673–684. [[CrossRef](#)]
11. Berenguer, M.; Lopez-Labrador, F.X.; Wright, T.L. Hepatitis C and liver transplantation. *J. Hepatol.* **2001**, *35*, 666–678. [[CrossRef](#)]
12. Berenguer, M.; Schuppan, D. Progression of liver fibrosis in post-transplant hepatitis C: Mechanisms, assessment and treatment. *J. Hepatol.* **2013**, *58*, 1028–1041. [[CrossRef](#)] [[PubMed](#)]
13. Gambato, M.; Gregori, J.; Quer, J.; Koutsoudakis, G.; González, P.; Caro-Pérez, N.; García-Cehic, D.; García-González, N.; González-Candelas, F.; Ignacio, E.J.; et al. Hepatitis C virus intrinsic molecular determinants may contribute to the development of cholestatic hepatitis after liver transplantation. *J. Gen. Virol.* **2019**, *100*, 63–68. [[CrossRef](#)]
14. Crespo, G.; Trota, N.; Londoño, M.C.; Mauro, E.; Baliellas, C.; Castells, L.; Castellote, J.; Tort, J.; Forn, X.; Navasa, M. The efficacy of direct anti-HCV drugs improves early post-liver transplant survival and induces significant changes in waiting list composition. *J. Hepatol.* **2018**, *69*, 11–17. [[CrossRef](#)] [[PubMed](#)]
15. Pawlotsky, J.M. Hepatitis C virus population dynamics during infection. *Curr. Top. Microbiol. Immunol.* **2006**, *299*, 261–284. [[CrossRef](#)]
16. Perales, C. Quasispecies dynamics and clinical significance of hepatitis C virus (HCV) antiviral resistance. *Int. J. Antimicrob. Agents* **2020**, *56*, 105562. [[CrossRef](#)] [[PubMed](#)]
17. Farci, P.; Strazzera, R.; Alter, H.J.; Farci, S.; Degioannis, D.; Coiana, A.; Peddis, G.; Usai, F.; Serra, G.; Chessa, L.; et al. Early changes in hepatitis C viral quasispecies during interferon therapy predict the therapeutic outcome. *Proc. Natl. Acad. Sci. USA* **2002**, *99*, 3081–3086. [[CrossRef](#)] [[PubMed](#)]
18. Vainio, E.J.; Chiba, S.; Ghabrial, S.A.; Maiss, E.; Roossinck, M.; Sabanadzovic, S.; Suzuki, N.; Xie, J.; Nibert, M.; Lefkowitz, E.J.; et al. ICTV virus taxonomy profile: Partitiviridae. *J. Gen. Virol.* **2018**, *99*, 17–18. [[CrossRef](#)]
19. Ogata, N.; Alter, H.J.; Miller, R.H.; Purcell, R.H. Nucleotide sequence and mutation rate of the H strain of hepatitis C virus. *Proc. Natl. Acad. Sci. USA* **1991**, *88*, 3392–3396. [[CrossRef](#)] [[PubMed](#)]
20. Vignuzzi, M.; Stone, J.K.; Arnold, J.J.; Cameron, C.E.; Andino, R. Quasispecies diversity determines pathogenesis through cooperative interactions within a viral population. *Nature* **2006**, *439*, 344–348. [[CrossRef](#)]
21. Holland, J.; Spindler, K.; Horodyski, F.; Grabau, E.; Nichol, S.; VandePol, S. Rapid evolution of RNA genomes. *Science* **1982**, *215*, 1577–1585. [[CrossRef](#)] [[PubMed](#)]
22. Domingo, E.; Sheldon, J.; Perales, C. Viral quasispecies evolution. *Microbiol. Mol. Biol. Rev.* **2012**, *76*, 159–216. [[CrossRef](#)] [[PubMed](#)]
23. Steinhauer, D.A.; Holland, J.J. Rapid Evolution of RNA Viruses. *Annu. Rev. Microbiol.* **1987**, *41*, 409–431. [[CrossRef](#)] [[PubMed](#)]
24. Duarte, E.A.; Novella, I.S.; Weaver, S.C.; Domingo, E.; Wain-Hobson, S.; Clarke, D.K.; Moya, A.; Elena, S.F.; de la Torre, J.C.; Holland, J.J. RNA virus quasispecies: Significance for viral disease and epidemiology. *Infect. Agents Dis.* **1994**, *3*, 201–214. [[PubMed](#)]
25. Domingo, E.; Sabo, D.; Taniguchi, T.; Weissmann, C. Nucleotide sequence heterogeneity of an RNA phage population. *Cell* **1978**, *13*, 735–744. [[CrossRef](#)]
26. Gregori, J.; Perales, C.; Rodríguez-Frias, F.; Esteban, J.I.; Quer, J.; Domingo, E. Viral quasispecies complexity measures. *Virology* **2016**, *493*, 227–237. [[CrossRef](#)] [[PubMed](#)]
27. Martell, M.; Esteban, J.I.; Quer, J.; Genescà, J.; Weiner, A.; Esteban, R.; Guardia, J.; Gómez, J. Hepatitis C virus (HCV) circulates as a population of different but closely related genomes: Quasispecies nature of HCV genome distribution. *J. Virol.* **1992**, *66*, 3225–3229. [[CrossRef](#)]
28. Bordería, A.; Stapleford, K.; Vignuzzi, M. RNA virus population diversity: Implications for inter-species transmission. *Curr. Opin. Virol.* **2011**, *1*, 643–648. [[CrossRef](#)]
29. Campagnola, G.; McDonald, S.; Beaucourt, S.; Vignuzzi, M.; Peersen, O.B. Structure-function relationships underlying the replication fidelity of viral RNA-dependent RNA polymerases. *J. Virol.* **2015**, *89*, 275–286. [[CrossRef](#)]
30. Pfeiffer, J.K.; Kirkegaard, K. Increased Fidelity Reduces Poliovirus Fitness and Virulence under Selective Pressure in Mice. *PLoS Pathog.* **2005**, *1*, e11. [[CrossRef](#)] [[PubMed](#)]
31. Quer, J.; Gregori, J.; Rodríguez-frias, F.; Buti, M.; Madejon, A.; Perez-del-pulgar, S.; Muñoz, J.M.; Cubero, M.; Caballero, A.; Domingo, E.; et al. High-Resolution Hepatitis C Virus Subtyping Using NS5B Deep Sequencing and Phylogeny, an Alternative to Current Methods. *J. Clin. Microbiol.* **2015**, *53*, 219–226. [[CrossRef](#)] [[PubMed](#)]
32. Ishak, K.; Baptista, A.; Bianchi, L.; Callea, F.; De Groote, J.; Gudat, F.; Denk, H.; Desmet, V.; Korb, G.; MacSween, R.N.M.; et al. Histological grading and staging of chronic hepatitis. *J. Hepatol.* **1995**, *22*, 696–699. [[CrossRef](#)]
33. Kuiken, C.; Mizokami, M.; Deleage, G.; Yusim, K.; Penin, F.; Shin-I, T.; Charavay, C.; Tao, N.; Crisan, D.; Grande, D.; et al. Hepatitis C databases, principles and utility to researchers. *Hepatology* **2006**, *43*, 1157–1165. [[CrossRef](#)]

34. Ramirez, C.; Gregori, J.; Buti, M.; Tabernero, D.; Camos, S.; Casillas, R.; Quer, J.; Esteban, R.; Homs, M.; Rodriguez-Frias, F. A comparative study of ultra-deep pyrosequencing and cloning to quantitatively analyze the viral quasispecies using hepatitis B virus infection as a model. *Antivir. Res.* **2013**, *98*, 273–283. [[CrossRef](#)] [[PubMed](#)]
35. Gregori, J.; Esteban, J.I.; Cubero, M.; Garcia-Cehic, D.; Perales, C.; Casillas, R.; Alvarez-Tejado, M.; Rodríguez-Frías, F.; Guardia, J.; Domingo, E.; et al. Ultra-deep pyrosequencing (UDPS) data treatment to study amplicon HCV minor variants. *PLoS ONE* **2013**, *8*, e83361. [[CrossRef](#)] [[PubMed](#)]
36. R Core Team. *R: A Language and Environment for Statistical Computing*; R Foundation for Statistical Computing: Vienna, Austria, 2013; pp. 1–12.
37. Pages, H.; Aboyoun, P.; Gentleman, R.; DebRoy, S. *Biostrings: String Objects Representing Biological Sequences, and Matching Algorithms*; R Package Version 2.24.1; Fred Hutchinson Cancer Research Center: Seattle, WA, USA, 2012.
38. Paradis, E.; Claude, J.; Strimmer, K. APE: Analyses of Phylogenetics and Evolution in R language. *Bioinformatics* **2004**, *20*, 289–290. [[CrossRef](#)] [[PubMed](#)]
39. Charif, D.; Lobry, J.R. *SeqinR 1.0-2: A Contributed Package to the R Project for Statistical Computing Devoted to Biological Sequences Retrieval and Analysis*; Springer: Berlin/Heidelberg, Germany, 2007; pp. 207–232.
40. Dray, S.; Dufour, A.B. The ade4 package: Implementing the duality diagram for ecologists. *J. Stat. Softw.* **2007**, *22*, 1–20. [[CrossRef](#)]
41. Hill, M.O. Diversity and evenness: A unifying notation and its consequences. *Ecology* **1973**, *54*, 427–432. [[CrossRef](#)]
42. Gotelli, N.J.; Hsieh, T.C.; Sander, E.L.; Colwell, R.K. *Rarefaction and Extrapolation with Hill Numbers: A Framework for Sampling and Estimation in Species Diversity Studies*; ESA: Washington DC, USA, 2014; Volume 84, pp. 45–67. [[CrossRef](#)]
43. Nei, M. *Molecular Evolutionary Genetics*; Columbia University: New York, NY, USA, 1987.
44. Nei, M.; Kumar, S. *Molecular Evolution and Phylogenetics*; Oxford University: New York, NY, USA, 2000.
45. Hudelot, C.; Gowri-Shankar, V.; Jow, H.; Rattray, M.; Higgs, P.G. RNA-based phylogenetic methods: Application to mammalian mitochondrial RNA sequences. *Mol. Phylogenet. Evol.* **2003**, *28*, 241–252. [[CrossRef](#)]
46. Dahari, H.; Feliu, A.; Garcia-Retortillo, M.; Forn, X.; Neumann, A.U. Second hepatitis C replication compartment indicated by viral dynamics during liver transplantation. *J. Hepatol.* **2005**, *42*, 491–498. [[CrossRef](#)] [[PubMed](#)]
47. Novella, I.S.; Elena, S.F.; Moya, A.; Domingo, E.; Holland, J.J. Size of genetic bottlenecks leading to virus fitness loss is determined by mean initial population fitness. *J. Virol.* **1995**, *69*, 2869–2872. [[CrossRef](#)] [[PubMed](#)]
48. Domingo, E. *Virus as Populations: Composition, Complexity, Dynamics and Biological Implications*; Academic Press: London, UK, 2016.
49. Pérez-Del-Pulgar, S.; Gregori, J.; Rodríguez-Frías, F.; González, P.; García-Cehic, D.; Ramírez, S.; Casillas, R.; Domingo, E.; Esteban, J.I.; Forn, X.; et al. Quasispecies dynamics in hepatitis C liver transplant recipients receiving grafts from hepatitis C virus infected donors. *J. Gen. Virol.* **2015**, *96*, 3493–3498. [[CrossRef](#)] [[PubMed](#)]
50. Farci, P.; Shimoda, A.; Coiana, A.; Diaz, G.; Peddis, G.; Melpolder, J.C.; Strazzera, A.; Chien, D.Y.; Munoz, S.J.; Balestrieri, A.; et al. The Outcome of Acute Hepatitis C Predicted by the Evolution of the Viral Quasispecies. *Science* **2000**, *288*, 339–344. [[CrossRef](#)] [[PubMed](#)]
51. Massagué, A.; Ramírez, S.; Carrión, J. A.; González, P.; Sánchez-Tapias, J.M.; Forn, X. Evolution of the NS3 and NS5B regions of the hepatitis C virus during disease recurrence after liver transplantation. *Am. J. Transplant.* **2007**, *7*, 2172–2179. [[CrossRef](#)] [[PubMed](#)]

4.1.3 Article 1 Supplementary material

Study of quasispecies complexity
and liver damage progression after
liver transplantation in hepatitis C
infected patients

Inclusion criteria

1. Recipient of the first orthotopic liver transplant
2. Adult of either sex
3. Age ≥ 18 years
4. Positive HCV RNA testing at 12 months before transplantation
5. Written informed consent for participation in the study
6. Able to participate in the study for the 12 months following transplantation

Exclusion criteria

1. Recipient of multiple organ transplants or a previous organ transplant
2. Split or living donor recipient infection
3. Recipient with ABO incompatibility
4. Recipient seropositive to HIV antibodies
5. Recipient due to fulminant liver failure
6. Recipient due to HCV infection under DAA treatment, with negative HCV RNA status
7. Known neoplasm or history of neoplastic disease, except basal cell skin carcinoma or hepatocarcinoma meeting the following criteria: no vascular invasion. Single nodule ≤ 5 cm diameter. or 2 or 3 three nodules < 3 cm (Milan's criteria)

8. Glomerular filtration rate <60 ml/min/1.73m² before transplantation or kidney dialysis requirement before transplantation
9. Critical illness with clinical instability that could affect the study goals
10. Patient treated with a new therapy under investigation within 1 month before transplantation with a drug that will be needed in the post-LT period
11. Patient with $<10^3$ viral particles 15 weeks post-LT

Figure S1. Continue

UPGMA tree (K80): P03

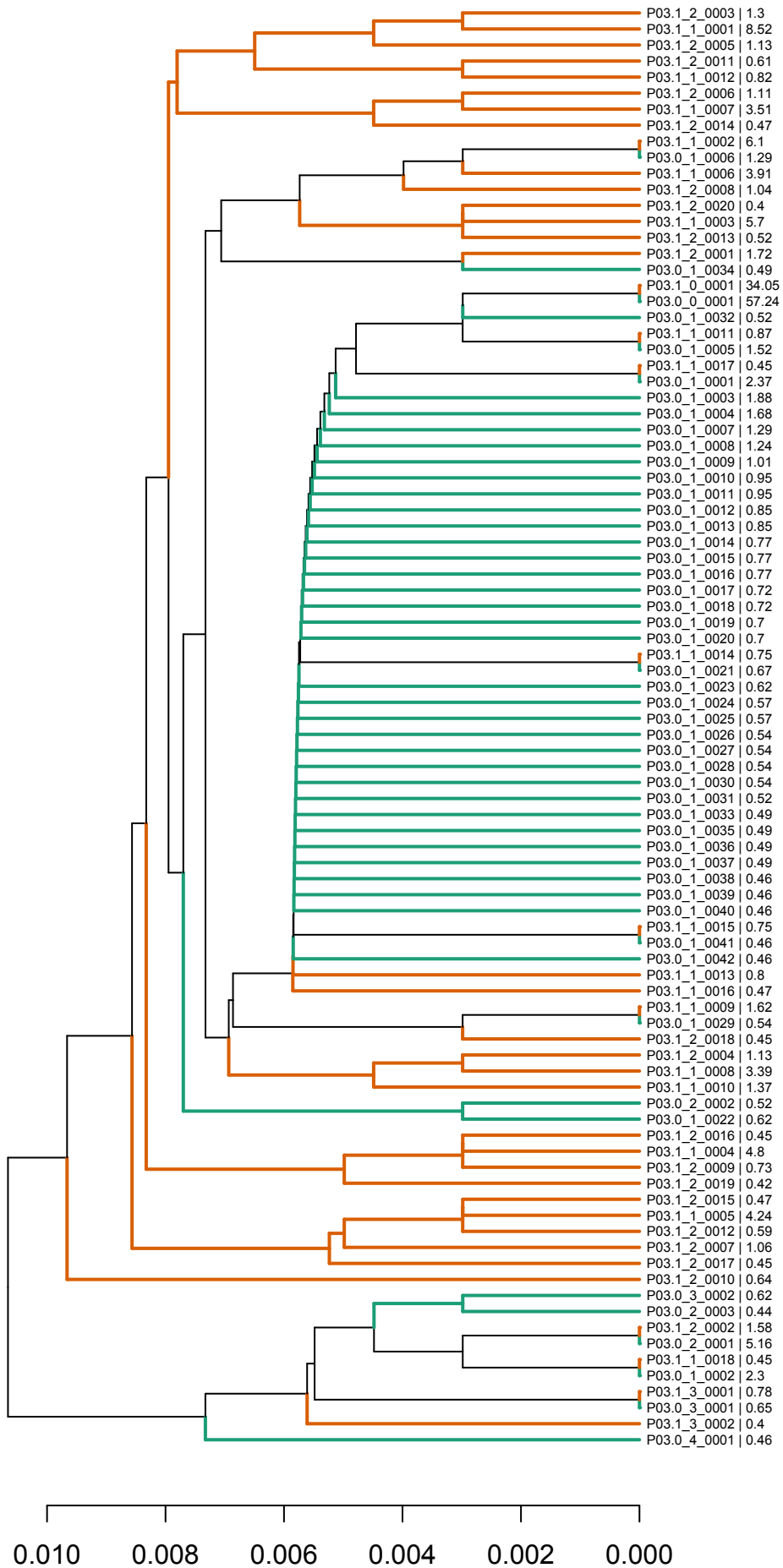


Figure S1. Continue

UPGMA tree (K80): P04

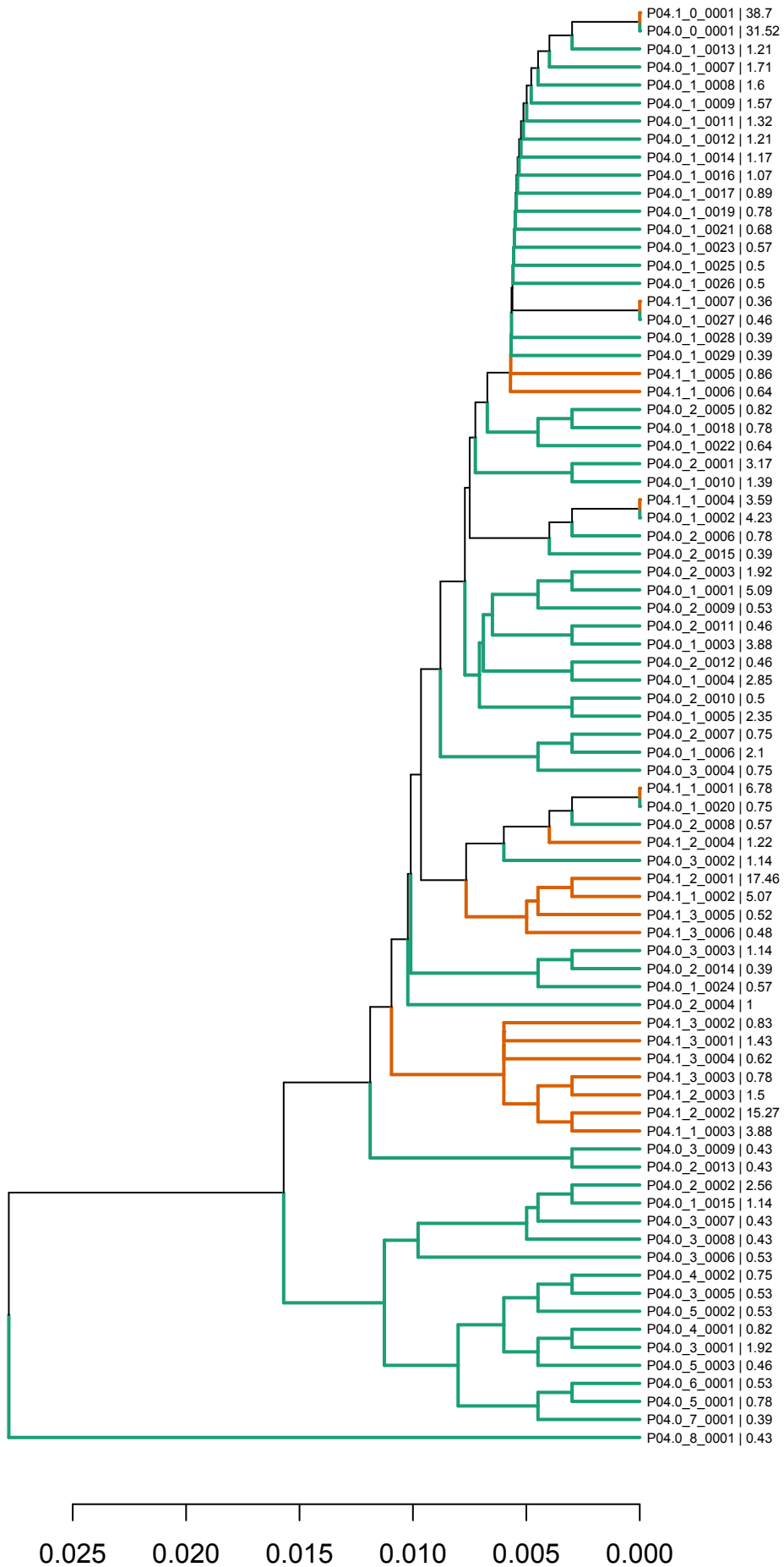


Figure S1. Continue

UPGMA tree (K80): P06

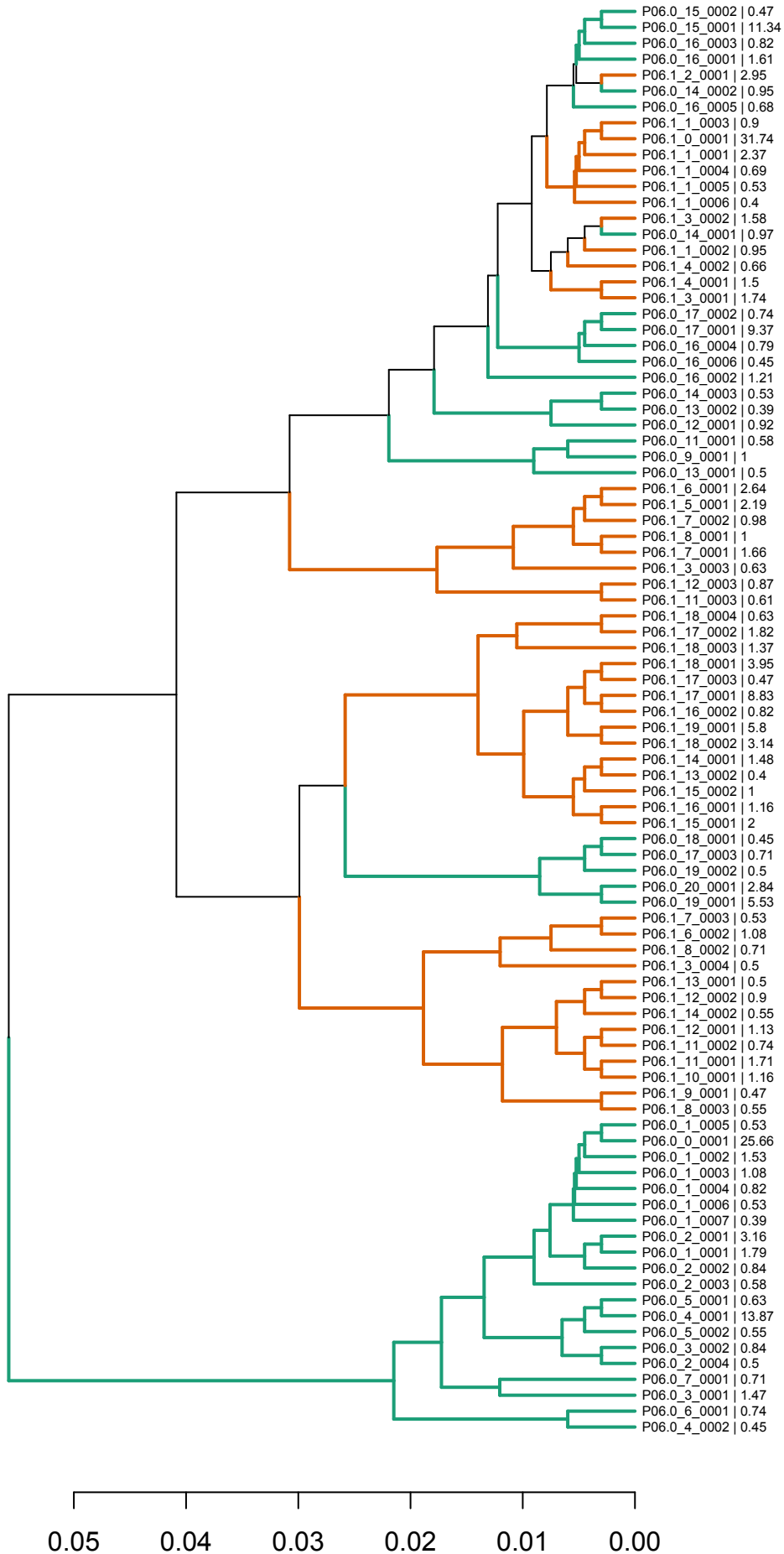


Figure S1. Continue

UPGMA tree (K80): P07

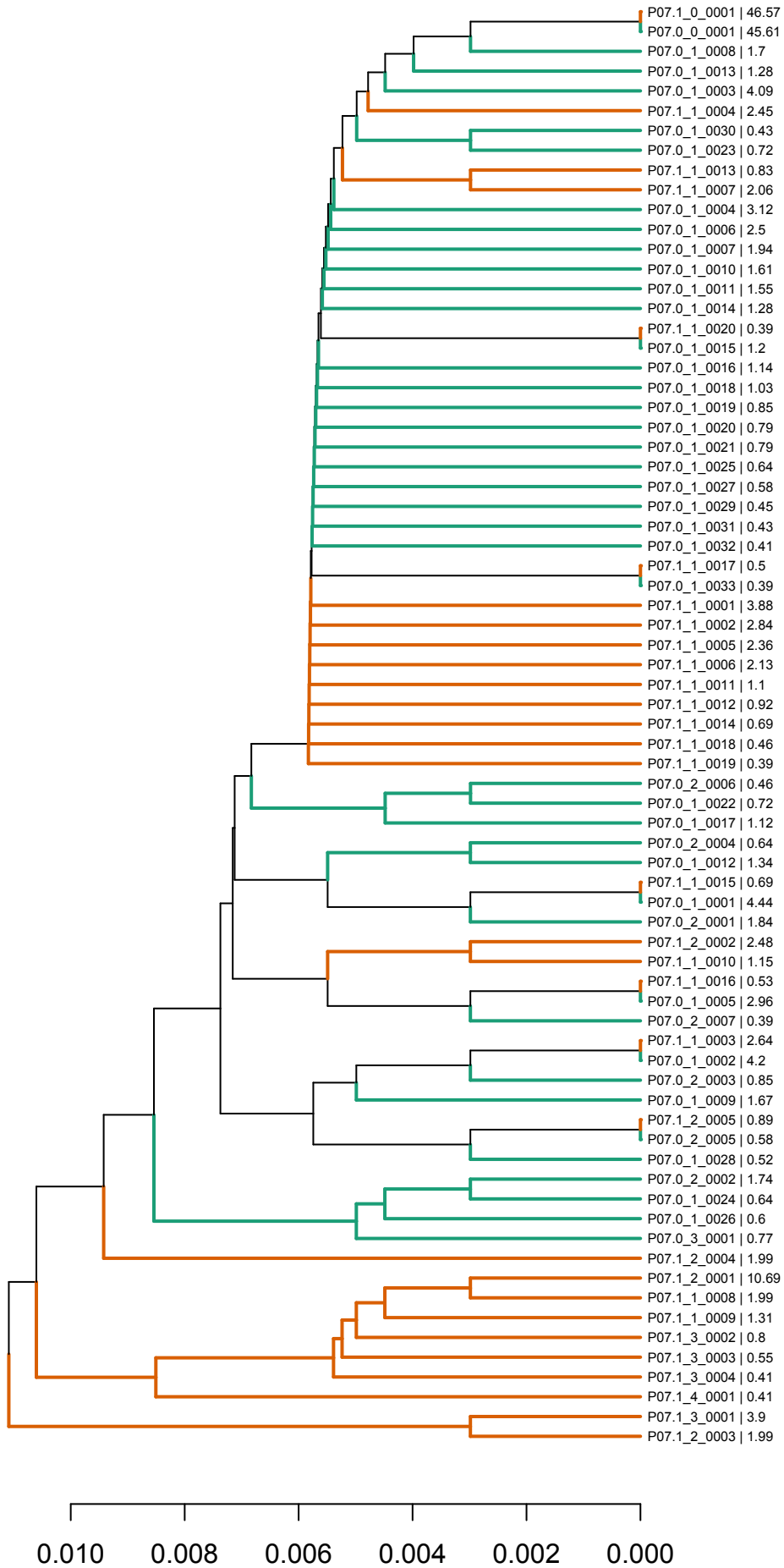
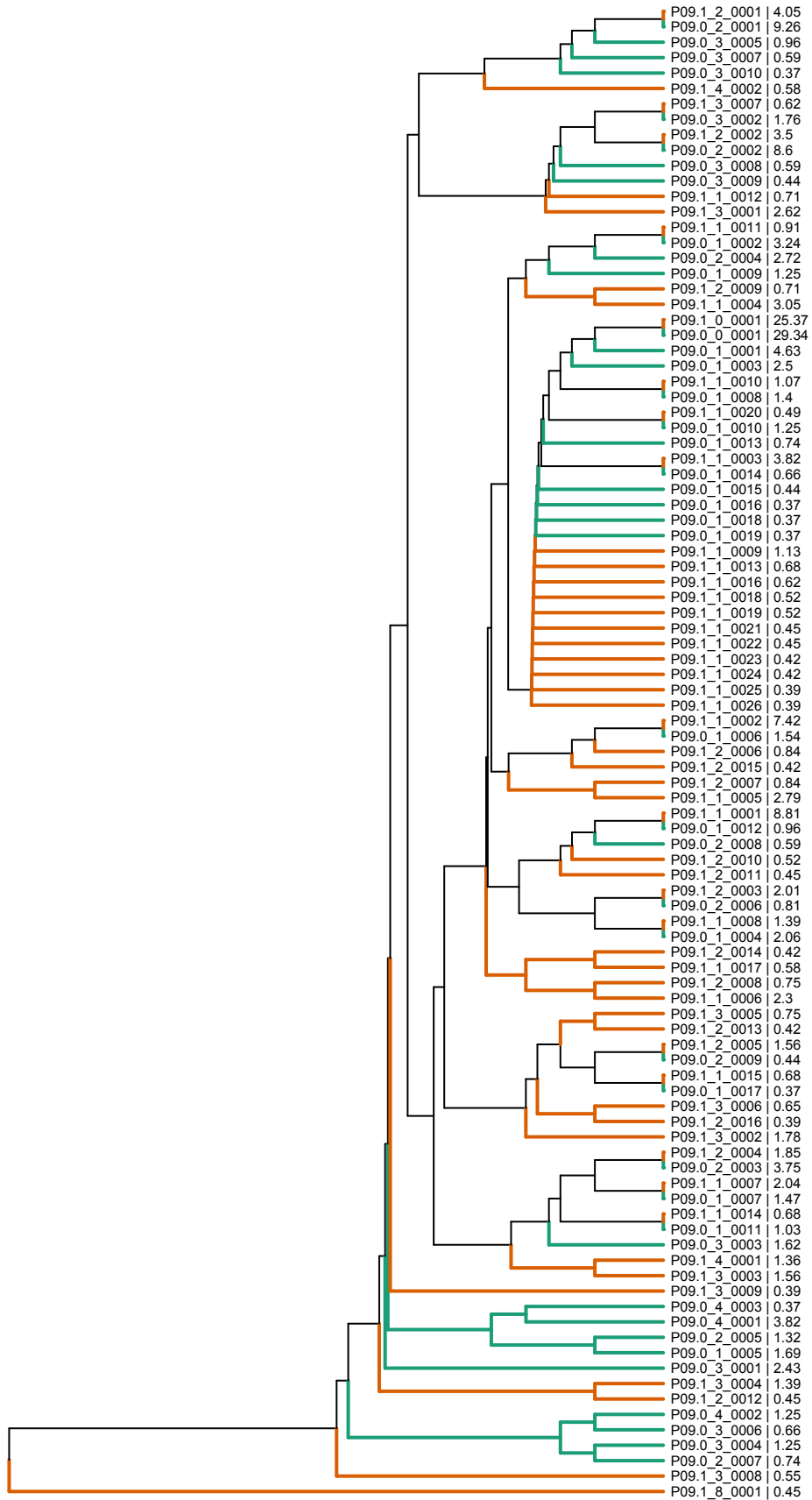


Figure S1. Continue

UPGMA tree (K80): P09



0.025 0.020 0.015 0.010 0.005 0.000

Figure S1. Continue

UPGMA tree (K80): P10

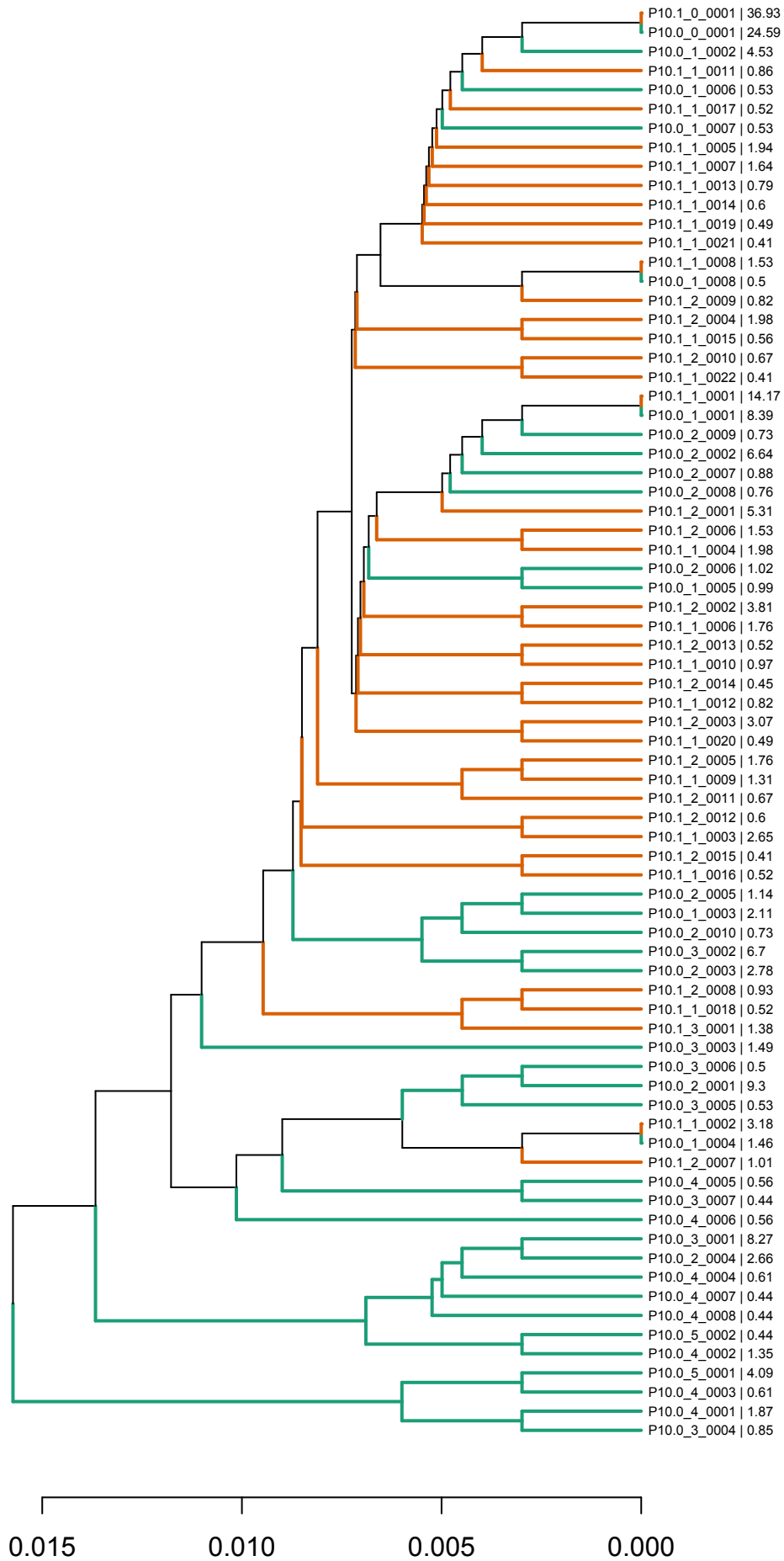


Table S1. Clinical data base, viral load and pre/post-LT viral complexity measures.

Patients	P01	P02	P03	P04	P05	P06	P07	P08	P09	P10
Subtype	3a	1a	1a	1b	1a	1b	1a	1b	1a	1b
Donor age	56	30	67	67	62	20	62	33	54	63
Receiver age	64	60	49	65	54	60	58	67	49	63
Liver damage^a	low	low	low	low	low	low	high	high	high	high
ISHAK^a	F0	F0	F0	F1	F2	F2	F3	F3	F4	F4
Viral load										
Pre-LT	2.00E+06	1.70E+06	8.40E+05	2.92E+06	1.20E+06	2.20E+06	1.50E+06	7.13E+05	1.30E+06	8.10E+05
Post-LT	6.22E+05	2.04E+05	1.10E+04	3.60E+05	3.00E+04	5.70E+06	2.20E+06	3.99E+06	1.50E+07	1.00E+06
Number of different mutations										
Pre-LT	39	49	44	42	19	38	33	12	28	22
Post-LT	35	19	22	11	22	24	25	33	37	26
Number of polymorphic sites										

Pre-LT	38	48	43	40	19	35	32	12	28	22
Post-LT	35	19	20	11	22	24	24	33	37	26
Number of nucleotides sequenced										
Pre-LT	772800	666288	1302000	944496	1614816	1276800	1734768	1445136	456960	1149120
Post-LT	589008	910560	1426992	1947456	660912	1274448	1465296	1187088	1036896	898800
Number of haplotypes										
Pre-LT	58	89	49	62	24	43	42	36	42	36
Post-LT	60	68	41	18	47	47	31	35	55	39
Abundance of dominant haplotype										
Pre-LT	34.00	17.40	57.24	31.52	51.48	25.66	45.61	22.90	29.34	24.59
Post-LT	25.44	11.77	34.05	38.70	34.98	31.74	46.57	55.19	25.37	36.93
MF min. minimum mutation frequency										
Pre-LT	5.05E-05	7.35E-05	3.38E-05	4.45E-05	1.18E-05	2.98E-05	1.90E-05	8.30E-06	6.13E-05	1.91E-05
Post-LT	5.94E-05	2.09E-05	1.54E-05	5.65E-06	3.33E-05	1.88E-05	1.71E-05	2.78E-05	3.57E-05	2.89E-05
MF max. maximum mutation frequency										
Pre-LT	2.80E-03	1.50E-02	1.57E-03	3.50E-03	1.98E-03	2.38E-02	1.86E-03	4.15E-03	4.06E-03	5.27E-03

Post-LT	4.45E-03	1.22E-02	2.52E-03	3.16E-03	3.84E-03	2.30E-02	2.50E-03	3.07E-03	3.67E-03	2.66E-03
Mfe. mutation frequency per entity										
Pre-LT	4.36E-03	1.62E-02	3.52E-03	6.24E-03	4.59E-03	2.80E-02	3.54E-03	6.45E-03	5.60E-03	7.52E-03
Post-LT	5.70E-03	1.32E-02	4.65E-03	5.46E-03	7.16E-03	2.76E-02	4.42E-03	1.04E-02	5.47E-03	4.20E-03
Δ. Nucleotide diversity										
Pre-LT	4.99E-03	2.19E-02	3.02E-03	6.54E-03	3.45E-03	3.04E-02	3.59E-03	7.07E-03	7.09E-03	8.32E-03
Post-LT	7.06E-03	1.45E-02	4.63E-03	4.80E-03	6.84E-03	2.69E-02	4.62E-03	5.72E-03	6.63E-03	4.51E-03
Δ[e]. Nucleotide diversity by entity										
Pre-LT	7.98E-03	2.40E-02	6.85E-03	1.12E-02	8.10E-03	3.29E-02	6.91E-03	1.04E-02	1.00E-02	1.19E-02
Post-LT	9.52E-03	1.55E-02	8.44E-03	8.03E-03	1.17E-02	2.85E-02	8.24E-03	1.77E-02	1.01E-02	7.70E-03
D1. Hill numbers										
Pre-LT	21.39	52.84	9.43	25.83	6.65	16.62	13.08	16.25	18.86	17.07
Post-LT	26.40	43.99	15.95	7.19	18.45	20.32	9.99	7.97	24.99	13.94
D2. Hill numbers										
Pre-LT	7.58	22.62	2.99	8.85	3.40	8.75	4.55	9.41	8.80	10.05
Post-LT	11.28	26.89	7.11	4.66	7.13	8.24	4.21	3.13	11.26	5.98
D_{∞}. Hill numbers										

Pre-LT	2.94	5.75	1.75	3.17	1.94	3.90	2.19	4.37	3.41	4.07
Post-LT	3.93	8.50	2.94	2.58	2.86	3.15	2.15	1.81	3.94	2.71

^a Data from post-LT samples.

4.2 Study 2

Partial restoration of immune response in hepatitis C patients after viral clearance by direct-acting antiviral therapy

4.2.1 Article 2 summary

4.2.1.1 Introduction

Hepatitis C is an infectious disease associated with significant liver-related morbidity and mortality, and although DAA-therapies eradicate HCV infection in more than 95% of treated patients, individuals with advanced liver disease are still at risk of developing HCC and other liver comorbidities after HCV elimination. Disease progression is closely related to immune responses such as HCV-specific CD4⁺ and CD8⁺ T cell responses, which are required for viral control and clearance. However, during chronic HCV infection, the constant exposure to viral antigens along with immunological factors results in varying degrees of functional impairment of HCV-specific T-cell effector functions, contributing to viral persistence and disease progression.

4.2.1.2 Hypothesis

The Characterization of the immunological status of patients that have resolved HCV infection by DAAs treatment would help to understand whether (i) the patient may evolve towards reversion of impaired liver functions and improvement of health's status or, (ii) the patient will evolve towards a worsening of the same or related liver disease.

4.2.1.3 Objectives

1. To investigate phenotypical changes in CD4⁺ T cells towards T cell exhaustion.
2. To evaluate functional changes in HCV-specific T cells by studying cytokines (IFN- γ and IL-2) secretion and proliferation capacity of both CD4⁺ and CD8⁺ T-cells after HCV clearance.

3. To determine if liver inflammation and fibrosis stage regression may occur after HCV elimination.

4.2.1.4 Study design

- Twenty-seven patients with HCV chronic infection undergoing DAA treatment and achieving SVR were included.
- The phenotypical and functional changes in both HCV-specific CD8+ and CD4+ T cells before treatment (baseline), at week 4 during treatment (W4), at the end of treatment (EOT) and 12 weeks after the end of treatment (FUW12), were determined.
- Cell surface expression of PD-1, TIM-3, and LAG-3, which have been identified as markers of exhausted T cells, were assessed by flow cytometry to determine CD4+ T cell exhaustion in baseline and FUW12 samples.
- To assess whether the impaired functionality of HCV-specific CD4+ and CD8+ T cells manifested by reduced IL2 and IFN- γ cytokine production is restored upon HCV clearance; firstly, IFN- γ spots forming cells (SFC) were analyzed by ELISpot assay after HCV Core, NS3 pool peptides and NS3 Helicase protein stimulation in baseline, W4, EOT, and FUW12 PBMC samples. Secondly, IL-2 and IFN- γ secretion, after HCV peptides stimulation, were analysed by intracellular cytokine staining in all patients at baseline, W4, EOT, and FUW12.

To further study functional responses to HCV after 5 days of incubation, HCV-specific CD4+ and CD8+ T cell proliferation was determined in all patients by carboxy-fluorescein diacetate succinimidyl ester (CFSE) dilution assay and the number of viable cells, that had proliferated at FUW12 versus baseline, was observed by flow cytometry.

- Transaminases, Fibrosis-4 (FIB-4) index, α -fetoprotein (AFP), and AST-to-platelet ratio index (APRI), were measured at baseline and FUW12 for each patient to determine liver inflammation and fibrosis stage.

4.2.1.5 Results according to objectives

4.2.1.5.1 Objective 1: To investigate phenotypical changes in CD4+ T cells towards T cell exhaustion.

Regarding exhausted T cell markers, we observed a slight, but not statistically significant, decrease of PD-1, TIM-3 and LAG-3 expression on CD4+ T cells in FUW12 samples compared to baseline.

However, significant decrease of PD-1 receptor expression at the surface of CD4+ T cells from FUW12 samples compared to baseline was observed in non-cirrhotic patients, treatment-naive patients and treatment-naive patients below 55 years of age, indicating a partial restoration of CD4 exhaustion phenotype as shown in Figure 12.

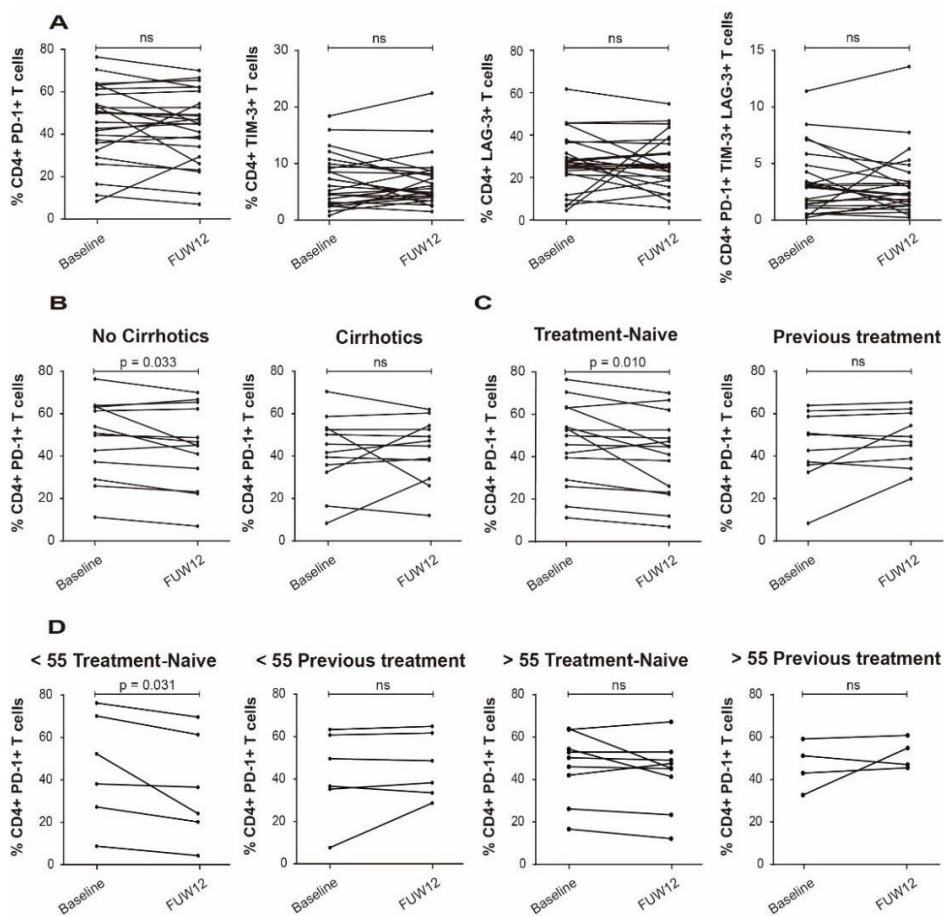


Figure 12. CD4+ T cell exhaustion markers expression. (A) Analysis of the frequencies of PD-1, TIM-3, LAG-3 markers among CD4+ T cells at baseline and FUW12, (N = 25). (B) Percent of PD-1 among CD4+ T cells according to score fibrosis. Non-cirrhotic patients (N = 13), liver stiffness < 9.5 KPa; Cirrhotic patients (N = 12), liver stiffness > 9.5 KPa. (C) Percent of CD4+ PD-1+ T cells in treatment-naive patients (N = 15), and in patients with previous IFN-based therapy (PEG-IFN- α + RBV) (N = 10). (D) Percent of CD4+ PD-1+ T cells in treatment-naive patients below 55 (N = 6), in patients below 55 with previous PEG-IFN- α + RBV treatment (N = 6), in treatment-naive patients over 55 (N = 9) and in patients below 55 previously treated with PEG-IFN- α + RBV (N = 4).

4.2.1.5.2 Objective 2: To evaluate functional changes in HCV-specific T cells by studying cytokines (IFN- γ and IL-2) secretion and proliferation capacity of both CD4+ and CD8+ T-cells after HCV clearance.

When studied IFN- γ secretion by HCV-specific CD4+ and CD8+ T cells by ELISpot, comparisons between baseline and FUW12 samples of all patients did not reveal any significant increase in IFN- γ production after HCV elimination. However, the number of IFN- γ SFC per 10^6 PBMCs significantly increased in FUW12 samples compared to baseline in G1b patients after stimulation with NS3 Helicase or Core peptides. Moreover, a similar increase was observed when comparing FUW12 versus W4 sample-pairs after stimulation with Core peptides, and FUW12 versus EOT sample-pairs after stimulation with NS3 31–44 peptides.

Furthermore, when we analyse the intracellular cytokine levels produced by HCV-specific CD4+ and CD8+ T cells, the percentages of CD4+ IFN- γ + T cells and CD4+ IL2+ T cells at FUW12 were not significantly higher than that observed in baseline or W4, independently of the HCV antigens used for stimulation. Contrary to what expected, T cells stimulated with NS3 31–44 peptides showed a significant decrease in IL2 production in CD4+ T cells between baseline or W4 and FUW12 samples and in CD8+ T cells between W4 and EOT, and between EOT and FUW12. Interestingly, a significant increase in IL2 production was observed in CD8+ T cells after stimulation with Core peptides when comparing baseline with W4, EOT and FUW12.

A significant increase of the proliferation capacity of both HCV CD4+ and CD8+ specific T-cells was observed between baseline and FUW12, when stimulated with NS3 Helicase and NS3 pooled peptides (Figure 13A). Moreover, when considering fibrosis score, proliferation capacity of CD4+ and CD8+ T cells significantly increased in non-cirrhotic patients after NS3 31–44 peptides stimulation compared with the cirrhotic ones (Figure 13B).

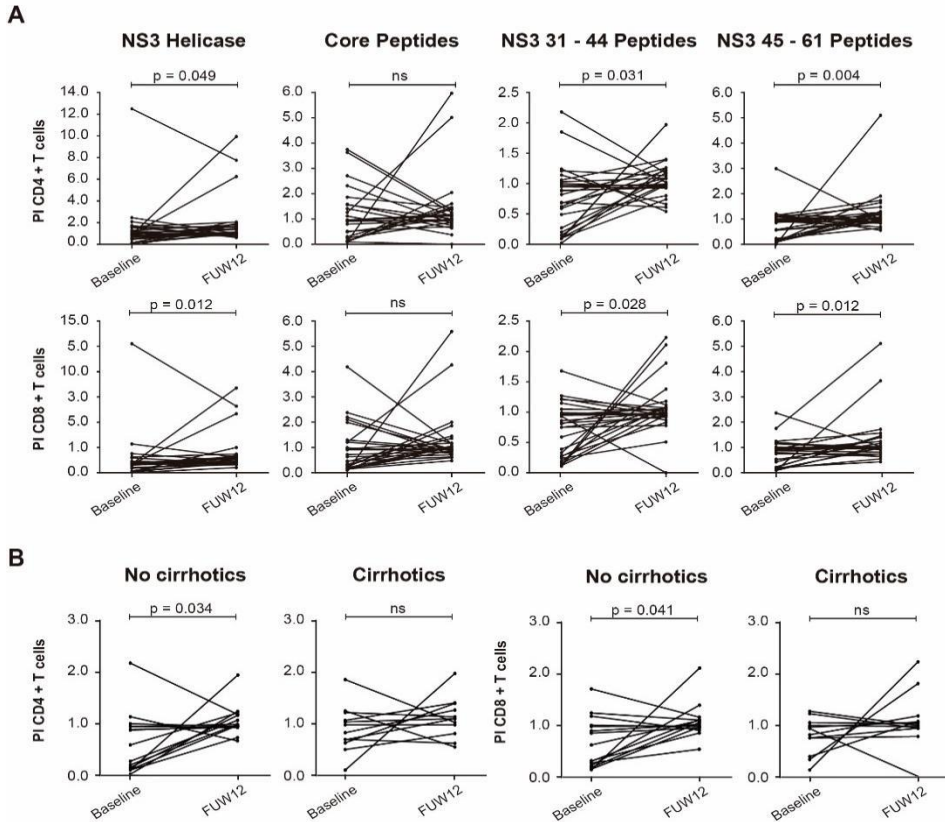


Figure 13. Proliferation responses of CD4+ and CD8+ HCV-specific T cells. Proliferation capacity was calculated as the proliferation index, at baseline and FUW12. (A) Proliferation index of CD4+ and CD8+ T cells (N = 27). (B) T cells proliferation index according to score fibrosis when stimulated with NS3 31–44 Peptides. CD4+ and CD8+ T cells of non-cirrhotic patients (N = 15) and (N = 12) respectively, liver stiffness < 9.5 KPa; CD4+ and CD8+ T cells of cirrhotic patients (N = 12) and (N = 12) respectively, liver stiffness > 9.5 KPa.

4.2.1.5.3 Objective 3. To determine if liver inflammation and fibrosis stage regression occurred after HCV elimination.

All liver inflammation and fibrosis markers tested showed a significant reduction 12 weeks after DAA-treatment as shown in Figure 14. These data indicate that

a reduction in liver inflammation and a fibrosis stage regression occurred in all patients that achieved SVR.

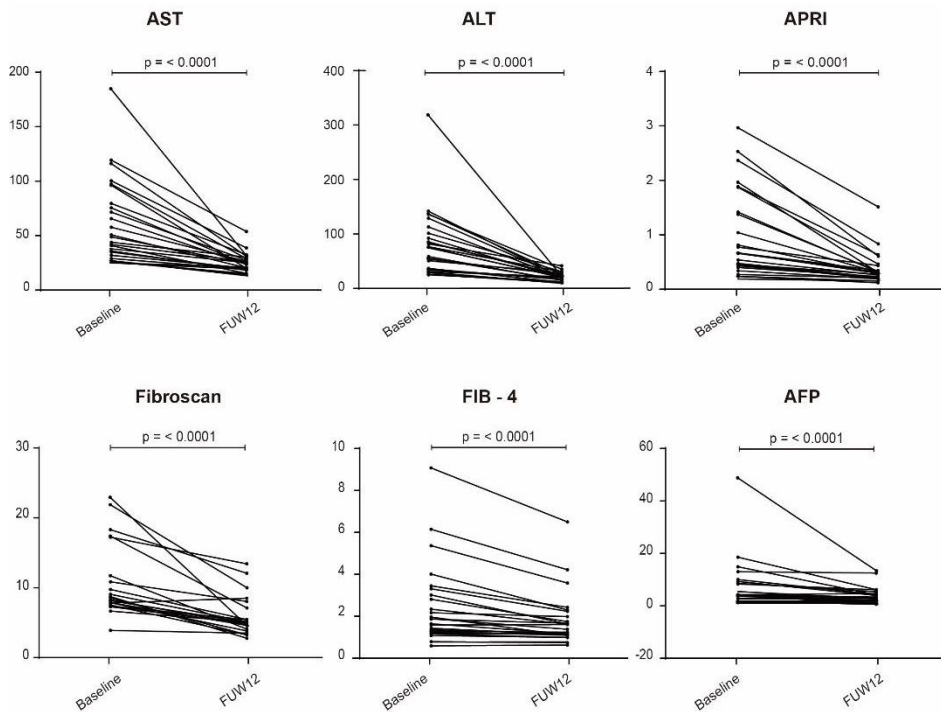


Figure 14. Liver inflammation and fibrosis markers. Levels of transaminases (AST, ALT), APRI, fibroscan, FIB-4 and AFP were measured at baseline and FUW12.

4.2.1.6 Conclusions

1. Restoration of CD4+ T cells exhausted phenotype is achieved in non-cirrhotic, treatment-naïve and patients below 55 years old treatment-naïve, while in cirrhotic, IFN- α previously treated and patients over 55 years old, HCV clearance does not fully revert the exhausted phenotype of CD4+ T cells.
2. HCV-specific CD4+ and CD8+ T cells remain in part functionally impaired, as cytokines production remained dysregulated upon HCV eradication, while the proliferative capacity of HCV-specific CD4+ and CD8+ T cells was restored.

- 3.** A reduction in liver inflammation and a fibrosis stage regression was achieved in all patients after DAA regimens, suggesting that a liver regeneration was ongoing.

4.2.2 Article 2

Partial restoration of immune response in hepatitis C patients after viral clearance by direct-acting antiviral therapy

Meritxell Llorens-Revull, Maria Isabel Costafreda, Angie Rico, Mercedes Guerrero-Murillo, Maria Eugenia Soria, Sofía Píriz-Ruzo, Elena Vargas-Accarino, Pablo Gabriel-Medina, Francisco Rodríguez-Frías, Mar Riveiro-Barciela, Celia Perales, Josep Quer, Silvia Sauleda, Juan Ignacio Esteban, Marta Bes

PLoS ONE16(7):e0254243.<https://doi.org/10.1371/journal.pone.0254243>

RESEARCH ARTICLE

Partial restoration of immune response in Hepatitis C patients after viral clearance by direct-acting antiviral therapy

Meritxell Llorens-Revull^{1,2,3}, Maria Isabel Costafreda^{1,4}, Angie Rico^{1,2,4}, Mercedes Guerrero-Murillo¹, Maria Eugenia Soria^{5,6}, Sofía Píriz-Ruzo¹, Elena Vargas-Accarino¹, Pablo Gabriel-Medina⁷, Francisco Rodríguez-Frías^{2,3,7,8}, Mar Riveiro-Barciela^{2,9}, Celia Perales^{2,5,6}, Josep Quer^{1,2,3}, Silvia Sauleda^{2,4}, Juan Ignacio Esteban^{1,2,3,9}, Marta Bes^{2,4*}



OPEN ACCESS

Citation: Llorens-Revull M, Costafreda MI, Rico A, Guerrero-Murillo M, Soria ME, Píriz-Ruzo S, et al. (2021) Partial restoration of immune response in Hepatitis C patients after viral clearance by direct-acting antiviral therapy. PLoS ONE 16(7): e0254243. <https://doi.org/10.1371/journal.pone.0254243>

Editor: Tatsuo Kanda, Nihon University School of Medicine, JAPAN

Received: April 7, 2021

Accepted: June 22, 2021

Published: July 9, 2021

Peer Review History: PLOS recognizes the benefits of transparency in the peer review process; therefore, we enable the publication of all of the content of peer review and author responses alongside final, published articles. The editorial history of this article is available here: <https://doi.org/10.1371/journal.pone.0254243>

Copyright: © 2021 Llorens-Revull et al. This is an open access article distributed under the terms of the [Creative Commons Attribution License](https://creativecommons.org/licenses/by/4.0/), which permits unrestricted use, distribution, and reproduction in any medium, provided the original author and source are credited.

Data Availability Statement: All relevant data are within the paper and its [Supporting Information](#) files.

1 Liver Diseases-Viral Hepatitis Laboratory, Liver Unit, Vall d'Hebron Institut de Recerca (VHIR), Hospital Universitari Vall d'Hebron (HUVH), Vall d'Hebron Barcelona Hospital Campus, Barcelona, Spain, **2** Centro de Investigación Biomédica en Red de Enfermedades Hepáticas y Digestivas (CIBERehd), Instituto de Salud Carlos III, Madrid, Spain, **3** Universitat Autònoma de Barcelona (UAB), Barcelona, Spain, **4** Transfusion Safety Laboratory, Banc de Sang i Teixits (BST), Barcelona, Spain, **5** Centro de Biología Molecular "Severo Ochoa" (CSIC-UAM), Campus de Cantoblanco, Madrid, Spain, **6** Department of Clinical Microbiology, IIS-Fundación Jiménez Díaz, UAM, Madrid, Spain, **7** Liver Pathology Laboratory, Biochemistry and Microbiology Unit, Vall d'Hebron Hospital Universitari (HUVH), Vall d'Hebron Barcelona Hospital Campus, Barcelona, Spain, **8** Clinical Biochemistry Unit, Vall d'Hebron Institut de Recerca (VHIR), Hospital Universitari Vall d'Hebron (HUVH), Vall d'Hebron Barcelona Hospital Campus, Barcelona, Spain, **9** Liver Unit, Department of Internal Medicine, Hospital Universitari Vall d'Hebron (HUVH), Vall d'Hebron Barcelona Hospital Campus, Barcelona, Spain

* mbes@bst.cat

Abstract

Background & aims

HCV CD4+ and CD8+ specific T cells responses are functionally impaired during chronic hepatitis C infection. DAAs therapies eradicate HCV infection in more than 95% of treated patients. However, the impact of HCV elimination on immune responses remain controversial. Here, we aimed to investigate whether HCV cure by DAAs could reverse the impaired immune response to HCV.

Methods

We analyzed 27 chronic HCV infected patients undergoing DAA treatment in tertiary care hospital, and we determined the phenotypical and functional changes in both HCV CD8+ and CD4+ specific T-cells before and after viral clearance. PD-1, TIM-3 and LAG-3 cell-surface expression was assessed by flow cytometry to determine CD4+ T cell exhaustion. Functional responses to HCV were analyzed by IFN- γ ELISPOT, intracellular cytokine staining (IL-2 and IFN- γ) and CFSE-based proliferation assays.

Results

We observed a significant decrease in the expression of PD-1 in CD4+ T-cells after 12 weeks of viral clearance in non-cirrhotic patients ($p = 0.033$) and in treatment-naive patients ($p = 0.010$), indicating a partial CD4 phenotype restoration. IFN- γ and IL-2 cytokines

Funding: This study was funded by Instituto de Salud Carlos III, cofinanced by the European Regional Development Fund (ERDF): grant numbers PI16/00337, PI18/00210 and PI19/00301. C.P. is supported by the Miguel Servet program of the Instituto de Salud Carlos III (CP14/00121 and CPII19/00001) cofinanced by the European Regional Development Fund (ERDF).

Competing interests: The authors have declared that no competing interests exist.

production by HCV-specific CD4⁺ and CD8⁺ T cells remained impaired upon HCV eradication. Finally, a significant increase of the proliferation capacity of both HCV CD4⁺ and CD8⁺ specific T-cells was observed after HCV elimination by DAAs therapies.

Conclusions

Our results show that in chronically infected patients HCV elimination by DAA treatment lead to partial reversion of CD4⁺ T cell exhaustion. Moreover, proliferative capacity of HCV-specific CD4⁺ and CD8⁺ T cells is recovered after DAA's therapies.

Introduction

Hepatitis C is an infectious disease caused by HCV, associated with significant liver-related morbidity and mortality. Approximately, 15–45% of infected people spontaneously clear the infection [1], but the vast majority of infections course asymptotically and become chronic. Of those with chronic HCV infection, 15–45% will silently develop advanced liver fibrosis/cirrhosis within 20–30 years [2] and 2–4% of all HCV cases will develop liver cancer or liver failure [3]. Short-duration therapy with Direct-Acting Antivirals (DAAs), lead to a Sustained Virological Response (SVR) in more than 95% of patients regardless of viral genotype and with minimal side effects [4]. However, individuals with advanced liver disease are still at risk of developing HCC [5] and many of them remain on liver transplant lists [6] after HCV infection cure.

HCV-specific T cell immune responses are required for viral control. HCV-specific CD4⁺ T cells have important helper functions, contributing to maintain the CD8⁺ T cell response and preventing viral escape from T cell response [7]. Lack or loss of helper functions by CD4⁺ T cells can result in a dysfunctional CD8⁺ T cell response and an immune response failure against the virus [8, 9]. HCV-specific CD8⁺ T cells play an essential role in HCV control since they may be involved not only in the elimination of infected hepatocytes but also in non-cytolytic effector mechanisms [10, 11]. Self-limiting HCV infections are associated with expansion of virus-specific CD8⁺ T cells, a broad CD4⁺ T cell responses, and a strong cytotoxic T lymphocyte response [12–15]. During chronic HCV infection, constant exposure to viral antigens along with immunological factors results in varying degrees of functional impairment of HCV-specific T-cell effector functions, contributing to viral persistence [16–18].

Several groups have investigated whether DAAs treatment, and the subsequent elimination of HCV, can restore the HCV-specific immune responses, although controversial results have been reported. For instance, it has been demonstrated that HCV-specific T cell functions does not completely ameliorate after SVR [19]. In contrast, other studies have observed an increase in T-cell functionality after DAA treatment [20]. It is known that, early impairment of proliferation may contribute to loss of T cell response and chronic HCV persistence [21]. Despite the fact that there is not yet a solid evidence that T cell proliferation is fully recovered after HCV cure, several studies have seen a rise in the proliferative profile of CD8 T cells in chronic HCV infected patients after DAA treatment [20, 22, 23]. While few have observed a partial or inexistent proliferative capacity recovery [24, 25]. Likewise, few and contradictory information have been reported about CD4⁺ T cell proliferative capacity after DAAs [24, 26].

Thus, there is still an open question on whether the elimination of HCV with DAAs results in a full, partial or inexistent restoration of the immune response.

In the present study, we investigate the phenotypical and functional changes of HCV-specific CD8⁺ and CD4⁺ T-cells responses in order to study the degree of immune restoration experienced by patients that achieved SVR after DAA treatment.

Materials and methods

Patients

Twenty-seven patients chronically infected with HCV were recruited from the Liver Disease Unit of Vall d'Hebron Hospital in Barcelona, Spain. The study was approved by the Institutional Review Board on Clinical Research of Vall d'Hebron Hospital (Code: HCV-SIR) and all subjects gave written informed consent in accordance with the 1975 Declaration of Helsinki.

Patient characteristics and clinical parameters are provided in Table 1 and the information of each patient is disclosed in S1 Table. All patients were HBV surface antigen and anti-HIV negative at the time of blood collection. The study included thirteen patients with HCV genotype 1a and fourteen patients with genotype 1b that received different combinations of IFN-

Table 1. Patient's characteristics.

Patient characteristics (N = 27)		
Age, mean (\pm SD)	55 (\pm 12.6)	
Gender, N Male (%)	12 (44.4)	
Liver stiffness, fibrosis score, N (%)		
< 9.5 KPa	15 (55.5)	
\geq 9.5 KPa	12 (44.5)	
HCV genotype 1 subtypes, N (%)		
1a	13 (48.1)	
1b	14 (51.9)	
DAAs treatment, N (%)		
SOF/LDV ^a	17 (63.0)	
SOF/LDV + RBV	4 (14.8)	
SOF / SMV ^b	1 (3.7)	
EBR / GZR + RBV ^c	2 (7.4)	
OBV/PTV/R + DSV + RBV ^d	3 (11.1)	
Previous treatment, N (%)		
Naive	16 (59.3)	
PEG-IFN / RBV	9 (33.3)	
PEG-IFN / RBV / BOC ^e	2 (7.4)	
Transaminase enzymes, mean (\pm SD)		
	Baseline	FUW12
ASG (UI/L) ^f	60.5 (\pm 38.7)	23.9 (\pm 8.4)
ALT (UI/L) ^g	79.7 (\pm 61.4)	19.9 (\pm 7.8)
Y-GT (UI/L) ^h	68.6 (\pm 62.8)	21.6 (\pm 7.9)
Bilirubin, mean (\pm SD)		
	Baseline	FUW12
Srm-bilirubin (ug/dL) ⁱ	0.8 (\pm 0.3)	0.8 (\pm 0.4)
Srm-esterified bilirubin (ug/dL) ^j	0.3 (\pm 0.1)	0.3 (\pm 0.1)

^a Sofosbuvir/Ledipasvir

^b Sofosbuvir / Simeprevir

^c Elbasvir / Grazoprevir

^d Ombitasvir/Paritaprevir/Ritonavir+Dasabuvir + Ribavirin

^e Pegylated Interferon- α / Boceprevir

^f Aspartate aminotransferase. Normal values <35–50 UI/L

^g Alanine aminotransferase. Normal values <50 UI/L

^h Gamma glutamyl transferase. Normal values <55 UI/L.

ⁱ Total Bilirubin. Normal values <1.20 ug/dL

^j Esterified bilirubin. Normal values <0.57 ug/dL

<https://doi.org/10.1371/journal.pone.0254243.t001>

free DAA therapies. Eleven patients had received IFN-based regimens before DAA therapy. Fifteen patients were non-cirrhotic with mild fibrosis grade based on transient elastography (Liver stiffness < 9.5 KPa) and 12 patients had an advanced stage of liver fibrosis or cirrhosis (Liver stiffness > 9.5 KPa). Blood samples used for this study were collected at the following times: prior to DAA treatment (baseline), at 4 weeks of treatment (W4), at the end of the treatment (EOT), and 12 weeks after the end of treatment (FUW12). All treated individuals included in this study achieved a SVR (i.e., undetectable HCV RNA by 12 weeks after treatment cessation) and patients 7 and 9 developed HCC after 61 and 55 month of follow up respectively.

Cell Isolation, cryopreservation and thawing

PBMCs were isolated from whole blood by density gradient centrifugation in BD Vacutainer-CPT Mononuclear Cell Preparation tubes (BD Biosciences, San Diego, CA). Samples were cryopreserved in medium containing 90% fetal calf serum (GIBCO BRL) and 10% DMSO (Sigma-Aldrich, St Louis, MO) and cryopreserved at -80°C . All assays were performed with thawed PBMCs maintained in completed RPMI 1640 (GIBCO/Invitrogen) supplemented with 10% heat-inactivated human AB serum, 2 mmol/L L-glutamine and 100 $\mu\text{g}/\text{mL}$ streptomycin.

Phenotypic analysis of CD4⁺ T cell

After being thawed, 1×10^6 PBMCs in completed medium were washed with PBS-0.5% fetal calf serum and stained with the fluorescently labeled anti-human antibodies CD4-FITC (BD Biosciences Cat#555346), PD1-PE (BD Biosciences Cat#557946), LAG3-BV421 (BD Biosciences Cat#565720), TIM3-AlexaFluor641 (BD Biosciences Cat#565558) and their corresponding isotype controls; FITC Mouse IgG1,k Isotype (BD Biosciences Cat#551954); PE Mouse IgG1,k Isotype (Beckman Coulter Cat#A07796), BV421 Mouse IgG1,k Isotype (BD Biosciences Cat#562438) and Alexa Fluor 647 Mouse IgG1 Isotype (BD Biosciences Cat#565571) at 4°C , for 30 min in the dark. For the identification and quantitation of exhausted CD4⁺ T cell subsets, 100,000 events were acquired per sample and analyzed in a Fortessa equipped with the FACS DIVA software (BD Biosciences, San Jose, CA). BD FACS Express software (BD Biosciences, San Jose, CA) was used for data analysis. Results were expressed as a percentage of positive cells.

HCV-specific CD4⁺ and CD8⁺ antigen-specific T cell responses

HCV antigens for PBMC stimulation. The 28 and 98 peptides (15–19-mers with 11–12 amino acid (aa) overlaps) spanning the core and nonstructural protein 3 (NS3), respectively, of HCV subtype 1a (H77) and 1b (J4) were obtained through the NIH Biodefense and Emerging Infectious Research Resources Repository, NIAID, NIH (peptide arrays, HCV Core and NS3 proteins, NR-3737, NR-3747, NR-3752, NR-37452). Purified recombinant HCV NS3-helicase (aa: 1207–1488) proteins derived from subtype 1a and 1b sequences and expressed in the yeast *Pichia pastoris* were purchased from Mikrogen (Neuried, Germany).

PBMCs were stimulated with 4 $\mu\text{g}/\text{mL}$ of overlapping HCV Core or NS3 pool peptides or 2 $\mu\text{g}/\text{mL}$ of NS3 Helicase protein subtype 1a or 1b. PBMCs stimulated with 1 $\mu\text{g}/\text{mL}$ of *Staphylococcus aureus* enterotoxin B (SEB; Sigma-Aldrich, Deisenhofer, Germany) or incubated with completed medium alone were used as positive and negative controls, respectively.

IFN- γ ELISpot assay. Freshly thawed PBMCs were cultured at a density of 5×10^5 cells per mL in completed medium and stimulated with HCV antigens as above. After overnight incubation at 37°C and 5% CO_2 , ELISPOT assays were performed according to previously published [27]. Results were expressed as the number of IFN- γ SFCs per 10^6 PBMCs (IFN- γ

SFCs/ 10^6 PBMCs). Median number of IFN- γ SFCs/ 10^6 PBMCs stimulated with different HCV antigens was compared between the time points. Assays with high background or no SEB response were excluded.

Intracellular cytokine staining. Freshly thawed PBMCs at a density of 1×10^6 cells per ml in completed medium supplemented with 0.67 μ L per ml of BD GolgiStop Protein Transport Inhibitor containing monensin (BD Biosciences, San Diego, CA) were stimulated with HCV antigens as described above and co-stimulated with 1 μ g/ml of anti-human CD28 antibody (BD Biosciences, Heidelberg, Germany). After 12–16 h of incubation at 37°C and 5% CO₂, cells were stained with anti-human CD4-FITC (BD Biosciences Cat#555346), anti-human CD8-PE (BD Biosciences Cat#555635) or the respective isotype control antibodies for 30 min at 4°C in complete darkness, and then fixed and permeabilized with BD Cytofix/Cytoperm solution (BD Biosciences, San Diego, CA) [27]. After permeabilization, cells were stained with anti-human IFN γ -APC (BD Biosciences Cat#554702) and anti-human IL2-PerCP-Cy5.5 (BD Biosciences Cat#560708) or the respective isotype control antibodies: APC-Mouse IgG1,k Isotype (BD Biosciences Cat#550854) and PerCP-Cy5.5 Rat IgG2a Isotype (BD Biosciences Cat#550765) at 4°C for 30 min in the dark, and washed twice with 1xBD Perm/Wash Buffer. Flow cytometry data was acquired using a FACSCalibur (BD Biosciences, San Jose, CA) and analyzed with CellQuest software (BD Biosciences, San Jose, CA). The number of viable cells that had produced IFN γ and IL2 was determined by gating on the CD4+ and CD8+ positive for those two markers and subtracting the background response.

Proliferation assay of HCV-specific CD4+ and CD8+ antigen-specific T cell. Antigen-specific T cell proliferation was determined in all patients by carboxy-fluorescein diacetate succinimidyl ester (CFSE) dilution assay as previously published [28]. After 5 days at 37°C, cells were washed and stained with anti-human CD4-PE (BD Biosciences Cat# 555347) and CD8-APC (BD Biosciences Cat# 555369) antibodies, and the viability dye 7-AAD. Flow cytometry analysis were performed on a FACSCalibur using CellQuest software (BD Biosciences, San Jose, CA). The number of viable cells that had proliferated was determined by gating on the CD4+CFSE^{low} and CD8+CFSE^{low}. Proliferation index was calculated as the ratio between CD4+ or CD8+ proliferative frequency (%) in the presence of specific antigen and that in the absence of antigen, as previously reported [28].

Statistical analysis

Results are presented as mean and SD. Comparisons between groups were performed with nonparametric Wilcoxon signed-rank test. P-values of less than 0.05 were considered significant. All Data was analyzed by GraphPad Prism 6.

Results

Partial reversion of the exhausted phenotype signatures in CD4+ T cells after DAA therapy depends on clinical parameters

Cell surface expression of Programmed cell death protein 1 (PD-1), T cell immunoglobulin and mucin domain-containing protein 3 (TIM-3), and Lymphocyte-activation gene 3 (LAG-3), which have been identified as markers of exhausted T cells, was tested by Flow Cytometry in baseline and FUW12 samples of the 27 patients. We observed a slight decrease of PD-1, TIM-3 and LAG-3 expression on CD4+ T cells in FUW12 samples compared to baseline samples, although the differences were not statistically different (Fig 1A). However, significant differences were observed when clinical parameters like fibrosis stage and previous IFN-based treatment were taken into account. By doing so, we observed that non-cirrhotic patients

showed a statistically significant decrease of PD-1 receptor expression at the surface of CD4+ T cells from FUW12 samples compared to baseline ($p = 0.033$), while cirrhotic patients did not show a clear tendency to reduce this T cell exhaustion marker (Fig 1B). Moreover, PD-1 surface expression in treatment-naive patients after HCV elimination at FUW12 was significantly lower than that at the baseline ($p = 0.010$), while in those patients who received previous IFN- α treatment, this decrease was not observed (Fig 1C).

In addition, only treatment-naive patients below 55 years of age showed a significant reduction of PD-1 expression (Fig 1D).

These data suggest that restoration of CD4+ T cells exhausted phenotype is achieved in non-cirrhotic, treatment-naive and treatment-naive below 55, while in cirrhotic, IFN- α previously treated and older age patients, HCV clearance does not fully revert the exhausted phenotype of CD4+ T cells.

HCV specific CD4+ and CD8+ T cells do not reverse the impaired cytokine production after HCV elimination by DAA regimens

We assessed whether the impaired functionality of HCV-specific CD4+ and CD8+ T cells manifested by reduced T helper 1 cytokine production (IL2 and IFN- γ) during chronic hepatitis C is restored upon HCV clearance with DAA treatments. To do so, PBMCs isolated from blood samples of patients with chronic HCV infection at baseline, W4, EOT, and FUW12 were stimulated with HCV antigens as described in the methods section. Comparisons between baseline and FUW12 samples of all patients included in the study did not reveal any significant increase in IFN- γ production after HCV elimination (Fig 2A). However, the number of IFN- γ SFC per 10^6 PBMCs significantly increased in FUW12 samples compared to baseline in G1b patients after stimulation with NS3 Helicase ($p = 0.042$) or Core peptides ($p = 0.013$). Moreover, a similar increase was observed when comparing FUW12 versus W4 sample-pairs after stimulation with Core peptides ($p = 0.021$), and FUW12 versus EOT sample-pairs after stimulation with NS3 31–44 peptides ($p = 0.023$) (Fig 2B).

To further study the immune response restoration status, intracellular cytokine levels produced by HCV-specific CD4+ and CD8+ T-cells after 16 hours of stimulation with HCV antigens was determined in all patients at baseline, W4, EOT, and FUW12. The percentages of CD4+ IFN- γ + T cells and CD4+ IL2+ T cells at FUW12 were not significantly higher than that observed in baseline or W4, independently of the HCV antigens used for stimulation (Fig 3A). T cells stimulated with NS3 31–44 peptides showed a significant decrease in IL2 production in CD4+ T cells between baseline or W4 and FUW12 samples ($p = 0.014$ and $p = 0.043$, respectively) and in CD8+ T cells between W4 and EOT ($p = 0.020$), and between EOT and FUW12 ($p = 0.040$). Interestingly, a significant increase in IL2 production was observed in CD8+ T cells after stimulation with Core peptides when comparing baseline with W4 ($p = 0.028$), EOT ($p = 0.031$) and FUW12 ($p = 0.029$).

Our data indicate that cytokine production by HCV-specific CD4+ and CD8+ T cells remains impaired after HCV elimination by DAA treatments. However IL2 production increases in CD8+ T cells stimulated with core antigen.

Proliferative capacity on HCV-specific CD4+ and CD8+ T cells is restored in the majority of chronic hepatitis C patients after HCV elimination with DAA treatments

To determine whether the limited proliferation capacity of HCV-specific CD4+ and CD8+ T cells observed during chronic HCV infection was reversed following the elimination of the virus with DAA therapy, the proliferative capacity of these cells before and after DAA therapy

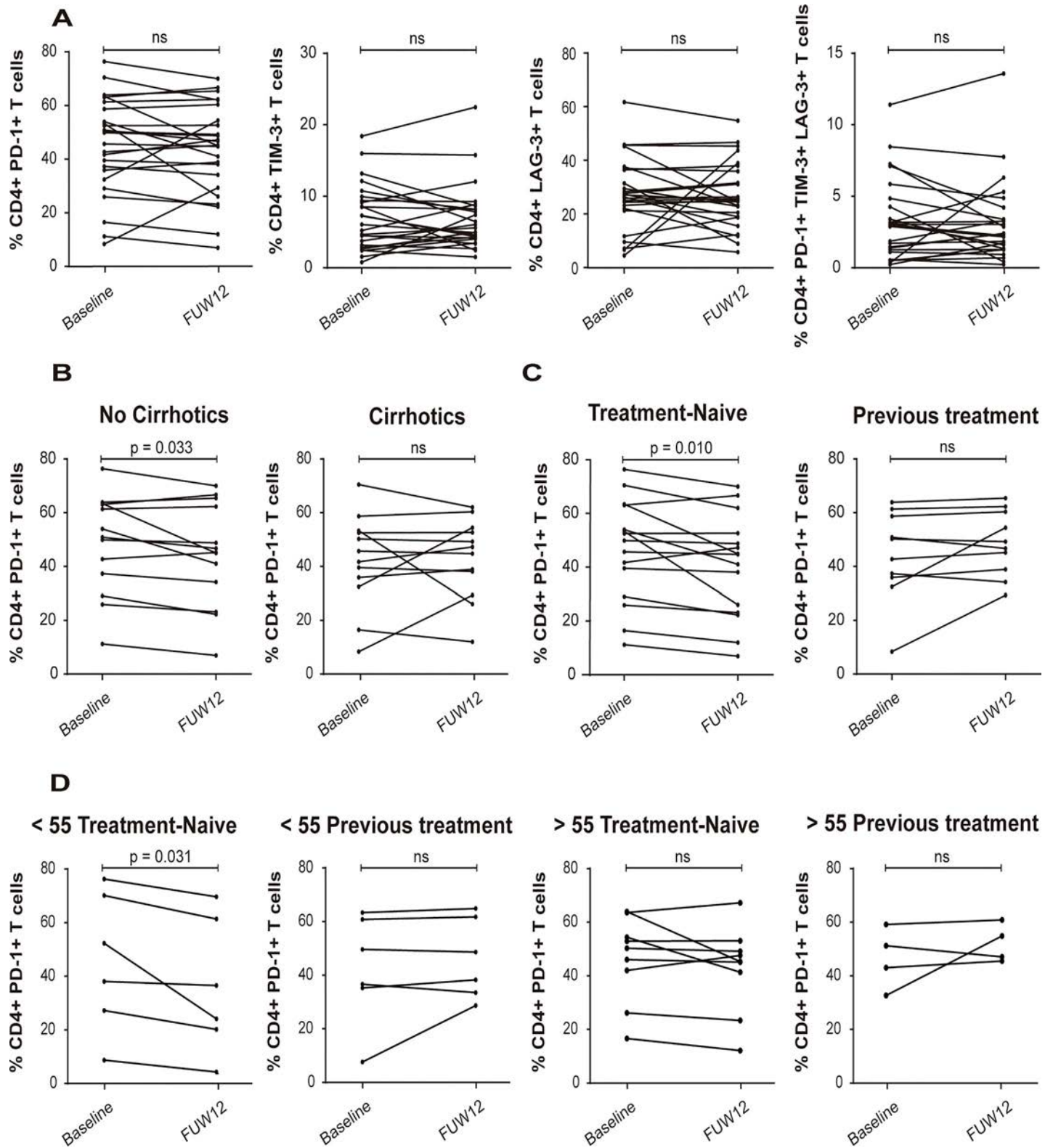


Fig 1. CD4+ T cell exhaustion markers expression. (A) Analysis of the frequencies of PD-1, TIM-3, LAG-3 markers among CD4+ T cells at baseline and FUW12, (N = 25). (B) Percent of PD-1 among CD4+ T cells according to score fibrosis. Non cirrhotic patients (N = 13), liver stiffness < 9.5 KPa; Cirrhotic patients (N = 12), liver stiffness \geq 9.5 KPa. (C) Percent of CD4+ PD-1+ T cells in treatment-naïve patients (N = 15), and in patients with previous IFN-based therapy (PEG-IFN- α + RBV) (N = 10). (D) Percent of CD4+ PD-1+ T cells in treatment-naïve patients below 55 (N = 6), in patients below 55 with previous PEG-IFN- α + RBV treatment (N = 6), in

treatment-naive patients over 55 ($N = 9$) and in patients below 55 previously treated with PEG-IFN- α + RBV ($N = 4$). Statistical significance was determined by nonparametric Wilcoxon signed-rank test and represented by p-value. $P < 0.05$ was considered statistically significant.

<https://doi.org/10.1371/journal.pone.0254243.g001>

was compared. A significant increase in the proliferative capacity of both CD4+ and CD8+ T cells between baseline and FUW12, after stimulation with NS3 Helicase ($p = 0.049$ and $p = 0.012$, CD4+ and CD8+ T cells, respectively), NS3 31–44 pooled peptides ($p = 0.031$ and $p = 0.028$, CD4+ and CD8+ T cells, respectively) and NS3 45–61 pooled peptides ($p = 0.004$ and $p = 0.012$, CD4+ and CD8+ T cells, respectively) was observed (Fig 4A). On the other hand, when considering fibrosis score, proliferation capacity of CD4+ and CD8+ T cells significantly increased in non-cirrhotic patients after NS3 31–44 peptides stimulation compared with cirrhotic ones ($p = 0.034$ and $p = 0.041$, respectively) (Fig 4B).

In summary, our data suggest that DAAs-mediated HCV clearance partially restores the proliferative capacity of virus-specific CD4+ and CD8+ T cells.

Liver inflammation and fibrosis markers

To determine if liver inflammation and fibrosis stage regression occurred after therapy-mediated HCV elimination, liver inflammation and fibrosis markers were measured at baseline and FUW12 for each patient. All markers including transaminases, Fibrosis-4 (FIB-4) index, α -fetoprotein (AFP), and AST-to-platelet ratio index (APRI) showed a significant reduction ($p = < 0.0001$) 12 weeks after DAA-treatment (Fig 5). These data indicate that a reduction in liver inflammation and a fibrosis stage regression was achieved in all patients after DAA regimens, suggesting that a liver regeneration was still ongoing.

Discussion

Persistent antigen stimulation, as in chronic infections, leads to T cell exhaustion and dysfunction, which results in an impaired immune response against the virus [29]. The exhaustion of HCV-specific T cells is characterized by up-regulation of PD-1 and other inhibitory receptors, low proliferative capacity, dysfunctional CD8 cytotoxicity, and impaired production of immunomodulatory cytokines [30–32].

In the present study we evaluated the degree of immune restoration by performing the analysis of phenotypic and functional changes in T cells before, during and after HCV elimination by DAA therapies.

Because host factors, including age and gender, can largely influence the immune response, the study cohort included both males and females in their middle age and elderly patients. Most patients with advanced liver fibrosis had abnormal baseline levels of liver inflammation and fibrosis markers, including transaminases, FIB-4, AFP, and APRI [33, 34]. All patients achieved SVR irrespective of the specific DAA treatment. HCV clearance was associated with decreased levels of liver inflammation and fibrosis markers, which correlates with the reduction of liver fibrosis related cytokines after HCV eradication by DAA treatment observed by Sasaki et al. [35].

Recent studies have demonstrated that DAA treatments reduce but do not eliminate the risk of developing HCC [36]. Indeed, 2 out of 27 patients who received DAA regimens in this study developed HCC at months 54 and 60 of follow-up, corresponding to a 5-years cumulative HCC rate of 7.4%. Despite the lack of specific predictors of HCC, several host factors, including liver fibrosis stage, older age, elevated AFP levels, and comorbidities such as diabetes and steatosis, have been associated with HCC occurrence [33, 37, 38]. Remarkably, patients who developed HCC were the oldest in our patients' cohort, suggesting that older age along

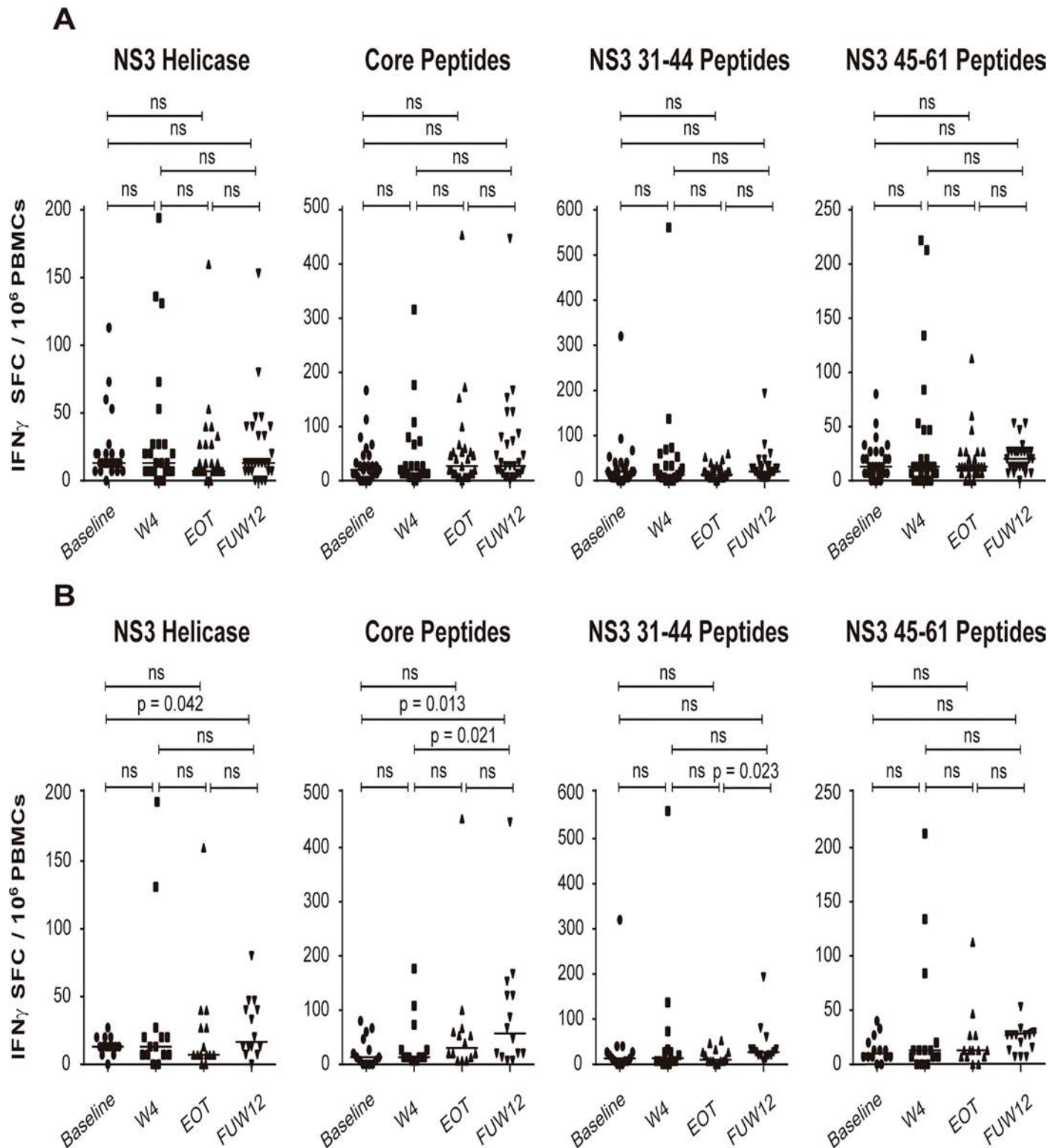


Fig 2. HCV specific T cells immune response analyzed by IFN- γ ELISPOT. Results were expressed as number of SFC producing IFN- γ . (A) IFN- γ production of 10⁶ PBMCs tested at baseline, W4, EOT, and FUW12. Total PBMCs were stimulated with HCV Peptides (NS3 Helicase, Core Peptides, NS3 31–44 Peptides and NS3 45–61 Peptides), (N = 27). (B) IFN- γ production of 10⁶ PBMCs tested in subtype 1b patients (N = 14). Horizontal bars represent median of IFN- γ SFC and each dot represents IFN- γ response from one patient. Median of IFN- γ SFC between different times were compared with Wilcoxon signed-rank test. P < 0.05 was considered statistically significant.

<https://doi.org/10.1371/journal.pone.0254243.g002>

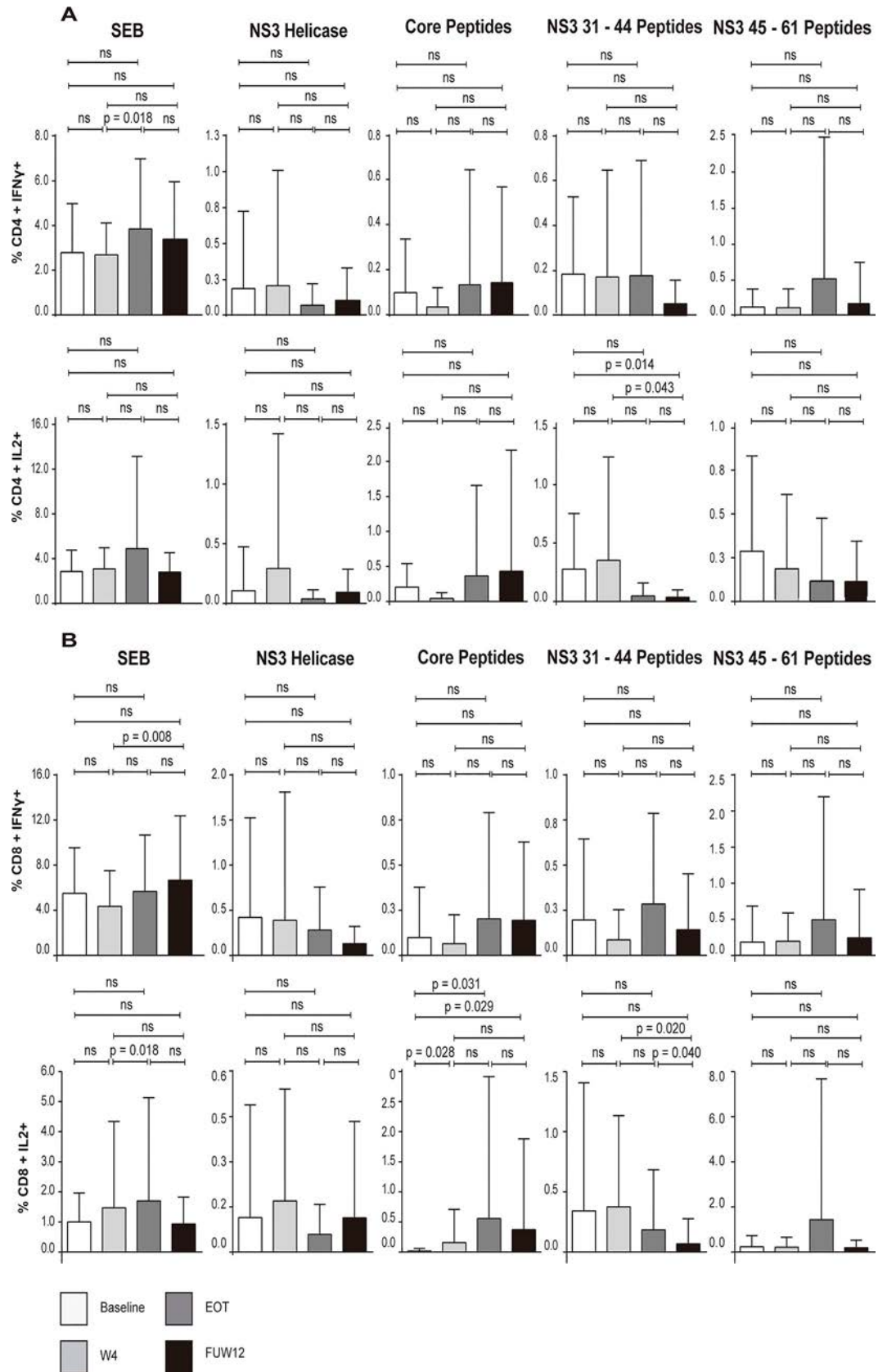


Fig 3. Intracellular cytokines staining (IFN- γ and IL-2) secreted by T cells of HCV-infected individuals. Frequencies of IFN- γ and IL-2 producing CD4+ and CD8+ specific T-cells were tested at 4 time points; baseline, W4, EOT and FUW12. T cells were stimulated with anti-CD28, monesin-containing transport inhibitor, HCV Peptides (NS3 Helicase, Core Peptides, NS3 31–44 Peptides, NS3 45–61 Peptides) and SEB as a positive control. (A) Percent CD4+ T cells producing IFN- γ and IL-2, (N = 22). (B) Percent CD8+ T cells producing IFN- γ and IL-2, (N = 22). Statistical significance was determined by Wilcoxon signed-rank test. $P < 0.05$ was considered statistically significant.

<https://doi.org/10.1371/journal.pone.0254243.g003>

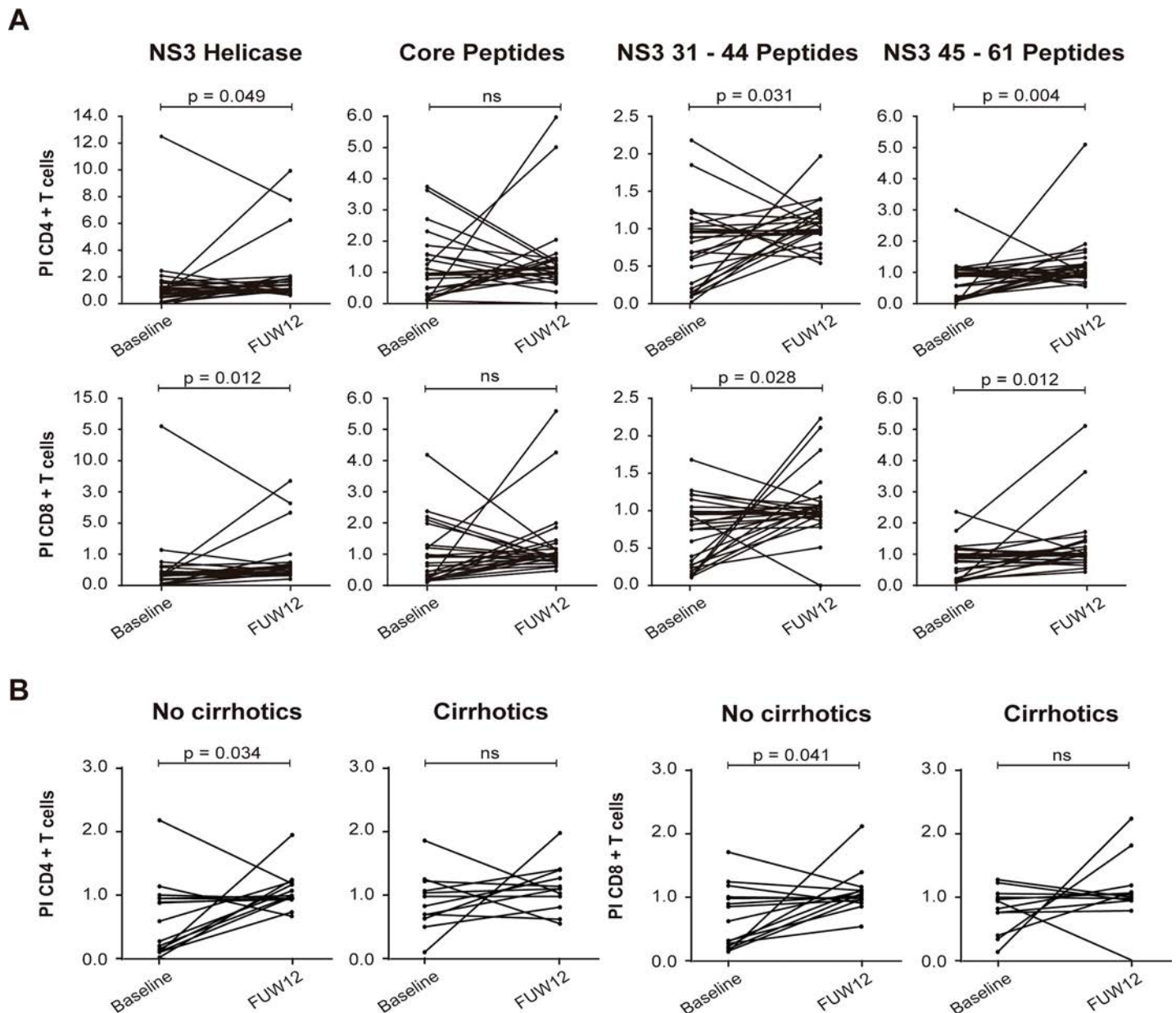


Fig 4. Proliferation responses of CD4+ and CD8+ HCV specific T-cells. In vitro expansion of PBMCs after 5 days of stimulation with HCV peptides (NS3 Helicase, Core Peptides, NS3 31–44 Peptides, NS3 45–61 Peptides). Proliferation capacity was calculated as the proliferation index, at baseline and FUW12, (A) Proliferation index of CD4+ and CD8+ T cells (N = 27). (B) T cells proliferation index according to score fibrosis when stimulated with NS3 31–44 Peptides. CD4+ and CD8+ T cells of non-cirrhotic patients (N = 15) and (N = 12) respectively, liver stiffness < 9.5 KPa; CD4+ and CD8+ T cells of cirrhotic patients (N = 12) and (N = 12) respectively, liver stiffness ≥ 9.5 KPa. Statistical significance was determined by nonparametric Wilcoxon signed-rank test and represented by p-value. $P < 0.05$ was considered statistically significant.

<https://doi.org/10.1371/journal.pone.0254243.g004>

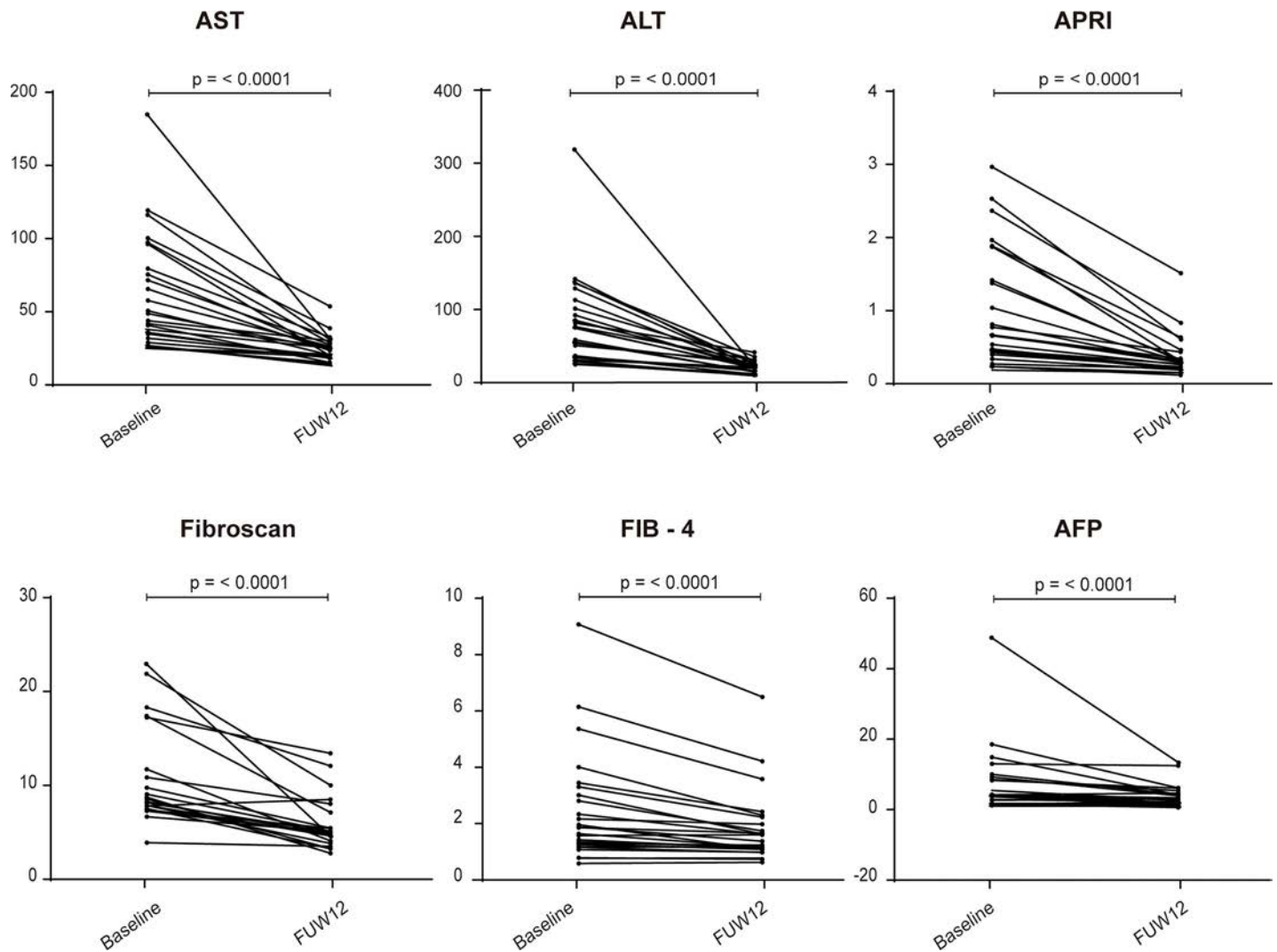


Fig 5. Liver inflammation and fibrosis markers. Levels of transaminases (AST, ALT), APRI, fibroscan, FIB-4 and AFP were measured at baseline and FUW12. Statistical significance was determined by Wilcoxon signed-rank test. $P < 0.05$ was considered statistically significant.

<https://doi.org/10.1371/journal.pone.0254243.g005>

with advanced fibrosis stage at baseline was a significant driving factor in the HCC development in these patients. Other host factors that may have contributed to the occurrence of HCC include the elevated AFP after DAA treatment in patient 7 and diabetes in patient 9.

To study the restoration of immune response after DAA treatment, we first characterized the exhausted phenotype of CD4⁺ T cells before and FUW12 by analyzing the expression of immune response inhibitory markers PD-1, TIM-3, and LAG-3 at the cell surface.

Interestingly, a significant decrease in cell surface expression of PD-1 was observed in FUW12 samples compared with its baseline pair in non-cirrhotic and treatment-naïve patients, suggesting that the immune response in these patients might have partly recovered. However, no significant differences were found when considering cirrhotic and IFN- α treated patients, which is in concordance with previous studies [25, 39], indicating that CD4 exhausted phenotype is not fully restored in all DAA-treated patients resolving infection.

The fact that after HCV eradication, PD1 expression levels were significantly reduced in treatment-naïve patients compared with IFN- α treated ones and in non-cirrhotic patients

compared with cirrhotic ones, suggests that cirrhotic's derived T cells show a deeper functional exhaustion than the non-cirrhotic ones, which may be associated with the difference in liver damage and more impaired HCV-specific immune response. Moreover, it is possible that treatment-naïve patients might be more receptive to respond to new treatment than IFN- α treated ones, as IFN-based therapies could have induced phenotypical changes towards T cells, making them to be less prone to switch off the exhausted phenotype. In addition, no significant differences in PD-1 levels at baseline and FUW12 were observed among treatment-naïve patients over 55 years of age, indicating that older patients may be less likely to reverse T cell exhaustion. Thus, failure to reverse the exhausted phenotype may have also contribute to HCC development in patients 7 and 9.

In summary, a partial restoration of the CD4+ T cell exhausted phenotype in patients with low grade of fibrosis, in treatment-naïve and in treatment-naïve patients below 55 years old, was observed.

Regarding the pro-inflammatory cytokines, it has been reported that NK and T cells produce high quantities of IFN- γ and other pro-inflammatory cytokines during acute infections, while production is decreased during chronic infections [24, 40, 41].

Interestingly, Sasaki et al. reported higher levels of pro-inflammatory cytokines, including IFN- γ and IL-2, in serum of rapid virological responders as compared with end of treatment responders, suggesting that enhanced host immune status may contribute in HCV clearance [35]. Here, we have measured IFN- γ and IL-2 production of lymphocytes stimulated in vitro, comparing the baseline and FUW12 samples of each patient and found that HCV clearance per se is not sufficient to reverse the decreased production of IFN- γ and IL-2 by HCV-specific T cells, suggesting that prolonged exposure to HCV antigens leads to long-lasting HCV-specific T cells that lack effector functions. Thus, we could show that impaired HCV-specific CD4+ and CD8+ T cells responses during chronic HCV infection are not restored following successful HCV clearance, at least in the short-time after HCV elimination, which is in line with recent published studies [25, 39, 41–43].

During chronic infections, virus-induced transcriptional reprogramming contributes to the maintenance of exhausted T cells in hyporesponsive states [8, 29, 44, 45]. As we have shown, T cell functionality remain impaired despite SVR, suggesting persistent transcription factor or epigenetic changes in HCV-specific T-cell after infection resolution. Moreover, those alterations have been reported to be directly associated with advanced liver diseases as HCC [46, 47].

The analysis of IFN- γ ELISPOT results by HCV subtypes revealed that patients with HCV subtype 1b showed higher IFN- γ restoration than those with HCV subtype 1a, which could be attributed to a different immunogenicity between subtypes [48], or due to T-cell-mediated protective immunity against other viral strains to which the patient was previously exposed [49].

Various studies point to the fact that a restoration of HCV-specific CD8+ T cells proliferation after DAAs treatment occurs [20, 22, 23]. But others reported that CD8 proliferation capacity was not restored after HCV elimination by DAAs in the majority of patients [24, 25]. However, little data was reported about the proliferative capacity of HCV-specific CD4+ T cells until now. A recently published study showed limited CD4+ T cell proliferative capacity of HCV specific CD4+ T-cells following DAA therapy [26]. In our study, we have observed a partial restoration of the proliferative capacity of CD4+ and CD8+ T cells after stimulation with NS3 Helicase protein and NS3 pooled peptides but not with structural HCV antigens (core), suggesting that restoration of T cell proliferation is HCV-epitope dependent, as core antigen has been related with the induction of T regs expansion and T cell exhaustion [50, 51] and non-structural antigens have been described to present a higher immunogenicity [28, 52,

53]. In accordance to our results, several studies confirmed a reinvigorated CD8+ T cell proliferative capacity after DAAs when stimulated with NS3 and NS4 peptides [20, 22, 23]. In addition, Burchill et al. also found a temporal increase in the proliferative response of CD4+ T cells when stimulating with NS3 and NS5 [24].

The discrepancies between our results and other studies pointing to a non-restoration of the proliferative capacity could be explained by different clinic-pathological conditions, by different DAA regimen used or due to the differences on immunogenicity between peptides.

Overall, our data suggest that clearance of persistent HCV antigens helps to partially increase the proliferative capacity of CD4+ and CD8+ T cells but is not sufficient to reverse T cell dysfunctionality.

The fact that those T cells remain dysfunctional after HCV clearance might have serious clinical implications. Additional immunological therapy may reduce the risk of developing HCC and other extrahepatic manifestations after DAA regimen [54]. Unfortunately, patients who have overcome the infection and cleared the virus are not protected against reinfection [55]. Moreover, no vaccine to prevent HCV infection is yet available, despite continuing efforts for its development [56]. Our study will provide information on the dynamics of HCV infection and immune response, which may be applicable to vaccine development and immunotherapy strategies, as well as on immune related liver remodeling that together with a correct diagnose and an early treatment will help to improve clinical outcomes.

Since this study has been limited to a low number of patients, similar studies with a higher number of patients need to be performed in order to avoid missing any biological significant trend. In addition, another limiting factor consists in the high intra-individual variability. Hence, we have designed the study so that each patient was their own control and comparisons were done intra-patient, avoiding additional genetic variations.

In conclusion, our study demonstrates a partial restoration of HCV-specific immune response in chronic HCV infected patients after the viral clearance induced by DAAs. Further investigations of HCV-specific T cell responses beyond 1 year of follow-up are needed to understand the long-term impact of HCV cure and their implications on HCV vaccine-design and HCV re-infections.

Supporting information

S1 Table. Clinical parameters of each patient. Age, gender, HCV genotype, previous Treatment, DAA regimens, fibroscan, transaminase enzymes (AST, ALT), APRI, FIB-4 and AFP levels were taken at baseline and FUW12.
(PDF)

Acknowledgments

The authors thank the Department of External extractions of Vall d'Hebron University Hospital (VHUH), especially to Francisco Tena who performed sample extractions and Judit Carbonell, who made the liver stiffness. Also thank Banc de Sang i Teixits (BST), Vall d'Hebron Institut de Recerca (VHIR), VHUH and Unitat d'Alta Tecnologia (UAT).

Author Contributions

Conceptualization: Maria Isabel Costafreda, Celia Perales, Silvia Sauleda, Juan Ignacio Esteban, Marta Bes.

Data curation: Meritxell Llorens-Revull, Mercedes Guerrero-Murillo, Juan Ignacio Esteban.

Formal analysis: Meritxell Llorens-Revull, Angie Rico, Maria Eugenia Soria, Pablo Gabriel-Medina, Francisco Rodríguez-Frías, Marta Bes.

Funding acquisition: Celia Perales, Josep Quer, Silvia Sauleda, Juan Ignacio Esteban, Marta Bes.

Investigation: Meritxell Llorens-Revull, Maria Isabel Costafreda, Angie Rico, Sofía Píriz-Ruzo, Elena Vargas-Accarino, Mar Riveiro-Barciela, Marta Bes.

Methodology: Meritxell Llorens-Revull, Maria Isabel Costafreda, Maria Eugenia Soria, Elena Vargas-Accarino, Pablo Gabriel-Medina, Francisco Rodríguez-Frías, Celia Perales, Marta Bes.

Project administration: Marta Bes.

Resources: Celia Perales, Juan Ignacio Esteban, Marta Bes.

Software: Mercedes Guerrero-Murillo.

Supervision: Maria Isabel Costafreda, Marta Bes.

Validation: Mar Riveiro-Barciela, Celia Perales, Marta Bes.

Writing – original draft: Meritxell Llorens-Revull.

Writing – review & editing: Maria Isabel Costafreda, Maria Eugenia Soria, Mar Riveiro-Barciela, Celia Perales, Josep Quer, Silvia Sauleda, Juan Ignacio Esteban, Marta Bes.

References

1. Micallef JM, Kaldor JM, Dore GJ. Spontaneous viral clearance following acute hepatitis C infection: A systematic review of longitudinal studies. *J Viral Hepat.* 2006; 13(1):34–41. <https://doi.org/10.1111/j.1365-2893.2005.00651.x> PMID: 16364080
2. Thein HH, Yi Q, Dore GJ, Krahn MD. Estimation of stage-specific fibrosis progression rates in chronic hepatitis C virus infection: A meta-analysis and meta-regression. *Hepatology.* 2008; 48(2):418–31. <https://doi.org/10.1002/hep.22375> PMID: 18563841
3. Gravit L. Introduction: A smouldering public-health crisis. *Nature [Internet].* 2011 Jun 8; 474(7350):S2–4. Available from: <http://www.nature.com/articles/474S2a> <https://doi.org/10.1038/474S2a> PMID: 21666731
4. Casey JL, Feld JJ, MacParland SA. Restoration of HCV-Specific Immune Responses with Antiviral Therapy: A Case for DAA Treatment in Acute HCV Infection. *Cells.* 2019; 8(4):317. <https://doi.org/10.3390/cells8040317> PMID: 30959825
5. Reig M, Mariño Z, Perelló C, Iñarrairaegui M, Ribeiro A, Lens S, et al. Unexpected high rate of early tumor recurrence in patients with HCV-related HCC undergoing interferon-free therapy. *J Hepatol [Internet].* 2016; 65(4):719–26. Available from: <https://doi.org/10.1016/j.jhep.2016.04.008> PMID: 27084592
6. Belli LS, Berenguer M, Cortesi PA, Strazzabosco M, Rockenschaub SR, Martini S, et al. Delisting of liver transplant candidates with chronic hepatitis C after viral eradication: A European study. *J Hepatol [Internet].* 2016; 65(3):524–31. Available from: <https://doi.org/10.1016/j.jhep.2016.05.010> PMID: 27212241
7. Thimme R, Oldach D, Chang KM, Steiger C, Ray SC, Chisari F V. Determinants of viral clearance and persistence during acute hepatitis C virus infection. *J Exp Med.* 2001; 194(10):1395–406. <https://doi.org/10.1084/jem.194.10.1395> PMID: 11714747
8. Zajac AJ, Blattman JN, Murali-Krishna K, Sourdive DJD, Suresh M, Altman JD, et al. Viral immune evasion due to persistence of activated T cells without effector function. *J Exp Med.* 1998; 188(12):2205–13. <https://doi.org/10.1084/jem.188.12.2205> PMID: 9858507
9. Gerlach JT, Diepolder HM, Jung MC, Gruener NH, Schraut WW, Zachoval R, et al. Recurrence of hepatitis C virus after loss of virus-specific CD4+ T- cell response in acute hepatitis C. *Gastroenterology.* 1999; 117(4):933–41. [https://doi.org/10.1016/s0016-5085\(99\)70353-7](https://doi.org/10.1016/s0016-5085(99)70353-7) PMID: 10500077
10. Jo J, Aichele U, Kersting N, Klein R, Aichele P, Bisse E, et al. Analysis of CD8 + T-Cell-Mediated Inhibition of Hepatitis C Virus Replication Using a Novel Immunological Model. *Gastroenterology [Internet].* 2009; 136(4):1391–401. Available from: <https://doi.org/10.1053/j.gastro.2008.12.034> PMID: 19185579

11. Neumann-Haefelin C, Thimme R. Adaptive Immune Responses in Hepatitis C Virus Infection. In: Bartenschlager R, editor. *Hepatitis C Virus: From Molecular Virology to Antiviral Therapy* [Internet]. Berlin, Heidelberg: Springer Berlin Heidelberg; 2013. p. 369: 243–262. Available from: https://doi.org/10.1007/978-3-642-27340-7_10
12. Cooper S, Erickson AL, Adams EJ, Kansopon J, Weiner AJ, Chien DY, et al. Analysis of a successful immune response against hepatitis C virus. *Immunity*. 1999; 10(4):439–49. [https://doi.org/10.1016/s1074-7613\(00\)80044-8](https://doi.org/10.1016/s1074-7613(00)80044-8) PMID: 10229187
13. Grakoui A, Shoukry NH, Woollard DJ, Han JH, Hanson HL, Ghayeb J, et al. HCV Persistence and Immune Evasion in the Absence of Memory T Cell Help. *Science* (80-). 2003; 302(5645):659–62. <https://doi.org/10.1126/science.1088774> PMID: 14576438
14. Lechner F, Wong DKH, Dunbar PR, Chapman R, Chung RT, Dohrenwend P, et al. Analysis of successful immune responses in persons infected with hepatitis C virus. *J Exp Med*. 2000; 191(9):1499–512. <https://doi.org/10.1084/jem.191.9.1499> PMID: 10790425
15. Bowen DG, Walker CM. Adaptive immune responses in acute and chronic hepatitis C virus infection. *Nature* [Internet]. 2005 Aug 17; 436(7053):946–52. Available from: <https://doi.org/10.1038/nature04079> PMID: 16107834
16. Bengsch B, Seigel B, Ruhl M, Timm J, Kuntz M, Blum HE, et al. Coexpression of PD-1, 2B4, CD160 and KLRG1 on exhausted HCV-specific CD8+ T cells is linked to antigen recognition and T cell differentiation. *PLoS Pathog*. 2010;6(6). <https://doi.org/10.1371/journal.ppat.1000947> PMID: 20548953
17. Klenerman P, Hill A. T cells and viral persistence: Lessons from diverse infections. *Nat Immunol*. 2005; 6(9):873–9. <https://doi.org/10.1038/ni1241> PMID: 16116467
18. Luxenburger H, Neumann-Haefelin C, Thimme R, Boettler T. HCV-Specific T Cell Responses During and After Chronic HCV Infection. *Viruses*. 2018; 10(11):645.
19. van der Ree MH, Stelma F, Willemse SB, Brown A, Swadling L, van der Valk M, et al. Immune responses in DAA treated chronic hepatitis C patients with and without prior RG-101 dosing. *Antiviral Res* [Internet]. 2017; 146(2017):139–45. Available from: <https://doi.org/10.1016/j.antiviral.2017.08.016> PMID: 28844749
20. Martin B, Hennecke N, Lohmann V, Kayser A, Neumann-Haefelin C, Kukulj G, et al. Restoration of HCV-specific CD8+ T cell function by interferon-free therapy. *J Hepatol* [Internet]. 2014; 61(3):538–43. Available from: <https://doi.org/10.1016/j.jhep.2014.05.043> PMID: 24905492
21. Folgieri A, Spada E, Pezzanera M, Ruggeri L, Mele A, Garbuglia AR, et al. Early impairment of hepatitis C virus specific T cell proliferation during acute infection leads to failure of viral clearance. *Gut*. 2006; 55(7):1012–9. <https://doi.org/10.1136/gut.2005.080077> PMID: 16484505
22. Wieland D, Kemming J, Schuch A, Emmerich F, Knolle P, Neumann-Haefelin C, et al. TCF1+ hepatitis C virus-specific CD8+ T cells are maintained after cessation of chronic antigen stimulation. *Nat Commun* [Internet]. 2017; 8(May):1–13. Available from: <https://doi.org/10.1038/ncomms15050> PMID: 28466857
23. Han JW, Sung PS, Kim KH, Hong S-H, Shin E-C, Jun Song M, et al. Dynamic Changes in Ex Vivo T-Cell Function After Viral Clearance in Chronic HCV Infection. *J Infect Dis*. 2019; 220(8):1290–301. <https://doi.org/10.1093/infdis/jiz291> PMID: 31152667
24. Burchill MA, Golden-Mason L, Wind-Rotolo M, Rosen HR. Memory re-differentiation and reduced lymphocyte activation in chronic HCV-infected patients receiving direct-acting antivirals. *J Viral Hepat*. 2015; 22(12):983–91. <https://doi.org/10.1111/jvh.12465> PMID: 26482547
25. Aregay A, Owusu Sekyere S, Deterding K, Port K, Dietz J, Berkowski C, et al. Elimination of hepatitis C virus has limited impact on the functional and mitochondrial impairment of HCV-specific CD8+ T cell responses. *J Hepatol* [Internet]. 2019; 71(5):889–99. Available from: <https://doi.org/10.1016/j.jhep.2019.06.025> PMID: 31295532
26. Hartnell F, Esposito I, Swadling L, Brown A, Phetsouphanh C, de Lara C, et al. Characterising HCV specific CD4+ T-cells following viral-vectored vaccination, directly acting anti-virals and spontaneous viral cure. *Hepatology*. 2020;
27. Bes M, Vargas V, Piron M, Casamitjana N, Esteban JI, Vilanova N, et al. T cell responses and viral variability in blood donation candidates with occult hepatitis B infection. *J Hepatol*. 2012; 56(4):765–74. <https://doi.org/10.1016/j.jhep.2011.11.011> PMID: 22173156
28. Bes M, Sauleda S, Casamitjana N, Piron M, Campos-Varela I, Quer J, et al. Reversal of nonstructural protein 3-specific CD4 + T cell dysfunction in patients with persistent hepatitis C virus infection. *J Viral Hepat*. 2012; 19(4):283–94. <https://doi.org/10.1111/j.1365-2893.2011.01549.x> PMID: 22404727
29. John Wherry E., Joseph N. Blattman, Kaja Murali-Krishna, Robbert van der Most and RA. Viral Persistence Alters CD8 T-Cell Immunodominance and Tissue Distribution and Results in Distinct Stages of Functional Impairment. *J Virol* [Internet]. 2003; 77(8):4911–4927. Available from: <https://jvi.asm.org/content/77/8/4911.short>

30. Yi JS, Cox MA, Zajac AJ. T-cell exhaustion: Characteristics, causes and conversion. *Immunology*. 2010; 129(4):474–81. <https://doi.org/10.1111/j.1365-2567.2010.03255.x> PMID: 20201977
31. Wherry EJ, Kurachi M. Molecular and cellular insights into T cell exhaustion. *Nat Rev Immunol*. 2015; 15(8):486–99. <https://doi.org/10.1038/nri3862> PMID: 26205583
32. Kahan SM, Wherry EJ, Zajac AJ. T cell exhaustion during persistent viral infections. *Virology* [Internet]. 2015; 479–480:180–93. Available from: <https://doi.org/10.1016/j.virol.2014.12.033> PMID: 25620767
33. Watanabe T, Tokumoto Y, Joko K, Michitaka K, Horiike N, Tanaka Y, et al. Predictors of hepatocellular carcinoma occurrence after direct-acting antiviral therapy in patients with hepatitis C virus infection. *Hepatol Res*. 2019; 49(2):136–46. <https://doi.org/10.1111/hepr.13278> PMID: 30335208
34. Loaeza-del-Castillo A, Paz-Pineda F, Oviedo-Cárdenas E, Sánchez-Ávila F, Vargas-Voráčková F. AST to platelet ratio index (APRI) for the noninvasive evaluation of liver fibrosis. *Ann Hepatol*. 2008; 7(4):350–7. PMID: 19034235
35. Sasaki R, Meyer K, Moriyama M, Kato N, Yokosuka O, Ray RB, et al. Rapid hepatitis C virus clearance by antivirals correlates with immune status of infected patients. *J Med Virol*. 2019; 91(3):411–8. <https://doi.org/10.1002/jmv.25310> PMID: 30192392
36. Kanwal F, Kramer J, Asch SM, Chayanupatkul M, Cao Y, El-Serag HB. Risk of Hepatocellular Cancer in HCV Patients Treated With Direct-Acting Antiviral Agents. *Gastroenterology* [Internet]. 2017; 153(4):996–1005.e1. Available from: <https://doi.org/10.1053/j.gastro.2017.06.012> PMID: 28642197
37. Peleg N, Issachar A, Sneh Arbib O, Cohen-Naftaly M, Harif Y, Oxtrud E, et al. Liver steatosis is a major predictor of poor outcomes in chronic hepatitis C patients with sustained virological response. *J Viral Hepat*. 2019; 26(11):1257–65. <https://doi.org/10.1111/jvh.13167> PMID: 31243878
38. Fujiwara N, Friedman SL, Goossens N, Hoshida Y. Risk factors and prevention of hepatocellular carcinoma in the era of precision medicine. *J Hepatol* [Internet]. 2018; 68(3):526–49. Available from: <https://doi.org/10.1016/j.jhep.2017.09.016> PMID: 28989095
39. Zhang C, Hua R, Cui Y, Wang S, Yan H, Li D, et al. Comprehensive mapping of antigen specific T cell responses in hepatitis C virus infected patients with or without spontaneous viral clearance. *PLoS One*. 2017; 12(2):1–16. <https://doi.org/10.1371/journal.pone.0171217> PMID: 28170421
40. Corado J, Toro F, Rivera H, Bianco NE, Deibis L, De Sanctis JB. Impairment of natural killer (NK) cytotoxic activity in hepatitis C virus (HCV) infection. *Clin Exp Immunol*. 1997; 109(3):451–7. <https://doi.org/10.1046/j.1365-2249.1997.4581355.x> PMID: 9328121
41. Pereira GL, Tarragô AM, Neves WLL, Da Silva Neto PV, De Souza PS, Dos Santos Affonso J, et al. Immunological Dynamics Associated with Direct-Acting Antiviral Therapies in Naive and Experimented HCV Chronic-Infected Patients. *Mediators Inflamm*. 2019;2019. <https://doi.org/10.1155/2019/4738237> PMID: 31780860
42. Hengst J, Falk CS, Schlaphoff V, Deterding K, Manns MP, Cornberg M, et al. Direct-acting antiviral-induced hepatitis c virus clearance does not completely restore the altered cytokine and chemokine milieu in patients with chronic hepatitis c. *J Infect Dis*. 2016; 214(12):1965–74. <https://doi.org/10.1093/infdis/jiw457> PMID: 27683821
43. Han Ji Won, Sung Pii Soo, Kim Kyung Hwan, Hong Seon-Hui, Eui-Cheol Shin MJSS-HP. Dynamic Changes in Ex Vivo T-Cell Function after Viral Clearance in Chronic HCV Infection. 2018;1–39. Available from: <https://pubmed.ncbi.nlm.nih.gov/31152667/>
44. Pereira RM, Hogan PG, Rao A, Martinez GJ. Transcriptional and epigenetic regulation of T cell hyporesponsiveness. *J Leukoc Biol*. 2017 Sep; 102(3):601–15. <https://doi.org/10.1189/jlb.2RI0317-097R> PMID: 28606939
45. Fuller MJ, Khanolkar A, Tebo AE, Zajac AJ. Maintenance, Loss, and Resurgence of T Cell Responses During Acute, Protracted, and Chronic Viral Infections. *J Immunol*. 2004; 172(7):4204–14. <https://doi.org/10.4049/jimmunol.172.7.4204> PMID: 15034033
46. Perez S, Kaspi A, Domovitz T, Davidovich A, Lavi-Itzkovitz A, Meirson T, et al. Hepatitis C virus leaves an epigenetic signature post cure of infection by direct-acting antivirals. *PLoS Genet*. 2019; 15(6):1–28. <https://doi.org/10.1371/journal.pgen.1008181> PMID: 31216276
47. Hamdane N, Jühling F, Crouchet E, El Saghire H, Thumann C, Oudot MA, et al. HCV-Induced Epigenetic Changes Associated With Liver Cancer Risk Persist After Sustained Virologic Response. *Gastroenterology* [Internet]. 2019; 156(8):2313–2329.e7. Available from: <https://doi.org/10.1053/j.gastro.2019.02.038> PMID: 30836093
48. Lange CM, Roomp K, Dragan A, Nattermann J, Michalk M, Spengler U, et al. HLA class i allele associations with HCV genetic variants in patients with chronic HCV genotypes 1a or 1b infection. *J Hepatol* [Internet]. 2010; 53(6):1022–8. Available from: <https://doi.org/10.1016/j.jhep.2010.06.011> PMID: 20800922

49. Sugimoto K, Kaplan DE, Ikeda F, Ding J, Schwartz J, Nunes FA, et al. Strain-Specific T-Cell Suppression and Protective Immunity in Patients with Chronic Hepatitis C Virus Infection. *J Virol*. 2005; 79(11):6976–83. <https://doi.org/10.1128/JVI.79.11.6976-6983.2005> PMID: 15890937
50. Doumba PP, Serti E, Boutsikou M, Konstadoulakis MM, Georgopoulou U, Koskinas J. Phenotypic and functional alterations of primary human PBMCs induced by HCV non-enveloped capsid-like particles uptake. *Cell Mol Life Sci*. 2013; 70(18):3463–74. <https://doi.org/10.1007/s00018-013-1344-y> PMID: 23645326
51. Zhai N, Chi X, Li T, Song H, Li H, Jin X, et al. Hepatitis C virus core protein triggers expansion and activation of CD4+CD25+regulatory T cells in chronic hepatitis C patients. *Cell Mol Immunol*. 2015; 12(6):743–9. <https://doi.org/10.1038/cmi.2014.119> PMID: 25531392
52. Smyk-Pearson S, Tester IA, Lezotte D, Sasaki AW, Lewinsohn DM, Rosen HR. Differential antigenic hierarchy associated with spontaneous recovery from hepatitis C virus infection: Implications for vaccine design. *J Infect Dis*. 2006; 194(4):454–63. <https://doi.org/10.1086/505714> PMID: 16845628
53. Diepolder HM, Zchoval R, Hoffmann RM, Jung MC, Pape GR, Wierenga EA, et al. Possible mechanism involving T-lymphocyte response to non-structural protein 3 in viral clearance in acute hepatitis C virus infection. *Lancet*. 1995; 346(8981):1006–7. [https://doi.org/10.1016/s0140-6736\(95\)91691-1](https://doi.org/10.1016/s0140-6736(95)91691-1) PMID: 7475549
54. Negro F. Natural History of Hepatic and Extrahepatic Hepatitis C Virus Diseases and Impact of Interferon-Free HCV Therapy. *Cold Spring Harb Perspect Med*. 2019;(Who 2017):a036921.
55. Aitken CK, Lewis J, Tracy SL, Spelman T, Bowden DS, Bharadwaj M, et al. High incidence of hepatitis C virus reinfection in a cohort of injecting drug users. *Hepatology*. 2008; 48(6):1746–52. <https://doi.org/10.1002/hep.22534> PMID: 18844233
56. Scott N, Wilson DP, Thompson AJ, Barnes E, El-Sayed M, Benzaken AS, et al. The case for a universal hepatitis C vaccine to achieve hepatitis C elimination. *BMC Med*. 2019; 17(1):1–12. <https://doi.org/10.1186/s12916-018-1207-3> PMID: 30651111

4.3 Study 3

Comparison of extracellular vesicle
isolation methods for miRNAs
sequencing

4.3.1 Article 3 summary

4.3.1.1 Introduction

The majority of miRNAs that are circulating freely are concentrated in exosomes, thus gaining stability. Furthermore, in a pathological process, injured cells secrete more exosomes than healthy cells, and therefore those exosomes are enriched with miRNAs involved in the pathogenesis. Moreover, exosomes provide relevant and real-time information on patient status from the different cells involved in the pathological process.

In the last few years, there has been increasing interest in miRNAs encapsulated in EVs as a novel source of clinical biomarker; however, discrepancies on miRNA patterns are still frequent between studies, which hampers the validation of specific miRNA signatures with diagnostic and/or prognostic value. This is partly due to differences in sample origin, EV-miRNA isolation and sequencing methods. Moreover, the separation of EVs from other particles, which also contain miRNAs, is difficult and varies depending on the isolation method used.

In this work, we have tested three methods to isolate and characterize exosomes from plasma samples. Despite these methods being adequate, they do not yield a pure exosome preparation. In consequence, to be cautious, we use the term EVs rather than exosomes in the third manuscript.

4.3.1.2 Hypothesis

Finding adequate methods of EV purification and miRNA sequencing would facilitate the discovery of miRNA as biomarkers of disease progression.

4.3.1.3 Objectives

1. To compare EVs isolated by different methods.
2. To analyse the yield, abundance and diversity of miRNAs obtained from different library preparation protocols.
3. To analyse the yield, abundance and diversity of miRNAs comparing different EV isolation methods.

4.3.1.4 Study design

- The same plasma sample from a blood donor was used for all the experiments.
- Three different EVs isolation methods were compared: (i) Size exclusion chromatography (SEC), (ii) Isopycnic ultracentrifugation using iodixanol gradients (GRAD), and (iii) their combination (SEC+GRAD). Experiments were performed in triplicate. EVs were characterized as depicted on Figure 15.

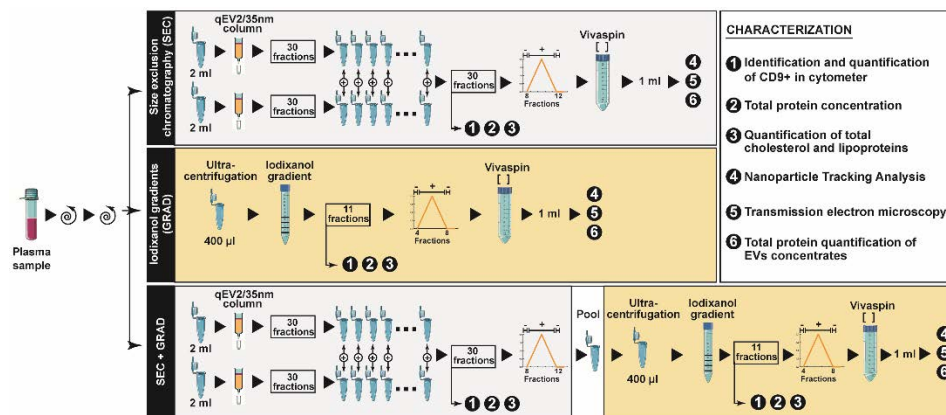


Figure 15. Diagram of EVs isolation methods used for the comparison.

- Prior to RNA extraction from the plasma sample, 52 spike-ins were added as controls. Quantity and quality of purified RNA were assessed.

Three different library preparation kits were compared; (i) NEBNext Multiplex Small RNA Library Prep Set for Illumina named as NEB; (ii) NEXTflex Small RNA-Seq Kit v3 named as NEXT; and (iii) SMARTer smRNA-seq kit named as SMARTer. Quantified libraries were mixed at the equimolar ratio and sequenced with the NextSeq 500 system (Illumina). Read trimming was performed using the specific guidelines for each library preparation kit. Reads with lengths corresponding to miRNAs were selected and mapped to a reference genome, and low expressed miRNAs were discarded. Mapped reads were quantified and normalized, and principal component analysis were performed to study the trend of aggregation between protocols and their corresponding replicas. In addition, analysis to determine the yield, abundance and diversity of miRNAs obtained from the three different library preparation kits were performed.

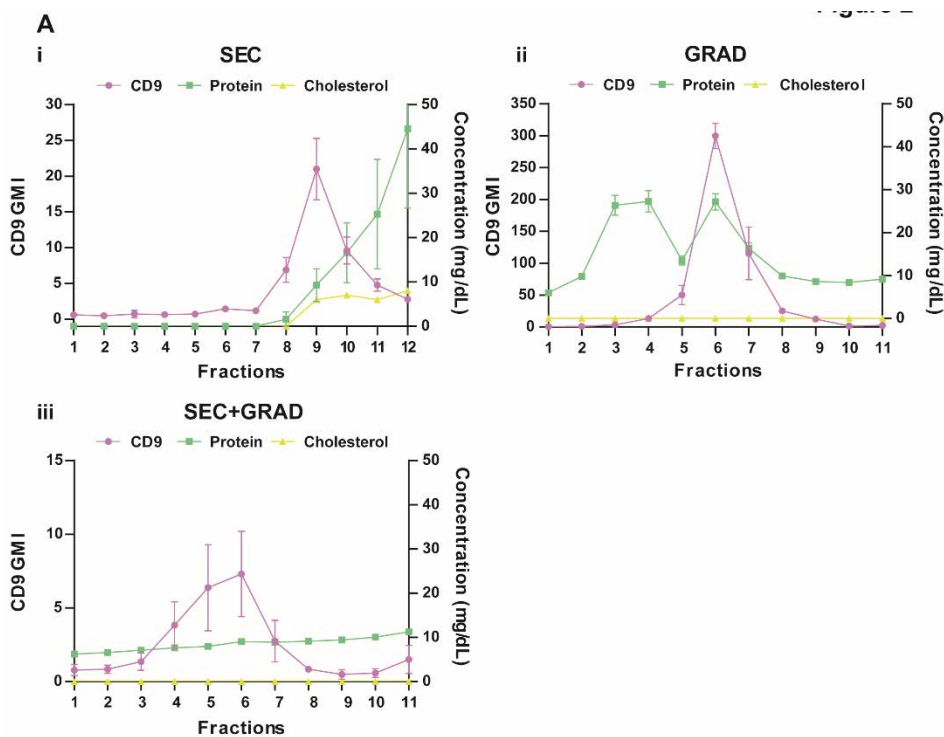
- RNA was extracted from the three replicas of the three EVs isolation methods. 52 spike-ins were added to the EVs concentrates prior to RNA extraction, and quantity and quality of purified RNA were determined.

NEBNext Multiplex Small RNA Library Prep Set for Illumina was used for library preparation. After size selection, elution and library quantification, libraries were sequenced using the NextSeq 500 system (Illumina). After sequencing, TruSeq 3' adapter was trimmed from samples, and reads corresponding to miRNAs were selected, mapped, quantified and normalized as above. Analysis to determine the yield, abundance and diversity of miRNAs obtained from SEC, GRAD and SEC+GRAD were performed.

4.3.1.5 Results according to objectives

4.3.1.5.1 Objective 1: To compare EVs isolated by different methods that range from more to less specific-methodology

The analysis of protein content showed that the three EV isolation methods removed most of the soluble plasma proteins being GRAD and SEC+GRAD those that produce a lower level of total cholesterol. In all the EVs preparations the size of the vesicles corresponded to that expected for EVs, and TEM images correlated with data obtained from NTA. Moreover, CD9 measurements presented the highest fluorescence intensity in EV fractions isolated by GRAD, followed by SEC and SEC+GRAD (Figure 16A). Based on the average EV concentration, the use of SEC allowed the recovery of a larger amount of EVs than GRAD or SEC+GRAD. GRAD yielded cleaner EV preparations, with a lower proportion of clumped vesicles. The purest EVs were obtained using SEC+GRAD, at the expense of a lower quantity of vesicles (Figure 16B).



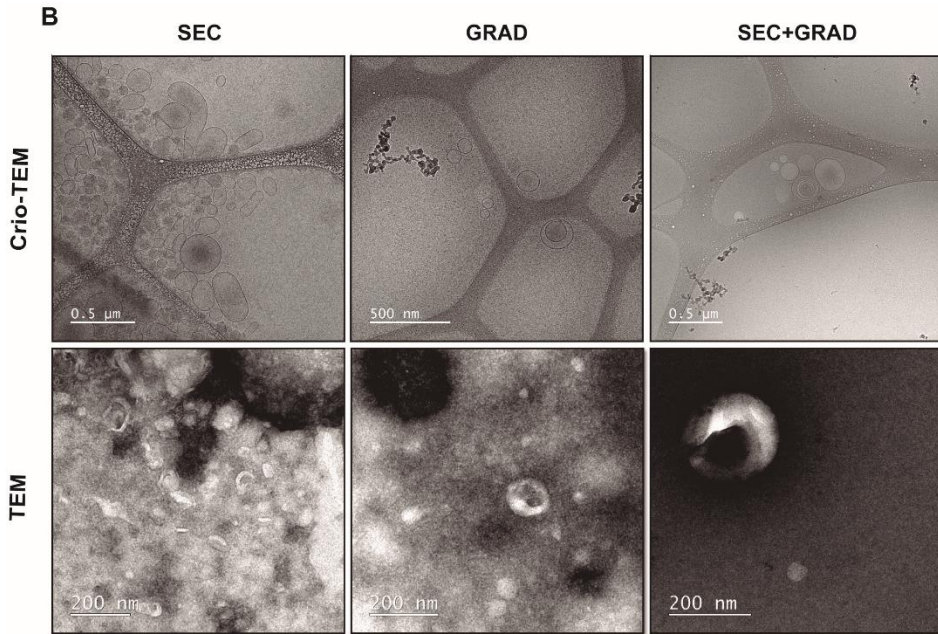


Figure 16. Characterization of three EVs isolation methods. (A) Detection of CD9, total cholesterol and total protein quantification. Codes for the quantifications are depicted in the box at the bottom right. The fractionation method is indicated in each panel, and fraction numbers in the abscissas. CD9 fluorescence intensity was measured as geometrical mean and plotted on the left axis. Total cholesterol and total proteins were measured as mg/dL and plotted on the right axis. (i) SEC extraction (ii) GRAD extraction, and (iii) SEC+GRAD extraction. (B) TEM and Cryo-TEM images of EVs extractions by SEC, GRAD, and SEC+GRAD.

4.3.1.5.2 Objective 2: To analyse the yield, abundance and diversity of miRNAs obtained from different library preparation kits.

The three library preparation protocols differed between them, being NEXT and NEB those that show the highest similarity among replicas in spike-in recovery. Using a principal component analysis (PCA), the samples were separated according to the three protocols used when the replicas were plotted together. NEB was the protocol that showed the highest reproducibility between replicas. Moreover, NEB was the protocol that on average detected

the largest number of different miRNAs, followed by NEXT and SMARTer (Figure 17).

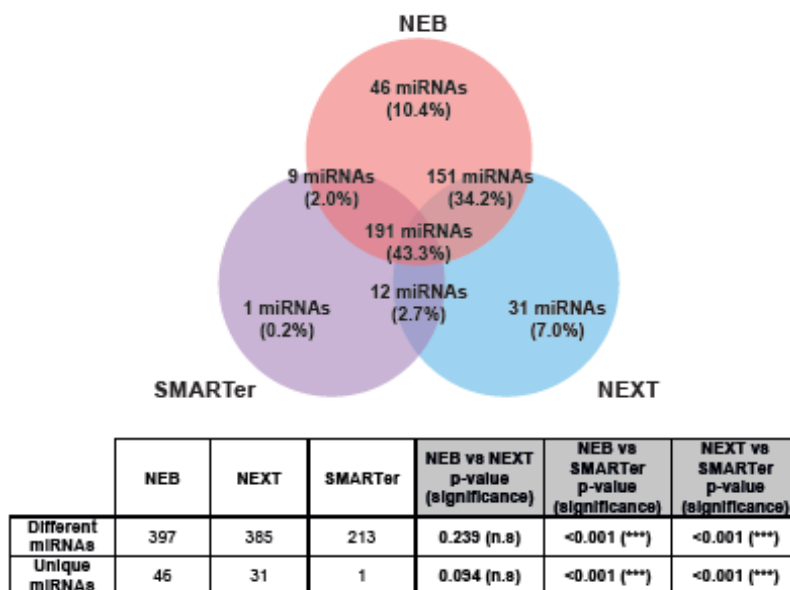


Figure 17. miRNAs detected by the three miRNAs sequencing protocols. Number and percentage of different miRNAs shared and unique among the three protocols.

4.3.1.5.3 Objective 3: To analyse the yield, abundance and diversity of miRNAs comparing different EV isolation methods

The samples were clearly separated according to the three methods with the replicas plotted together, being the GRAD method the one that showed the highest reproducibility among replicas. Replicas from GRAD method showed a higher number of reads corresponding to miRNAs than those obtained with SEC and SEC+GRAD. Moreover, GRAD method detected highest number and more different miRNAs, followed by SEC and SEC+GRAD method as depicted on Figure 18.

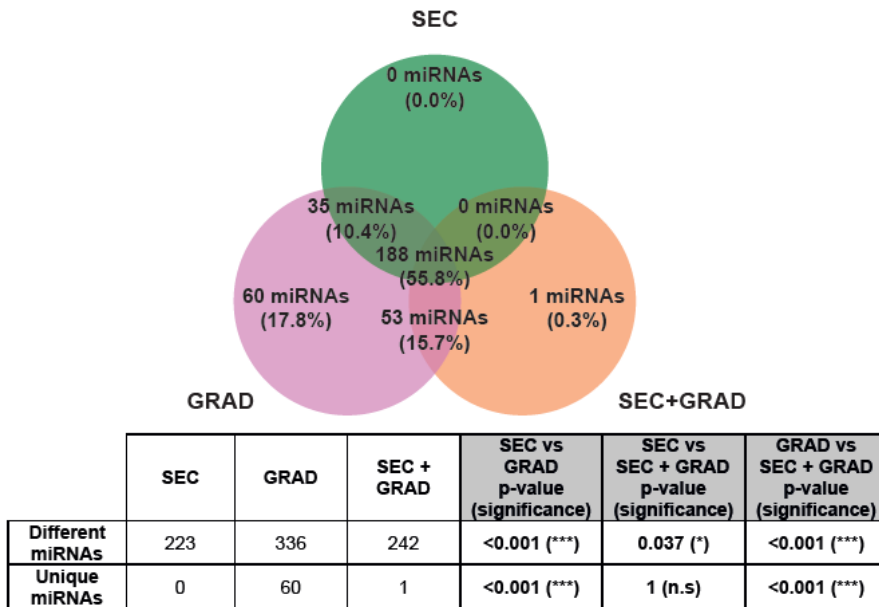


Figure 18. miRNAs detected with the three EV isolation methods. isolation method. Number and percentage of miRNAs different, shared and unique among the three methods.

4.3.1.6 Conclusions

1. The GRAD method provides a good balance between EV purity and yield.
2. NEB protocol yields a broad coverage of sequenced miRNAs.
3. GRAD method provides the best results for detecting miRNAs from EVs. Therefore, it should be considered a reliable method for identification of new clinical biomarkers.

4.3.2 Article 3

Comparison of extracellular vesicle isolation methods for miRNAs sequencing

Meritxell Llorens-Revull, Brenda Martínez-González, Josep Quer, Juan Ignacio Esteban, Gonzalo Núñez-Moreno, Pablo Minguez, Idoia Burgui, Ricardo Ramos-Ruiz, María Eugenia Soria, Angie Rico, Mar Riveiro, Silvia Sauleda, Maria Piron, Irene Corrales, Francesc E Borràs, Francisco-Rodríguez Frías, Ariadna Rando, Clara Ramírez, Silvia Camós, Esteban Domingo, Marta Bes, Celia Perales*, Maria Isabel Costafreda*

1 Comparison of extracellular vesicle isolation methods 2 for miRNAs sequencing

3 4 Authors

5 Meritxell Llorens-Revull^{a,b,c}, Brenda Martínez-González^{d,e}, Josep Quer^{a,b}, Juan
6 Ignacio Esteban^{a,b,c}, Gonzalo Núñez-Moreno^{f,g,h}, Pablo Minguez^{f,g,h}, Idoia Burguiⁱ,
7 Ricardo Ramos-Ruizⁱ, María Eugenia Soria^{d,j}, Angie Rico^k, Mar Riveiro^{a,b}, Silvia
8 Sauleda^{b,k}, Maria Piron^{b,k}, Irene Corrales^{l,m,n}, Francesc E Borràs^{o,p,q}, Francisco-
9 Rodríguez Frías^{b,u}, Ariadna Rando^{b,r}, Clara Ramírez-Serra^r, Silvia Camós^s,
10 Esteban Domingo^j, Marta Bes^{b,k}, Celia Perales^{d,e*}, Maria Isabel Costafreda^{b,t*}

11 a Liver Diseases-Viral Hepatitis, Liver Unit, Vall d'Hebron Institut de Recerca (VHIR), Hospital
12 Universitari Vall d'Hebron (HUVH), Vall d'Hebron Barcelona Hospital Campus, Barcelona, Spain

13 b Centro de Investigación Biomédica en Red de Enfermedades Hepáticas y Digestivas
14 (CIBERehd), Instituto de Salud Carlos III, Madrid, Spain

15 c Biochemistry and Molecular Biology Department, Universitat Autònoma de Barcelona (UAB),
16 Bellaterra, Spain

17 d Department of Clinical Microbiology, IIS-Fundación Jiménez Díaz, Madrid, Spain

18 e Centro Nacional de Biotecnología (CNB-CSIC). Consejo Superior de Investigaciones
19 Científicas (CSIC), Madrid, Spain.

20 f Department of Genetics & Genomics, Instituto de Investigación Sanitaria-Fundación Jiménez
21 Díaz University Hospital, Universidad Autónoma de Madrid (IIS-FJD, UAM), Madrid, Spain.

22 g CIBER de Enfermedades Raras (CIBERER), Instituto de Salud Carlos III, Madrid, Spain.

23 h Bioinformatics Unit, Instituto de Investigación Sanitaria-Fundación Jiménez Díaz University
24 Hospital, Universidad Autónoma de Madrid (IIS-FJD, UAM), Madrid, Spain.

25 i Unidad de Genómica, "Scientific Park of Madrid", Campus de Cantoblanco, 28049 Madrid,
26 Spain.

27 j Centro de Biología Molecular "Severo Ochoa" (CSIC-UAM), Consejo Superior de
28 Investigaciones Científicas (CSIC), Madrid, Spain

29 k Transfusion Safety Laboratory, Blood and Tissue Bank of Catalonia (BST), Barcelona, Spain

30 l Congenital Coagulopathies Laboratory, Banc de Sang i Teixits (BST), Barcelona, Spain

31 m Transfusional Medicine, Vall d'Hebron Institut de Recerca (VHIR), Universitat Autònoma de
32 Barcelona (UAB), Barcelona, Spain

33 n CIBER de Enfermedades Cardiovasculares (CIBERCV), Barcelona, Spain

34 o REMAR-IVECAT Group, Germans Trias i Pujol Research Institute (IGTP), Can Ruti Campus,
35 Badalona, Spain

36 p Nephrology Unit, Germans Trias i Pujol University Hospital, Badalona, Spain

37 q Department of Cell Biology, Physiology & Immunology, UAB, Barcelona, Spain
38 r Clinical Biochemistry Research Group, Vall d'Hebron Research Institute (VHIR), Biochemical
39 Core Facilities, Vall d'Hebron University Hospital, Autonomous University Barcelona, Barcelona,
40 Spain
41 s Clinical Biochemistry Laboratory, ICS-IAS Girona Clinical Laboratory, Doctor Josep Trueta
42 University Hospital, Girona, Spain.
43 t Enteric Virus Laboratory, Department of Genetics, Microbiology and Statistics, School of
44 Biology, and Institute of Nutrition and Safety, University of Barcelona (UB), Barcelona, Spain
45 u Department of Basic Sciences, Universitat Internacional de Catalunya, Sant Cugat del Vallès,
46 Barcelona, Spain

47
48 * Authors to whom correspondence should be addressed: Maria Isabel Costafreda:
49 mcostafreda@ub.edu and Celia Perales: celia.perales@cnb.csic.es

50 51 **Abstract**

52 Background & aims

53 MicroRNAs (miRNAs) encapsulated in extracellular vesicles (EVs) are potential
54 diagnostic and prognostic biomarkers. However, discrepancies in miRNA patterns and
55 their validation are still frequent due to differences in sample origin, EVs isolation, miRNA
56 extraction and sequencing methods. Selecting appropriate EVs isolation methods is
57 therefore a critical step for miRNA-based biomarker discovery. The aim of the present
58 comparative study is to find the most suitable EVs isolation method for miRNAs
59 sequencing, adequate for clinical application.

60 Material & Methods

61 EVs were isolated by Size Exclusion Chromatography (SEC), iodixanol gradients
62 (GRAD) and the combination of both (SEC+GRAD), using the same plasma sample, in
63 triplicate isolation assays. Isolated EVs were characterized and RNA was extracted.
64 Three different protocols for miRNA library preparation were compared: NEBNext,
65 NEXTFlex and SMARTer smRNA-seq. The miRNAs encapsulated into EVs were
66 sequenced using NextSeq 500 system (Illumina). The yield, abundance, and diversity of
67 miRNAs using the three EVs isolation protocols were analyzed and compared.

68 Results

69 The majority of lipoproteins, total cholesterol and plasma proteins were removed
70 from the EVs-containing fractions by using SEC, GRAD, and SEC+GRAD. SEC method
71 recovered a larger amount of EVs followed by GRAD and SEC+GRAD, while GRAD and
72 SEC+GRAD yielded the purest EVs. NEBNext was the library preparation kit that
73 showed the highest reproducibility among replicas, higher number of reads
74 corresponding to miRNAs and more different miRNAs, followed by NEXTFlex and

75 SMARTer smRNA-seq. GRAD exhibited the highest reproducibility among replicas, a
76 higher number of reads corresponding to miRNAs, and more different miRNAs, followed
77 by SEC and SEC+GRAD.

78 Conclusions

79 These results render the GRAD method to isolate EVs as one of the most
80 appropriate to detect miRNAs from EVs.

81

82 **Introduction**

83 MicroRNAs (miRNAs) are small and highly conserved non-coding RNAs of 20-30
84 nucleotides in length that play a critical role as post-transcriptional regulators of gene
85 expression¹. They are involved in biological processes such as development, cell
86 proliferation and differentiation, apoptosis, immune regulation, and metabolism². In
87 addition, they also participate in pathological processes, displaying a significant role in
88 primary tumor growth cancer progression, angiogenesis, pre-metastatic niche formation
89 metastatic cell migration, and drug anti-cancer resistance³. miRNAs are present in many
90 body fluids associated with RNA binding proteins (RBPs), with high and low density
91 lipoproteins, or encapsulated in extracellular vesicles (EVs)⁴⁻⁶. EVs are lipid membrane
92 vesicles secreted by all cell types⁷. The majority of miRNAs that are circulating freely are
93 concentrated in EVs⁸. Furthermore, in a pathological process, injured cells secrete more
94 EVs than healthy cells, and those EVs are enriched with miRNAs involved in the
95 pathogenesis⁹.

96 EVs travel through body fluids, including blood, urine, saliva, bile, ascites fluid,
97 breast milk, semen, and amniotic fluid, and reach distant cells¹⁰. Three main subtypes of
98 EVs have been described: (i) apoptotic bodies that range in size from 500 nm to 5 μ m,
99 (ii) microvesicles (MVs) from 100 nm to 1 μ m, and (iii) exosomes from 30 nm to 150 nm,
100 which differ among them in size, origin, content and function¹¹. EVs, and particularly
101 exosomes, serve as functional vehicles of intercellular communication because they
102 carry a complex cargo, with nucleic acids, lipids, and proteins that are capable of
103 modulating and reprogramming recipient cells¹². Furthermore, the content, size and
104 membrane composition of EVs varies depending on the cell of origin, its state (e.g.,
105 differentiated, stressed, stimulated), and environmental conditions¹³. Relevant
106 differences in the transcriptomic pattern have been observed between EVs and EV-
107 producing cells, indicating a selective incorporation of certain cellular RNAs into the
108 EVs¹⁴, with a selective enrichment of smaller RNAs as compared to the cell
109 transcriptome¹⁵. Moreover, the RNA cargo of EVs varies among cell types, and can also
110 be affected by exogenous stimuli^{16,17}.

111 The study of miRNA content within circulating EVs rather than total miRNAs in
112 plasma has several advantages. Firstly, EVs provide relevant information on patient
113 status, and may offer prognostic information on a broad range of diseases¹⁸. Secondly,
114 the use of circulating EVs allows to compile real-time information from the different cells
115 involved in the pathological process (e.g., injured cells, immune cells, and metastatic
116 cells)^{19,20}. Thirdly, the increased stability of EV-miRNAs and their accessibility in
117 biological fluids make them an attractive alternative as a minimally invasive diagnostic
118 test, known as liquid biopsy²¹. Finally, EVs transfer miRNAs from donor to recipient cells,
119 thereby regulating gene expression locally and distantly during both physiological and
120 pathological processes. Such transfer capability converts EV-miRNAs not only in
121 potential diagnostic and prognostic biomarkers but also in potential vehicles of
122 therapeutic agents^{22,23}.

123 For all these reasons, it is important to have reproducible methods to isolate EVs
124 from biological samples with high yield. Discrepancies on miRNA patterns are still
125 frequent among studies, which hampers the validation of specific miRNA signatures with
126 diagnostic and/or prognostic value. This is partly due to differences in sample origin and
127 EV-miRNA isolation and sequencing methods²⁴⁻²⁶. Moreover, the separation of EVs from
128 other particles such as lipoproteins, which also contain miRNAs, is difficult and varies
129 depending on the isolation method used²⁷. Hence, EV purification methods that result in
130 minimal contaminants are necessary to enable the precise characterization of miRNA
131 content within EVs. Since many years, ultracentrifugation has been used as the gold
132 standard method for EV isolation, as it allows the sedimentation of a wide range of
133 vesicles; however, ultracentrifugation is a time consuming procedure that requires
134 expensive equipment and yields low-purity EVs, which is why an increasing number of
135 laboratories are currently using other methodologies²⁸. Precipitation-based methods also
136 result in high EVs recovery, without specific infrastructure requirements²⁹, but the low
137 purity of isolated EVs is a major problem. Isopycnic ultracentrifugation using iodixanol
138 gradients has the same requirements than ultracentrifugation in terms of time and
139 equipment, but it provides higher EV purity because it discriminates vesicles subtypes
140 according to their density³⁰. Finally, size exclusion chromatography (SEC) is widely used
141 for size-based particle isolation, and leads to large EV batches that are well separated
142 from smaller particles and proteins³¹.

143 Selecting the appropriate isolation method is therefore a critical step for miRNA-
144 based biomarker discovery. Initially, we focus our study in miRNAs encapsulated within
145 exosomes, since these are the most studied vesicles in cellular communication.
146 However, we are aware that some microvesicles with a size and density similar to
147 exosomes, can remain in our samples after the centrifugation steps because of the

148 difficulty to completely separate microvesicles from exosomes³². For that reason,
149 although the majority of the vesicles recovered in the final sample are exosome-like, from
150 now on we will refer to EVs as to all vesicles mixed in our final solution, regardless of the
151 method of isolation. Hence, in the present study, we analysed the yield, abundance and
152 diversity of miRNAs obtained from the same plasma sample but using three different EV
153 isolation methods in triplicate isolation assays. The aim is establishing the most suitable
154 method to assess circulating miRNAs profiles for clinical applications.

155

156 **Materials and Methods**

157 **Plasma isolation.** Plasma was isolated from whole blood from a donor by centrifugation.
158 Plasma aliquots were frozen at -80°C until use.

159 **Cell debris, apoptotic bodies and microvesicles removal.** Plasma samples were
160 centrifuged at 1,200xg for 20 min at 4°C. Supernatants were subsequently centrifuged
161 at 10,000xg for 30 min at 4°C, and the clarified supernatants were used for further
162 experimentation.

163 **Extracellular vesicles isolation methods.** To identify the best EVs isolation method
164 among those currently available, intended for miRNA sequencing, two different methods
165 and their combination were performed in triplicate and compared (Fig 1). All buffers were
166 filtered with 0.22 µm filters.

167 1. Size exclusion chromatography (SEC) was applied to separate vesicles
168 according to their size. qEV2/35nm columns (Izon Science Ltd) were used for optimal
169 recovery of vesicles between 35 and 350 nm. Two ml of clarified supernatants (by two
170 successive centrifugations, as detailed above), were fractionated through the
171 qEV2/35nm column following the manufacturer instructions. PBS (1X) was used as
172 elution buffer and 30 fractions of 2 ml were collected. The procedure was repeated twice
173 per sample (4 ml each) combining the corresponding fractions. Three independent
174 experiments were performed by using different aliquots of the same plasma sample.

175 2. Isopycnic ultracentrifugation using iodixanol gradients (GRAD) was used to
176 separate vesicles by their density. Four ml of clarified supernatant were concentrated by
177 ultracentrifugation at 100,000xg for 3 h, at 4°C, using a TH-641 rotor (ThermoFisher
178 Scientific). The pellet was resuspended in 400 µl of PBS, loaded onto 8-40% iodixanol
179 step gradient prepared with OptiPrep™ (Sigma-Aldrich), and centrifuged at 140,000xg
180 during 18 h at 4°C. Eleven fractions of 1 ml were collected from the top of the gradient.
181 The density of each fraction was determined by the absorbance of iodixanol at 240 nm.

182 3. Combination of SEC and GRAD (SEC+GRAD) were used to separate vesicles
183 by size and density. EVs from 4 ml of clarified supernatant were purified by SEC as
184 described above. Then, fractions containing EVs were pooled together, concentrated,
185 and purified by isopycnic ultracentrifugation as above.

186 **EVs characterization.**

187 EVs marker detection. Fifty μ l of SEC fractions containing EVs or 12.5 μ l of GRAD
188 and SEC+GRAD fractions (fractions 1 to 15, and 1 to 11, respectively), were mixed with
189 0.5 μ l of aldehyde/sulfate-latex beads, 4% w/v, 4 μ m (ThermoFisher Scientific) and PBS
190 up to 55 μ l, and incubated for 15 min at room temperature (RT). Non-specific binding
191 was blocked with 5% filtered BSA Blocker™ (Thermo Scientific™), overnight at RT in an
192 orbital shaker. CD9 tetraspanin staining was performed with the primary antibody Pure
193 Anti-Human CD9 (Immunostep SL) at RT for 30 min, washed, and subsequently stained
194 with the FITC-labeled Goat F (ab')₂ Anti-Mouse IgG (H+L) secondary antibody
195 (SouthernBiotech,) for 30 min at RT in darkness (the protocol has been adapted from³³).
196 For the identification and quantitation of CD9+ subsets, 100,000 events were acquired
197 per sample in a FACSCalibur cytometer (BD Biosciences, San Jose, CA). FlowJo
198 software (BD Biosciences, San Jose, CA) was used for data analysis.

199 Total protein concentration. Total protein concentration was measured using the
200 Thermo Scientific™ Pierce™ BCA assay kit (Thermo Scientific™). In brief, 25 μ l of the
201 first 20 fractions from SEC or 6.25 μ l of all gradient fractions in PBS up to 25 μ l were
202 incubated with BCA reagent and 4% Cupric Sulfate, at 37°C for 30 min in darkness.
203 Absorbance was measured at 562 nm on a Varioskan™ LUX multimode microplate
204 reader (Thermo Scientific™).

205 Lipoproteins detection. Total cholesterol, apolipoprotein A (apoA), and
206 Apolipoprotein B (apoB) were measured using the OLYMPUS AU2700 chemistry
207 analyzer (Beckman-Coulter).

208 Concentration of fractions containing EVs. Fractions containing EVs isolated by
209 SEC, GRAD or SEC+GRAD methods were pooled and concentrated down to 1 ml with
210 Vivaspin® 20 Ultrafiltration Unit of 100K MWCO PES (Sartorius), following the
211 manufacturer's instructions.

212 Total protein quantification of EV concentrates. Total protein in EV concentrates
213 was quantified by using the BCA method.

214 Nanoparticle Tracking Analysis (NTA). Size and concentration of purified EVs
215 were assessed with a Nanosight N300 instrument (Malvern Panalytical).

216 Transmission electron microscopy (TEM). Morphological analyses of the EVs in
217 each concentrate were performed by TEM and Cryo-TEM.

218 **RNA extraction.** RNA was extracted from 250 µl of the plasma sample or from 250 µl
219 EVs isolation samples using a miRNeasy Mini kit (QIAGEN) following the manufacturer's
220 instructions. Purified RNA was eluted in 20 µl of nuclease-free water. To monitor the
221 purification and amplification of miRNAs, 52 spike-ins (synthetic miRNAs at different
222 concentrations) (QIAseq miRNA Library QC PCR Assay Kit) were added to the initial
223 sample before RNA extraction. Quantity and quality of the purified RNA were determined
224 using NanoDrop and Bioanalyzer 2100 (Agilent Technologies, Santa Clara, CA, USA).
225 The RNA concentrations obtained ranged between 164 pg/µl and 349 pg/µl.

226 **Library preparation, size selection and sequencing.** Libraries of small RNA using
227 three different protocols: (i) NEBNext Multiplex Small RNA Library Prep Set for Illumina
228 (New England BioLabs, Ipswich, MA, USA); (ii) NEXTFlex Small RNA-Seq Kit v3
229 (PerkinElmer, Waltham, MA, USA); and (iii) SMARTer smRNA-seq kit (Clontech
230 Laboratories, CA, USA), according to the manufacturer's guidelines. The amount of RNA
231 was 0.7 ng for the Plasma 1 sample and 1 ng for the Plasma 2 sample. The size profile
232 of the individual libraries was analyzed using High Sensitivity DNA Assay on a
233 Bioanalyzer 2100 (Agilent Technologies, Santa Clara, CA, USA). Size selection of
234 fragments was carried out using 5% Mini-PROTEAN TBE Gel precast polyacrylamide
235 gel (Bio-Rad Laboratories). Electrophoresis was performed at 120 V during 1 h in tris-
236 borate-EDTA (TBE) buffer. The band of interest was eluted following the NEXTFlex kit
237 guidelines. Libraries were quantified by qPCR using KAPA Sybr fast master Mix (2x)
238 optimized for LightCycler 480 (KAPA Biosystems), and an in-house standard library from
239 Fundación Parque Científico de Madrid. Quantified libraries were mixed at equimolar
240 ratios and sequenced with a NextSeq 500/550 High Output Kit v2.5 (75 Cycles) using
241 the NextSeq 500 system (Illumina).

242 **Bioinformatics analyses.** Read trimming was performed with cutadapt (version 3.2)³⁴
243 following the guidelines of each library preparation kit. Samples prepared with NEXTFlex
244 kit were trimmed by removing the 3' adapter 'TGGAATTCTCGGGTGCCAAGG', plus 4
245 bases from both ends of each read. TruSeq 3' adapter
246 'AGATCGGAAGAGCACACGTCTGAACTCCAGTCA' was trimmed from samples
247 prepared with the NEBNext kit. Samples prepared with SMARTer were trimmed by
248 removing the 3' PolyA adapter ('AAAAAAAAA') plus 3 extra bases at the 5' end.

249 After adapter trimming, reads with lengths between 17 and 25 nucleotides were
250 selected and mapped using Bowtie 2 (version 2.3.4.3)³⁵ to the hg38 reference genome
251 using default parameters. Quantification was performed using HTSeq (version 0.13.5)³⁶
252 with default parameters using mature miRNA coordinates provided by miRBase v22.1
253 (<https://www.mirbase.org/ftp/22.1/genomes/hsa.gff3>). Low expressed miRNAs (those

254 with less than 50 reads in total) were discarded. Principal component analysis was
255 performed using TMM normalized counts.

256 For spike-in analysis, selected reads between 17 and 25 nucleotides were
257 mapped using Bowtie 2 (version 2.3.4.3) to the QIAseq™ miRNA Library QC Spike-In
258 sequences. Mapping parameters were tuned for "perfect match" as recommended in
259 QIAseq™ miRNA Library QC Spike-Ins protocol by setting the following parameters: "--
260 end-to-end -N 0 --mp 10000 --np 10000 --rdg 10000 --rfg 10000". Mapped reads were
261 quantified and normalized by dividing them by the total number of mapped spike-in per
262 sample. Heatmaps were plotted using the "pheatmap" R package over the log2
263 normalized values.

264 **Statistics.** The statistical significances of different comparisons were calculated by the
265 proportion test, using software R version 4.0.2. *, $p < 0.05$.

266 **Ethics approval.** The study was approved by the Research Ethics Committee with
267 Medicines and University Hospital Research Projects Commission of Vall d'Hebron
268 Barcelona Hospital Campus [PR(AG)414/2018].

269 **Data Availability Statement:** Fastq files of samples included in this study were
270 uploaded to GEO database.

271

272 **Results**

273 **1. Comparative characterization of three EVs isolation methods**

274 We measured CD9, apoA, apoB, total cholesterol, and total protein concentration
275 in fractions 1 to 20 for SEC extractions, and all fractions extracted by GRAD and
276 SEC+GRAD. The tetraspanin CD9 is one of the most common proteins at the surface of
277 EVs, and is, therefore, considered an EV marker³⁷. ApoA is the major component of high-
278 density lipoprotein (HDL) particles and is commonly used as an HDL marker³⁸. ApoB is
279 the primary apolipoprotein of chylomicrons, very-low-density lipoprotein (VLDL),
280 intermediate-density lipoprotein (IDL), low-density lipoprotein (LDL), and lipoprotein (a)
281 (Lp(a)). Hence, apoB is used as a marker of these lipoproteins³⁹.

282 Total cholesterol, apoA and apoB measurements performed directly on the
283 plasma sample, display concentration values of 169 mg/dL, 124 mg/dL and 102 mg/dL
284 respectively. Whereas in SEC fractions (Fig. 2A), CD9 tetraspanin reached the highest
285 concentration in fractions 8-12, indicating that EVs were mainly located in these fractions,
286 which, in turn, presented low amounts of protein, cholesterol, and lipoproteins (Fig. S1).
287 Protein concentration started to rise from fraction 8, and achieved its maximum at
288 fractions 18-19, followed by a decrease in subsequent fractions (Fig. S1). An increase in

289 total cholesterol values was observed from fraction 9, reaching a plateau phase between
290 fractions 14-16, and decreasing afterwards. A similar trend was observed with HDL,
291 since apoA presented a progressive increase from fraction 16 to 18 with a subsequent
292 decline. We were not able to detect apoB, the marker of chylomicrons, VLDL, IDL, LDL,
293 and Lp(a), in any SEC fraction. In the case of GRAD (Fig. 2A), fractions 5-8 contained
294 the highest amount of CD9 marker, and therefore of EVs. Most proteins were likely
295 pelleted with the GRAD method and the remaining proteins were mainly found in the first
296 fractions of the GRAD, and co-purified with those fractions containing the highest CD9
297 values. Total cholesterol, apoA and apoB were under the limit of detection, (<20 mg/dL,
298 <5,13 mg/dL and <24,40 mg/dL, respectively). Among the fractions extracted by
299 SEC+GRAD (Fig. 2A), the highest levels of CD9 fluorescence were detected in fractions
300 4-7. Protein concentration was reduced and showed a slight and continuous increase
301 from the first fraction. Total cholesterol, apoA and apoB were not detected in any fraction.

302 The five fractions containing the highest EVs concentration were pooled in nine
303 final samples (three per each replica); corresponding to fractions 8-12 for the SEC, and
304 to fractions 4-8 for the GRAD and SEC+GRAD. Total protein in each EV pool was
305 quantified and compared with the protein content in the original plasma sample. The
306 comparison indicated that most of the protein plasma content had been removed, with a
307 decrease from about 147 mg/ml, to 1,86 mg/ml for the SEC extractions, 2,02 mg/ml for
308 GRAD fractionations, and 1,50 mg/ml for the combination of SEC+GRAD.

309 Furthermore, EVs size distribution and concentration of each pool were
310 measured by nanosight (Table 1). Particle size distribution was represented as mean,
311 mode, and percentage of particles present in the sample with the indicated size or
312 smaller (D values; D10, D50 and D90 correspond to the 10%, 50% and 90% of particles
313 under the reported particle size). Based on the mean concentration of EV in each pool,
314 the conclusion is that the use of SEC allowed the recovery of a larger amount of EVs
315 than GRAD or SEC+GRAD; the mean number of particles/ml recovered by the three
316 procedures was $7.49 \times 10^{11} \pm 5.5 \times 10^{10}$, $8.51 \times 10^9 \pm 1.98 \times 10^8$ and $3.83 \times 10^9 \pm 5.53 \times 10^8$,
317 respectively. SEC+GRAD, yielded the largest average particle size followed by GRAD
318 and SEC, with mean size values of 170.5 ± 4.57 nm, 136.5 ± 4 nm and 133.37 ± 1.93 nm,
319 respectively.

320 Finally, purified EVs were visualized by TEM and Cryo-TEM in all the pools
321 analysed (Fig. 2B). The cup-shape is due to the drying process during sample
322 preparation for negative staining⁴⁰. The size of the vesicles corresponded to that
323 expected for EVs. TEM images correlated with data obtained from nanosight
324 quantifications. Thus, SEC pools presented a higher quantity of EVs with an apparent
325 low purity. In contrast, GRAD yielded a cleaner EVs preparation, with a lower proportion

326 of clumped vesicles. The purest EVs isolation was achieved using SEC+GRAD at the
327 expense of a lower yield in vesicles.

328 **2. miRNA library evaluation for next-generation sequencing.**

329 To determine which protocol is more effective to detect miRNAs in plasma
330 samples from patients, we compared three different protocols for miRNA library
331 preparation: i) NEBNext Multiplex Small RNA Library Prep Set for Illumina (named as
332 NEB); ii) NEXTFlex Small RNA-Seq Kit v3 (named as NEXT) and iii) SMARTer smRNA-
333 seq kit (named as SMARTer) (detailed in Materials and Methods). To this aim, we
334 isolated small-RNAs from a plasma sample of a donor, and prepared libraries using the
335 three protocols. We analysed two replicas with each protocol [Replica 1 (R1) and Replica
336 2 (R2)]. The resulting RNA libraries were sequenced using Illumina technology (see
337 Materials and Methods).

338 We evaluated the protocols considering the following aspects: i) the recovery of
339 synthetic miRNAs used as control (called spike-ins), ii) the reproducibility between
340 replicas, iii) the number of sequencing reads corresponding to miRNAs, and iv) the
341 number of different miRNAs detected. Spike-ins were used as a control of purification
342 and amplification of miRNAs. The number of counts that corresponds to these spike-ins
343 were depicted as a heat map (Fig. S1). The three protocols differed, being NEXT and
344 NEB those that shown the highest similarity in spike-in recovery between replicas. Using
345 a principal component analysis (PCA) (Fig. 3A), the samples were separated according
346 to the three protocols used when the replicas were plotted together.

347 Regarding miRNA detection, we selected reads between 17 and 25 nucleotides
348 as miRNAs that were aligned to the human genome and mapped against miRNAs
349 coordinates. The total number of reads that correspond to miRNAs is represented in
350 Table S1. The two replicates sequenced by NEB and NEXT protocols resulted in a higher
351 number of miRNAs reads than samples processed with SMARTer.

352 NEB was the protocol that on average detected the largest number of different
353 miRNAs, followed by NEXT and SMARTer (Fig. 3B and Table S2). Considering the
354 number of different miRNAs, the reproducibility between replicas was analysed and
355 depicted as Venn diagrams (Fig. 3C); NEB was the protocol that showed the highest
356 reproducibility (84.1%) between replicas. The largest number of miRNAs was detected
357 with the NEB protocol [397 out of 441 (90%) different miRNAs found in total, considering
358 the three protocols] (Fig.3D). Based on these results, the NEB protocol was selected as
359 the most adequate to sequence miRNAs in a human plasma.

360 **3. Selection of a EVs isolation method according to miRNA sequence recovery**

361 To determine the EVs isolation method that allowed detection of more miRNAs,
362 we isolated miRNAs from the three replicas of each EVs isolation method (SEC, GRAD
363 and SEC+GRAD) using NEB protocol. Using a principal component analysis (PCA) (Fig.
364 4A), the samples were separated according to the three isolation methods used when
365 the replicas were plotted together.

366 Using the bioinformatics methods previously described^{34–36}, replicas from GRAD
367 method showed a high number of miRNA reads than the number obtained with SEC and
368 SEC+GRAD (Table S3). GRAD was the method that detected the largest number of
369 different miRNAs, followed by SEC and SEC+GRAD (Fig. 4B and Table S4).

370 The reproducibility among replicas was analysed and depicted as Venn diagrams
371 (Fig. 4C); GRAD was the method that showed the highest reproducibility (72.3%) among
372 replicas. The highest number of miRNAs was detected with GRAD [336 out of 337
373 (99.7%) different miRNAs, considering the three EVs isolation methods] (Fig. 4D). These
374 results render the GRAD method as one of the most appropriate to detect miRNAs from
375 EVs isolated from human plasma.

376

377 **Discussion**

378 In the present work, we have conducted a study to compare different EV isolation
379 methods in order to find the best approach for miRNA biomarker recovery and
380 identification. By comparing three different methods, SEC, GRAD and the combination
381 of SEC+GRAD, we have shown that the method used can influence the final result. Each
382 method allows isolation of a diverse size range of vesicles, but it varies regarding
383 lipoprotein and protein contaminants depletion, EVs recovery yield, miRNA profiles, cost-
384 effectiveness, and clinical applicability. For that reason, it is important to choose the
385 methodology depending on the forthcoming application of the purified EVs.

386 The analysis of protein content showed that all three EV isolation methods
387 removed most of the overabundant soluble plasma proteins, although SEC extractions
388 are the ones recovering more impurities. As far as lipoproteins is concern, it is expected
389 that SEC could not separate EVs from apoB-containing lipoproteins such as
390 chylomicrons, LDL, IDL, VLDL and Lp(a) because of their size overlap (30-5000nm vs
391 18-1200 nm), whereas GRAD could not separate EVs from apoA-containing lipoproteins
392 (HDL) because of their density overlap (~1.1 g/mL vs 1.08-1.19 g/mL)³². Therefore, by
393 combining SEC+GRAD should provide the highest lipoprotein removal. However, all
394 GRAD and SEC fractions tested negative for apoA and apoB in EVs-containing fractions,
395 suggesting that the combination of initial centrifugations with fractioning methodologies
396 eliminate the vast majority of lipoproteins. However, certain degree of lipoprotein

397 contamination cannot be excluded based on the physical properties of these particles,
398 which would explain the high quantity of particles detected in NTA and TEM analyses,
399 and the low fluorescence intensity in CD9 analyses in SEC fractions.

400 According to CD9 fluorescent intensity in tagged EVs, GRAD provided a higher
401 proportion of pure EVs than SEC. According to NTA measurements, the concentration
402 of recovered particles by GRAD and SEC+GRAD was two orders of magnitude lower
403 than that of SEC extractions, but showing the highest degree of purity by TEM and Cryo-
404 TEM images.

405 In consequence, GRAD is the methodology showing the best balance between
406 EVs purity and yield. Next step was to study the cargo in miRNAs of the EVs isolated by
407 the three methods.

408 Firstly, when testing the efficacy of three commercial protocols of miRNAs library
409 preparation, NEB, NEXT and SMARTer, NEB was the protocol that showed the highest
410 reproducibility between replicas and resulted in the highest and different number of
411 miRNAs followed by NEXT and SMARTer. Similar results were observed in other studies
412 published with NEB kit when compared with other commercial kits^{25,41-43}.

413 Secondly, when testing the efficacy of the three EV isolation methods for miRNA-
414 sequencing, GRAD method showed the highest reproducibility from replicas and
415 detected the higher number and more different miRNAs than those obtained with SEC
416 and SEC+GRAD. Conversely, Buschmann et al. conclude that less specific EVs isolation
417 methods yielded more RNA and obtained higher number of miRNAs than more specific
418 methods. This could be attributed to extreme alterations in miRNA expression as they
419 work with sepsis patients, different subpopulations of vesicles isolated or a more
420 abundant co-isolation of non-vesicular extracellular RNA that mask those miRNAs
421 coming from EVs. Besides, highly abundant miRNAs are less affected by library
422 preparation-induced biases than low-abundance transcripts⁴⁴. MiRNAs related to
423 pathologies that induce small differences in their expression levels and/or are
424 underrepresented in plasma samples can be enriched by isolating the miRNAs within
425 EVs⁹. Thus, the study of miRNAs with GRAD may allow detecting less abundant
426 circulating miRNAs that nevertheless may play significant roles in pathogenesis that
427 would be concealed by more abundant miRNAs if other methods are used.

428 In addition to miRNAs, EVs contain messenger RNAs, transfer RNA, long non-
429 coding RNAs, and circular RNAs, among others⁴⁵. Depending on the EVs isolation
430 methodology, different types of vesicles with different sizes and cargos are isolated. In
431 our study, SEC proved to be the less discriminative method allowing to recover more
432 different type of particles, and depending on the aim of the study this methodology could
433 represent the best choice since despite showing lower miRNA abundance and diversity

434 than GRAD, other RNA types might have been isolated and sequenced. Although further
435 investigation would be required to confirm this hypothesis, the results obtained by
436 SEC+GRAD are consistent with a pre-selection of less miRNA-enriched vesicles by
437 SEC.

438 In conclusion, all methods assessed in this study successfully detected miRNAs
439 from plasma samples, although the number of mapped miRNAs varied considerably
440 across EV isolation methods and library preparation kits. In our case, the method that
441 provided the best balance between EV's purity, yield and miRNA-sequencing was the
442 GRAD. Hence, isopycnic centrifugation using GRAD methodology, followed by NGS
443 sequencing using NEB kit should be considered, as a reliable protocol for the
444 identification of clinical biomarkers.

445

446 **Acknowledgments**

447 The authors thank Jose Amable Bernabe for NTA analysis which has
448 been performed by the ICTS "NANBIOSIS", more specifically by the Unit 6. Unit of the
449 CIBER in Bioengineering, Biomaterials & Nanomedicine (CIBER-BBN) at the Barcelona
450 Materials Science Institute, and Martí de Cabo Jaume for TEM analysis at the UAB
451 Microscopy Service. We extend our thanks to Miriam Moron Font for cytometry advises
452 and UAT staff, especially Irene Sales Pardo. We also want to thank Francesc Canals
453 Suris and Luna Martín Castel for total protein quantification at the proteomics laboratory
454 of Vall d'Hebron Institute of Oncology (VHIO) and Fundación Parque Científico de Madrid
455 for small RNA-sequencing performance. Finally, Laura Martin-Fernández and Nina
456 Borràs from Congenital Coagulopathies Laboratory of Banc de Sang i Teixits of
457 Catalonia for their technical recommendations.

458

459 **Funding**

460 This study was funded by Instituto de Salud Carlos III, cofinanced by the European
461 Regional Development Fund (ERDF): grant numbers PI18/00210, PI19/00301,
462 PI19/00533, and PI22/00258; Centro para el Desarrollo Tecnológico Industrial (CDTI)
463 from the Spanish Ministry of Economy and Business, grant number IDI-20200297; C.P.
464 is supported by the Miguel Servet program of the Instituto de Salud Carlos III
465 (CP14/00121 and CPII19/00001) cofinanced by the European Regional Development
466 Fund (ERDF). M.LL. is a recipient of a predoctoral fellowship from Instituto de Salud
467 Carlos III (FI20/00313), cofinanced by the European Regional Development Fund
468 (ERDF). B.M.-G. is supported by predoctoral contract PFIS FI19/00119 from ISCIII
469 cofinanced by Fondo Social Europeo (FSE).

470

471 **Disclosure statement**

472 The authors reported no potential conflict of interest.

473

474 **Figure legends**

475 **Figure 1. Diagram of EVs isolation methods used for the comparison.**

476 **Figure 2. Characterization of three EVs isolation methods. (A)** Detection of CD9,
477 total cholesterol and total protein. Codes for the quantifications are depicted above the
478 graph. The fractionation method is indicated in each panel, and fraction number in the
479 abscissas. CD9 fluorescence intensity was measured as geometrical mean and plotted
480 on the left axis as the three replica's mean. Total cholesterol and total proteins were
481 measured as mg/dL and plotted on the right axis. Total protein was represented as the
482 mean of the three replicas. (i) SEC means..., (ii) GRAD means..., and (iii) SEC+GRAD
483 means... (see Materials and Methods). **(B)** TEM and Cryo-TEM images of EVs
484 extractions by SEC, GRAD, and SEC+GRAD.

485 **Figure 3. miRNAs detected by the three miRNAs sequencing protocols.** NEB refers
486 to NEB Multiplex Small RNA Library Prep Set for Illumina, NEXT refers to NEXTFlex
487 Small RNA-Seq Kit v3 and SMARTer refers to SMARTer smRNA-seq kit (see Materials
488 and Methods). **(A)** Plot of principal component analysis (PCA) of components Dim1 and
489 Dim2. Each protocol is represented by a different color and symbol. The two replicas are
490 depicted in the plot (Replica 1 and Replica 2). The third point is the centroid of the two
491 replicas of each library protocol. **(B)** Number of different miRNAs identified in each
492 replica of each protocol. **(C)** Number and percentage of miRNAs detected in each replica
493 of the three protocols, represented as a Venn diagram. **(D)** Number and percentage of
494 miRNAs shared and unique among the three protocols.

495 **Figure 4. miRNAs detected with the three EV isolation methods.** SEC refers to Size
496 exclusion chromatography, GRAD refers to iodixanol gradient and SEC+GRAD refers to
497 size exclusion and iodixanol gradient. **(A)** Plot of principal component analysis (PCA) of
498 components Dim1 and Dim2. Each method is represented by a different color and
499 symbol. The three replicas are depicted in the plot (R1, R2 and R3). The fourth point is
500 the centroid of the three replicas of each EV isolation method. **(B)** Number of different
501 miRNAs detected in replicas (R1, R2 and R3) from each EVs isolation method. **(C)**
502 Number and percentage of miRNAs detected in each replica represented as a Venn

503 diagram. **(D)** Number and percentage of miRNAs shared and unique among the three
504 methods.

505 **Figure S1. Characterization of all SEC fractions.** CD9, ApoA, total cholesterol and
506 total protein quantification. CD9 fluorescence intensity was measured as geometrical
507 mean and plotted on the left axis. ApoA, total cholesterol and total proteins were
508 measured as mg/dL and plotted on the right axis and fraction number in the abscissas.
509 Instead of the three replicates one replica was represented from fractions 15 to 30.

510 **Figure S2. Heat map of normalized NOISEq counts of different spike-ins identified**
511 **in the two replicas from each protocol (SMARTer, NEB and NEXT).** Spike-ins with a
512 higher number of counts are depicted with red and yellow colors, and those with a lower
513 number of counts are depicted with blue colors.

514 **References**

- 515 1. M. Bhaskaran, M. Mohan. MicroRNAs: History, Biogenesis, and Their Evolving
516 Role in Animal Development and Disease. 2014;51(4):759-774.
517 doi:10.1177/0300985813502820
- 518 2. Huntzinger E, Izaurralde E. Gene silencing by microRNAs: Contributions of
519 translational repression and mRNA decay. *Nat Rev Genet.* 2011;12(2):99-110.
520 doi:10.1038/nrg2936
- 521 3. Steinbichler TB, Dudás J, Riechelmann H, Skvortsova II. The role of exosomes in
522 cancer metastasis. *Semin Cancer Biol.* 2017;44:170-181.
523 doi:10.1016/j.semcancer.2017.02.006
- 524 4. Vickers KC, Palmisano BT, Shoucri BM, Shamburek RD, Remaley AT.
525 MicroRNAs are transported in plasma and delivered to recipient cells by high-
526 density lipoproteins. *Nat Cell Biol.* 2011;13(4):423-433. doi:10.1038/ncb2210
- 527 5. Mitchell PS, Parkin RK, Kroh EM, et al. Circulating microRNAs as stable blood-
528 based markers for cancer detection. *Proc Natl Acad Sci U S A.*
529 2008;105(30):10513-10518. doi:10.1073/pnas.0804549105
- 530 6. Winter J, Diederichs S. Argonaute proteins regulate microRNA stability: Increased
531 microRNA abundance by Argonaute proteins is due to microRNA stabilization.
532 *RNA Biol.* 2011;8(6):1149-1157. doi:10.4161/rna.8.6.17665
- 533 7. Simons M, Raposo G. Exosomes - vesicular carriers for intercellular
534 communication. *Curr Opin Cell Biol.* 2009;21(4):575-581.

535 doi:10.1016/j.ceb.2009.03.007

536 8. Gallo A, Tandon M, Alevizos I, Illei GG. The majority of microRNAs detectable in
537 serum and saliva is concentrated in exosomes. *PLoS One*. 2012;7(3):1-5.
538 doi:10.1371/journal.pone.0030679

539 9. Sun Z, Shi K, Yang S, et al. Effect of exosomal miRNA on cancer biology and
540 clinical applications. *Mol Cancer*. 2018;17(147):1-19. doi:10.1186/s12943-018-
541 0897-7

542 10. Colombo M, Raposo G, Théry C. Biogenesis, secretion, and intercellular
543 interactions of exosomes and other extracellular vesicles. *Annu Rev Cell Dev Biol*.
544 2014;30(1):255-289. doi:10.1146/annurev-cellbio-101512-122326

545 11. Laura M. Doyle, Michael Zhuo Wang. Overview of Extracellular Vesicles, Their
546 Origin, Composition, Purpose, and Methods for Exosome Isolation and Analysis.
547 *Cells*. 2019;8(727):41-68. doi:10.3390/cells8070727

548 12. Raposo G, Stoorvogel W. Extracellular vesicles: Exosomes, microvesicles, and
549 friends. *J Cell Biol*. 2013;200(4):373-383. doi:10.1083/jcb.201211138

550 13. Zaborowski MP, Balaj L, Breakefield XO, Lai CP. Extracellular Vesicles:
551 Composition, Biological Relevance, and Methods of Study. *Bioscience*.
552 2015;65(8):783-797. doi:10.1093/biosci/biv084

553 14. O'Grady T, Njock MS, Lion M, et al. Sorting and packaging of RNA into
554 extracellular vesicles shape intracellular transcript levels. *BMC Biol*. 2022;20(1):1-
555 21. doi:10.1186/s12915-022-01277-4

556 15. Baglio SR, Rooijers K, Koppers-Lalic D, et al. Human bone marrow- and adipose-
557 mesenchymal stem cells secrete exosomes enriched in distinctive miRNA and
558 tRNA species. *Stem Cell Res Ther*. 2015;6(127):1-20. doi:10.1186/s13287-015-
559 0116-z

560 16. D'souza RF, Woodhead JST, Zeng N, et al. Circulatory exosomal miRNA following
561 intense exercise is unrelated to muscle and plasma miRNA abundances. *Am J*
562 *Physiol - Endocrinol Metab*. 2018;315(4):E723-E733.
563 doi:10.1152/ajpendo.00138.2018

564 17. Matsuzaki J, Ochiya T. Extracellular microRNAs and oxidative stress in liver injury:
565 A systematic mini review. *J Clin Biochem Nutr*. 2018;63(1):6-11.
566 doi:10.3164/jcfn.17-123

- 567 18. Zhang Y, Liu Y, Liu H, Tang WH. Exosomes: Biogenesis, biologic function and
568 clinical potential. *Cell Biosci.* 2019;9(19):1-18. doi:10.1186/s13578-019-0282-2
- 569 19. Johan Skog, Wurdinger T, Rijn S van, et al. Glioblastoma microvesicles transport
570 RNA and protein that promote tumor growth and provide diagnostic biomarkers.
571 *Nat Cell Biol.* 2008;10(12):1470–1476. doi:10.1038/ncb1800
- 572 20. Chaput N, Théry C. Exosomes: Immune properties and potential clinical
573 implementations. *Semin Immunopathol.* 2011;33(5):419-440.
574 doi:10.1007/s00281-010-0233-9
- 575 21. de Miguel Pérez D, Rodriguez Martínez A, Ortigosa Palomo A, et al. Extracellular
576 vesicle-miRNAs as liquid biopsy biomarkers for disease identification and
577 prognosis in metastatic colorectal cancer patients. *Sci Rep.* 2020;10(3974):1-13.
578 doi:10.1038/s41598-020-60212-1
- 579 22. Valadi H, Ekström K, Bossios A, Sjöstrand M, Lee JJ, Lötvall JO. Exosome-
580 mediated transfer of mRNAs and microRNAs is a novel mechanism of genetic
581 exchange between cells. *Nat Cell Biol.* 2007;9(6):654-659. doi:10.1038/ncb1596
- 582 23. Kyoung Mi Kim, Kotb Abdelmohsen, Maja Mustapic, Dimitrios Kapogiannis,
583 Myriam Gorospe. RNA in extracellular vesicles. *Wiley Interdiscip Rev RNA.*
584 2017;8(4):1-20. doi:10.1002/wrna.1413
- 585 24. Buschmann D, Kirchner B, Hermann S, et al. Evaluation of serum extracellular
586 vesicle isolation methods for profiling miRNAs by next-generation sequencing. *J*
587 *Extracell vesicles.* 2018;7(1). doi:10.1080/20013078.2018.1481321
- 588 25. Coenen-Stass AML, Magen I, Brooks T, et al. Evaluation of methodologies for
589 microRNA biomarker detection by next generation sequencing. *RNA Biol.*
590 2018;15(8):1133-1145. doi:10.1080/15476286.2018.1514236
- 591 26. Witwer KW, Buzás EI, Bemis LT, et al. Standardization of sample collection,
592 isolation and analysis methods in extracellular vesicle research. *J Extracell*
593 *Vesicles.* 2013;2(1). doi:10.3402/jev.v2i0.20360
- 594 27. Michell DL, Vickers KC. Lipoprotein carriers of microRNAs. *Biochim Biophys Acta*
595 *- Mol Cell Biol Lipids.* 2016;1861(12):2069-2074.
596 doi:10.1016/j.bbalip.2016.01.011
- 597 28. Théry C, Clayton A, Amigorena S, Raposo and G. Isolation and Characterization
598 of Exosomes from Cell Culture Supernatants. *Curr Protoc Cell Biol.*
599 2006;30:3.22.1–3.22.29. doi:10.1002/0471143030.cb0322s30

- 600 29. Coughlan C, Bruce KD, Burgy O, et al. Exosome Isolation by Ultracentrifugation
601 and Precipitation and Techniques for Downstream Analyses. *Curr Protoc Cell Biol.*
602 2020;88(1):e110. doi:10.1002/cpcb.110
- 603 30. Crescitelli R, Lässer C, Lötvall J. Isolation and characterization of extracellular
604 vesicle subpopulations from tissues. *Nat Protoc.* 2021;16(3):1548-1580.
605 doi:10.1038/s41596-020-00466-1
- 606 31. Böing AN, van der Pol E, Grootemaat AE, Coumans FAW, Sturk A, Nieuwland R.
607 Single-step isolation of extracellular vesicles by size-exclusion chromatography. *J*
608 *Extracell Vesicles.* 2014;3(1):23430. doi:10.3402/jev.v3.23430
- 609 32. Brennan K, Martin K, FitzGerald SP, et al. A comparison of methods for the
610 isolation and separation of extracellular vesicles from protein and lipid particles in
611 human serum. *Sci Rep.* 2020;10(1):1-13. doi:10.1038/s41598-020-57497-7
- 612 33. Monguió-Tortajada M, Morón-Font M, Gámez-Valero A, Carreras-Planella L,
613 Borràs FE, Franquesa M. Extracellular-Vesicle Isolation from Different Biological
614 Fluids by Size-Exclusion Chromatography. *Curr Protoc Stem Cell Biol.*
615 2019;49(1):1-24. doi:10.1002/cpsc.82
- 616 34. Martin M. Cutadapt removes adapter sequences from high-throughput
617 sequencing reads. *EMBnet.journal.* 2013;7(10):2803-2809.
618 doi:10.14806/ej.17.1.200
- 619 35. Langmead B, Salzberg SL. Fast gapped-read alignment with Bowtie 2. *Nat*
620 *Methods.* 2012;9(4):357-359. doi:10.1038/nmeth.1923
- 621 36. Anders S, Pyl PT, Huber W. HTSeq-A Python framework to work with high-
622 throughput sequencing data. *Bioinformatics.* 2015;31(2):166-169.
623 doi:10.1093/bioinformatics/btu638
- 624 37. Andreu Z, Yáñez-Mó M. Tetraspanins in extracellular vesicle formation and
625 function. *Front Immunol.* 2014;5(442):1-12. doi:10.3389/fimmu.2014.00442
- 626 38. Phillips MC. New insights into the determination of HDL structure by
627 apolipoproteins. *J Lipid Res.* 2013;54(8):2034-2048. doi:10.1194/jlr.R034025
- 628 39. Behbodikhah J, Ahmed S, Elyasi A, et al. Apolipoprotein b and cardiovascular
629 disease: Biomarker and potential therapeutic target. *Metabolites.* 2021;11(690):1-
630 26. doi:10.3390/metabo11100690
- 631 40. Jung MK, Mun JY. Sample preparation and imaging of exosomes by transmission

632 electron microscopy. *J Vis Exp*. 2018;2018(131):5-9. doi:10.3791/56482

633 41. Huang X, Yuan T, Tschannen M, et al. Characterization of human plasma-derived
634 exosomal RNAs by deep sequencing. *BMC Genomics*. 2013;14(1):1-14.
635 doi:10.1186/1471-2164-14-319

636 42. Baldrich P, Tamim S, Mathioni S, Meyers B. Ligation bias is a major contributor to
637 nonstoichiometric abundances of secondary siRNAs and impacts analyses of
638 microRNAs. *bioRxiv*. 2020:1-44. doi:10.1101/2020.09.14.296616

639 43. Dard-Dascot C, Naquin D, d'Aubenton-Carafa Y, Alix K, Thermes C, van Dijk E.
640 Systematic comparison of small RNA library preparation protocols for next-
641 generation sequencing. *BMC Genomics*. 2018;19(1):1-16. doi:10.1186/s12864-
642 018-4491-6

643 44. Buschmann D, Kirchner B, Hermann S, et al. Evaluation of serum extracellular
644 vesicle isolation methods for profiling miRNAs by next-generation sequencing. *J*
645 *Extracell Vesicles*. 2018;7(1481321):1-18. doi:10.1080/20013078.2018.1481321

646 45. Schulz-Siegmund M, Aigner A. Nucleic acid delivery with extracellular vesicles.
647 *Adv Drug Deliv Rev*. 2021;173:89-111. doi:10.1016/j.addr.2021.03.005

648

Figure 1

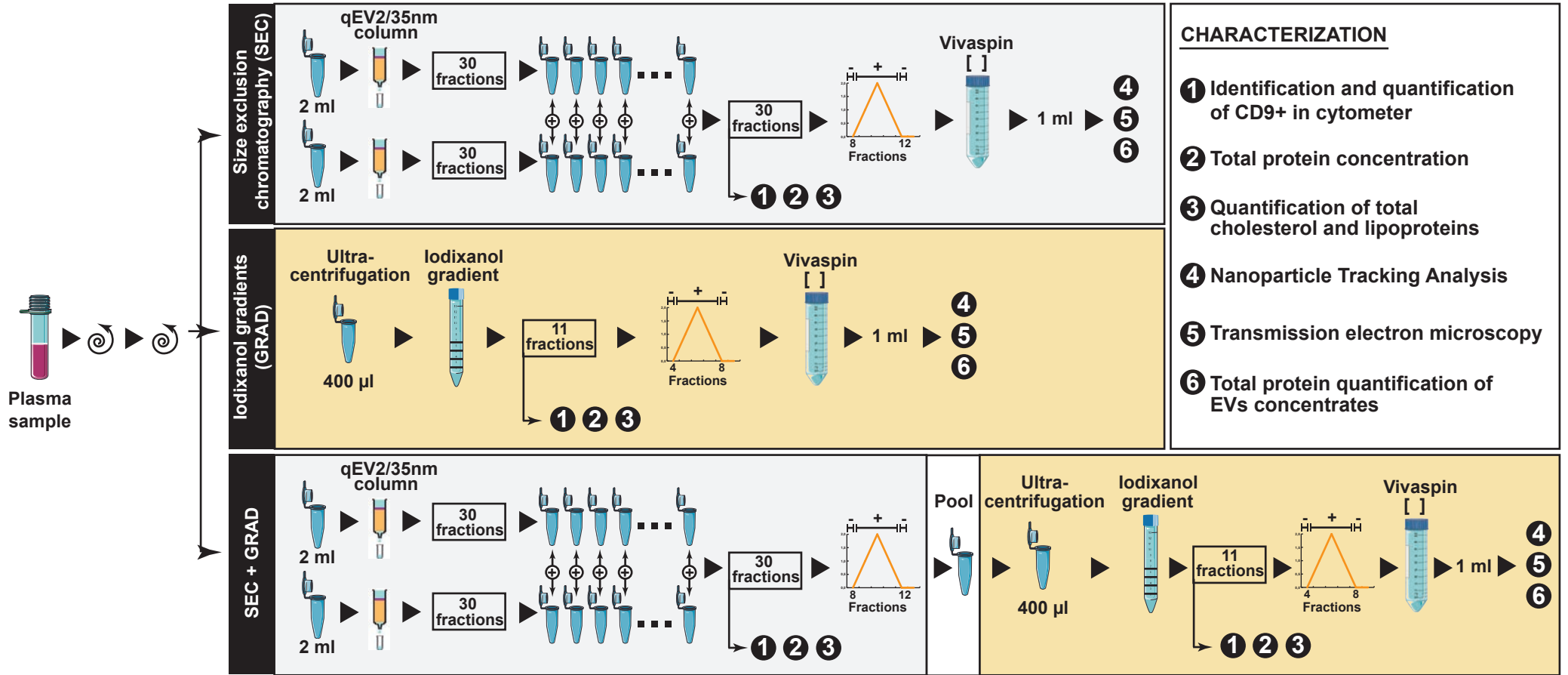
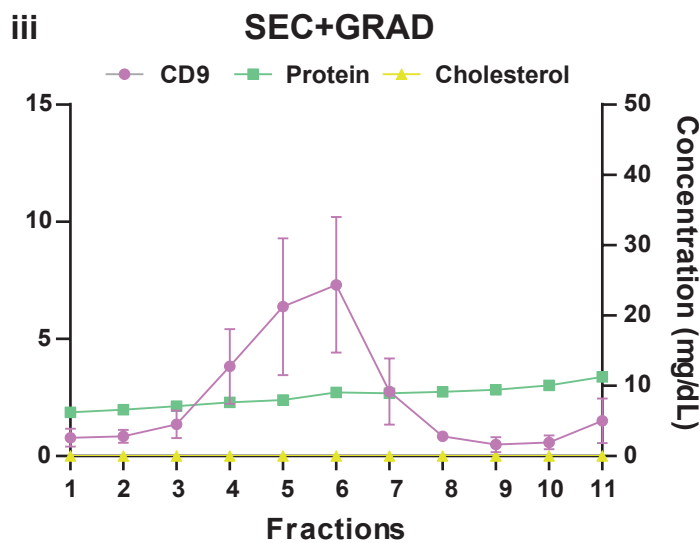
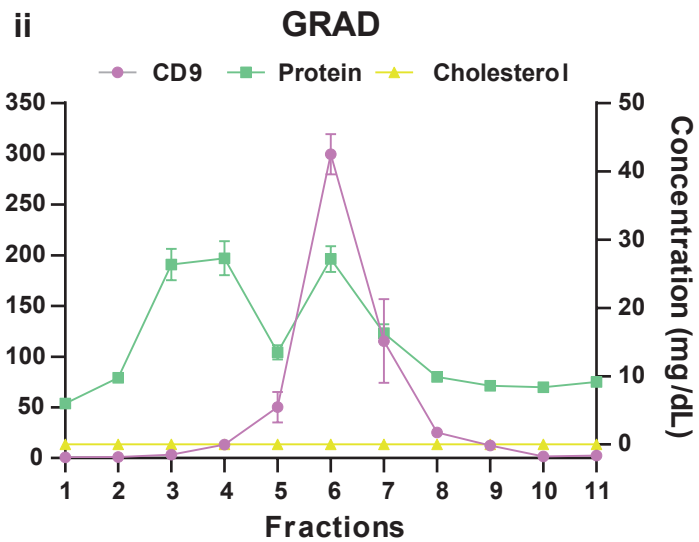
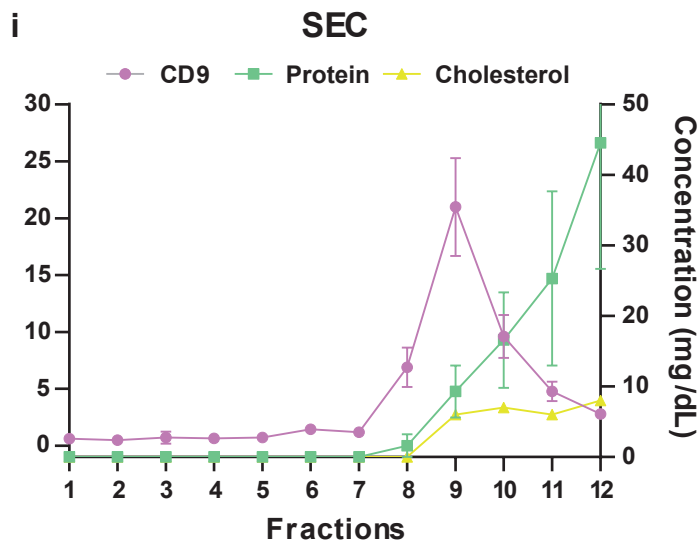


Figure 2

A



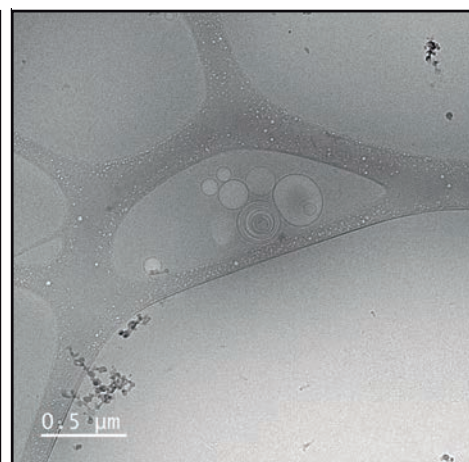
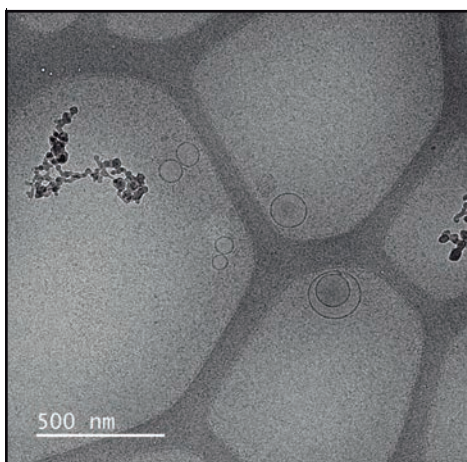
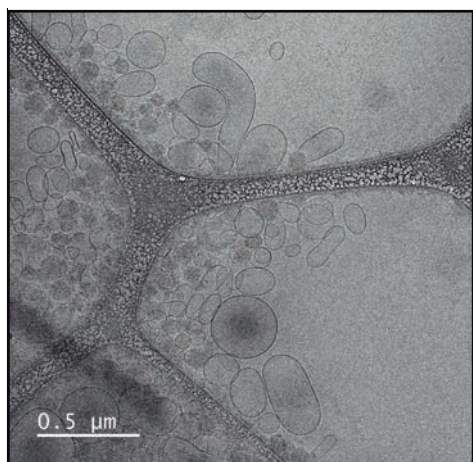
B

SEC

GRAD

SEC+GRAD

Cryo-TEM



TEM

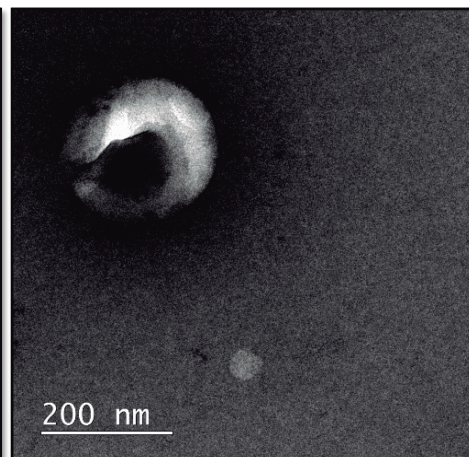
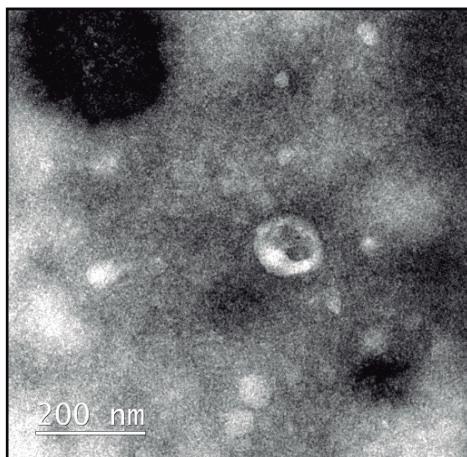
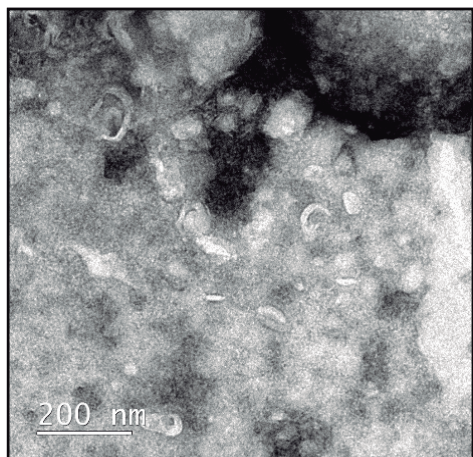
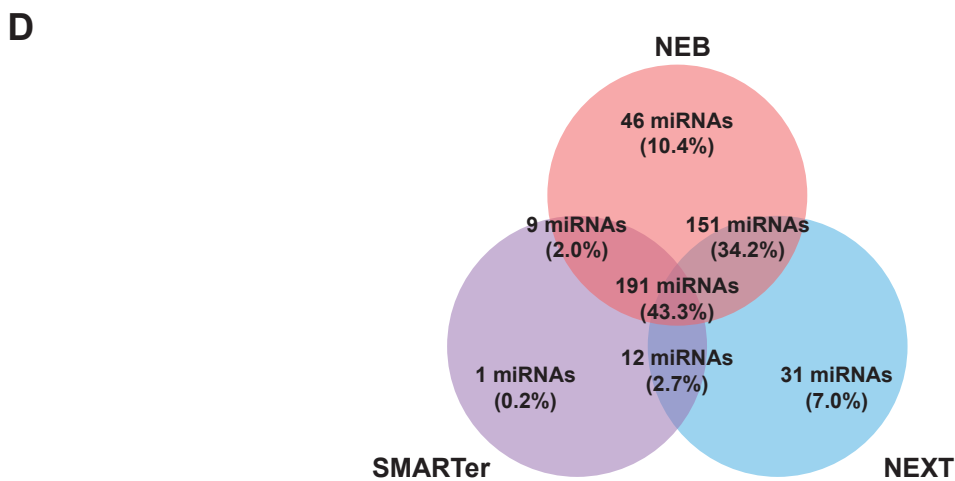
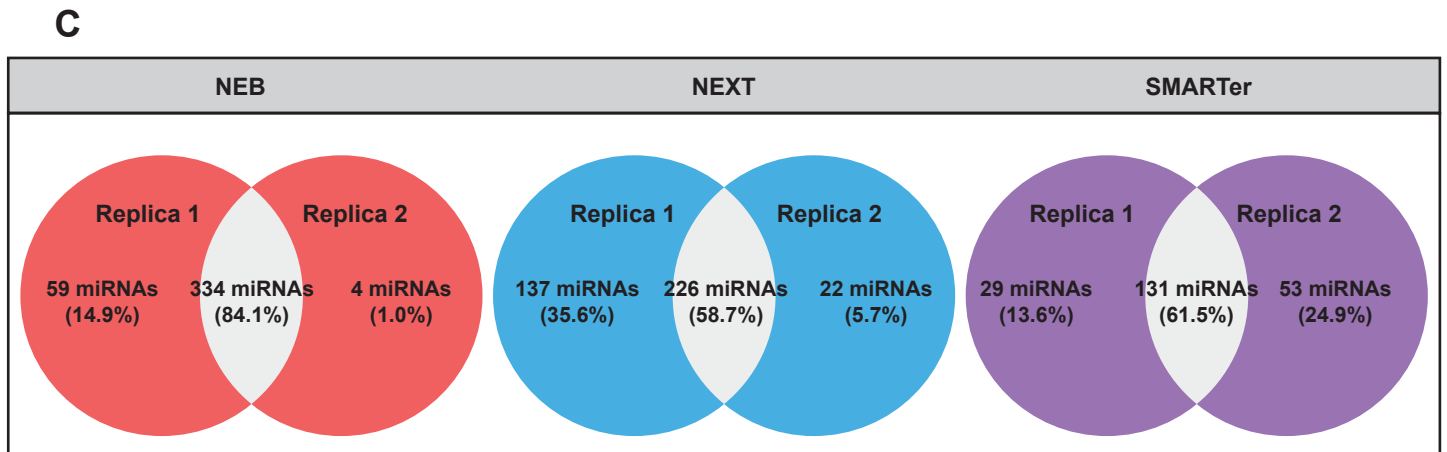
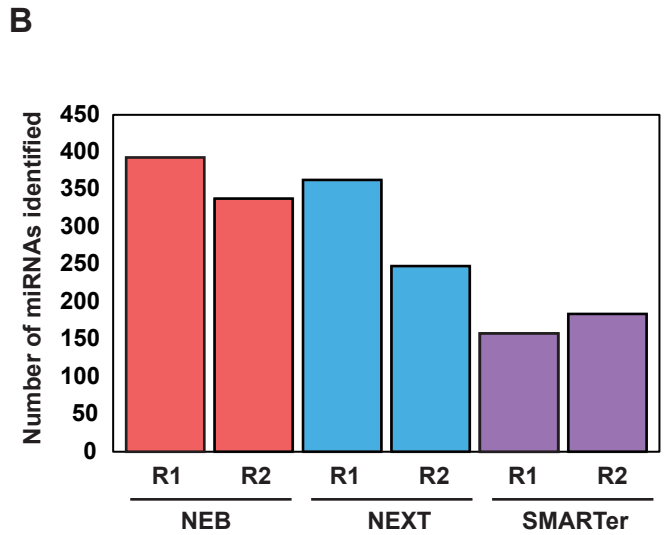
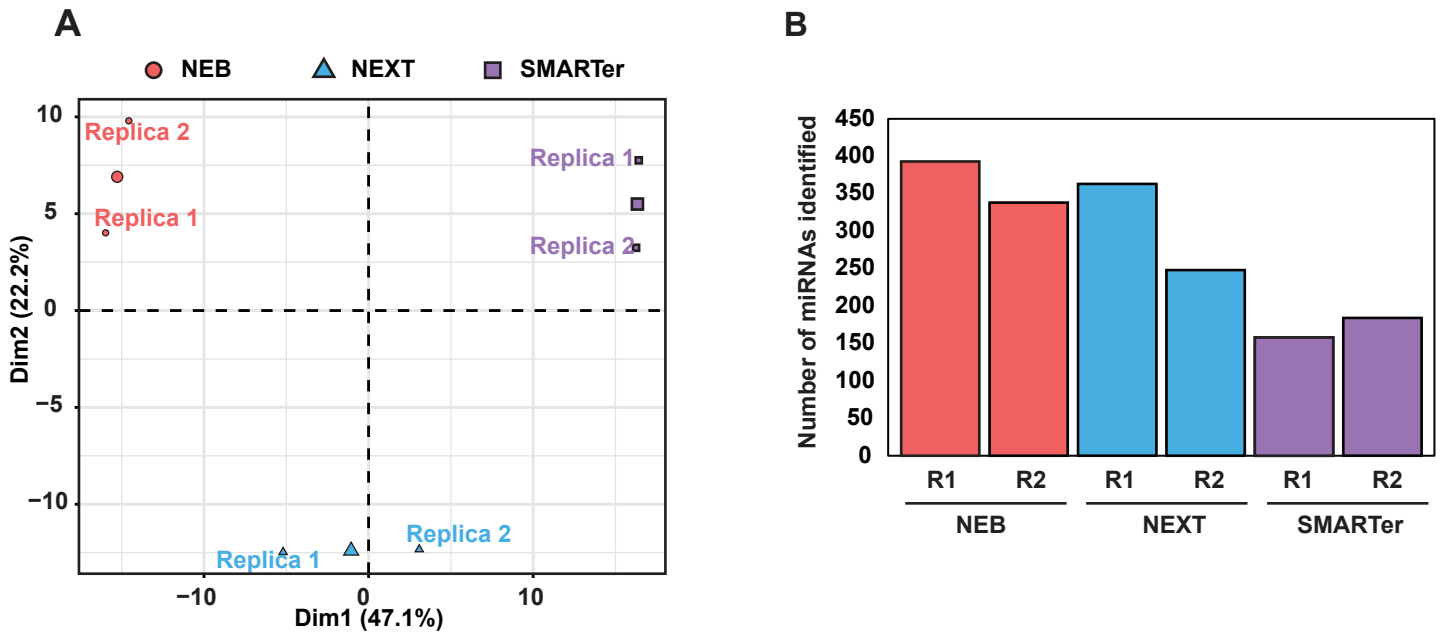
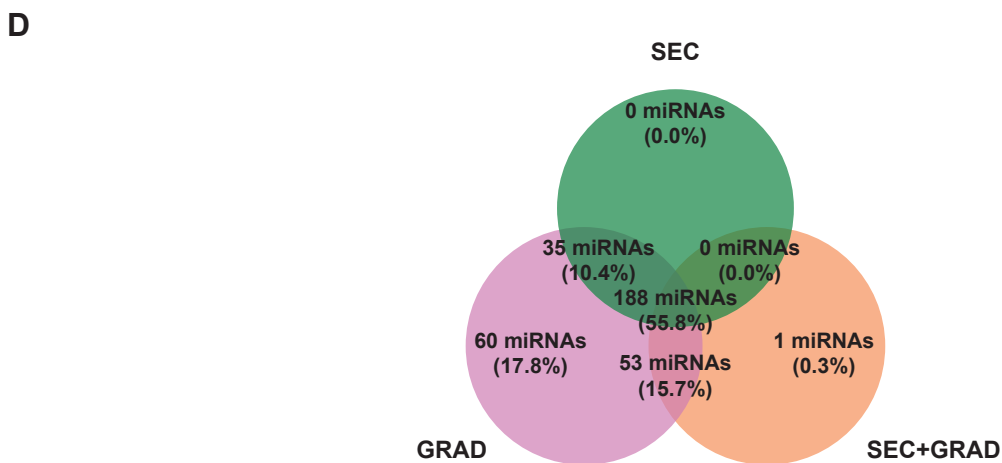
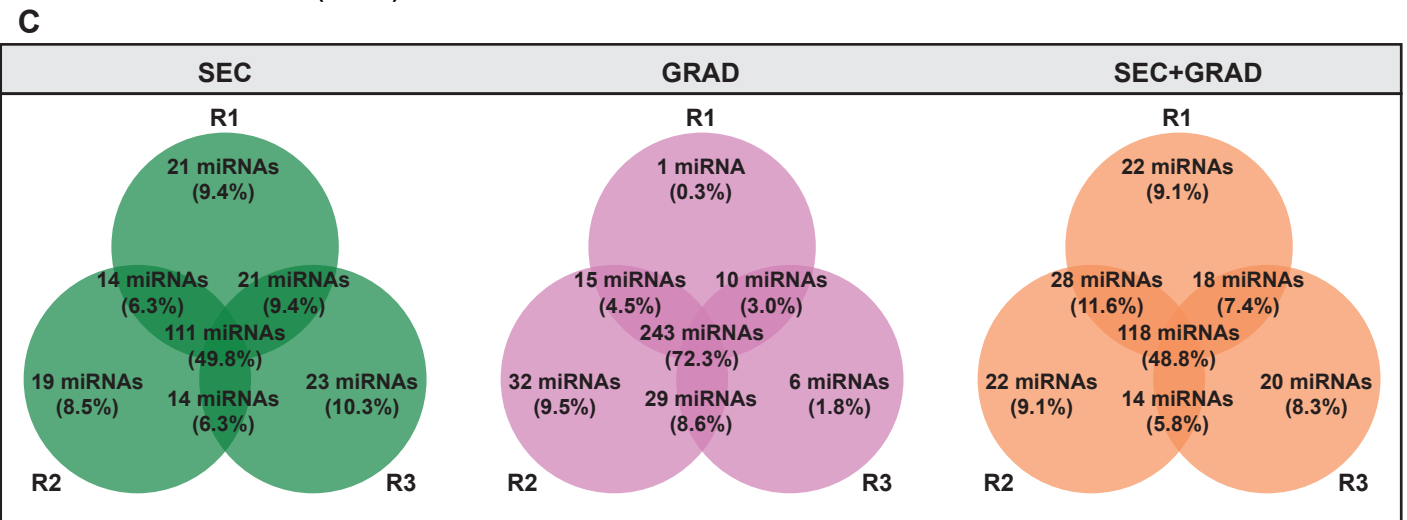
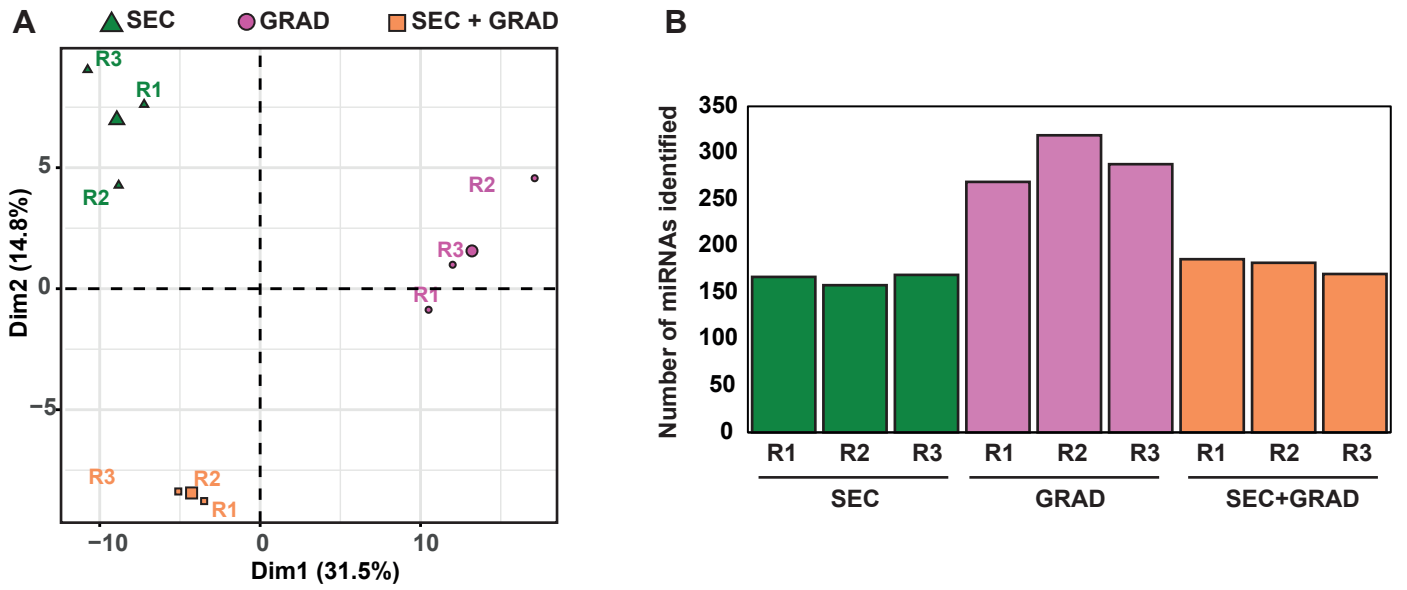


Figure 3



	NEB	NEXT	SMARTer	NEB vs NEXT p-value (significance)	NEB vs SMARTer p-value (significance)	NEXT vs SMARTer p-value (significance)
Different miRNAs	397	385	213	0.239 (n.s)	<0.001 (***)	<0.001 (***)
Unique miRNAs	46	31	1	0.094 (n.s)	<0.001 (***)	<0.001 (***)

Figure 4



	SEC	GRAD	SEC + GRAD	SEC vs GRAD p-value (significance)	SEC vs SEC + GRAD p-value (significance)	GRAD vs SEC + GRAD p-value (significance)
Different miRNAs	223	336	242	<0.001 (***)	0.037 (*)	<0.001 (***)
Unique miRNAs	0	60	1	<0.001 (***)	1 (n.s)	<0.001 (***)

Table 1. NTA parameters of each replica

EVs isolation methods	Concentration (particles/ml)	Mean (nm)	Mode (nm)	D10 (nm)	D50 (nm)	D90 (nm)
SEC1	1.29x10 ¹² +/- 1.24x10 ¹¹	128.4+/-1.5	96.4+/-5.4	80.9+/-2.1	116.2+/-1.3	194.1+/-2.1
SEC2	5.63x10 ¹¹ +/- 3.89x10 ¹⁰	134.5+/-2.4	108.4+/-4.1	87.6+/-0.8	121.2+/-1.6	206.7+/-8.5
SEC3	3.93x10 ¹¹ +/- 2.22x10 ⁹	137.2+/-1.9	114.8+/-7.7	78.3+/-2.3	124.2+/-1.8	215.7+/-3.4
GRAD1	7.29x10 ⁹ +/- 8.16x10 ⁷	134.7+/-1.2	95.5+/-1.1	86.1+/-2.8	120.6+/-1.2	200.9+/-4.7
GRAD2	9.55x10 ⁹ +/- 1.95x10 ⁸	133.7+/-1.6	94.3+/-2.5	82.8+/-1.4	120.2+/-1.8	203.7+/- 3.3
GRAD3	8.68x10 ⁹ +/- 3.18x10 ⁸	141.1+/-9.2	95.1+/-4.0	85.3+/-5.0	123.7+/-6.7	215.9+/-14.0
SEC+GRAD1	4.90x10 ⁹ +/- 2.23x10 ⁸	164.2+/-2.7	129.1+/-8.1	94.1+/-2.9	146.2+/-3.2	259.4+/-11.2
SEC+GRAD2	4.30x10 ⁹ +/- 1.31x10 ⁹	179.7+/-7.3	140.4+/-28.7	96.1+/-3.9	161.0+/-14.4	277.6+/-12.5
SEC+GRAD3	2.29x10 ⁹ +/- 1.25x10 ⁸	167.6+/-3.	111.5+/-2.5	94.9+/-9.0	148.3+/-2.9	278.9+/-16.8

4.3.3 Article 3 Supplementary material

Comparison of extracellular vesicle
isolation methods for miRNAs
sequencing

Figure S1

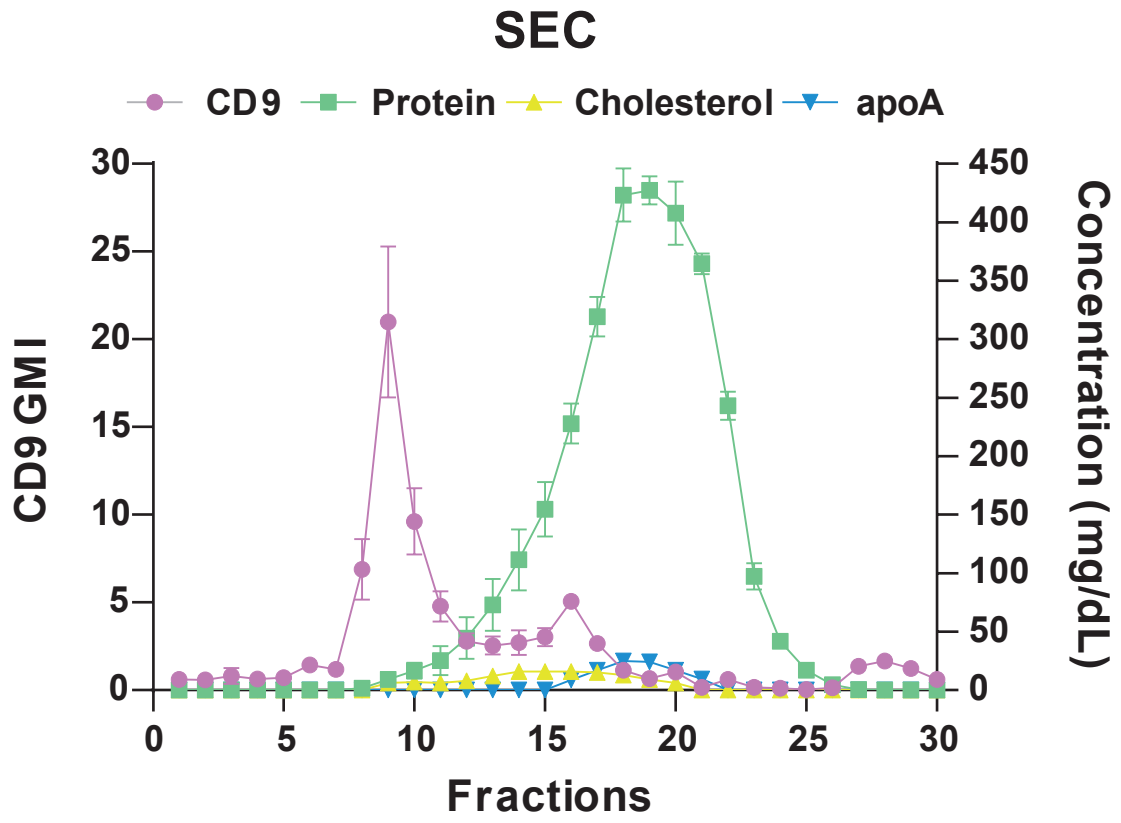


Figure S2

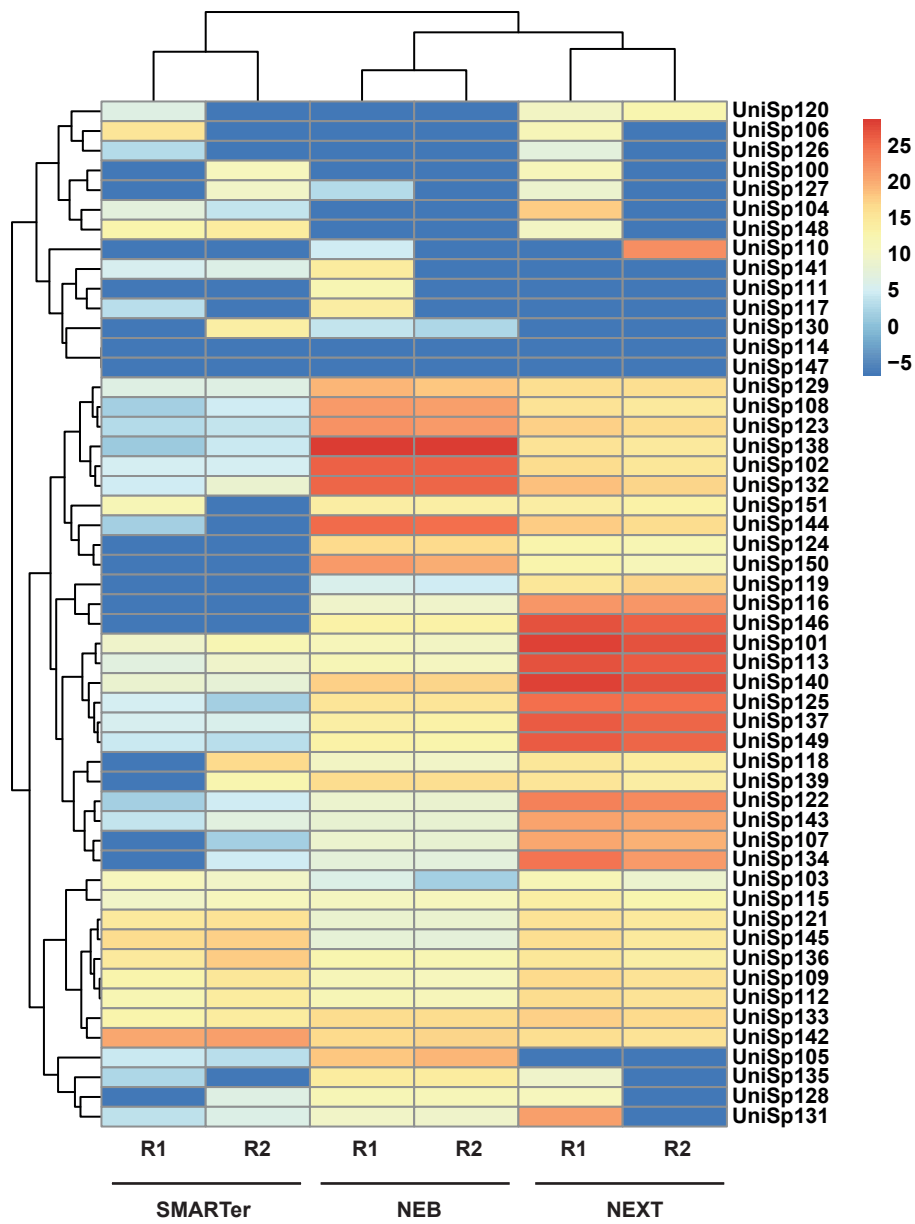


Table S1. Number of reads that remain after each of the steps of different library preparation methods in the bioinformatics process obtained by the ultra-deep sequencing analysis.

Library preparation method	Replica	Initial reads	Post-trimming ^a	Too short ^b	Too long ^c	Aligned 0 times ^d	Aligned exactly 1 time ^e	Aligned >1 times ^f	No feature ^g	Final reads ^h
NEBNext Multiplex Small RNA Library Prep Set for Illumina	1	11,892,073	2,701,556	486,910	8,703,607	634,166	785,411	1,281,979	413,514	1,653,876
	2	12,339,551	2,715,473	631,422	8,992,656	664,003	775,349	1,276,121	402,348	1,649,122
NextFlex Small RNA-Seq v3	1	18,689,055	8,063,509	1,850,873	8,774,673	2,055,648	2,228,291	3,779,570	1,184,404	4,823,457
	2	11,750,617	5,001,162	1,470,510	5,278,945	1,798,933	1,239,603	1,962,626	682,706	2,519,523
SMARTer smRNA-Seq Kit for Illumina	1	8,738,639	468,249	1,577,605	6,692,785	115,613	61,746	290,890	347,252	5,384
	2	8,727,581	395,306	1,374,911	6,957,364	91,132	56,476	247,698	285,256	18,918

^a Number of reads between 17 and 25 nucleotides after trimming according to kit manufacturer instructions.

^b Number of reads discarded to be shorter than 17 nucleotides.

^c Number of reads discarded to be longer than 25 nucleotides.

^d Number of reads discarded because do not map to human reference genome (assembly hg38).

^e Number of reads that map one time to human reference genome (assembly hg38).

^f Number of reads that map more than one time to human reference genome (assembly hg38).

^g Number of reads discarded because do not map to miRNAs coordinates.

^h Number of reads after each of the steps in the bioinformatics process.

Table S2. Normalized counts of miRNAs detected using three different library preparation and filtered by abundance (miRNAs with at least 50 reads).

Accession Number ^a	NEBNext ^b		NEXTFlex ^c		SMARTer ^d	
	Replica 1	Replica 2	Replica 1	Replica 2	Replica 1	Replica 2
MIMAT0000062	20955.5	19262.1	29495.8	27959.7	22795.2	34786.5
MIMAT0000062_1	23376.0	19940.0	29928.9	28755.3	22795.2	37721.2
MIMAT0000062_2	22924.3	20133.0	29687.4	29337.8	25210.6	39868.5
MIMAT0000063	69745.9	150564.7	43189.6	68745.2	82575.9	94052.4
MIMAT0000064	2175.0	2211.6	806.5	1808.9	603.8	2290.5
MIMAT0000065	2527.1	1269.6	4470.8	5498.1	4377.9	1717.9
MIMAT0000066	1408.3	1493.0	1687.9	1219.6	2113.5	1861.0
MIMAT0000067	32428.1	28905.8	26390.8	27383.0	20530.7	33498.1
MIMAT0000067_1	45014.8	43239.4	27893.9	28879.4	19021.1	35072.8
MIMAT0000068	18.5	66.0	385.2	134.4	0.0	0.0
MIMAT0000069	384.5	347.9	12147.5	13791.4	1207.7	2218.9
MIMAT0000069_1	370.6	358.0	12187.2	13883.9	3321.2	3221.0
MIMAT0000070	433.1	203.1	160.6	0.0	3925.0	787.3
MIMAT0000072	4.6	0.0	258.4	0.0	0.0	0.0
MIMAT0000073	250.2	71.1	102.5	618.7	6189.4	1789.4
MIMAT0000074	169.1	213.3	79.5	120.1	7699.0	3292.5
MIMAT0000074_1	159.8	286.9	77.2	116.6	7699.0	3722.0
MIMAT0000075	901.0	721.1	486.1	2531.0	301.9	429.5
MIMAT0000076	119624.9	103900.0	105219.8	129114.9	2566.3	6871.4
MIMAT0000077	8927.0	10669.6	7823.8	9284.3	452.9	429.5
MIMAT0000078	440.1	137.1	23312.7	28109.6	30645.2	53038.7
MIMAT0000079	2.3	12.7	59.7	0.0	0.0	0.0
MIMAT0000080	6992.9	6055.9	13673.0	16933.7	5736.5	10020.8
MIMAT0000080_1	6891.0	6388.5	13781.2	16404.0	3472.1	12025.0
MIMAT0000081	29713.4	29487.3	4984.8	4458.9	22191.3	17965.9
MIMAT0000082	120820.1	106444.2	17445.2	21690.1	301.9	572.6
MIMAT0000082_1	116623.0	106444.2	16577.7	20490.1	452.9	143.2
MIMAT0000083	4065.1	3382.2	9703.9	9973.6	603.8	143.2
MIMAT0000084	16197.8	14529.1	5981.2	6957.8	1811.5	214.7
MIMAT0000085	275.6	248.8	820.4	1016.2	0.0	0.0
MIMAT0000086	1570.4	1307.7	3734.2	6456.8	2113.5	1861.0
MIMAT0000087	3909.9	2861.6	5508.7	4021.2	452.9	0.0
MIMAT0000088	491.1	652.6	124.9	64.9	754.8	0.0
MIMAT0000090	247.8	162.5	64.1	0.0	0.0	930.5
MIMAT0000092	23864.8	24205.8	37890.9	42738.0	8906.7	23548.9
MIMAT0000092_1	22449.5	23246.0	35166.6	38624.4	9812.5	24407.8
MIMAT0000093	870.9	716.0	4627.0	7978.6	5434.6	5225.1

MIMAT0000094	136.7	17.8	48.2	0.0	0.0	0.0
MIMAT0000095	57.9	0.0	112.4	168.9	0.0	0.0
MIMAT0000096	1556.5	1912.0	2804.8	4320.4	1660.6	715.8
MIMAT0000097	28335.2	29616.8	1687.4	2487.9	0.0	0.0
MIMAT0000098	6620.0	6441.9	684.5	1.7	0.0	0.0
MIMAT0000099	9191.0	9653.9	2550.6	3121.0	905.8	214.7
MIMAT0000099_1	9612.6	10568.0	2581.8	2984.8	603.8	429.5
MIMAT0000100	30.1	2.5	268.8	454.4	2415.4	3793.6
MIMAT0000100_1	18.5	0.0	249.8	420.5	2566.3	3364.1
MIMAT0000101	1028.4	774.4	3033.2	2398.9	0.0	0.0
MIMAT0000101_1	1109.5	703.3	2875.7	2337.4	0.0	0.0
MIMAT0000104	180.7	66.0	320.7	153.4	0.0	0.0
MIMAT0000222	12721.1	11489.7	1084.0	748.5	1509.6	357.9
MIMAT0000227	379.9	322.5	1823.8	1760.1	754.8	2719.9
MIMAT0000231	1894.7	1406.7	388.5	198.2	452.9	0.0
MIMAT0000231_1	1836.8	1322.9	397.1	176.4	301.9	0.0
MIMAT0000232	322.0	286.9	1885.3	1466.6	0.0	143.2
MIMAT0000232_1	296.5	281.8	1879.3	1457.4	452.9	214.7
MIMAT0000242_1	85.7	33.0	0.0	0.0	0.0	0.0
MIMAT0000243	321547.7	360489.9	3939.9	2659.7	0.0	0.0
MIMAT0000244	690.3	553.5	1248.5	960.5	0.0	1073.7
MIMAT0000244_1	704.2	604.3	1214.1	888.1	0.0	787.3
MIMAT0000245	137636.4	142058.5	52009.5	56214.1	754.8	0.0
MIMAT0000250	1362.0	1561.6	806.5	735.3	0.0	357.9
MIMAT0000252	854.7	700.8	238.6	426.8	0.0	0.0
MIMAT0000252_1	910.3	721.1	238.9	430.8	0.0	0.0
MIMAT0000252_2	942.7	713.5	236.0	436.6	0.0	0.0
MIMAT0000253	45304.4	55247.1	5628.4	6087.5	0.0	0.0
MIMAT0000254	61926.1	77937.0	6771.6	9017.7	0.0	143.2
MIMAT0000255	0.0	0.0	65.7	52.3	0.0	0.0
MIMAT0000256	3092.3	2303.0	1188.6	1721.1	0.0	0.0
MIMAT0000256_1	2964.9	2460.4	1184.7	1727.4	0.0	0.0
MIMAT0000257	530.4	335.2	134.8	183.8	0.0	0.0
MIMAT0000257_1	460.9	388.5	124.9	170.0	0.0	0.0
MIMAT0000259	2652.2	3460.9	1751.3	3446.1	0.0	0.0
MIMAT0000261	3020.4	4740.6	619.3	1023.1	1660.6	357.9
MIMAT0000264	53.3	0.0	49.8	0.0	0.0	0.0
MIMAT0000265	74.1	66.0	0.0	0.0	0.0	0.0
MIMAT0000271	20.8	116.8	36.2	0.0	0.0	71.6
MIMAT0000272	2413.6	2455.4	904.3	457.8	0.0	0.0
MIMAT0000278	5600.8	2595.0	3030.4	1785.4	3170.2	357.9

MIMAT0000279	8588.8	8602.7	1646.5	1705.0	603.8	715.8
MIMAT0000280	576.8	358.0	12257.6	12464.4	43929.8	67712.0
MIMAT0000281	5285.8	5657.3	1551.6	580.8	452.9	143.2
MIMAT0000318	111.2	71.1	127.5	0.0	0.0	0.0
MIMAT0000414	23174.5	19995.9	39860.7	47158.4	14039.4	12239.7
MIMAT0000415	151557.3	144879.5	17704.7	22014.7	8755.8	5511.4
MIMAT0000416	416.9	228.5	743.2	931.8	0.0	930.5
MIMAT0000416_1	421.6	243.8	653.2	938.7	452.9	1145.2
MIMAT0000417	85.7	40.6	3718.0	3270.9	452.9	572.6
MIMAT0000418	187.6	78.7	1099.1	1788.3	2868.3	8589.3
MIMAT0000419	17754.4	17611.6	10260.1	9037.8	0.0	1145.2
MIMAT0000420	60.2	10.2	276.7	248.2	603.8	0.0
MIMAT0000421	1314537.7	1453863.0	138996.8	158159.1	29739.4	48171.4
MIMAT0000423	664.8	815.1	606.5	514.1	0.0	214.7
MIMAT0000423_1	750.5	787.1	618.8	530.8	0.0	143.2
MIMAT0000424	24411.4	30089.1	1370.1	2349.5	0.0	71.6
MIMAT0000424_1	14859.0	16898.1	927.3	1307.5	0.0	0.0
MIMAT0000425	69.5	68.6	37.6	0.0	13737.5	3650.4
MIMAT0000426	16.2	63.5	136.6	0.0	0.0	0.0
MIMAT0000427	0.0	0.0	0.0	84.4	0.0	0.0
MIMAT0000427_1	0.0	0.0	0.0	85.6	0.0	0.0
MIMAT0000431	101.9	86.3	145.5	0.0	0.0	0.0
MIMAT0000432	4.6	0.0	47.7	0.0	0.0	0.0
MIMAT0000433	10416.4	11238.3	6038.6	9689.3	15549.0	5654.6
MIMAT0000434	555.9	464.7	341.9	449.2	7850.0	3364.1
MIMAT0000435	23105.0	23378.1	11082.8	11873.3	301.9	572.6
MIMAT0000436	945.0	799.8	1080.1	1033.4	10869.2	715.8
MIMAT0000437	0.0	0.0	289.2	0.0	754.8	787.3
MIMAT0000438	1948.0	1223.9	190.4	175.2	0.0	0.0
MIMAT0000440	8584.2	7391.5	15001.9	15461.9	18568.3	12382.8
MIMAT0000442	2.3	0.0	0.0	182.7	0.0	0.0
MIMAT0000442_1	2.3	0.0	0.0	168.9	0.0	0.0
MIMAT0000442_2	4.6	0.0	0.0	170.6	0.0	0.0
MIMAT0000443	5327.5	8389.4	3354.8	2528.2	905.8	1503.1
MIMAT0000444	1714.1	1868.8	3805.4	2856.7	74273.0	287597.0
MIMAT0000445	48412.8	45631.3	12224.7	20177.6	9661.5	6298.8
MIMAT0000446	528.1	840.5	0.0	0.0	0.0	0.0
MIMAT0000447	6529.6	5383.0	476.7	161.4	301.9	787.3
MIMAT0000449	23702.6	18645.1	28003.7	27081.9	18568.3	23405.7
MIMAT0000451	956.6	441.8	3308.1	4322.2	17813.4	53682.9
MIMAT0000453	0.0	0.0	98.6	0.0	0.0	0.0

MIMAT0000454	27.8	233.6	0.0	0.0	0.0	0.0
MIMAT0000455	5735.1	2983.5	3435.9	6293.7	3321.2	1145.2
MIMAT0000456	2717.0	1404.2	2935.7	2654.0	2264.4	1646.3
MIMAT0000460	595.3	586.5	312.4	413.0	151.0	214.7
MIMAT0000460_1	484.1	520.5	558.0	411.3	452.9	0.0
MIMAT0000461	25.5	58.4	64.9	0.0	151.0	0.0
MIMAT0000462	157.5	210.8	0.0	197.6	0.0	357.9
MIMAT0000510	46837.8	21384.8	14197.4	8556.5	151.0	858.9
MIMAT0000617	127.4	101.6	137.2	0.0	0.0	0.0
MIMAT0000646	741.2	530.7	332.0	373.4	0.0	0.0
MIMAT0000680	118.1	119.3	625.3	348.7	0.0	0.0
MIMAT0000681	32.4	96.5	518.4	619.8	1207.7	858.9
MIMAT0000682	539.7	248.8	0.0	0.0	0.0	0.0
MIMAT0000688	0.0	0.0	25.3	0.0	603.8	143.2
MIMAT0000689	5390.0	6459.6	789.1	524.5	0.0	0.0
MIMAT0000691	30.1	35.5	147.1	0.0	603.8	357.9
MIMAT0000692	11498.1	6881.1	19926.9	26585.6	0.0	71.6
MIMAT0000693	3495.3	3839.2	540.0	0.0	1962.5	357.9
MIMAT0000703	88.0	116.8	691.3	842.1	151.0	0.0
MIMAT0000707	2358.0	2440.1	668.6	923.7	151.0	0.0
MIMAT0000720	4.6	0.0	20.1	0.0	0.0	858.9
MIMAT0000721	115.8	30.5	1896.6	2228.9	0.0	214.7
MIMAT0000722	148.2	119.3	0.0	158.0	0.0	0.0
MIMAT0000727	169.1	157.4	597.2	492.9	603.8	0.0
MIMAT0000728	3233.5	4273.4	885.6	968.5	301.9	0.0
MIMAT0000729	9.3	0.0	103.5	0.0	151.0	429.5
MIMAT0000729_1	30.1	0.0	87.9	0.0	0.0	214.7
MIMAT0000732	2812.0	2800.7	77.2	143.0	301.9	0.0
MIMAT0000733	593.0	454.5	99.6	384.9	0.0	0.0
MIMAT0000736	1637.6	1505.7	37.3	181.5	0.0	0.0
MIMAT0000737	3534.7	3813.8	2760.5	4922.5	1811.5	1503.1
MIMAT0000750	335.9	269.2	179.9	446.3	754.8	787.3
MIMAT0000751	1040.0	601.8	259.5	283.2	0.0	143.2
MIMAT0000752	3604.2	4288.6	820.9	1495.3	1962.5	3077.8
MIMAT0000753	150.6	0.0	1511.9	1573.4	5283.6	6585.1
MIMAT0000754	11.6	0.0	33.6	116.0	151.0	214.7
MIMAT0000755	108.9	33.0	133.5	0.0	0.0	0.0
MIMAT0000756	57.9	2.5	147.1	209.1	1358.7	572.6
MIMAT0000757	78473.7	86443.2	4832.3	5943.8	2717.3	10020.8
MIMAT0000759	8164.9	7840.9	1579.2	2203.0	151.0	286.3
MIMAT0000760	60.2	0.0	188.8	0.0	0.0	71.6

MIMAT0000762	0.0	0.0	25.6	0.0	0.0	0.0
MIMAT0000764	55.6	96.5	103.0	0.0	0.0	0.0
MIMAT0000765	233.9	246.3	7986.7	9940.9	2566.3	3507.3
MIMAT0000772	67.2	142.2	170.3	418.8	151.0	71.6
MIMAT0001340	17416.2	19731.8	7633.9	10677.9	301.9	501.0
MIMAT0001343	210.8	134.6	62.8	0.0	0.0	0.0
MIMAT0001536	48.6	20.3	27.1	0.0	0.0	0.0
MIMAT0001545	37.1	0.0	39.1	0.0	0.0	0.0
MIMAT0001545_1	32.4	0.0	40.9	0.0	0.0	0.0
MIMAT0001618	71.8	71.1	123.3	0.0	301.9	143.2
MIMAT0001621	192.3	228.5	131.2	0.0	0.0	0.0
MIMAT0001629	6.9	0.0	116.6	0.0	0.0	0.0
MIMAT0001629_1	2.3	0.0	117.6	0.0	0.0	0.0
MIMAT0001630	9.3	0.0	0.3	553.2	0.0	0.0
MIMAT0001631	38927.6	35853.0	36311.1	47680.0	6642.3	2648.4
MIMAT0001635	85.7	86.3	276.2	0.0	0.0	0.0
MIMAT0001636	30.1	0.0	44.9	0.0	0.0	0.0
MIMAT0001639	34512.8	40431.1	4898.0	5745.1	2113.5	4366.2
MIMAT0002171	104.2	0.0	38.1	0.0	0.0	0.0
MIMAT0002173	37.1	109.2	285.0	107.4	1207.7	3149.4
MIMAT0002174	1107.2	1376.2	2414.4	819.2	452.9	1431.5
MIMAT0002175	2388.1	2419.8	531.7	318.2	0.0	0.0
MIMAT0002176	958.9	2920.0	1252.2	1777.4	301.9	214.7
MIMAT0002177	57302.8	83477.5	28584.1	27261.2	4679.8	13528.1
MIMAT0002177_1	63362.2	92697.2	28600.0	27322.6	6642.3	13098.6
MIMAT0002178	48.6	0.0	88.7	526.2	0.0	0.0
MIMAT0002808	289.5	134.6	0.0	0.0	452.9	0.0
MIMAT0002809	14861.3	13480.4	1445.4	1236.8	1962.5	3507.3
MIMAT0002813	90.3	48.2	84.2	0.0	0.0	0.0
MIMAT0002814	213.1	157.4	71.2	0.0	0.0	0.0
MIMAT0002816	25.5	0.0	451.9	868.6	0.0	0.0
MIMAT0002817	755.1	634.8	502.2	1647.5	0.0	143.2
MIMAT0002818	23.2	0.0	21.6	0.0	0.0	143.2
MIMAT0002821	227.0	86.3	0.0	0.0	0.0	0.0
MIMAT0002859	30.1	157.4	0.0	0.0	0.0	0.0
MIMAT0002859_1	30.1	129.5	0.0	0.0	0.0	0.0
MIMAT0002870	178.4	137.1	115.3	172.3	0.0	0.0
MIMAT0002871	55.6	10.2	165.6	123.5	0.0	0.0
MIMAT0002874	18.5	129.5	0.0	199.9	0.0	0.0
MIMAT0002875	0.0	0.0	47.7	0.0	0.0	0.0
MIMAT0002876	30.1	0.0	216.4	87.3	452.9	0.0

MIMAT0002888	3770.9	3478.7	32.9	66.6	0.0	143.2
MIMAT0002891	30.1	0.0	52.4	196.5	0.0	0.0
MIMAT0003161	39.4	139.7	0.0	0.0	0.0	0.0
MIMAT0003180	6.9	0.0	1147.9	841.0	0.0	357.9
MIMAT0003218	484.1	942.0	388.3	0.0	0.0	357.9
MIMAT0003220	11.6	0.0	103.0	455.0	0.0	0.0
MIMAT0003239	0.0	58.4	578.1	701.4	1962.5	3292.5
MIMAT0003241	39.4	0.0	87.4	0.0	452.9	0.0
MIMAT0003249	6965.1	5504.9	1456.9	871.4	0.0	0.0
MIMAT0003251	0.0	0.0	0.0	54.0	0.0	0.0
MIMAT0003251_1	0.0	0.0	0.0	54.0	0.0	0.0
MIMAT0003251_2	0.0	0.0	0.0	58.0	0.0	0.0
MIMAT0003266	30.1	0.0	118.1	0.0	0.0	0.0
MIMAT0003283	74.1	96.5	0.0	0.0	0.0	0.0
MIMAT0003297	416.9	698.3	242.0	198.8	301.9	429.5
MIMAT0003321	92.7	43.2	72.8	0.0	0.0	0.0
MIMAT0003322	134.3	149.8	3307.3	3786.8	0.0	0.0
MIMAT0003329	111.2	154.9	1.3	0.0	0.0	0.0
MIMAT0003330	509.6	540.8	0.0	0.0	0.0	0.0
MIMAT0003332	44.0	0.0	175.5	286.7	0.0	1073.7
MIMAT0003338	53.3	193.0	178.1	0.0	151.0	501.0
MIMAT0003339	148.2	231.1	347.3	691.1	0.0	1288.4
MIMAT0003389	20.8	63.5	56.8	0.0	0.0	0.0
MIMAT0003393	549.0	479.9	2585.2	2874.6	603.8	787.3
MIMAT0003884	60.2	45.7	52.2	0.0	0.0	71.6
MIMAT0003885	11.6	0.0	74.6	0.0	151.0	0.0
MIMAT0003886	111.2	124.4	0.0	0.0	0.0	0.0
MIMAT0003888	9.3	0.0	65.5	0.0	0.0	0.0
MIMAT0003945	0.0	0.0	0.0	236.1	0.0	0.0
MIMAT0004481	521.2	578.9	48.2	0.0	603.8	572.6
MIMAT0004481_1	437.8	571.3	48.0	0.0	905.8	1360.0
MIMAT0004482	199.2	766.8	512.1	272.3	2415.4	9018.7
MIMAT0004484	11822.4	25381.5	13493.6	16784.9	19172.1	130485.1
MIMAT0004485	11.6	116.8	0.0	0.0	0.0	0.0
MIMAT0004486	48.6	109.2	47.7	0.0	452.9	1717.9
MIMAT0004494	20.8	0.0	114.7	184.4	0.0	143.2
MIMAT0004495	393.8	386.0	18.3	725.5	151.0	0.0
MIMAT0004496	9.3	83.8	123.6	0.0	0.0	357.9
MIMAT0004497	120.4	167.6	0.0	0.0	0.0	286.3
MIMAT0004498	85.7	38.1	0.0	287.8	0.0	0.0
MIMAT0004500	48.6	114.3	40.4	0.0	301.9	572.6

MIMAT0004501	108.9	116.8	0.0	0.0	0.0	0.0
MIMAT0004502	5529.0	5085.9	1422.0	263.7	603.8	286.3
MIMAT0004518	4486.7	4933.6	1241.8	1964.0	0.0	143.2
MIMAT0004549	233.9	286.9	0.0	0.0	0.0	0.0
MIMAT0004551	90.3	76.2	0.0	0.0	0.0	0.0
MIMAT0004552	845.4	1254.3	108.7	0.0	0.0	0.0
MIMAT0004556	104.2	81.3	44.3	0.0	2113.5	2863.1
MIMAT0004558	356.7	586.5	14.6	640.5	0.0	0.0
MIMAT0004563	322.0	233.6	1897.3	1487.3	151.0	143.2
MIMAT0004568	90.3	147.3	40.9	0.0	0.0	0.0
MIMAT0004570	5464.1	4303.9	162.5	1552.7	603.8	1073.7
MIMAT0004585	18.5	0.0	39.1	0.0	603.8	1789.4
MIMAT0004586	92.7	38.1	268.6	360.8	1358.7	858.9
MIMAT0004587	53.3	0.0	97.8	0.0	0.0	0.0
MIMAT0004589	48.6	121.9	0.0	0.0	0.0	0.0
MIMAT0004597	6881.7	6274.3	1398.0	1544.7	452.9	71.6
MIMAT0004600	690.3	289.5	2382.4	525.0	1056.7	858.9
MIMAT0004601	535.1	434.2	320.0	467.6	0.0	143.2
MIMAT0004602	118.1	30.5	0.0	0.0	0.0	0.0
MIMAT0004603	44.0	127.0	0.0	0.0	0.0	0.0
MIMAT0004606	20.8	0.0	43.0	0.0	0.0	0.0
MIMAT0004608	71.8	104.1	0.0	0.0	0.0	0.0
MIMAT0004610	525.8	515.4	102.0	194.7	0.0	715.8
MIMAT0004611	136.7	53.3	0.0	0.0	151.0	0.0
MIMAT0004614	829.2	782.1	462.1	0.0	0.0	0.0
MIMAT0004672	1535.7	1371.1	284.5	0.0	754.8	0.0
MIMAT0004674	27.8	0.0	21.4	0.0	0.0	0.0
MIMAT0004678	108.9	40.6	0.0	0.0	0.0	0.0
MIMAT0004680	945.0	1183.2	530.1	402.7	1207.7	858.9
MIMAT0004682	1711.7	1152.8	61.3	868.6	452.9	0.0
MIMAT0004683	0.0	0.0	58.9	377.4	151.0	0.0
MIMAT0004688	78.8	127.0	0.0	0.0	0.0	0.0
MIMAT0004690	41.7	0.0	16.9	0.0	0.0	0.0
MIMAT0004692	7710.9	8244.7	2077.0	4641.0	0.0	0.0
MIMAT0004694	1239.2	1241.7	119.4	0.0	0.0	787.3
MIMAT0004697	46.3	2.5	1627.2	1814.7	0.0	286.3
MIMAT0004699	53.3	0.0	93.1	0.0	0.0	0.0
MIMAT0004701	229.3	304.7	187.8	0.0	0.0	0.0
MIMAT0004702	426.2	302.2	708.5	329.7	0.0	0.0
MIMAT0004703	993.7	1069.0	474.1	1086.3	0.0	0.0
MIMAT0004748	211764.7	287940.9	42571.3	57079.8	23248.1	11237.6

MIMAT0004749	252.5	274.2	210.7	0.0	0.0	0.0
MIMAT0004761	1176.7	3374.5	1153.9	2370.2	301.9	0.0
MIMAT0004762	354.4	391.0	362.5	572.7	0.0	0.0
MIMAT0004762_1	257.1	284.4	236.3	550.9	0.0	0.0
MIMAT0004766	25.5	38.1	75.4	0.0	0.0	0.0
MIMAT0004767	201.5	639.9	0.0	380.9	905.8	0.0
MIMAT0004774	542.0	624.6	448.8	440.6	0.0	0.0
MIMAT0004775	51.0	43.2	388.8	112.0	0.0	0.0
MIMAT0004776	125.1	27.9	0.0	0.0	452.9	0.0
MIMAT0004780	4.6	0.0	100.1	0.0	0.0	143.2
MIMAT0004792	90.3	144.7	0.0	0.0	0.0	0.0
MIMAT0004793	0.0	0.0	0.0	0.0	2868.3	3936.7
MIMAT0004795	0.0	0.0	25.0	0.0	0.0	0.0
MIMAT0004796	41.7	68.6	32.3	0.0	0.0	0.0
MIMAT0004797	37.1	139.7	0.0	0.0	0.0	0.0
MIMAT0004799	108.9	35.5	0.0	0.0	0.0	0.0
MIMAT0004801	34.7	0.0	0.0	63.2	0.0	644.2
MIMAT0004808	1223.0	1279.7	774.5	704.9	2264.4	2004.2
MIMAT0004809	4.6	27.9	125.2	0.0	0.0	143.2
MIMAT0004810	1690.9	1399.1	183.6	223.5	452.9	71.6
MIMAT0004813	78.8	177.7	52.9	0.0	0.0	0.0
MIMAT0004814	555.9	299.6	55.0	418.8	0.0	71.6
MIMAT0004819	731.9	840.5	31.3	0.0	0.0	0.0
MIMAT0004909	44.0	63.5	120.0	0.6	0.0	0.0
MIMAT0004921	308.1	477.4	59.2	49.4	0.0	0.0
MIMAT0004945	7852.2	7053.8	236.3	970.8	1056.7	286.3
MIMAT0004947	34.7	175.2	970.6	726.1	0.0	2863.1
MIMAT0004948	60.2	33.0	42.2	0.0	0.0	0.0
MIMAT0004949	37.1	73.6	87.4	195.9	301.9	71.6
MIMAT0004954	10448.8	13673.4	1012.6	1013.3	301.9	286.3
MIMAT0004955	48.6	134.6	255.6	0.0	1056.7	3221.0
MIMAT0004957	264.1	307.2	77.7	463.0	0.0	0.0
MIMAT0004959	18.5	0.0	41.2	0.0	0.0	0.0
MIMAT0004984	134.3	180.3	0.0	0.0	0.0	0.0
MIMAT0004984_1	148.2	167.6	0.0	0.0	0.0	0.0
MIMAT0004984_2	127.4	180.3	0.0	0.0	0.0	0.0
MIMAT0004984_3	143.6	167.6	0.0	0.0	0.0	0.0
MIMAT0004984_4	180.7	180.3	0.0	0.0	0.0	0.0
MIMAT0004985	115.8	294.5	265.7	0.0	0.0	0.0
MIMAT0005577	0.0	0.0	43.5	0.0	0.0	0.0
MIMAT0005582	97.3	116.8	0.0	0.0	0.0	0.0

MIMAT0005583	0.0	0.0	0.0	159.1	0.0	0.0
MIMAT0005584	0.0	99.0	0.0	0.0	754.8	1861.0
MIMAT0005593	11.6	0.0	36.0	0.0	0.0	0.0
MIMAT0005792	1857.7	1277.2	340.8	264.2	0.0	71.6
MIMAT0005792_1	1697.8	1081.7	347.9	279.8	151.0	71.6
MIMAT0005793	711.1	617.0	166.9	94.2	0.0	0.0
MIMAT0005793_1	715.7	540.8	207.6	96.5	0.0	0.0
MIMAT0005797	576.8	812.5	304.3	23.0	151.0	0.0
MIMAT0005825	201.5	134.6	0.0	0.0	0.0	0.0
MIMAT0005874	48.6	99.0	78.8	0.0	0.0	0.0
MIMAT0005875	51.0	81.3	0.0	258.5	0.0	0.0
MIMAT0005882	20.8	0.0	92.6	0.0	0.0	0.0
MIMAT0005884	27.8	0.0	0.0	164.9	0.0	0.0
MIMAT0005892	46.3	50.8	143.4	0.0	0.0	0.0
MIMAT0005898	120.4	121.9	0.0	0.0	1207.7	644.2
MIMAT0005901	13.9	22.9	366.9	649.1	0.0	0.0
MIMAT0005911	16.2	38.1	633.4	1223.6	603.8	357.9
MIMAT0005919	90.3	121.9	0.0	0.0	0.0	0.0
MIMAT0005919_1	85.7	129.5	0.0	0.0	0.0	0.0
MIMAT0005933	0.0	0.0	88.4	0.0	0.0	0.0
MIMAT0005948	613.8	589.1	418.5	0.0	301.9	0.0
MIMAT0005949	0.0	0.0	197.9	0.0	2717.3	4079.9
MIMAT0005950	9.3	7.6	91.3	0.0	0.0	0.0
MIMAT0005951	3493.0	3143.5	130.1	0.0	0.0	0.0
MIMAT0006764	150.6	157.4	89.2	48.8	0.0	0.0
MIMAT0006764_1	122.8	114.3	84.5	36.8	0.0	0.0
MIMAT0006789	206.2	114.3	37.8	0.0	301.9	0.0
MIMAT0007881	275.6	370.7	120.2	0.0	0.0	143.2
MIMAT0007883	0.0	0.0	28.9	0.0	0.0	0.0
MIMAT0010133	423.9	246.3	100.1	0.0	0.0	0.0
MIMAT0010214	9.3	15.2	92.3	68.4	0.0	0.0
MIMAT0011161	0.0	0.0	43.8	0.0	0.0	0.0
MIMAT0011778	0.0	0.0	18.0	0.0	0.0	0.0
MIMAT0014982	150.6	55.9	55.5	0.0	0.0	0.0
MIMAT0015004	23.2	0.0	0.3	339.5	0.0	0.0
MIMAT0015006	162.1	317.4	0.0	0.0	0.0	0.0
MIMAT0015032	104.2	53.3	0.0	0.0	0.0	0.0
MIMAT0015032_1	141.3	53.3	0.0	0.0	0.0	0.0
MIMAT0015041	16.2	33.0	1235.0	1826.2	5585.6	3650.4
MIMAT0015043	90.3	601.8	0.0	0.0	0.0	0.0
MIMAT0015050	2290.8	2823.5	782.8	782.4	754.8	429.5

MIMAT0015054	32.4	129.5	92.3	0.0	0.0	0.0
MIMAT0016847	71.8	53.3	2.1	0.0	0.0	0.0
MIMAT0016916	0.0	0.0	35.7	0.0	0.0	0.0
MIMAT0017981	57.9	104.1	0.0	0.0	0.0	0.0
MIMAT0017982	104.2	195.5	0.0	0.0	0.0	143.2
MIMAT0017988	16.2	0.0	38.9	0.0	0.0	0.0
MIMAT0017990	69.5	73.6	1298.4	1597.0	0.0	0.0
MIMAT0017994	2230.6	2272.5	322.6	273.4	0.0	143.2
MIMAT0017997	13.9	0.0	24.0	0.6	0.0	0.0
MIMAT0018104	39.4	307.2	0.0	367.6	0.0	0.0
MIMAT0018195	2.3	0.0	24.8	0.0	0.0	0.0
MIMAT0018205	18.5	0.0	96.5	0.0	0.0	0.0
MIMAT0018356	0.0	0.0	0.3	253.9	0.0	0.0
MIMAT0018926	11.6	33.0	31.0	0.0	0.0	0.0
MIMAT0018926_1	27.8	20.3	39.1	0.0	0.0	0.0
MIMAT0018965	1285.5	952.2	351.5	465.3	301.9	71.6
MIMAT0019048	0.0	60.9	77.7	0.0	0.0	0.0
MIMAT0019074	104.2	78.7	0.3	0.0	0.0	0.0
MIMAT0019198	39.4	86.3	0.0	0.0	0.0	0.0
MIMAT0019214	13.9	0.0	66.5	0.0	0.0	0.0
MIMAT0019734	44.0	0.0	71.7	0.0	0.0	0.0
MIMAT0019739	78.8	93.9	225.0	0.0	0.0	0.0
MIMAT0019772	0.0	96.5	20.1	0.0	0.0	0.0
MIMAT0019855	69.5	25.4	0.0	442.9	0.0	0.0
MIMAT0019856	25.5	0.0	63.1	0.0	0.0	0.0
MIMAT0019880	99.6	116.8	0.0	0.0	0.0	0.0
MIMAT0019892	11.6	0.0	51.4	0.0	0.0	0.0
MIMAT0020924	55.6	71.1	0.0	0.0	0.0	143.2
MIMAT0021120	44.0	104.1	0.0	1.7	0.0	0.0
MIMAT0022697	220.0	162.5	616.5	1001.8	0.0	429.5
MIMAT0022700	0.0	0.0	92.1	0.0	0.0	0.0
MIMAT0022714	141.3	190.4	0.0	0.0	452.9	0.0
MIMAT0022720	57.9	50.8	87.4	0.0	0.0	0.0
MIMAT0022726	41.7	0.0	307.7	356.7	452.9	1360.0
MIMAT0022727	132.0	22.9	98.8	0.0	0.0	0.0
MIMAT0022842	27.8	0.0	54.0	227.5	3623.1	9090.3
MIMAT0025479	0.0	0.0	3.1	33.9	0.0	286.3
MIMAT0025479_1	0.0	0.0	2.9	36.8	0.0	214.7
MIMAT0025479_2	0.0	0.0	5.0	29.9	0.0	214.7
MIMAT0025479_3	0.0	0.0	8.3	50.6	0.0	357.9
MIMAT0025483	18.5	48.2	73.0	0.0	0.0	0.0

MIMAT0025848	0.0	0.0	15.6	137.9	0.0	71.6
MIMAT0025848_1	0.0	0.0	13.3	121.8	0.0	214.7
MIMAT0026555	0.0	0.0	44.3	0.0	0.0	0.0
MIMAT0026555_1	0.0	0.0	55.5	0.0	0.0	0.0
MIMAT0026559	171.4	91.4	91.3	0.0	0.0	0.0
MIMAT0026606	4.6	0.0	24.0	0.0	0.0	0.0
MIMAT0026721	0.0	0.0	38.3	0.0	0.0	0.0
MIMAT0027032	2.3	2.5	58.7	0.6	0.0	0.0
MIMAT0027366	0.0	0.0	0.0	125.2	0.0	0.0
MIMAT0027369	2.3	60.9	8.9	0.0	0.0	0.0
MIMAT0027384	37.1	121.9	98.3	0.0	0.0	0.0
MIMAT0027395	60.2	142.2	0.0	0.0	0.0	0.0
MIMAT0027507	0.0	0.0	449.8	221.7	0.0	0.0
MIMAT0027518	0.0	0.0	97.3	0.0	0.0	357.9
MIMAT0027530	11.6	165.0	0.0	0.0	0.0	0.0
MIMAT0027539	0.0	0.0	62.8	0.0	0.0	0.0
MIMAT0027587	630.0	637.3	87.1	0.0	0.0	0.0
MIMAT0027588	37.1	93.9	42.5	0.0	0.0	0.0
MIMAT0027604	143.6	40.6	69.4	0.0	0.0	0.0
MIMAT0027617	0.0	0.0	25.8	0.0	0.0	0.0
MIMAT0030021	155.2	292.0	0.0	0.0	0.0	0.0
MIMAT0030413	637.0	561.2	17060.3	24216.0	754.8	3722.0
MIMAT0030414	3015.8	10232.8	1051.4	631.3	2566.3	3865.2
MIMAT0030428	0.0	0.0	34.9	0.0	0.0	0.0
MIMAT0030999	0.0	0.0	79.5	0.0	0.0	0.0
MIMAT0031180	0.0	0.0	12.5	23.0	0.0	0.0
MIMAT0039763	9.3	20.3	14.9	0.6	0.0	0.0
MIMAT0039764	616.1	1000.4	117.1	0.0	0.0	0.0
MIMAT0041618	0.0	0.0	42.5	0.0	0.0	0.0
MIMAT0041629	53.3	38.1	34.9	259.7	0.0	0.0
MIMAT0041630	57.9	246.3	25.0	0.0	0.0	0.0
MIMAT0041997	20.8	0.0	28.7	0.0	0.0	0.0
MIMAT0044657	129.7	190.4	0.0	0.0	0.0	0.0
MIMAT0044658	208.5	162.5	0.0	0.0	0.0	0.0
MIMAT0049032	0.0	0.0	102.2	0.6	24606.7	30778.2

^a Accession number of miRNAs in miRbase (the microRNA database) (<https://www.mirbase.org/index.shtml>)

^b NEBNext Multiplex Small RNA Library Prep Set for Illumina.

^c NEXTFlex Small RNA-Seq Kit v3.

^d SMARTer smRNA-seq kit.

Table S3. Number of reads that remain after each of the steps of different EVs isolation methods in the bioinformatics process obtained by the ultra-deep sequencing analysis.

Isolation methods	Replica	Initial reads	Post-trimming ^a	Too short ^b	Too long ^c	Aligned 0 times ^d	Aligned exactly 1 time ^e	Aligned >1 times ^f	No feature ^g	Final reads ^h
Size exclusion chromatography (SEC)	1	52,212,398	14,869,057	15,021,795	22,321,546	6,518,235	643,691	7,707,131	8,120,100	230,722
	2	11,845,277	2,866,224	6,138,591	2,840,462	1,962,382	217,196	686,646	870,412	33,430
	3	13,457,256	4,050,107	7,021,869	2,385,280	2,612,502	329,589	1,108,016	1,341,088	96,517
Iodixanol gradients	1	22,927,102	5,503,171	14,513,590	2,910,341	2,661,171	763,814	2,078,186	1,831,390	1,010,610
	2	19,791,596	7,534,761	8,199,092	4,057,743	3,536,190	1,195,765	2,802,806	1,979,942	2,018,629
	3	14,796,045	5,223,574	6,714,444	2,858,027	2,509,192	812,122	1,902,260	1,484,901	1,229,481
SEC + Iodixanol gradients	1	20,277,248	7,604,405	8,439,115	4,233,728	5,101,523	480,885	2,021,997	2,383,242	119,640
	2	17,261,430	5,452,052	8,571,717	3,237,661	3,726,289	391,554	1,334,209	1,662,167	63,596
	3	22,873,867	7,761,546	12,309,751	2,802,570	5,108,336	650,194	2,003,016	2,523,274	129,936

^a Number of reads between 17 and 25 nucleotides after trimming according to kit manufacturer instructions.

^b Number of reads discarded to be shorter than 17 nucleotides.

^c Number of reads discarded to be longer than 25 nucleotides.

^d Number of reads discarded because do not map to human reference genome (assembly hg38).

^e Number of reads that map one time to human reference genome (assembly hg38).

^f Number of reads that map more than one time to human reference genome (assembly hg38).

^g Number of reads discarded because do not map to miRNAs coordinates.

^h Number of reads after each of the steps in the bioinformatics process.

Table S4. Normalized counts of miRNAs detected using three different EVs isolation methods and filtered by abundance (miRNAs with at least 50 reads).

Accession Number ^a	SEC ^b			GRAD ^c			SEC + GRAD ^d		
	R1	R2	R3	R1	R2	R3	R1	R2	R3
MIMAT0000062	15754,4	6086,6	4868,5	10488,2	10738,7	10522,4	9542,1	9454,2	10963,7
MIMAT0000062_1	16424,7	6486,6	4956,3	10949,6	11003,6	10795,8	10158,6	10181,5	11847,9
MIMAT0000062_2	16151,2	6186,6	5229,1	10933,0	11042,5	10870,5	10132,6	10058,9	11725,0
MIMAT0000063	189016,8	42643,9	59573,3	75981,4	78065,5	71599,1	76615,0	74547,1	67494,9
MIMAT0000064	4091,2	662,4	1488,8	1406,0	1563,3	1534,5	1528,1	1487,2	2125,3
MIMAT0000065	450,9	62,5	887,7	670,4	742,6	1077,5	655,5	1168,5	1011,1
MIMAT0000066	998,0	562,4	1382,4	282,6	327,4	327,5	138,9	416,7	392,6
MIMAT0000067	15378,7	7886,4	7901,5	14882,1	15146,2	14775,2	14981,8	13025,1	13743,2
MIMAT0000067_1	19731,3	10648,5	11540,2	18609,1	18973,3	19004,8	15619,9	14994,4	16225,4
MIMAT0000069	90,2	225,0	0,0	234,5	214,7	246,6	464,5	392,2	130,9
MIMAT0000069_1	78,2	200,0	4,6	239,9	194,0	236,8	468,9	424,9	91,2
MIMAT0000070	336,7	12,5	13,9	233,3	197,9	221,3	4,3	0,0	646,3
MIMAT0000072	0,0	0,0	0,0	17,2	40,2	17,5	0,0	0,0	142,7
MIMAT0000073	0,0	12,5	4,6	38,0	62,2	9,8	160,6	0,0	154,6
MIMAT0000074	0,0	0,0	0,0	28,5	12,0	3,6	0,0	0,0	0,0
MIMAT0000074_1	0,0	0,0	4,6	23,8	10,0	6,7	0,0	0,0	0,0
MIMAT0000075	622,2	0,0	388,4	262,4	572,9	407,0	998,5	204,3	662,2
MIMAT0000076	12204,3	13598,1	26783,7	12613,3	12238,5	11736,6	12871,9	10500,2	11693,2
MIMAT0000077	6402,8	162,5	383,7	710,1	744,6	800,0	659,9	171,6	951,6
MIMAT0000078	619,2	0,0	0,0	0,0	66,4	1,0	0,0	179,8	0,0
MIMAT0000080	532,1	949,9	453,1	958,9	879,0	915,6	269,2	719,1	741,5
MIMAT0000080_1	562,1	1212,3	517,8	983,3	937,3	921,7	334,3	408,6	769,2
MIMAT0000081	5347,7	3037,1	2991,4	7081,2	8961,0	8260,1	10484,2	7403,2	8441,8
MIMAT0000082	10668,3	10985,9	13542,1	11663,3	10360,7	10873,6	8947,4	10737,1	12303,9
MIMAT0000082_1	10388,7	11010,9	13093,6	11885,3	10520,4	11136,7	8778,1	11170,2	12684,5
MIMAT0000083	1136,3	2149,7	901,6	1188,7	1325,3	1369,5	1697,4	1846,7	2093,6
MIMAT0000084	958,9	4699,3	2376,5	1956,4	1907,9	1604,1	1888,5	2304,3	3136,4
MIMAT0000085	3,0	12,5	499,3	3,0	41,5	59,8	73,8	8,2	0,0
MIMAT0000086	1497,0	1224,8	1021,8	166,8	422,6	305,9	0,0	8,2	460,0
MIMAT0000087	766,5	1562,3	3070,0	324,8	382,8	309,5	1224,2	1307,4	154,6
MIMAT0000088	171,3	25,0	462,3	54,0	109,8	121,2	112,9	237,0	210,2
MIMAT0000090	3,0	0,0	9,2	106,9	91,7	125,9	173,7	326,9	0,0
MIMAT0000092	3483,9	3849,5	2774,1	11250,0	9875,9	11006,2	9511,8	8539,0	8628,2
MIMAT0000092_1	3387,8	3637,0	2533,7	11067,1	9373,3	10005,5	8860,6	9160,1	8378,4
MIMAT0000093	0,0	0,0	0,0	174,6	218,3	314,1	195,4	187,9	230,0
MIMAT0000094	0,0	0,0	263,5	44,5	12,0	0,0	0,0	138,9	0,0
MIMAT0000095	0,0	0,0	0,0	110,4	91,0	81,0	117,2	106,2	198,3
MIMAT0000096	270,5	262,5	18,5	463,1	284,0	430,7	17,4	0,0	170,5
MIMAT0000097	5122,2	4311,9	4383,0	3126,2	4063,8	3603,4	2522,3	2672,0	2930,3
MIMAT0000098	5876,7	699,9	2353,3	374,7	754,0	743,8	1033,2	359,5	218,1
MIMAT0000099	2573,1	674,9	2926,6	2231,4	2840,6	2715,2	2800,1	2598,5	1954,8
MIMAT0000099_1	2558,1	787,4	3033,0	2411,9	2949,8	2890,6	3295,0	2672,0	1958,8
MIMAT0000100	0,0	0,0	0,0	31,5	5,5	21,1	47,8	0,0	0,0
MIMAT0000100_1	0,0	0,0	0,0	26,7	3,9	20,6	78,1	0,0	0,0

MIMAT0000101	0,0	412,4	203,4	158,5	130,8	147,5	338,6	163,4	281,5
MIMAT0000101_1	3,0	412,4	272,8	155,6	146,7	165,1	343,0	163,4	253,8
MIMAT0000104	0,0	12,5	268,2	33,3	37,6	23,7	4,3	8,2	142,7
MIMAT0000222	324,6	487,4	425,4	1325,3	1868,0	1844,5	1905,8	2851,8	2589,2
MIMAT0000227	0,0	0,0	0,0	0,0	18,1	15,0	0,0	0,0	202,2
MIMAT0000231	120,2	12,5	217,3	47,5	54,7	61,4	0,0	0,0	4,0
MIMAT0000231_1	135,3	0,0	263,5	51,1	47,6	54,7	4,3	0,0	0,0
MIMAT0000232	3,0	287,5	1243,7	37,4	70,3	36,1	104,2	0,0	206,2
MIMAT0000232_1	0,0	350,0	1003,3	44,5	71,6	38,7	95,5	16,3	222,0
MIMAT0000243	16085,1	25083,9	18124,0	32092,3	47595,1	46380,5	24328,6	27169,7	20908,3
MIMAT0000244	201,4	12,5	730,5	239,9	181,4	340,4	191,0	89,9	305,3
MIMAT0000244_1	156,3	12,5	776,7	220,3	182,3	346,1	147,6	171,6	230,0
MIMAT0000245	6483,9	11348,4	8220,5	10520,9	10798,6	10791,6	6021,4	7632,0	7018,3
MIMAT0000250	580,2	774,9	1498,0	216,7	428,5	261,0	790,1	416,7	0,0
MIMAT0000252	141,3	562,4	4,6	571,2	518,2	578,7	455,8	433,1	519,4
MIMAT0000252_1	177,4	437,4	0,0	554,0	482,6	555,5	421,1	514,8	574,9
MIMAT0000252_2	156,3	374,9	4,6	549,2	484,2	551,9	468,9	424,9	491,7
MIMAT0000253	6565,1	8348,8	9658,4	4589,2	6370,7	4840,8	6338,3	6929,3	6106,3
MIMAT0000254	17732,3	22796,8	20005,7	7267,7	9140,7	8861,0	15099,0	13123,2	15920,1
MIMAT0000256	745,5	175,0	850,7	237,5	336,5	292,5	677,2	441,3	559,1
MIMAT0000256_1	775,5	275,0	721,3	219,7	326,8	323,9	685,9	441,3	571,0
MIMAT0000257	0,0	212,5	0,0	45,7	38,5	81,5	69,5	16,3	4,0
MIMAT0000257_1	0,0	200,0	4,6	49,9	39,8	81,0	43,4	89,9	0,0
MIMAT0000259	2876,7	474,9	443,9	1875,7	2272,9	1914,1	2926,0	947,9	1526,6
MIMAT0000261	2197,4	325,0	1382,4	3275,8	3904,2	3911,8	3898,5	2680,2	2712,2
MIMAT0000263	0,0	0,0	0,0	0,0	25,6	0,0	325,6	0,0	0,0
MIMAT0000264	523,0	112,5	4,6	15,4	16,5	8,3	0,0	0,0	35,7
MIMAT0000267	138,3	0,0	0,0	0,6	5,8	0,0	0,0	8,2	0,0
MIMAT0000272	12,0	0,0	9,2	141,3	209,2	145,5	4,3	0,0	7,9
MIMAT0000275	3,0	0,0	0,0	42,2	30,1	67,6	0,0	0,0	0,0
MIMAT0000275_1	3,0	0,0	0,0	33,8	30,8	62,9	4,3	0,0	0,0
MIMAT0000278	3,0	1024,9	4,6	213,8	145,7	107,8	751,0	16,3	0,0
MIMAT0000279	643,3	100,0	957,1	1309,8	717,7	984,7	751,0	792,6	571,0
MIMAT0000280	0,0	25,0	0,0	35,6	48,6	32,0	0,0	0,0	0,0
MIMAT0000281	6,0	0,0	531,7	422,8	454,1	385,8	86,8	0,0	574,9
MIMAT0000318	3,0	0,0	0,0	41,6	0,6	0,5	73,8	8,2	0,0
MIMAT0000414	7220,4	4224,4	1484,1	6413,2	6583,2	6249,0	7801,3	7893,5	8564,7
MIMAT0000415	16947,8	15422,8	17587,6	36271,8	33614,2	34463,4	32624,8	34997,8	38291,5
MIMAT0000416	186,4	0,0	4,6	5,9	74,2	16,5	191,0	8,2	0,0
MIMAT0000416_1	162,3	0,0	0,0	3,0	79,7	15,5	178,0	8,2	0,0
MIMAT0000417	0,0	0,0	0,0	0,0	82,9	6,7	4,3	187,9	0,0
MIMAT0000418	0,0	687,4	4,6	28,5	37,6	0,5	4,3	89,9	0,0
MIMAT0000419	3315,6	2462,1	1830,9	1830,0	2016,4	1862,0	1888,5	1740,5	2395,0
MIMAT0000420	6,0	0,0	0,0	20,8	11,3	0,0	0,0	0,0	0,0
MIMAT0000421	96600,6	41831,5	61062,0	82821,0	95959,7	96922,0	15815,3	14945,4	10816,9
MIMAT0000423	405,8	0,0	4,6	21,4	79,0	62,9	0,0	0,0	4,0
MIMAT0000423_1	375,7	0,0	0,0	19,0	68,0	77,9	0,0	0,0	0,0
MIMAT0000424	3655,3	2812,1	1673,7	3534,7	3868,6	3684,4	1654,0	1250,2	2006,4

MIMAT0000424_1	2543,1	1074,8	841,5	2156,0	2538,8	2061,7	646,9	735,4	1296,6
MIMAT0000425	0,0	0,0	0,0	6,5	26,9	0,0	0,0	0,0	0,0
MIMAT0000431	0,0	0,0	0,0	81,3	20,7	58,8	147,6	0,0	333,1
MIMAT0000433	42,1	2274,7	2297,9	2323,4	3048,5	2677,0	4063,4	4265,4	4908,9
MIMAT0000434	0,0	12,5	0,0	454,8	410,7	426,1	91,2	866,2	456,0
MIMAT0000435	6474,9	7948,9	9399,5	1638,2	1791,9	1755,3	6481,5	4298,1	1268,9
MIMAT0000436	0,0	399,9	4,6	1490,3	1183,4	1310,7	1115,7	1266,6	1316,4
MIMAT0000437	0,0	0,0	402,2	0,0	0,3	0,0	438,5	8,2	321,2
MIMAT0000438	0,0	212,5	9,2	50,5	24,6	73,8	0,0	16,3	0,0
MIMAT0000440	1536,1	1687,3	887,7	730,3	1088,5	1470,6	1532,5	2353,3	182,4
MIMAT0000443	1325,6	3712,0	5071,9	982,1	978,4	728,3	1832,0	1291,1	824,8
MIMAT0000444	3,0	674,9	4,6	24,9	186,9	81,0	65,1	8,2	194,3
MIMAT0000445	9973,9	31658,0	26349,1	11507,1	13744,5	14782,9	19939,5	25306,6	21059,0
MIMAT0000446	24,0	50,0	9,2	55,8	58,9	36,1	138,9	16,3	4,0
MIMAT0000447	0,0	12,5	184,9	394,9	276,3	105,2	169,3	0,0	4,0
MIMAT0000449	411,8	1312,3	2265,5	1005,8	858,9	1740,8	811,8	1233,9	559,1
MIMAT0000451	3,0	387,4	4,6	323,0	519,8	192,9	1002,8	1103,1	1605,9
MIMAT0000454	28208,2	25,0	0,0	136,0	20,4	5,2	230,1	490,3	0,0
MIMAT0000455	487,0	187,5	23,1	545,7	600,1	501,9	277,8	441,3	812,9
MIMAT0000456	682,4	599,9	610,3	1034,9	1139,7	1023,9	555,7	1707,8	1697,1
MIMAT0000458	0,0	0,0	0,0	28,5	0,0	19,6	0,0	0,0	0,0
MIMAT0000460	0,0	150,0	0,0	89,1	64,1	89,2	160,6	122,6	0,0
MIMAT0000460_1	0,0	150,0	9,2	92,0	72,2	86,7	186,7	65,4	0,0
MIMAT0000461	0,0	0,0	0,0	0,0	16,8	0,5	0,0	0,0	0,0
MIMAT0000462	2278,5	287,5	0,0	0,0	45,0	34,6	0,0	0,0	0,0
MIMAT0000510	1196,4	1787,2	1770,8	1732,6	1933,8	2032,3	1059,3	1225,7	1126,1
MIMAT0000617	0,0	0,0	0,0	26,1	47,6	28,4	0,0	269,7	0,0
MIMAT0000646	348,7	1687,3	1479,5	118,2	88,4	148,6	738,0	0,0	705,8
MIMAT0000680	0,0	187,5	0,0	137,8	79,3	66,0	0,0	498,5	0,0
MIMAT0000681	3,0	374,9	0,0	42,2	6,8	29,4	0,0	0,0	0,0
MIMAT0000682	1424,8	0,0	4,6	17,8	40,8	59,8	4,3	0,0	0,0
MIMAT0000688	0,0	0,0	0,0	0,0	17,2	0,0	0,0	0,0	0,0
MIMAT0000689	1163,3	1487,3	938,6	425,7	636,1	625,2	616,5	482,1	749,4
MIMAT0000692	435,9	512,4	420,7	978,5	759,5	855,2	586,1	604,7	1447,3
MIMAT0000693	219,4	512,4	13,9	442,4	486,4	680,9	325,6	106,2	1030,9
MIMAT0000703	0,0	0,0	4,6	38,6	18,8	55,2	0,0	0,0	0,0
MIMAT0000705	0,0	0,0	0,0	42,8	0,0	28,4	4,3	8,2	0,0
MIMAT0000707	276,6	424,9	494,7	1936,3	1935,1	2176,2	1332,8	2410,5	2617,0
MIMAT0000722	6,0	25,0	18,5	18,4	20,1	14,4	13,0	16,3	0,0
MIMAT0000727	0,0	0,0	0,0	62,3	76,1	105,7	130,2	0,0	222,0
MIMAT0000728	279,6	162,5	420,7	188,8	377,3	278,5	4,3	8,2	7,9
MIMAT0000732	225,4	62,5	161,8	299,9	287,3	352,3	60,8	187,9	388,6
MIMAT0000733	3,0	12,5	4,6	52,3	24,6	24,8	0,0	8,2	4,0
MIMAT0000736	0,0	12,5	0,0	43,9	29,5	146,0	8,7	16,3	0,0
MIMAT0000737	0,0	0,0	0,0	209,6	236,1	168,2	147,6	0,0	0,0
MIMAT0000750	3,0	12,5	0,0	221,5	134,7	160,9	4,3	40,9	0,0
MIMAT0000751	0,0	0,0	9,2	96,2	23,6	30,9	0,0	122,6	0,0
MIMAT0000752	9,0	0,0	13,9	226,8	184,3	150,1	247,5	8,2	35,7

MIMAT0000753	0,0	0,0	1063,4	0,0	0,0	16,0	0,0	849,8	233,9
MIMAT0000754	0,0	0,0	0,0	0,0	23,6	0,5	0,0	0,0	0,0
MIMAT0000755	0,0	0,0	0,0	0,0	22,0	20,6	0,0	0,0	0,0
MIMAT0000756	0,0	0,0	0,0	4,2	32,1	0,0	0,0	0,0	0,0
MIMAT0000757	10857,6	8611,3	10726,4	7843,6	9608,1	10209,8	5287,7	4584,1	4361,7
MIMAT0000759	745,5	399,9	83,2	399,0	610,8	421,9	17,4	286,0	285,5
MIMAT0000763	0,0	0,0	0,0	0,0	0,0	0,0	0,0	0,0	257,7
MIMAT0000764	0,0	0,0	0,0	7,7	9,4	36,6	0,0	0,0	0,0
MIMAT0000772	0,0	25,0	0,0	11,9	0,6	42,3	0,0	0,0	0,0
MIMAT0001080	0,0	0,0	0,0	36,2	0,0	26,8	212,7	179,8	0,0
MIMAT0001340	414,8	2337,2	596,4	3095,3	2622,0	2520,2	1775,6	1029,6	1827,9
MIMAT0001343	0,0	0,0	0,0	7,7	30,1	0,5	0,0	0,0	222,0
MIMAT0001413	0,0	0,0	0,0	7,7	100,7	28,4	0,0	0,0	0,0
MIMAT0001545	0,0	0,0	0,0	11,3	12,0	0,0	4,3	0,0	0,0
MIMAT0001545_1	0,0	0,0	0,0	8,3	12,0	0,0	0,0	0,0	0,0
MIMAT0001618	0,0	0,0	0,0	17,8	0,3	18,1	0,0	0,0	0,0
MIMAT0001620	0,0	0,0	13,9	0,0	21,7	0,0	0,0	0,0	0,0
MIMAT0001621	0,0	0,0	0,0	7,7	21,4	42,3	0,0	0,0	0,0
MIMAT0001631	7436,8	14098,0	6250,9	26772,8	34652,5	35062,7	33809,9	47704,3	38699,9
MIMAT0001639	610,2	1287,3	929,3	2115,6	2081,2	1905,9	625,1	514,8	158,6
MIMAT0002174	3,0	225,0	13,9	206,0	123,7	174,9	178,0	89,9	4,0
MIMAT0002175	3,0	275,0	416,1	163,3	129,5	179,0	0,0	81,7	186,4
MIMAT0002176	0,0	362,4	0,0	133,6	114,0	130,5	269,2	0,0	0,0
MIMAT0002177	19653,2	9748,6	8151,2	32782,8	34142,1	28120,5	27593,2	23051,3	23743,4
MIMAT0002177_1	20134,1	10111,1	8706,0	34112,3	35436,9	29662,8	28570,0	20624,5	24504,7
MIMAT0002808	264,5	0,0	0,0	42,8	39,8	25,3	0,0	8,2	0,0
MIMAT0002809	2170,3	2249,7	3754,2	2153,0	2227,5	2659,0	6225,4	7713,7	8981,1
MIMAT0002814	0,0	0,0	9,2	36,8	0,3	0,5	69,5	0,0	0,0
MIMAT0002817	0,0	624,9	0,0	17,2	72,5	71,7	0,0	0,0	0,0
MIMAT0002821	0,0	12,5	4,6	0,0	0,3	1,5	0,0	8,2	210,2
MIMAT0002870	0,0	0,0	0,0	0,0	27,2	48,0	0,0	0,0	0,0
MIMAT0002874	0,0	0,0	0,0	15,4	23,3	35,6	0,0	0,0	4,0
MIMAT0002875	0,0	0,0	0,0	16,0	0,0	0,0	208,4	0,0	0,0
MIMAT0002888	814,6	1249,8	4,6	899,6	780,8	873,3	898,6	572,0	1225,2
MIMAT0002891	0,0	0,0	0,0	35,0	40,2	23,7	0,0	8,2	0,0
MIMAT0003218	213,4	25,0	4,6	86,1	103,0	57,3	0,0	179,8	4,0
MIMAT0003239	0,0	0,0	0,0	0,0	19,4	0,0	0,0	0,0	0,0
MIMAT0003241	0,0	0,0	0,0	0,0	39,2	0,0	0,0	0,0	4,0
MIMAT0003249	279,6	62,5	878,5	408,5	392,5	435,9	134,6	40,9	4,0
MIMAT0003266	360,7	50,0	0,0	0,0	0,0	18,1	0,0	0,0	0,0
MIMAT0003297	0,0	0,0	0,0	71,8	24,6	18,1	0,0	0,0	0,0
MIMAT0003321	60,1	0,0	0,0	0,0	24,6	0,0	0,0	0,0	0,0
MIMAT0003322	0,0	0,0	0,0	7,7	0,3	0,0	334,3	318,7	0,0
MIMAT0003329	0,0	0,0	0,0	21,4	20,7	1,0	0,0	424,9	0,0
MIMAT0003330	3,0	212,5	0,0	0,0	9,4	1,5	0,0	0,0	0,0
MIMAT0003338	0,0	0,0	0,0	4,8	25,3	25,8	0,0	0,0	0,0
MIMAT0003339	3,0	0,0	0,0	14,3	0,3	29,9	0,0	0,0	0,0
MIMAT0003385	0,0	0,0	0,0	13,7	0,3	0,0	165,0	0,0	0,0

MIMAT0003389	0,0	0,0	0,0	0,0	22,7	0,0	0,0	0,0	0,0
MIMAT0003393	6,0	37,5	9,2	238,1	196,3	185,7	182,3	16,3	134,8
MIMAT0003884	0,0	0,0	0,0	19,0	0,0	15,0	0,0	0,0	0,0
MIMAT0003886	3,0	12,5	0,0	41,6	23,6	1,5	0,0	0,0	0,0
MIMAT0004481	0,0	0,0	46,2	32,1	103,6	83,6	65,1	0,0	4,0
MIMAT0004481_1	0,0	0,0	64,7	40,4	104,3	53,1	91,2	0,0	4,0
MIMAT0004482	0,0	0,0	0,0	36,2	48,3	29,9	91,2	0,0	0,0
MIMAT0004484	3649,3	1287,3	980,2	2600,7	3405,1	2048,8	1319,8	1062,3	1859,7
MIMAT0004495	72,1	0,0	0,0	32,7	10,4	23,7	0,0	0,0	0,0
MIMAT0004497	0,0	0,0	0,0	39,2	52,5	22,2	0,0	8,2	182,4
MIMAT0004498	3,0	0,0	0,0	0,0	0,0	9,8	0,0	8,2	130,9
MIMAT0004500	0,0	0,0	0,0	15,4	0,3	0,0	134,6	0,0	0,0
MIMAT0004501	0,0	0,0	0,0	22,0	0,0	13,9	0,0	114,4	122,9
MIMAT0004502	3,0	0,0	9,2	48,7	212,1	252,2	460,2	482,1	289,5
MIMAT0004505	0,0	0,0	0,0	0,0	24,6	0,0	0,0	0,0	0,0
MIMAT0004518	2991,0	1137,3	1655,2	2582,9	2438,0	2423,8	2470,2	2255,3	2843,0
MIMAT0004549	0,0	0,0	0,0	0,0	17,5	0,0	0,0	0,0	0,0
MIMAT0004552	330,7	0,0	0,0	113,4	64,8	99,5	4,3	147,1	0,0
MIMAT0004558	0,0	12,5	0,0	33,8	47,0	78,9	0,0	0,0	0,0
MIMAT0004563	3,0	399,9	1188,2	35,0	68,7	34,0	104,2	8,2	206,2
MIMAT0004568	0,0	0,0	0,0	0,0	8,7	51,1	0,0	0,0	0,0
MIMAT0004570	327,7	537,4	887,7	368,1	694,7	537,5	507,9	57,2	384,6
MIMAT0004571	0,0	0,0	0,0	0,0	17,8	0,0	0,0	0,0	0,0
MIMAT0004586	0,0	0,0	0,0	22,6	0,3	76,9	0,0	0,0	0,0
MIMAT0004594	0,0	0,0	4,6	0,0	26,6	21,7	0,0	0,0	0,0
MIMAT0004597	1611,2	899,9	1160,5	548,6	987,1	778,9	764,1	1470,8	900,1
MIMAT0004600	838,7	637,4	0,0	364,0	837,2	624,6	4,3	433,1	400,5
MIMAT0004601	0,0	0,0	0,0	64,7	50,2	30,4	0,0	237,0	0,0
MIMAT0004608	0,0	0,0	0,0	0,0	23,6	0,0	0,0	0,0	0,0
MIMAT0004610	3,0	150,0	0,0	144,9	83,9	115,0	112,9	196,1	499,6
MIMAT0004614	0,0	0,0	4,6	83,7	79,0	62,4	4,3	0,0	0,0
MIMAT0004615	769,5	0,0	0,0	20,2	0,0	21,1	0,0	0,0	23,8
MIMAT0004672	378,8	12,5	13,9	315,9	242,3	336,3	308,2	196,1	7,9
MIMAT0004678	0,0	0,0	4,6	23,2	8,1	24,8	0,0	0,0	0,0
MIMAT0004680	261,5	0,0	198,8	171,0	227,0	172,3	0,0	73,5	0,0
MIMAT0004682	3,0	25,0	13,9	18,4	102,3	213,5	494,9	171,6	0,0
MIMAT0004688	0,0	0,0	0,0	57,0	76,1	101,6	0,0	237,0	0,0
MIMAT0004692	9,0	300,0	148,0	552,2	336,5	408,0	377,7	24,5	709,8
MIMAT0004693	0,0	0,0	0,0	35,6	31,1	15,0	0,0	0,0	0,0
MIMAT0004694	1355,7	12,5	1308,4	403,2	381,5	330,6	885,6	1307,4	678,0
MIMAT0004699	0,0	0,0	0,0	10,1	58,6	57,8	0,0	0,0	0,0
MIMAT0004700	0,0	0,0	0,0	0,0	19,4	13,9	0,0	0,0	0,0
MIMAT0004701	0,0	0,0	0,0	0,0	57,6	0,0	0,0	0,0	0,0
MIMAT0004702	0,0	0,0	0,0	30,9	22,0	80,5	0,0	73,5	0,0
MIMAT0004703	6,0	0,0	13,9	136,0	73,2	48,5	8,7	0,0	0,0
MIMAT0004748	11302,5	6111,6	4498,6	15829,1	16968,2	17199,5	10527,6	9797,4	11340,3
MIMAT0004749	3,0	125,0	4,6	65,3	88,1	69,1	321,3	0,0	206,2
MIMAT0004761	0,0	12,5	0,0	306,4	456,0	339,9	0,0	0,0	218,1

MIMAT0004762	0,0	12,5	0,0	126,5	226,7	117,6	178,0	114,4	71,4
MIMAT0004762_1	3,0	0,0	4,6	101,5	93,9	61,4	117,2	171,6	63,4
MIMAT0004767	117,2	0,0	0,0	42,8	63,2	44,9	0,0	0,0	0,0
MIMAT0004774	3,0	12,5	4,6	57,6	105,6	164,5	0,0	171,6	0,0
MIMAT0004775	0,0	0,0	0,0	0,0	0,0	30,4	21,7	0,0	0,0
MIMAT0004776	0,0	0,0	0,0	11,9	40,5	16,5	0,0	0,0	0,0
MIMAT0004792	0,0	0,0	0,0	86,1	24,6	51,6	0,0	130,7	0,0
MIMAT0004796	0,0	0,0	0,0	4,8	8,4	8,8	0,0	8,2	0,0
MIMAT0004797	0,0	0,0	0,0	0,0	22,3	0,0	0,0	155,3	0,0
MIMAT0004799	0,0	0,0	0,0	19,0	0,3	25,8	4,3	0,0	4,0
MIMAT0004808	3,0	0,0	235,8	216,7	197,6	184,7	8,7	0,0	170,5
MIMAT0004810	3,0	0,0	4,6	105,7	211,2	69,6	151,9	8,2	0,0
MIMAT0004813	0,0	0,0	0,0	0,0	17,8	21,7	0,0	0,0	0,0
MIMAT0004814	3,0	0,0	554,8	37,4	52,8	44,4	0,0	0,0	4,0
MIMAT0004819	387,8	25,0	4,6	68,3	109,8	77,9	0,0	8,2	0,0
MIMAT0004920	0,0	0,0	0,0	0,0	16,2	16,0	0,0	0,0	0,0
MIMAT0004921	0,0	12,5	0,0	11,3	29,5	19,6	0,0	0,0	0,0
MIMAT0004928	0,0	0,0	0,0	0,0	20,7	0,0	0,0	0,0	0,0
MIMAT0004945	21,0	50,0	411,5	408,5	406,8	362,6	4,3	269,7	7,9
MIMAT0004947	0,0	0,0	0,0	0,0	13,0	15,5	0,0	0,0	0,0
MIMAT0004949	0,0	0,0	50,9	13,7	13,6	11,9	0,0	0,0	31,7
MIMAT0004954	336,7	474,9	32,4	979,7	850,1	859,8	243,1	24,5	0,0
MIMAT0004957	3,0	0,0	4,6	72,4	1,9	69,1	0,0	0,0	0,0
MIMAT0004959	0,0	0,0	0,0	0,0	20,1	0,0	0,0	0,0	0,0
MIMAT0004976	0,0	0,0	0,0	0,0	29,5	0,0	0,0	0,0	0,0
MIMAT0004982	0,0	0,0	351,4	0,0	13,0	16,0	0,0	0,0	0,0
MIMAT0004984	3,0	12,5	0,0	22,0	29,8	30,9	0,0	8,2	35,7
MIMAT0004984_1	3,0	25,0	0,0	23,8	31,1	27,3	0,0	0,0	39,7
MIMAT0004984_2	0,0	50,0	0,0	19,6	26,6	32,5	0,0	8,2	39,7
MIMAT0004984_3	0,0	50,0	0,0	18,4	30,1	30,9	0,0	0,0	27,8
MIMAT0004984_4	3,0	62,5	0,0	17,8	32,4	35,6	4,3	0,0	39,7
MIMAT0004985	0,0	0,0	0,0	66,5	59,3	28,4	4,3	0,0	0,0
MIMAT0005458	0,0	0,0	0,0	13,7	0,0	13,9	0,0	0,0	0,0
MIMAT0005580	0,0	0,0	0,0	0,0	21,4	0,0	0,0	0,0	0,0
MIMAT0005582	174,3	0,0	448,5	35,6	20,4	34,0	0,0	0,0	0,0
MIMAT0005792	0,0	12,5	37,0	80,2	110,1	150,6	17,4	228,8	83,3
MIMAT0005792_1	0,0	0,0	27,7	85,5	99,8	163,0	13,0	237,0	75,3
MIMAT0005793	0,0	0,0	0,0	46,9	55,4	73,2	4,3	24,5	35,7
MIMAT0005793_1	0,0	0,0	4,6	45,1	54,4	78,9	4,3	8,2	27,8
MIMAT0005797	0,0	0,0	9,2	73,0	88,7	1,5	0,0	204,3	0,0
MIMAT0005825	0,0	25,0	13,9	149,6	139,9	80,5	199,7	0,0	154,6
MIMAT0005874	0,0	0,0	0,0	0,0	24,6	0,0	0,0	0,0	0,0
MIMAT0005884	0,0	0,0	4,6	23,8	21,7	14,4	0,0	0,0	0,0
MIMAT0005919	0,0	0,0	0,0	0,0	13,9	11,3	0,0	8,2	0,0
MIMAT0005919_1	0,0	0,0	0,0	0,0	15,2	7,2	0,0	0,0	0,0
MIMAT0005933	0,0	0,0	0,0	0,0	27,9	0,0	0,0	0,0	0,0
MIMAT0005936	0,0	0,0	0,0	28,5	35,3	15,5	52,1	0,0	71,4
MIMAT0005943	0,0	0,0	0,0	0,0	12,3	18,6	0,0	130,7	4,0

MIMAT0005948	3,0	0,0	18,5	0,0	25,3	16,5	0,0	0,0	0,0
MIMAT0005950	0,0	37,5	0,0	16,6	21,1	0,0	0,0	0,0	0,0
MIMAT0005951	330,7	762,4	32,4	530,8	302,8	417,3	199,7	220,6	222,0
MIMAT0006764	0,0	0,0	0,0	25,5	11,3	15,0	8,7	24,5	7,9
MIMAT0006764_1	0,0	0,0	0,0	25,5	11,0	13,4	0,0	8,2	11,9
MIMAT0006789	0,0	0,0	4,6	0,0	21,4	17,5	65,1	204,3	0,0
MIMAT0007881	0,0	0,0	0,0	5,3	15,5	0,0	0,0	0,0	0,0
MIMAT0010133	468,9	0,0	0,0	24,9	49,2	37,1	134,6	8,2	4,0
MIMAT0015006	0,0	0,0	0,0	0,0	0,0	45,4	0,0	0,0	0,0
MIMAT0015032	315,6	0,0	4,6	87,9	78,4	134,6	4,3	49,0	249,8
MIMAT0015032_1	321,6	0,0	0,0	78,4	80,0	133,6	4,3	65,4	297,4
MIMAT0015043	51,1	75,0	203,4	12,5	9,7	22,7	91,2	130,7	138,8
MIMAT0015050	0,0	0,0	4,6	87,3	268,8	69,6	0,0	0,0	230,0
MIMAT0016888	0,0	12,5	0,0	0,0	23,0	19,6	0,0	0,0	0,0
MIMAT0017981	0,0	0,0	0,0	0,0	13,9	36,6	0,0	0,0	0,0
MIMAT0017982	0,0	0,0	9,2	42,8	81,9	21,7	0,0	0,0	0,0
MIMAT0017990	0,0	0,0	0,0	58,2	17,8	36,6	99,8	8,2	0,0
MIMAT0017994	174,3	399,9	32,4	410,3	256,8	415,7	182,3	539,3	186,4
MIMAT0018104	0,0	0,0	0,0	5,3	16,5	32,5	0,0	0,0	0,0
MIMAT0018187_1	0,0	0,0	0,0	0,0	11,3	0,0	43,4	65,4	0,0
MIMAT0018965	0,0	325,0	0,0	12,5	21,1	97,0	0,0	16,3	4,0
MIMAT0019000	0,0	0,0	0,0	0,0	17,8	0,0	143,3	0,0	0,0
MIMAT0019210	0,0	0,0	0,0	0,0	21,7	0,0	0,0	0,0	0,0
MIMAT0019214	0,0	0,0	0,0	0,0	17,5	0,0	0,0	0,0	0,0
MIMAT0019226	2002,0	0,0	0,0	0,0	0,0	0,5	0,0	0,0	0,0
MIMAT0019743	0,0	0,0	0,0	0,0	16,8	0,0	0,0	0,0	0,0
MIMAT0019772	0,0	0,0	0,0	0,0	17,5	0,0	0,0	0,0	0,0
MIMAT0019855	3,0	0,0	0,0	3,6	0,3	34,0	0,0	0,0	198,3
MIMAT0019856	0,0	0,0	166,4	0,0	37,9	11,9	34,7	24,5	0,0
MIMAT0019880	0,0	0,0	0,0	0,0	21,4	17,0	0,0	0,0	0,0
MIMAT0020924	0,0	0,0	0,0	0,0	24,0	6,2	0,0	0,0	0,0
MIMAT0021043	0,0	0,0	0,0	0,0	18,1	16,5	0,0	0,0	0,0
MIMAT0022693	0,0	0,0	0,0	12,5	16,2	17,5	0,0	416,7	0,0
MIMAT0022710	0,0	0,0	0,0	0,0	19,4	0,0	169,3	0,0	0,0
MIMAT0022714	3,0	0,0	4,6	10,7	16,8	0,5	0,0	0,0	0,0
MIMAT0022727	0,0	0,0	0,0	19,6	12,6	0,0	0,0	0,0	174,5
MIMAT0026482	0,0	0,0	0,0	0,0	23,3	0,0	0,0	0,0	0,0
MIMAT0027369	0,0	0,0	0,0	0,0	46,0	15,0	0,0	0,0	154,6
MIMAT0027384	0,0	0,0	0,0	52,3	0,0	23,7	0,0	0,0	210,2
MIMAT0027395	0,0	0,0	0,0	16,6	42,4	0,0	0,0	0,0	0,0
MIMAT0027445	0,0	0,0	0,0	20,8	0,0	12,4	0,0	0,0	0,0
MIMAT0027513	0,0	0,0	0,0	0,0	20,1	0,0	0,0	0,0	0,0
MIMAT0027530	0,0	0,0	0,0	20,2	10,4	0,0	0,0	0,0	0,0
MIMAT0027539	0,0	0,0	0,0	0,0	21,1	0,0	0,0	0,0	0,0
MIMAT0027587	0,0	437,4	4,6	27,9	104,3	82,5	0,0	0,0	0,0
MIMAT0027616	0,0	0,0	0,0	0,0	18,5	0,0	0,0	0,0	0,0
MIMAT0027637	291,6	0,0	0,0	0,0	25,9	0,0	0,0	0,0	0,0
MIMAT0027689	0,0	0,0	0,0	20,8	0,0	9,3	99,8	0,0	0,0

MIMAT0030021	0,0	0,0	0,0	21,4	19,8	5,2	156,3	0,0	0,0
MIMAT0030413	0,0	12,5	0,0	54,6	56,7	64,0	0,0	0,0	0,0
MIMAT0030414	1509,0	1424,8	1262,2	989,2	1203,5	1256,0	473,2	49,0	83,3
MIMAT0039764	0,0	0,0	0,0	102,1	9,7	99,5	4,3	212,5	0,0
MIMAT0044657	0,0	0,0	0,0	7,1	21,1	3,1	0,0	0,0	0,0

^a Accession number of miRNAs in miRbase (the microRNA database) (<https://www.mirbase.org/index.shtml>)

^b Size exclusion chromatography.

^c Isopycnic ultracentrifugation using iodixanol gradients.

^d Size exclusion chromatography and isopycnic ultracentrifugation using iodixanol gradients.

5. DISCUSSION

Although the number of new HCV positive infections has been greatly reduced since the introduction of DAAs-based treatments, about 58 million people worldwide are still chronically infected and close to 290.000 patients died of chronic HCV infection in 2019. Therefore, HCV infection and its repercussions continue to be a global public health problem nowadays.

In long-time chronic HCV infection with end-stage liver disease (chronic liver failure), LT is the only solution patients have to survive. In the patients with detectable circulating viral RNA before surgery, reinfection of the engrafted liver is universal after LT, and an active infection is reestablished in all of them due to the immunosuppression treatment they have to endure²⁰³. After the primary HCV target organ is removed, there is a substantial reduction in the overall VL, because the main factory of viral production (the liver) is removed, and the transfusions using blood from uninfected donors. However, reinfection of the new liver graft is achieved by viral particles remaining in the bloodstream. Moreover, liver replacement causes a drastic change in the environment in which the virus was adapted to replicate and therefore changes would be expected to occur in the composition of the quasispecies following LT. Thus, the number of viral particles (population size) that initiate the reinfection, the differences in the liver graft, the immunosuppression status, and patient characteristics, may influence the evolutionary outcome and affect the viral quasispecies composition^{43,44,204}.

5.1 Quasispecies dynamics before and after LT, and parameters that would be predictive of fibrosis progression at one year after LT

In this scenario, during graft reinfection, a genetic phenomenon known as “bottlenecking” is expected²⁰⁵, in which a subset of virions is selected in the absence of an effective immune response, with still limited heterogeneity²⁰⁶. Conversely, based on the results of the unidimensional and principal component

analysis of our first study, we could not confirm changes towards lower viral complexity after transplantation, as HCV dynamics varied between patients without resulting in a consistent viral complexity pattern after LT. In addition, the phylogenetic studies revealed three different patterns of viral behavior after liver graft reinfection.

In the first pattern, observed in most of the patients, the master sequence was conserved, but the mutant spectra differed. Only some sequences were the same as the pre-LT ones, suggesting that the reinfection of the liver was caused by the most prevalent pre-LT sequences.

In the second pattern, observed in two patients, the master sequence differed from the pre-LT one, and the mutant spectra were completely different, suggesting that reinfection of the liver graft was caused by a minor genome from the pre-LT quasispecies.

In the third pattern, observed in one patient, the pre-LT quasispecies was maintained after liver transplantation, suggesting massive reinfection of the liver graft by most of the pre-LT virions.

The small sample size does not allow us to reach conclusions on a possible effect of viral subtype in the quasispecies behavior after LT. However, pattern one has been found in patients with subtype 1a and 1b, suggesting that in most of the cases, and independently of the liver damage progression, HCV reinfection follows this particular pattern in which the master sequence remains after LT but with different mutant spectra. Interestingly, in the patient that had a cholestatic fibrosis hepatitis (P10), the master sequence remained dominant after LT as previously reported by Gambato et al. in which 62% of cholestatic patients showed the remaining of master sequence compared with the 11% in the patients with mild recurrence²⁰⁷.

Even so, we cannot ignore the reduced patients with which we work as the main limitation of this study and a possible bias of the results. Most patients were

efficiently treated with DAAs before or soon after LT, thus limiting the number of samples fulfilling inclusion criteria for our study that required patients with at least one year of follow-up in the absence of treatment.

Although DAA treatment before LT would be the best option, drug-to-drug interactions between some DAAs and various immunosuppressive agents may jeopardize this approach. Furthermore, some DAAs should be avoided in patients with severely impaired liver function and renal dysfunction because of complications, the most common being renal failure. An alternative protocol is to apply the treatment soon after the LT or when the risk of rejection has decreased and immunosuppressive rejection medication is stable²⁰⁸. Hence, the question arises as to when would be the best time to start DAA treatment.

It is widely recognized that liver fibrosis rapidly progresses in some patients, leading to cirrhosis at one year post-LT (fast-progressors), whereas others show minimal changes in the transplanted graft at the same time point (slow-progressors). A parameter that would be predictive of fast fibrosis progression at one year after LT would be useful to decide the time to start a DAA therapy. In general, fast progressors should be treated earlier after LT than slow progressors, once the patient's health status has improved.

In this situation and having as precedent studies in which quasispecies composition has been related to viral persistence, disease progression, and response to antiviral agents, we hypothesized that virological factors such as viral complexity and viral load might predict fast progression of liver damage in liver-transplanted patients^{209–211}. Furthermore, reports have shown that some amino acid signatures in the NS5B region of HCV, that is the region we have amplified in our first study, are specific to patients developing cholestatic fibrosis hepatitis, which is a severe variant of HCV infection recurrence after

LT²⁰⁷. Therefore, our hypothesis was that complexity studies based on this region will reveal some clues of fibrosis progression.

After conducting an exhaustive analysis of changes in the HCV quasispecies complexity measures (qD , Mf_{max} , and π) obtained before LT and 15 days following LT, none of the measures studied were significantly associated with progression to more aggressive liver damage at one year following the procedure. This may be because the viral quasispecies is a highly variable and dynamic population that fluctuates over time, and the results may vary according to the moment at which the sample is collected and analyzed. Hence, we cannot exclude that the analysis of samples taken at a later point after LT might have led to the identification of a complexity index predictive of fast liver damage progression.

Interestingly, we observed a significant increase in VL values from pre-LT to 15 days post-LT in all patients who had an advanced stage of fibrosis one year after the procedure, in accordance with previous findings²¹². Our results support the notion that the difference in VL before and after LT may be of value in predicting fibrosis progression. Thus, VL changes may be a useful criterion to determine whether to administer DAA-treatment as soon as possible after LT or delay it until the patient is clinically stable.

Thus, DAA-treatment is necessary to eliminate the virus in those chronic patients undergoing LT, but even after infection resolution many of them remain on transplant lists²¹³. Much hinges on the sequels of long periods of silent and persistent antigen stimulation along with immunological factors that lead to fibrogenesis induced by chronic inflammation, and consequently has a direct effect on the development of advanced or end-stage liver diseases, even after infection resolution²¹⁴. According, recent studies have demonstrated that DAA treatments reduce but do not eliminate the risk of developing HCC²¹⁵. Indeed,

we observed that 2 out of 27 patients who received DAA regimens in our second study developed HCC at months 54 and 60 of follow-up, corresponding to a 5-years cumulative HCC rate of 7.4%.

Despite the lack of specific predictors of HCC, several host factors, including liver fibrosis stage, older age, elevated AFP levels, and comorbidities such as diabetes and steatosis, have been associated with HCC occurrence²¹⁶⁻²¹⁸. Remarkably, patients who developed HCC were the oldest in our patients' cohort, suggesting that older age along with advanced fibrosis stage at baseline was a significant driving factor in the HCC development in these patients. Other host factors that may have contributed to the occurrence of HCC include the elevated AFP after DAA treatment in patient 7 and diabetes in patient 9. Moreover, dysregulations in the functions or expression of immunological components play a key role in HCC progression, as immune response is shift towards tumor tolerance²¹⁹.

5.2 Relevance of cellular immune response, liver inflammation and fibrosis regression, after HCV elimination mediated by DAAs

In infectious diseases, an effective immune response is essential for viral control and disease's outcome, whilst a dysregulated immune system leads to disease progression²¹⁵. In an HCV infection context, spontaneous resolution infections are associated with expansion of HCV-specific CD8+ T cells, a broad CD4+ T cell responses, and a strong cytotoxic T lymphocyte response, while chronic infections leads to T cell exhaustion and dysfunction, resulting in varying degrees of functional impairment of the immune response^{100-105,220}. The exhaustion of HCV-specific T cells is characterized by up-regulation of PD-1 and other inhibitory receptors, low proliferative capacity, dysfunctional CD8 cytotoxicity, and impaired production of immunomodulatory cytokines^{123,221,222}. With that in mind, in the second study we evaluated the degree of immune restoration by performing the analysis of phenotypic and functional changes in

T cells before, during and after HCV elimination by DAA therapies in patients with chronic HCV infection.

Because host factors, including age and gender, can largely influence the immune response, the study cohort included both males and females in their middle age and elderly patients. Moreover, all patients achieved SVR irrespective of the specific DAA treatment.

To study the restoration of immune response after DAA treatment, we first characterized the exhausted phenotype of CD4+ T cells before and FUW12 by analyzing the expression of immune response inhibitory markers PD-1, TIM-3, and LAG-3 at the cell surface. Interestingly, a significant decrease in cell surface expression of PD-1 was observed in FUW12 samples compared with its baseline pair in non-cirrhotic and treatment-naive patients, suggesting that the immune response in these patients might have partly recovered. However, no significant differences were found when considering cirrhotic and previous IFN- α treated patients, which is in concordance with previous studies^{133,223}, indicating that CD4 exhausted phenotype is not fully restored in all DAA-treated patients resolving infection. The fact that after HCV eradication, PD1 expression levels were significantly reduced in non-cirrhotic patients compared with cirrhotic ones, suggests that cirrhotic's derived T cells show a deeper functional exhaustion than the non-cirrhotic ones, which may be associated with the difference in liver damage and more impaired HCV-specific immune response. Moreover, PD1 expression level were also reduced in treatment-naive patients compared with IFN- α treated ones, therefore it is possible that treatment-naive patients might be more receptive to respond to new treatment than IFN- α treated ones, as IFN-based therapies could have induced phenotypical changes towards T cells, making them to be less prone to switch off the exhausted phenotype. In addition, no significant differences in PD-1 levels at baseline and FUW12 were

observed among treatment-naïve patients over 55 years of age, indicating that older patients may be less likely to reverse T cell exhaustion. Thus, failure to reverse the exhausted phenotype may have also contribute to HCC development in patients 7 and 9.

In summary, a partial restoration of the CD4+ T cell exhausted phenotype in patients with low grade of fibrosis, in treatment-naïve and in treatment-naïve patients below 55 years old, was observed. This results shows that those with high grade of fibrosis and older than 55 should be subjected to a strict surveillance to prevent the development of an HCC.

Regarding the pro-inflammatory cytokines, it has been reported that NK and T cells produce high quantities of IFN- γ and other pro-inflammatory cytokines during acute infections, while production is decreased during chronic infections^{134,224,225}. Interestingly, Sasaki et al. reported higher levels of pro-inflammatory cytokines, including IFN- γ and IL-2, in serum of rapid virological responders as compared with end of treatment responders, suggesting that enhanced host immune status may contribute in HCV clearance²²⁶. Here, we have measured IFN- γ and IL-2 production of lymphocytes stimulated *in vitro*, comparing the baseline and FUW12 samples of each patient. We found that HCV clearance *per se* is not sufficient to revert the decreased production of IFN- γ and IL-2 by HCV-specific T cells, suggesting that prolonged exposure to HCV antigens leads to long-lasting HCV-specific T cells that lack effector functions. Thus, we have shown that impaired HCV-specific CD4+ and CD8+ T cells responses during chronic HCV infection are not restored following successful HCV clearance, at least in the short-time after HCV elimination, which is in line with recent published studies^{133,223,225,227,228}.

During chronic infections, virus-induced transcriptional reprogramming contributes to the maintenance of exhausted T cells in hyporesponsive

states^{111,220,229,230}. As we have shown, T cell functionality remains impaired despite SVR, suggesting persistent transcription factor or epigenetic changes in HCV-specific T-cell after infection resolution. Moreover, those alterations have been reported to be directly associated with advanced liver diseases as HCC^{231,232}.

The analysis of IFN- γ ELISPOT results by HCV subtypes revealed that patients with HCV subtype 1b showed higher IFN- γ restoration than those with HCV subtype 1a, which could be attributed to a different immunogenicity between subtypes²³³, or due to T-cell-mediated protective immunity against other viral strains to which the patient was previously exposed²³⁴.

Various studies point to the fact that a restoration of HCV-specific CD8+ T cells proliferation after DAAs treatment occurs^{129,131,132}. But others reported that CD8 proliferation capacity was not restored after HCV elimination by DAAs in the majority of patients^{133,134}. However, little data was reported about the proliferative capacity of HCV-specific CD4+ T cells until now. A published study showed limited CD4+ T cell proliferative capacity of HCV specific CD4+ T-cells following DAA therapy¹³⁵.

In our study, we have observed a partial restoration of the proliferative capacity of both CD4+ and CD8+ T cells after stimulation with NS3 Helicase protein and NS3 pooled peptides but not with structural HCV antigens (core), suggesting that restoration of T cell proliferation is HCV-epitope dependent. In accordance, core antigen has been related with the induction of T regs expansion and T cell exhaustion^{235,236}, and NS antigens have been described to present a higher immunogenicity^{237–239}. In conformity to our results, several studies confirmed a reinvigorated CD8+ T cell proliferative capacity after DAAs when stimulated with NS3 and NS4 peptides^{129,131,132}. In addition, Burchill et al. also found a temporal increase in the proliferative response of CD4+ T cells when stimulating with NS3 and NS5¹³⁴. The discrepancies between our results and other studies pointing to

a non-restoration of the proliferative capacity could be explained by different clinic-pathological conditions, by different DAA regimen used or due to the differences on immunogenicity between peptides.

Overall, our data suggest that clearance of persistent HCV antigens helps to partially increase the proliferative capacity of CD4+ and CD8+ T cells but is not sufficient to reverse T cell dysfunctionality, 12 weeks after finishing treatment.

Regarding liver inflammation and fibrosis during and after HCV infection, most patients with advanced liver fibrosis had abnormal baseline levels of liver inflammation and fibrosis markers, including transaminases, FIB-4, AFP, and APRI, as expected after years of chronic injury^{216,240}. Our results point that HCV clearance was associated with decreased levels of liver inflammation since all fibrosis markers studied were reduced after DAA-treatment. Furthermore, apart from a reduction in liver inflammation, a fibrosis stage regression was achieved in all patients after DAA regimens, suggesting that a liver regeneration was still ongoing in the majority of patients 12 weeks after treatment. However, we have observed that HCC was developed in two patients after 61 and 55 month of follow up.

The fact that those T cells remain dysfunctional after HCV clearance might have serious clinical implications. Additional immunological therapy may reduce the risk of developing HCC and other extrahepatic manifestations after DAA regimen²⁴¹. Unfortunately, patients who have overcome the infection and cleared the virus are not protected against reinfection²⁴² and HCC. Moreover, no vaccine to prevent HCV infection is yet available, despite continuing efforts for its development²⁴³. Hence, our studies will provide information on the dynamics of HCV infection and immune response, which may be applicable to vaccine development and immunotherapy strategies, as well as on immune related liver remodeling that together with a correct diagnose and an early

treatment will help to improve clinical outcomes. Nonetheless, further investigations of HCV-specific T cell responses beyond 1 year of follow-up are needed to understand the long-term impact of HCV cure and their implications on HCV vaccine-design and HCV re-infections.

5.3 Development of new strategies for biomarker-discovery to predict advanced liver diseases in patients after HCV infection

Besides immune response dysregulation, HCV infection's traces in the host, mentioned previously, makes evident the need of follow-up studies focused on biomarkers. Those studies may help clinicians to act in advance and improve the quality of life of the patients who in many cases received the medical discharge once the harmful stimuli was removed, but nevertheless continue having HCV infection-related diseases. In fact, late patient diagnosis reduces their therapeutic options and decrease the patients' survival rate²⁴⁴.

Finding new biomarkers for disease diagnosis and prognosis remains challenging despite considerable improvements. Recently, the use of miRNAs within EVs as clinical biomarkers has attracted increasing interest because EVs have been shown to provide an enriched source of miRNAs with higher diagnostic and prognostic potential than total cell-free RNA. Therefore, the analysis of EV-miRNAs may allow to detect subtle disease-induced miRNA dysregulations that play significant roles in pathogenesis and can therefore influence the clinical outcomes. However, discrepancies on miRNA patterns are still frequent between studies, which hampers the validation of specific miRNA signatures with diagnostic and/or prognostic value. Hence, the choice of EV isolation method as well as library preparation kit should depend on the downstream application. Due to the large discrepancy between methods and the high variability between samples and diseases, it would be advisable to use specific methods that allow the isolation of EV-miRNAs, which are functionally secreted

as intercellular mediators and may therefore be more sensitive and specific biomarkers.

Consequently, in the third work, we have conducted a study to compare different EV isolation methods in order to find the best approach for miRNA biomarker recovery and identification. By comparing three different methods, SEC, GRAD and the combination of SEC+GRAD, we have shown that the method used can influence the final result. Each method allows isolation of a diverse size range of vesicles, but it varies regarding lipoprotein and protein contaminants depletion, EVs recovery yield, miRNA profiles, cost-effectiveness, and clinical applicability. For that reason, it is important to choose the methodology depending on the forthcoming application of the purified EVs.

The analysis of protein content showed that all three EV isolation methods removed most of the overabundant soluble plasma proteins, although SEC extractions are the ones recovering more impurities. As far as lipoproteins is concern, it is expected that SEC could not separate EVs from apoB-containing lipoproteins such as chylomicrons, LDL, IDL, VLDL and Lp(a) because of their size overlap (30-5000nm vs 18-1200 nm), whereas GRAD could not separate EVs from apoA-containing lipoproteins (HDL) because of their density overlap (~1.1 g/mL vs 1.08-1.19 g/mL)²⁴⁵. Thus, by combining SEC+GRAD should provide the highest lipoprotein removal. However, all GRAD and SEC fractions tested negative for apoA and apoB in EVs-containing fractions, suggesting that the combination of initial centrifugations with fractioning methodologies eliminate the vast majority of lipoproteins. However, certain degree of lipoprotein contamination cannot be excluded based on the physical properties of these particles, which would explain the high quantity of particles detected in NTA and TEM analyses, and the low fluorescence intensity in CD9 analyses in SEC fractions.

According to CD9 fluorescent intensity in tagged EVs, GRAD provided a higher proportion of pure EVs than SEC. According to NTA measurements, the concentration of recovered particles by GRAD and SEC+GRAD was two orders of magnitude lower than that of SEC extractions, but showing the highest degree of purity by TEM and Cryo-TEM images. In consequence, GRAD is the methodology showing the best balance between EVs purity and yield.

Next step was to study the cargo in miRNAs of the EVs isolated by the three methods. Firstly, when testing the efficacy of three commercial protocols of miRNAs library preparation, NEB, NEXT and SMARTer, NEB was the protocol that showed the highest reproducibility between replicas and resulted in the highest and different number of miRNAs followed by NEXT and SMARTer. Similar results were observed in other studies published with NEB kit when compared with other commercial kits^{166,184,246,247}.

Secondly, when testing the efficacy of the three EV isolation methods for miRNA-sequencing, GRAD method showed the highest reproducibility from replicas and detected the higher number and more different miRNAs than those obtained with SEC and SEC+GRAD. Conversely, Buschmann et al. conclude that less specific EVs isolation methods yielded more RNA and obtained higher number of miRNAs than more specific methods. This could be attributed to extreme alterations in miRNA expression as they work with sepsis patients, different subpopulations of vesicles isolated or a more abundant co-isolation of non-vesicular extracellular RNA that mask those miRNAs coming from EVs. Besides, highly abundant miRNAs are less affected by library preparation-induced biases than low-abundance transcripts²⁴⁸. MiRNAs related to pathologies that induce small differences in their expression levels and/or are underrepresented in plasma samples can be enriched by isolating the miRNAs within EVs¹⁷¹. Thus, the study of miRNAs with GRAD method may allow detecting less abundant circulating miRNAs that nevertheless may play

significant roles in pathogenesis that would be concealed by more abundant miRNAs if other methods are used.

In addition to miRNAs, EVs contain messenger RNAs, transfer RNA, long non-coding RNAs, and circular RNAs, among others¹⁶⁵. Depending on the EVs isolation methodology, different types of vesicles with different sizes and cargos are isolated. In our study, SEC proved to be the less discriminative method allowing to recover more different type of particles, and depending on the aim of the study this methodology could represent the best choice since despite showing lower miRNA abundance and diversity than GRAD, other RNA types might have been isolated and sequenced. Although further investigation would be required to confirm this hypothesis, the results obtained by SEC+GRAD are consistent with a pre-selection of less miRNA-enriched vesicles by SEC.

In conclusion, all methods assessed in this study successfully detected miRNAs from plasma samples, although the number of mapped miRNAs varied considerably across EV isolation methods and library preparation kits. In our case, the method that provided the best balance between EV's purity, yield and miRNA-sequencing was the GRAD. Hence, isopycnic centrifugation using GRAD methodology, followed by NGS sequencing using NEB kit should be considered, as a reliable protocol for the identification of clinical biomarkers. Finding new non-invasive biomarkers to predict HCC prognosis and other liver-advanced diseases is crucial in the actual era of hepatitis C infection.

6. CONCLUSIONS

6.1 Principal conclusions

1. An increase in viral load 15 days after LT was associated with fast progression to liver fibrosis one year after transplantation. This suggests DAA-therapy should be started as soon as possible following LT.
2. A partial restoration of the immune response is achieved in chronic HCV infected patients 12 weeks after viral clearance induced by DAAs.
3. Isopycnic ultracentrifugation using iodixanol gradients is one of the most appropriate method to detect miRNAs within EVs, and should therefore be considered as a reliable method for the identification of new clinical biomarkers.

6.2 Secondary conclusions

1. HCV kinetics before and after LT differed among patients. Changes towards lower viral complexity or homogenization of the viral population were not generalized phenomena after liver graft reinfection.
2. None of the viral diversity indices studied at 15 days after LT were significantly associated with liver damage progression one year after transplantation.
3. An increase in viral load 15 days after LT shows predictive capacity of fast progression to fibrosis at one year of the LT.
4. Restoration of CD4⁺ T cells exhaustion was achieved in non-cirrhotic patients, treatment-naive and treatment-naive below 55 years old.
5. A partial restoration of the T cell functions was observed after viral clearance, since cytokine production by HCV-specific CD4⁺ and CD8⁺ T cells remained impaired after HCV elimination, whilst the proliferative capacity of HCV-specific CD4⁺ and CD8⁺ T cells was partly restored.
6. A reduction in liver inflammation and a fibrosis stage regression was achieved in all patients after DAA regimens, suggesting that a liver regeneration was still ongoing.

6 | CONCLUSIONS

7. GRAD method maintains a good balance between EVs purity and yield.
8. NEB kit showed the highest reproducibility among replicas, provided a broader coverage of sequenced miRNAs, and better overall results regarding miRNA-detection than NEXT and SMARTer protocols.
9. GRAD method showed the highest reproducibility among replicas, presented a higher number of miRNAs, and detected more different miRNAs than SEC and SEC+GRAD. Hence, GRAD is one of the most appropriate methods to detect miRNAs from EVs by next generation sequencing.

V. FUTURE PERSPECTIVES

The studies included in this Doctoral Thesis open up new lines of research on long-term effects of Hepatitis C Virus infection as detailed below.

V.I Multi-centric studies

One limitation of this thesis is the reduced number of patients that were included in the first two studies. It would be interesting to increase the number of patients and extend to additional cohorts from other hospitals to make our results more robust and eliminate possible bias introduced by doing it with patients from a single hospital.

V.II Epigenetic studies

Some reports pointed to high rates of *de novo* HCC and HCC-recurrence in cirrhotic patients after DAA treatment^{249,250}. It is well known, that apart from the direct involvement of the immune response, other mechanisms such as epigenetic dysregulations may also contribute to the progression towards advanced liver diseases and HCC development. In this line, it has been reported that HCV reprogram host's gene expression through epigenetic modifications in the transcriptome of host cells that persist after virus eradication with DAAs-based treatment^{231,251}. Furthermore, it has been reported that epigenetic modifications affect the expression of tumor suppressor genes or oncogenes promoting tumor initiation and progression. Hence, these epigenetic modifications may contribute to the HCC risk despite HCV eradication^{232,252}.

The identification of epigenetic signatures will bring light to HCC prevention by serving as clinical strategies for early detection, and by identifying novel host targets for the development of drugs that may revert the epigenetic processes and consequently reduce HCC risk²⁵³.

To this end, RNA-seq together with DNA-seq methylation studies may give relevant, detailed and more in-depth information of the state of damage caused by long-term HCV infection. It would be interesting to study differential gene expression profiles, and epigenetic changes occurred in groups of genes with specific immunological functions by analyzing RNA and DNA extracted from pre-treatment PBMCs and their respective follow-up, in a cohort of chronic infected patients with different stages of fibrosis.

Until now, considering that global DNA hypomethylation has been associated with predictive capacity of cancer risk²⁵⁴, a first screening on the percentage of methylation and hydroxymethylation between pre-treatment DNA samples and their respective 2 years follow-up samples has been carried out. Preliminary results from a cohort of 20 HCV-chronic infected patients; 10 non-cirrhotic (elastography <12 KPa, F0-F1), and 10 cirrhotic (elastography >12 KPa, F3-F4), shown differences between the two groups. Cirrhotic patients showed lower levels of methylation and hydroxymethylation than non-cirrhotic ones, both in pre-treatment and follow-up, indicating that different epigenetic signatures may occurred within patients depending on the fibrosis stage.

V.III EV's effect in immune response

As explained in the introduction section, EVs (especially exosomes), by transmitting information from cell to cell, have become functional vehicles of intercellular communication¹⁴⁰. Moreover, exosomes are active mediators of the immune system. They have a pivotal role in immune stimulation, in immune suppression and maintenance of peripheral tolerance by inducing T cell anergy and activating induced cell death and Treg cells^{187,194}. Additionally, EVs, mainly exosomes, have shown the ability to inhibit or induce the expression of chemokines and cytokines, modulate the activation and proliferation of T cells, upregulate the expression of inhibitory receptors in T cells and promote T cell exhaustion, accelerating, among other pathologies, HCC progression^{195,196,198}.

In a situation of advanced liver damage such as the one that we have seen that occur in patients with advanced fibrosis after HCV infection resolution, and taking as a precedent the results obtained in the immune response study, we propose that EVs may be closely involved in T cell-exhaustion not only during active infection but also after SVR. Demonstrating a role of EVs in the generation and maintenance of an exhausted T-cell phenotype will help to understand immune response alterations caused by a chronic infection and to propose new therapeutic solutions.

To study the role of EVs in T-cell exhaustion, the experiment will consist in isolating EVs from an active and chronic infection showing a T-cell exhaustion profile, and to co-culture these EVs with T-cells isolated from the same patient after recovering immune functionalities. The rationale is to study whether or not EVs from chronic samples will induce exhaustion in the recovered immune cells. For this purpose, a cell culture with purified EVs from plasma samples faced with post-treatment PBMCs should be done to test phenotypic and functional changes induced. With all the evidences presented about EV's role in the induction of T cell exhaustion, we hypothesized that EVs most likely derived from exhausted cells, in contact with follow-up PBMCs would revert PD1 expression levels of CD4 and CD8 T cells like in chronic infections.

Preliminary results from a cohort of 30 HCV-chronic infected patients; 15 non-cirrhotic (elastography <12 KPa, F0-F1), and 15 cirrhotic (elastography >12 KPa, F3-F4), have shown that FWU-PBMCs in contact with EVs increased their PD1 levels to similar or higher values than those detected in Pre-TX PBMCs in the majority of patients. Those results suggest that indeed EVs induce phenotypical changes toward an exhaustion phenotype in both CD4 and CD8 T cells.

V.IV EVs-miRNAs to monitor HCV-patients follow-up

It is widely known, and as explained in this thesis, that during HCV infection miRNAs content in EVs is closely linked to HCV infection outcome by promoting an efficient viral replication, liver damage progression, and HCC development¹⁹⁹⁻²⁰¹. In addition, an active infection and/or liver damage induce a dysregulation of the endogenous miRNAs encapsulated in EVs. Moreover, viral eradication mediated by DAAs does not imply the cure of liver disease that can progress to a worsening state in patients with advanced fibrosis, still at risk of developing HCC²⁵⁵. Thereby, HCC prevention is the most efficient measure to reduce HCC-related mortality.

For that reason, as seen that patients with advanced cirrhosis may need exhaustive follow-up for surveillance of HCC is essential to establish diagnostic tools as a panel of biomarkers that may predict the risk to evolve towards advanced liver diseases and HCC despite viral eradication.

To do so, once selected the most accurate approach for EVs isolation and miRNAs sequencing, GRAD method based on the results obtained from the third study of the thesis, the next step is to apply these methodologies in a cohort of cirrhotic and non-cirrhotic patients who have achieved SVR mediated by DAAs. By analyzing EVs-miRNAs present in pre-treatment and follow-up plasma samples with different stages of fibrosis, we can monitor the clinical evolution of HCV-patients after infection resolution with diverse degrees of liver damage. Hence, could be of clinical utility to perform a longitudinal study to analyze the expression changes of miRNAs in circulating EVs of HCV-infected patients before treatment, 12 weeks of the end of treatment and from one to four years of follow-up.

7. REFERENCES

1. Feinstone SM, Kapikian AZ, Purcell RH, Alter HJ, Holland P V. Transfusion-Associated Hepatitis Not Due to Viral Hepatitis Type A or B. *N Engl J Med*. 1975;292(15):767-770. doi:10.1056/nejm197504102921502
2. Bradley DW. The agents of non-A, non-B viral hepatitis. *J Virol Methods*. 1985;10(4):307-319. doi:10.1016/0166-0934(85)90047-3
3. Dienstag JL, Alter HJ. Non-A, non-B hepatitis: Evolving epidemiologic and clinical perspective. *Semin Liver Dis*. 1986;6(1):67-81. doi:10.1055/s-2008-1040795
4. Choo QL, Kuo G, Weiner AJ, Overby LR, Bradley DW, Houghton M. Isolation of a cDNA clone derived from a blood-borne non-A, non-B viral hepatitis genome. *Science* (80-). 1989;244(4902):359-362. doi:10.1126/science.2523562
5. Houghton M. The long and winding road leading to the identification of the hepatitis C virus. *J Hepatol*. 2009;51(5):939-948. doi:10.1016/j.jhep.2009.08.004
6. Ghany MG, Lok ASF, Dienstag JL, et al. The 2020 Nobel Prize for Medicine or Physiology for the Discovery of Hepatitis C Virus: A Triumph of Curiosity and Persistence. *Hepatology*. 2021;74(5):2813-2823. doi:10.1002/hep.31830
7. Micallef JM, Kaldor JM, Dore GJ. Spontaneous viral clearance following acute hepatitis C infection: A systematic review of longitudinal studies. *J Viral Hepat*. 2006;13(1):34-41. doi:10.1111/j.1365-2893.2005.00651.x
8. Grebely J, Page K, Sacks-Davis R, et al. The effects of female sex, viral genotype, and IL28B genotype on spontaneous clearance of acute hepatitis C virus infection. *Hepatology*. 2014;59(1):109-120. doi:10.1002/hep.26639

9. Sun J, Rajsbaum R, Yi M. Immune and non-immune responses to hepatitis C virus infection. *World J Gastroenterol*. 2015;21(38):10739-10748. doi:10.3748/wjg.v21.i38.10739
10. Thein HH, Yi Q, Dore GJ, Krahn MD. Estimation of stage-specific fibrosis progression rates in chronic hepatitis C virus infection: A meta-analysis and meta-regression. *Hepatology*. 2008;48(2):418-431. doi:10.1002/hep.22375
11. Westbrook RH, Dusheiko G. Natural history of hepatitis C. *J Hepatol*. 2014;61(1):S58-S68. doi:10.1016/j.jhep.2014.07.012
12. Gravitz L. Introduction: A smouldering public-health crisis. *Nature*. 2011;474(7350):S2-S4. doi:10.1038/474S2a
13. Prieto M, Berenguer M, Rayón JM, et al. High incidence of allograft cirrhosis in hepatitis C virus genotype 1b infection following transplantation: Relationship with rejection episodes. *Hepatology*. 1999;29(1):250-256. doi:10.1002/hep.510290122
14. Garcia-Retortillo M, Forns X, Feliu A, et al. Hepatitis C virus kinetics during and immediately after liver transplantation. *Hepatology*. 2002;35(3):680-687. doi:10.1053/jhep.2002.31773
15. Berenguer M, Prieto M, Rayón JM, et al. Natural history of clinically compensated hepatitis C virus-related graft cirrhosis after liver transplantation. *Hepatology*. 2000;32(4):852-858. doi:10.1053/jhep.2000.17924
16. Martini S. Hepatitis C and liver transplantation. *Minerva Gastroenterol Dietol*. 2018;64(2):158-169. doi:10.23736/S1121-421X.17.02448-5
17. Mason Andrew I., Y.N. JL, Nicole H, et al. Association of diabetes mellitus and chronic hepatitis C infection. *Hepatology*. 1999;29(2):328-333.

- doi:10.1002/hep.510290235
18. Goossens N, Negro F. Cardiovascular Manifestations of Hepatitis C Virus. *Clin Liver Dis.* 2017;21(3):465-473. doi:10.1016/j.cld.2017.03.003
 19. Carrier P, Jaccard A, Jacques J, et al. HCV-associated B-cell non-Hodgkin lymphomas and new direct antiviral agents. *Liver Int.* 2015;35(10):2222-2227. doi:10.1111/liv.12897
 20. Wu HL, Duan ZP, Zheng SJ. Hepatitis C virus infection and autoimmunity. *World Chinese J Dig.* 2012;20(28):2678-2684. doi:10.11569/wcjd.v20.i28.2678
 21. Alter HJ, Holland P V., Morrow AG, Purcell RH, Feinstone SM, Moritsugu Y. Clinical and Serological Analysis of Transfusion-Associated Hepatitis. *Lancet.* 1975;306(7940):838-841. doi:10.1016/S0140-6736(75)90234-2
 22. Zuckerman AJ. The elusive hepatitis C virus: A Cause Of Parenteral Non-A, Non-B Hepatitis. *Br Med J.* 1989;299(6704):871-873. doi:10.1136/bmj.299.6704.871
 23. Grebely J, Larney S, Peacock A, et al. Global, regional, and country-level estimates of hepatitis C infection among people who have recently injected drugs. *Addiction.* 2019;114(1):150-166. doi:10.1111/add.14393
 24. Platt L, Easterbrook P, Gower E, et al. Prevalence and burden of HCV co-infection in people living with HIV: A global systematic review and meta-analysis. *Lancet Infect Dis.* 2016;16(7):797-808. doi:10.1016/S1473-3099(15)00485-5
 25. Catanese MT, Uryu K, Kopp M, et al. Ultrastructural analysis of hepatitis C virus particles. *Proc Natl Acad Sci.* 2013;110(23):9505-9510. doi:10.1073/pnas.1307527110

26. Merz A, Long G, Hiet MS, et al. Biochemical and morphological properties of hepatitis C virus particles and determination of their lipidome. *J Biol Chem.* 2011;286(4):3018-3032. doi:10.1074/jbc.M110.175018
27. Honda M, Beard MR, Ping L-H, Lemon SM. A Phylogenetically Conserved Stem-Loop Structure at the 5' Border of the Internal Ribosome Entry Site of Hepatitis C Virus Is Required for Cap-Independent Viral Translation. *J Virol.* 1999;73(2):1165-1174. doi:10.1128/jvi.73.2.1165-1174.1999
28. Friebe P, Boudet J, Simorre J-P, Bartenschlager R. Kissing-Loop Interaction in the 3' End of the Hepatitis C Virus Genome Essential for RNA Replication. *J Virol.* 2005;79(1):380-392. doi:10.1128/jvi.79.1.380-392.2005
29. Choo QL, Richman KH, Han JH, et al. Genetic organization and diversity of the hepatitis C virus. *Proc Natl Acad Sci U S A.* 1991;88(6):2451-2455. doi:10.1073/pnas.88.6.2451
30. Takamizawa A, Mori C, Fuke I, et al. Structure and Organization of the Hepatitis C Virus Genome Isolated from Human Carriers. *J Virol.* 1991;65(3):1105-1113. doi:10.1128/JVI.65.3.1105-1113.1991
31. Abdel-Hakeem MS, Shoukry NH. Protective immunity against hepatitis C: Many shades of gray. *Front Immunol.* 2014;5(274):1-19. doi:10.3389/fimmu.2014.00274
32. Lindenbach BD, Rice CM. Unravelling hepatitis C virus replication from genome to function. *Nature.* 2005;436(7053):933-938. doi:10.1038/nature04077
33. Dubuisson J. Hepatitis C virus proteins. *World J Gastroenterol.* 2007;13(17):2406-2415. doi:10.3748/wjg.v13.i17.2406
34. Holland J, Spindler K, Horodyski F, Grabau E, Nichol S, VandePol S. Rapid

- evolution of RNA genomes. *Science (80-)*. 1982;215(4540):1577-1585. doi:10.1126/science.7041255
35. Martell M, Esteban JI, Quer J, et al. Hepatitis C virus (HCV) circulates as a population of different but closely related genomes: quasispecies nature of HCV genome distribution. *J Virol*. 1992;66(5):3225-3229. doi:10.1128/JVI.66.5.3225-3229.1992
 36. Smith DB, Bukh J, Kuiken C, et al. Flaviviridae: Hepacivirus C Classification. International Committee of Taxonomy of Viruses. https://ictv.global/sg_wiki/flaviviridae/hepacivirus. Published 2022.
 37. Domingo E. Quasispecies. *Encycl Virol*. 1999:1431–1436. doi:10.1006/rwvi.1999.0240
 38. Eigen M, Schuster P. The Hypercycle: A Principle of Natural Self-Organization Part. *Naturwissenschaften*. 1977;64(11):541-565. doi:10.1007/BF00450633
 39. Okamoto H, Kojima M, Okada SI, et al. Genetic drift of hepatitis C virus during an 8.2-year infection in a chimpanzee: Variability and stability. *Virology*. 1992;190(2):894-899. doi:10.1016/0042-6822(92)90933-G
 40. Ogata N, Alter HJ, Miller RH, Purcell RH. Nucleotide sequence and mutation rate of the H strain of hepatitis C virus. *Proc Natl Acad Sci U S A*. 1991;88(8):3392-3396. doi:10.1073/pnas.88.8.3392
 41. Neumann AU, Lam NP, Dahari H, et al. Hepatitis C viral dynamics in vivo and the antiviral efficacy of interferon- α therapy. *Science (80-)*. 1998;282(5386):103-107. doi:10.1126/science.282.5386.103
 42. Perales C, Lorenzo-Redondo R, López-Galíndez C, Martínez MA, Domingo E. Mutant spectra in virus behavior. *Future Virol*. 2010;5(6):679-698. doi:10.2217/fvl.10.61

43. Domingo E, Sheldon J, Perales C. Viral Quasispecies Evolution. *Microbiol Mol Biol Rev.* 2012;76(2):159-216. doi:10.1128/membr.05023-11
44. Novella IS, Elena SF, Moya A, Domingo E, Holland JJ. Size of genetic bottlenecks leading to virus fitness loss is determined by mean initial population fitness. *J Virol.* 1995;69(5):2869-2872. doi:10.1128/jvi.69.5.2869-2872.1995
45. Lázaro E, Escarmís C, Domingo E, Manrubia SC. Modeling Viral Genome Fitness Evolution Associated with Serial Bottleneck Events: Evidence of Stationary States of Fitness. *J Virol.* 2002;76(17):8675-8681. doi:10.1128/jvi.76.17.8675-8681.2002
46. Gregori J, Perales C, Rodriguez-Frias F, Esteban JI, Quer J, Domingo E. Viral quasispecies complexity measures. *Virology.* 2016;493:227-237. doi:10.1016/j.virol.2016.03.017
47. Farci P, Bukh J, Purcell RH. The quasispecies of hepatitis C virus and the host immune response. *Springer Semin Immunopathol.* 1997;19(1):5-26. doi:10.1007/BF00945022
48. Biebricher CK, Eigen M. The error threshold. *Virus Res.* 2005;107(2):117-127. doi:10.1016/j.virusres.2004.11.002
49. Domingo E, Martín V, Perales C, Grande-Pérez A, García-Arriaza J, Arias A. Viruses as quasispecies: Biological implications. *Curr Top Microbiol Immunol.* 2006;299:51-82. doi:10.1007/3-540-26397-7_3
50. Simmonds P, Becher P, Bukh J, et al. ICTV virus taxonomy profile: Flaviviridae. *J Gen Virol.* 2017;98(1):2-3. doi:10.1099/jgv.0.000672
51. Guntipalli P, Pakala R, Gara SK, et al. Worldwide prevalence, genotype distribution and management of hepatitis C. *Acta Gastroenterol Belg.* 2021;84(4):637-656. doi:10.51821/84.4.015

52. Messina JP, Humphreys I, Flaxman A, et al. Global distribution and prevalence of hepatitis C virus genotypes. *Hepatology*. 2015;61(1):77-87. doi:10.1002/hep.27259
53. McMahon BJ, Bruden D, Townshend-Bulson L, et al. Infection With Hepatitis C Virus Genotype 3 is an Independent Risk Factor for End-stage Liver Disease, Hepatocellular Carcinoma, and Liver-related Death. *Clin Gastroenterol Hepatol*. 2017;15(3):431-437. doi:10.1016/j.cgh.2016.10.012.Infection
54. Park HK, Lee SS, Im C Bin, et al. Hepatitis C virus genotype affects survival in patients with hepatocellular carcinoma. *BMC Cancer*. 2019;19(1):1-9. doi:10.1186/s12885-019-6040-3
55. Raimondi S, Bruno S, Mondelli MU, Maisonneuve P. Hepatitis C virus genotype 1b as a risk factor for hepatocellular carcinoma development: A meta-analysis. *J Hepatol*. 2009;50(6):1142-1154. doi:10.1016/j.jhep.2009.01.019
56. Poynard T, Leroy V, Cohard M, et al. Meta-analysis of interferon randomized trials in the treatment of viral hepatitis C: Effects of dose and duration. *Hepatology*. 1996;24(4):778-789. doi:10.1053/jhep.1996.v24.pm0008855176
57. Tine' F, Magrin S, Craxi' A, Pagliaro L. Interferon for non-A, non-B chronic hepatitis. A meta-analysis of randomised clinical trials. *J Hepatol*. 1991;13(2):192-199. doi:10.1016/0168-8278(91)90814-R
58. Reichard O, Norkrans G, Frydén A, Braconier JH, Sönnernborg A, Weiland O. Randomised, double-blind, placebo-controlled trial of interferon α -2b with and without ribavirin for chronic hepatitis C. *Lancet*. 1998;351(9096):83-87. doi:10.1016/S0140-6736(97)06088-1

59. Poynard T, Marcellin P, Lee SS, et al. Randomised trial of interferon α 2b plus ribavirin for 48 weeks or for 24 weeks versus interferon α 2b plus placebo for 48 weeks for treatment of chronic infection with hepatitis C virus. *Lancet*. 1998;352(9138):1426-1432. doi:10.1016/S0140-6736(98)07124-4
60. Davis GL, Esteban-Mur R, Rustgi V, et al. Interferon Alfa-2b Alone or in Combination with Ribavirin for the Treatment of Relapse of Chronic Hepatitis C. *N Engl J Med*. 1998;339(21):1493-1499. doi:10.1056/nejm199811193392102
61. Fried MW, Shiffman ML, Reddy KR, et al. Peginterferon Alfa-2a plus Ribavirin for Chronic Hepatitis C Virus Infection. *N Engl J Med*. 2002;347(13):975-982. doi:10.1056/NEJMoa020047
62. Jacobson IM, McHutchison JG, Dusheiko G, et al. Telaprevir for Previously Untreated Chronic Hepatitis C Virus Infection. *N Engl J Med*. 2011;364(25):2405-2416. doi:10.1056/nejmoa1012912
63. Poordad F, Jonathan McCone J, Bacon BR, et al. Boceprevir for Untreated Chronic HCV Genotype 1 Infection. *N Engl J Med*. 2011;364(13):1195-1206. doi:10.1056/NEJMoa1010494
64. Zoratti MJ, Siddiqua A, Morassut RE, et al. Pangenotypic direct acting antivirals for the treatment of chronic hepatitis C virus infection: A systematic literature review and meta-analysis. *EClinicalMedicine*. 2020;18(100237):1-6. doi:10.1016/j.eclinm.2019.12.007
65. Hartlage AS, Kapoor A. Hepatitis c virus vaccine research: Time to put up or shut up. *Viruses*. 2021;13(8):1-17. doi:10.3390/v13081596
66. Bartenschlager R, Baumert TF, Bukh J, et al. Critical challenges and emerging opportunities in hepatitis C virus research in an era of potent

- antiviral therapy: Considerations for scientists and funding agencies. *Virus Res.* 2018;248:53-62. doi:10.1016/j.virusres.2018.02.016
67. Isakov V, Tsyrcunov V, Nikityuk D. Is elimination of hepatitis C virus realistic by 2030: Eastern Europe. *Liver Int.* 2021;41(S1):50-55. doi:10.1111/liv.14836
68. Mescher MF, Curtsinger JM, Agarwal P, et al. Signals required for programming effector and memory development by CD8+ T cells. *Immunol Rev.* 2006;211:81-92. doi:10.1111/j.0105-2896.2006.00382.x
69. Schwerk J, Negash A, Savan R, Gale M. Innate immunity in Hepatitis C virus infection. *Cold Spring Harb Perspect Med.* 2021;11(2):1-15. doi:10.1101/cshperspect.a036988
70. Guo JT, Sohn JA, Zhu Q, Seeger C. Mechanism of the interferon alpha response against hepatitis C virus replicons. *Virology.* 2004;325(1):71-81. doi:10.1016/j.virol.2004.04.031
71. Lionel B. Ivashkiv^{1, 2 3} and Laura T. Donlin¹. Regulation of type I interferon responses Lionel. *Bone.* 2008;23(1):1-7. doi:10.1038/nri3581.Regulation
72. Pujantell M, Franco S, Galván-Femenía I, et al. ADAR1 affects HCV infection by modulating innate immune response. *Antiviral Res.* 2018;156:116-127. doi:10.1016/j.antiviral.2018.05.012
73. Taylor DR, Puig M, Darnell MER, Mihalik K, Feinstone SM. New Antiviral Pathway That Mediates Hepatitis C Virus Replicon Interferon Sensitivity through ADAR1. *J Virol.* 2005;79(10):6291-6298. doi:10.1128/jvi.79.10.6291-6298.2005
74. Dolganiuc A, Chang S, Kodys K, et al. Hepatitis C Virus (HCV) Core Protein-Induced, Monocyte-Mediated Mechanisms of Reduced IFN- α and

- Plasmacytoid Dendritic Cell Loss in Chronic HCV Infection. *J Immunol.* 2006;177(10):6758-6768. doi:10.4049/jimmunol.177.10.6758
75. Lin W, Choe WH, Hiasa Y, et al. Hepatitis C virus expression suppresses interferon signaling by degrading STAT1. *Gastroenterology.* 2005;128(4):1034-1041. doi:10.1053/j.gastro.2005.02.006
76. Shrivastava A, Manna SK, Ray R, Aggarwal BB. Ectopic Expression of Hepatitis C Virus Core Protein Differentially Regulates Nuclear Transcription Factors. *J Virol.* 1998;72(12):9722-9728. doi:10.1128/jvi.72.12.9722-9728.1998
77. Nguyen H, Sankaran S, Dandekar S. Hepatitis C virus core protein induces expression of genes regulating immune evasion and anti-apoptosis in hepatocytes. *Virology.* 2006;354(1):58-68. doi:10.1016/j.virol.2006.04.028
78. Taylor DR, Shi ST, Romano PR, Barber GN, Lai MMC. Inhibition of the interferon-inducible protein kinase PKR by HCV E2 protein. *Science (80-)*. 1999;285(5424):107-110. doi:10.1126/science.285.5424.107
79. Qi H, Chu V, Wu NC, et al. Systematic identification of anti-interferon function on hepatitis C virus genome reveals p7 as an immune evasion protein. *Proc Natl Acad Sci U S A.* 2017;114(8):2018-2023. doi:10.1073/pnas.1614623114
80. Li XD, Sun L, Seth RB, Pineda G, Chen ZJ. Hepatitis C virus protease NS3/4A cleaves mitochondrial antiviral signaling protein off the mitochondria to evade innate immunity. *Proc Natl Acad Sci U S A.* 2005;102(49):17717-17722. doi:10.1073/pnas.0508531102
81. Li K, Foy E, Ferreon JC, et al. Immune evasion by hepatitis C virus NS3/4A protease-mediated cleavage of the Toll-like receptor 3 adaptor protein

- TRIF. *Proc Natl Acad Sci U S A*. 2005;102(8):2992-2997. doi:10.1073/pnas.0408824102
82. Vazquez C, Tan CY, Horner SM. Hepatitis C Virus Infection Is Inhibited by a Noncanonical Antiviral Signaling Pathway Targeted by NS3-NS4A. *J Virol*. 2019;93(23):1-19. doi:10.1128/jvi.00725-19
83. Chen Y, He L, Peng Y, et al. The hepatitis C virus protein NS3 suppresses TNF- α -stimulated activation of NF- κ B by targeting LUBAC. *Sci Signal*. 2015;8(403):1-11. doi:10.1126/scisignal.aab2159
84. Otsuka M, Kato N, Moriyama M, et al. Interaction between the HCV NS3 protein and the host TBK1 protein leads to inhibition of cellular antiviral responses. *Hepatology*. 2005;41(5):1004-1012. doi:10.1002/hep.20666
85. Nitta S, Sakamoto N, Nakagawa M, et al. Hepatitis C virus NS4B protein targets STING and abrogates RIG-I-mediated type I interferon-dependent innate immunity. *Hepatology*. 2013;57(1):46-58. doi:10.1002/hep.26017
86. Liang Y, Cao X, Ding Q, Zhao Y, He Z, Zhong J. Hepatitis C virus NS4B induces the degradation of TRIF to inhibit TLR3-mediated interferon signaling pathway. *PLoS Pathog*. 2018;14(5):1-19. doi:10.1371/journal.ppat.1007075
87. Gale MJ, Korth MJ, Tang NM, et al. Evidence that hepatitis C virus resistance to interferon is mediated through repression of the PKR protein kinase by the nonstructural 5A protein. *Virology*. 1997;230(2):217-227. doi:10.1006/viro.1997.8493
88. Hiet MS, Bauhofer O, Zayas M, et al. Control of temporal activation of hepatitis C virus-induced interferon response by domain 2 of nonstructural protein 5A. *J Hepatol*. 2015;63(4):829-837. doi:10.1016/j.jhep.2015.04.015

89. Çevik RE, Cesarec M, Da Silva Filipe A, Licastro D, McLauchlan J, Marcello A. Hepatitis C Virus NS5A Targets Nucleosome Assembly Protein NAP1L1 To Control the Innate Cellular Response. *J Virol.* 2017;91(18):1-20. doi:10.1128/jvi.00880-17
90. Li H, Jiang JD, Peng ZG. MicroRNA-mediated interactions between host and hepatitis C virus. *World J Gastroenterol.* 2016;22(4):1487-1496. doi:10.3748/wjg.v22.i4.1487
91. Grünvogel O, Colasanti O, Lee JY, et al. Secretion of Hepatitis C Virus Replication Intermediates Reduces Activation of Toll-Like Receptor 3 in Hepatocytes. *Gastroenterology.* 2018;154(8):2237-2251.e16. doi:10.1053/j.gastro.2018.03.020
92. Wong MT, Chen SSL. Emerging roles of interferon-stimulated genes in the innate immune response to hepatitis C virus infection. *Cell Mol Immunol.* 2016;13(1):11-35. doi:10.1038/cmi.2014.127
93. Neumann-Haefelin C, Thimme R. Adaptive Immune Responses in Hepatitis C Virus Infection. In: Bartenschlager R, ed. *Hepatitis C Virus: From Molecular Virology to Antiviral Therapy.* Berlin, Heidelberg: Springer Berlin Heidelberg; 2013:369: 243-262. doi:10.1007/978-3-642-27340-7_10
94. Jo J, Aichele U, Kersting N, et al. Analysis of CD8 + T-Cell-Mediated Inhibition of Hepatitis C Virus Replication Using a Novel Immunological Model. *Gastroenterology.* 2009;136(4):1391-1401. doi:10.1053/j.gastro.2008.12.034
95. Swain SL, McKinstry KK, Strutt TM. Expanding roles for CD4 + T cells in immunity to viruses. *Nat Rev Immunol.* 2012;12(2):136-148. doi:10.1038/nri3152

96. Mosmann TR, Cherwinski H, Bond MW, Giedlin MA, Coffman RL. Two types of murine helper T cell clone. I. Definition according to profiles of lymphokine activities and secreted proteins. *J Immunol.* 1986;136(7):2348-2357.
97. Rehermann B. Hepatitis C virus versus innate and adaptive immune responses: a tale of coevolution and coexistence. *Sci Med.* 2009;119(7):1745-1754. doi:10.1172/JCI39133.vitro
98. Farci P, Alter HJ, Govindarajan S, et al. Lack of protective immunity against reinfection with hepatitis C virus. *Science (80-).* 1992;258(5079):135-140. doi:10.1126/science.1279801
99. Thimme R, Oldach D, Chang KM, Steiger C, Ray SC, Chisari F V. Determinants of viral clearance and persistence during acute hepatitis C virus infection. *J Exp Med.* 2001;194(10):1395-1406. doi:10.1084/jem.194.10.1395
100. Grakoui A, Shoukry NH, Woollard DJ, et al. HCV Persistence and Immune Evasion in the Absence of Memory T Cell Help. *Science (80-).* 2003;302(5645):659-662. doi:10.1126/science.1088774
101. Cooper S, Erickson AL, Adams EJ, et al. Analysis of a successful immune response against hepatitis C virus. *Immunity.* 1999;10(4):439-449. doi:10.1016/S1074-7613(00)80044-8
102. Bowen DG, Walker CM. Adaptive immune responses in acute and chronic hepatitis C virus infection. *Nature.* 2005;436(7053):946-952. doi:10.1038/nature04079
103. Lechner F, Wong DKH, Dunbar PR, et al. Analysis of successful immune responses in persons infected with hepatitis C virus. *J Exp Med.* 2000;191(9):1499-1512. doi:10.1084/jem.191.9.1499

104. Klenerman P, Hill A. T cells and viral persistence: Lessons from diverse infections. *Nat Immunol.* 2005;6(9):873-879. doi:10.1038/ni1241
105. Bengsch B, Seigel B, Ruhl M, et al. Coexpression of PD-1, 2B4, CD160 and KLRG1 on exhausted HCV-specific CD8+ T cells is linked to antigen recognition and T cell differentiation. *PLoS Pathog.* 2010;6(6):1-14. doi:10.1371/journal.ppat.1000947
106. Luxenburger H, Neumann-Haefelin C, Thimme R, Boettler T. HCV-Specific T Cell Responses During and After Chronic HCV Infection. *Viruses.* 2018;10(11):645. doi:10.3390/v10110645
107. Penna A, Missale G, Lamonaca V, et al. Intrahepatic and circulating HLA class II-restricted, hepatitis C virus-specific T cells: Functional characterization in patients with chronic hepatitis C. *Hepatology.* 2002;35(5):1225-1236. doi:10.1053/jhep.2002.33153
108. Accapezzato D, Francavilla V, Paroli M, et al. Hepatic expansion of a virus-specific regulatory CD8+ T cell population in chronic hepatitis C virus infection. *J Clin Invest.* 2004;113(7):963-972. doi:10.1172/JCI200420515
109. Semmo N, Day CL, Ward SM, et al. Preferential loss of IL-2-secreting CD4+ T helper cells in chronic HCV infection. *Hepatology.* 2005;41(5):1019-1028. doi:10.1002/hep.20669
110. Boettler T, Spangenberg HC, Neumann-Haefelin C, et al. T Cells with a CD4+ CD25+ regulatory phenotype suppress in vitro proliferation of virus-specific CD8+ T cells during chronic hepatitis C virus infection. *J Virol.* 2005;79(12):7860-7867. doi:10.1128/JVI.79.12.7860
111. Zajac AJ, Blattman JN, Murali-Krishna K, et al. Viral immune evasion due to persistence of activated T cells without effector function. *J Exp Med.* 1998;188(12):2205-2213. doi:10.1084/jem.188.12.2205

112. Gerlach JT, Diepolder HM, Jung MC, et al. Recurrence of hepatitis C virus after loss of virus-specific CD4+ T- cell response in acute hepatitis C. *Gastroenterology*. 1999;117(4):933-941. doi:10.1016/S0016-5085(99)70353-7
113. Zhao B Bin, Zheng SJ, Gong LL, et al. T Lymphocytes from Chronic HCV-Infected Patients Are Primed for Activation-Induced Apoptosis and Express Unique Pro-Apoptotic Gene Signature. *PLoS One*. 2013;8(10):1-13. doi:10.1371/journal.pone.0077008
114. Heim MH, Thimme R. Innate and adaptive immune responses in HCV infections. *J Hepatol*. 2014;61(1):S14-S25. doi:10.1016/j.jhep.2014.06.035
115. Shimizu YK, Hijikata M, Iwamoto A, Alter HJ, Purcell RH, Yoshikura H. Neutralizing antibodies against hepatitis C virus and the emergence of neutralization escape mutant viruses. *J Virol*. 1994;68(3):1494-1500. doi:10.1128/jvi.68.3.1494-1500.1994
116. Tsai SL, Chen YM, Chen MH, et al. Hepatitis C virus variants circumventing cytotoxic T lymphocyte activity as a mechanism of chronicity. *Gastroenterology*. 1998;115(4):954-966. doi:10.1016/S0016-5085(98)70268-9
117. Sarobe P, Lasarte JJ, Casares N, et al. Abnormal Priming of CD4 + T Cells by Dendritic Cells Expressing Hepatitis C Virus Core and E1 Proteins . *J Virol*. 2002;76(10):5062-5070. doi:10.1128/jvi.76.10.5062-5070.2002
118. Auffermann-Gretzinger S, Keeffe EB, Levy S. Impaired dendritic cell maturation in patients with chronic, but not resolved, hepatitis C virus infection. *Blood*. 2001;97(10):3171-3176. doi:10.1182/blood.V97.10.3171

119. Lee CH, Choi YH, Yang SH, Lee CW, Ha SJ, Sung YC. Hepatitis C virus core protein inhibits interleukin 12 and nitric oxide production from activated macrophages. *Virology*. 2001;279(1):271-279. doi:10.1006/viro.2000.0694
120. Yao ZQ, Eisen-Vandervelde A, Waggoner SN, Cale EM, Hahn YS. Direct Binding of Hepatitis C Virus Core to gC1qR on CD4 + and CD8 + T Cells Leads to Impaired Activation of Lck and Akt . *J Virol*. 2004;78(12):6409-6419. doi:10.1128/jvi.78.12.6409-6419.2004
121. Urbani S, Boni C, Missale G, et al. Virus-Specific CD8 + Lymphocytes Share the Same Effector-Memory Phenotype but Exhibit Functional Differences in Acute Hepatitis B and C . *J Virol*. 2002;76(24):12423-12434. doi:10.1128/jvi.76.24.12423-12434.2002
122. Gruener NH, Lechner F, Jung M-C, et al. Sustained Dysfunction of Antiviral CD8 + T Lymphocytes after Infection with Hepatitis C Virus . *J Virol*. 2001;75(12):5550-5558. doi:10.1128/jvi.75.12.5550-5558.2001
123. Wherry EJ, Kurachi M. Molecular and cellular insights into T cell exhaustion. *Nat Rev Immunol*. 2015;15(8):486-499. doi:10.1038/nri3862
124. Radziewicz H, Ibegbu CC, Hon H, et al. Impaired Hepatitis C Virus (HCV)-Specific Effector CD8 + T Cells Undergo Massive Apoptosis in the Peripheral Blood during Acute HCV Infection and in the Liver during the Chronic Phase of Infection . *J Virol*. 2008;82(20):9808-9822. doi:10.1128/jvi.01075-08
125. Harryvan TJ, de Lange S, Hawinkels LJAC, Verdegaal EME. The ABCs of antigen presentation by stromal non-professional antigen-presenting cells. *Int J Mol Sci*. 2022;23(1):137. doi:10.3390/ijms23010137
126. Harari A, Vallelian F, Meylan PR, Pantaleo G. Functional Heterogeneity of

- Memory CD4 T Cell Responses in Different Conditions of Antigen Exposure and Persistence. *J Immunol.* 2005;174(2):1037-1045. doi:10.4049/jimmunol.174.2.1037
127. Chung JB, Wells AD, Adler S, Jacob A, Turka LA, Monroe JG. Incomplete Activation of CD4 T Cells by Antigen-Presenting Transitional Immature B Cells: Implications for Peripheral B and T Cell Responsiveness. *J Immunol.* 2003;171(4):1758-1767. doi:10.4049/jimmunol.171.4.1758
128. van der Ree MH, Stelma F, Willemse SB, et al. Immune responses in DAA treated chronic hepatitis C patients with and without prior RG-101 dosing. *Antiviral Res.* 2017;146(2017):139-145. doi:10.1016/j.antiviral.2017.08.016
129. Martin B, Hennecke N, Lohmann V, et al. Restoration of HCV-specific CD8+ T cell function by interferon-free therapy. *J Hepatol.* 2014;61(3):538-543. doi:10.1016/j.jhep.2014.05.043
130. Folgori A, Spada E, Pezzanera M, et al. Early impairment of hepatitis C virus specific T cell proliferation during acute infection leads to failure of viral clearance. *Gut.* 2006;55(7):1012-1019. doi:10.1136/gut.2005.080077
131. Han JW, Sung PS, Kim KH, et al. Dynamic Changes in Ex Vivo T-Cell Function After Viral Clearance in Chronic HCV Infection. *J Infect Dis.* 2019;220(8):1290-1301. doi:10.1093/infdis/jiz291
132. Wieland D, Kemming J, Schuch A, et al. TCF1+ hepatitis C virus-specific CD8+ T cells are maintained after cessation of chronic antigen stimulation. *Nat Commun.* 2017;8:1-13. doi:10.1038/ncomms15050
133. Aregay A, Owusu Sekyere S, Deterding K, et al. Elimination of hepatitis C virus has limited impact on the functional and mitochondrial impairment

- of HCV-specific CD8+ T cell responses. *J Hepatol.* 2019;71(5):889-899. doi:10.1016/j.jhep.2019.06.025
134. Burchill MA, Golden-Mason L, Wind-Rotolo M, Rosen HR. Memory re-differentiation and reduced lymphocyte activation in chronic HCV-infected patients receiving direct-acting antivirals. *J Viral Hepat.* 2015;22(12):983-991. doi:10.1111/jvh.12465
135. Hartnell F, Esposito I, Swadling L, et al. Characterising HCV specific CD4+ T-cells following viral-vectored vaccination, directly acting anti-virals and spontaneous viral cure. *Hepatology.* 2020;72(5):1541-1555. doi:10.1002/hep.31160
136. Raposo G, Nijman HW, Stoorvogel W, et al. B lymphocytes secrete antigen-presenting vesicles. *J Exp Med.* 1996;183(3):1161-1172. doi:10.1084/jem.183.3.1161
137. Johnstone RM, Adam M, Hammond JR, Orr L, Turbide C. Vesicle formation during reticulocyte maturation. Association of plasma membrane activities with released vesicles (exosomes). *J Biol Chem.* 1987;262(19):9412-9420. doi:10.1016/s0021-9258(18)48095-7
138. Harding C, Heuser J, Stahl P. Receptor-mediated endocytosis of transferrin and recycling of the transferrin receptor in rat reticulocytes. *J Cell Biol.* 1983;97(2):329-339. doi:10.1083/jcb.97.2.329
139. Colombo M, Raposo G, Théry C. Biogenesis, secretion, and intercellular interactions of exosomes and other extracellular vesicles. *Annu Rev Cell Dev Biol.* 2014;30(1):255-289. doi:10.1146/annurev-cellbio-101512-122326
140. Raposo G, Stoorvogel W. Extracellular vesicles: Exosomes, microvesicles, and friends. *J Cell Biol.* 2013;200(4):373-383. doi:10.1083/jcb.201211138

141. Zaborowski MP, Balaj L, Breakefield XO, Lai CP. Extracellular Vesicles: Composition, Biological Relevance, and Methods of Study. *Bioscience*. 2015;65(8):783-797. doi:10.1093/biosci/biv084
142. Yáñez-Mó M, Siljander PRM, Andreu Z, et al. Biological properties of extracellular vesicles and their physiological functions. *J Extracell Vesicles*. 2015;4(2015):1-60. doi:10.3402/jev.v4.27066
143. Battistelli M, Falcieri E. Apoptotic bodies: Particular extracellular vesicles involved in intercellular communication. *Biology (Basel)*. 2020;9(1):21. doi:10.3390/biology9010021
144. Laura M. Doyle, Michael Zhuo Wang. Overview of Extracellular Vesicles, Their Origin, Composition, Purpose, and Methods for Exosome Isolation and Analysis. *Cells*. 2019;8(727):41-68. doi:10.3390/cells8070727
145. Fadeel B, Orrenius S. Apoptosis: A basic biological phenomenon with wide-ranging implications in human disease. *J Intern Med*. 2005;258(6):479-517. doi:10.1111/j.1365-2796.2005.01570.x
146. Heijnen HFG, Schiel AE, Fijnheer R, Geuze HJ, Sixma JJ. Activated platelets release two types of membrane vesicles: Microvesicles by surface shedding and exosomes derived from exocytosis of multivesicular bodies and α -granules. *Blood*. 1999;94(11):3791-3799. doi:10.1182/blood.v94.11.3791
147. Théry C, Boussac M, Véron P, et al. Proteomic Analysis of Dendritic Cell-Derived Exosomes: A Secreted Subcellular Compartment Distinct from Apoptotic Vesicles. *J Immunol*. 2001;166(12):7309-7318. doi:10.4049/jimmunol.166.12.7309
148. Livshits MA, Khomyakova E, Evtushenko EG, et al. Isolation of exosomes by differential centrifugation: Theoretical analysis of a commonly used

- protocol. *Sci Rep*. 2015;5(17319):1-14. doi:10.1038/srep17319
149. He C, Zheng S, Luo Y, Wang B. Exosome theranostics: Biology and translational medicine. *Theranostics*. 2018;8(1):237-255. doi:10.7150/thno.21945
150. Théry C, Clayton A, Amigorena S, Raposo and G. Isolation and Characterization of Exosomes from Cell Culture Supernatants. *Curr Protoc Cell Biol*. 2006;30:3.22.1–3.22.29. doi:10.1002/0471143030.cb0322s30
151. Coughlan C, Bruce KD, Burgy O, et al. Exosome Isolation by Ultracentrifugation and Precipitation and Techniques for Downstream Analyses. *Curr Protoc Cell Biol*. 2020;88(1):e110. doi:10.1002/cpcb.110
152. Crescitelli R, Lässer C, Lötvall J. Isolation and characterization of extracellular vesicle subpopulations from tissues. *Nat Protoc*. 2021;16(3):1548-1580. doi:10.1038/s41596-020-00466-1
153. Böing AN, van der Pol E, Grootemaat AE, Coumans FAW, Sturk A, Nieuwland R. Single-step isolation of extracellular vesicles by size-exclusion chromatography. *J Extracell Vesicles*. 2014;3(1):23430. doi:10.3402/jev.v3.23430
154. Zhou X, Xie F, Wang L, et al. The function and clinical application of extracellular vesicles in innate immune regulation. *Cell Mol Immunol*. 2020;17(4):323-334. doi:10.1038/s41423-020-0391-1
155. Möbius W, van Donselaar E, Ohno-Iwashita Y, et al. Recycling compartments and the internal vesicles of multivesicular bodies harbor most of the cholesterol found in the endocytic pathway. *Traffic*. 2003;4(4):222-231. doi:10.1034/j.1600-0854.2003.00072.x
156. Buschow SI, Nolte-t Hoen ENM, van Niel G, et al. MHC II In dendritic cells

- is targeted to lysosomes or t cell-induced exosomes via distinct multivesicular body pathways. *Traffic*. 2009;10(10):1528-1542. doi:10.1111/j.1600-0854.2009.00963.x
157. Llorente A, Skotland T, Sylvänne T, et al. Molecular lipidomics of exosomes released by PC-3 prostate cancer cells. *Biochim Biophys Acta - Mol Cell Biol Lipids*. 2013;1831(7):1302-1309. doi:10.1016/j.bbaliip.2013.04.011
158. Février B, Raposo G. Exosomes: Endosomal-derived vesicles shipping extracellular messages. *Curr Opin Cell Biol*. 2004;16(4):415-421. doi:10.1016/j.ceb.2004.06.003
159. Elzanowska J, Semira C, Costa-Silva B. DNA in extracellular vesicles: biological and clinical aspects. *Mol Oncol*. 2021;15(6):1701-1714. doi:10.1002/1878-0261.12777
160. Ghanam J, Chetty VK, Barthel L, Reinhardt D, Hoyer PF, Thakur BK. DNA in extracellular vesicles: from evolution to its current application in health and disease. *Cell Biosci*. 2022;12(1):1-13. doi:10.1186/s13578-022-00771-0
161. O'Grady T, Njock MS, Lion M, et al. Sorting and packaging of RNA into extracellular vesicles shape intracellular transcript levels. *BMC Biol*. 2022;20(1):1-21. doi:10.1186/s12915-022-01277-4
162. Matsuzaki J, Ochiya T. Extracellular microRNAs and oxidative stress in liver injury: A systematic mini review. *J Clin Biochem Nutr*. 2018;63(1):6-11. doi:10.3164/jcbtn.17-123
163. D'souza RF, Woodhead JST, Zeng N, et al. Circulatory exosomal miRNA following intense exercise is unrelated to muscle and plasma miRNA abundances. *Am J Physiol - Endocrinol Metab*. 2018;315(4):E723-E733.

- doi:10.1152/ajpendo.00138.2018
164. Baglio SR, Rooijers K, Koppers-Lalic D, et al. Human bone marrow- and adipose-mesenchymal stem cells secrete exosomes enriched in distinctive miRNA and tRNA species. *Stem Cell Res Ther.* 2015;6(127):1-20. doi:10.1186/s13287-015-0116-z
165. Schulz-Siegmund M, Aigner A. Nucleic acid delivery with extracellular vesicles. *Adv Drug Deliv Rev.* 2021;173:89-111. doi:10.1016/j.addr.2021.03.005
166. Huang X, Yuan T, Tschannen M, et al. Characterization of human plasma-derived exosomal RNAs by deep sequencing. *BMC Genomics.* 2013;14(1):1-14. doi:10.1186/1471-2164-14-319
167. M. Bhaskaran, M. Mohan. MicroRNAs: History, Biogenesis, and Their Evolving Role in Animal Development and Disease. 2014;51(4):759-774. doi:10.1177/0300985813502820
168. Richard W. Carthew, Erik J. Sontheimer. Origins and Mechanisms of miRNAs and siRNAs Richard. *Cell.* 2009;136(4):642-655. doi:10.1016/j.cell.2009.01.035.Origins
169. Huntzinger E, Izaurralde E. Gene silencing by microRNAs: Contributions of translational repression and mRNA decay. *Nat Rev Genet.* 2011;12(2):99-110. doi:10.1038/nrg2936
170. Steinbichler TB, Dudás J, Riechelmann H, Skvortsova II. The role of exosomes in cancer metastasis. *Semin Cancer Biol.* 2017;44:170-181. doi:10.1016/j.semcancer.2017.02.006
171. Sun Z, Shi K, Yang S, et al. Effect of exosomal miRNA on cancer biology and clinical applications. *Mol Cancer.* 2018;17(147):1-19. doi:10.1186/s12943-018-0897-7

172. Vickers KC, Palmisano BT, Shoucri BM, Shamburek RD, Remaley AT. MicroRNAs are transported in plasma and delivered to recipient cells by high-density lipoproteins. *Nat Cell Biol.* 2011;13(4):423-433. doi:10.1038/ncb2210
173. Mitchell PS, Parkin RK, Kroh EM, et al. Circulating microRNAs as stable blood-based markers for cancer detection. *Proc Natl Acad Sci U S A.* 2008;105(30):10513-10518. doi:10.1073/pnas.0804549105
174. Winter J, Diederichs S. Argonaute proteins regulate microRNA stability: Increased microRNA abundance by Argonaute proteins is due to microRNA stabilization. *RNA Biol.* 2011;8(6):1149-1157. doi:10.4161/rna.8.6.17665
175. Gallo A, Tandon M, Alevizos I, Illei GG. The majority of microRNAs detectable in serum and saliva is concentrated in exosomes. *PLoS One.* 2012;7(3):1-5. doi:10.1371/journal.pone.0030679
176. Wei H, Chen Q, Lin L, et al. Regulation of exosome production and cargo sorting. *Int J Biol Sci.* 2020;17(1):163-177. doi:10.7150/ijbs.53671
177. Zhang Y, Liu Y, Liu H, Tang WH. Exosomes: Biogenesis, biologic function and clinical potential. *Cell Biosci.* 2019;9(19):1-18. doi:10.1186/s13578-019-0282-2
178. Johan Skog, Wurdinger T, Rijn S van, et al. Glioblastoma microvesicles transport RNA and protein that promote tumor growth and provide diagnostic biomarkers. *Nat Cell Biol.* 2008;10(12):1470–1476. doi:10.1038/ncb1800
179. Chaput N, Théry C. Exosomes: Immune properties and potential clinical implementations. *Semin Immunopathol.* 2011;33(5):419-440. doi:10.1007/s00281-010-0233-9

180. de Miguel Pérez D, Rodríguez Martínez A, Ortigosa Palomo A, et al. Extracellular vesicle-miRNAs as liquid biopsy biomarkers for disease identification and prognosis in metastatic colorectal cancer patients. *Sci Rep.* 2020;10(3974):1-13. doi:10.1038/s41598-020-60212-1
181. Valadi H, Ekström K, Bossios A, Sjöstrand M, Lee JJ, Lötvall JO. Exosome-mediated transfer of mRNAs and microRNAs is a novel mechanism of genetic exchange between cells. *Nat Cell Biol.* 2007;9(6):654-659. doi:10.1038/ncb1596
182. Kyoung Mi Kim, Kotb Abdelmohsen, Maja Mustapic, Dimitrios Kapogiannis, Myriam Gorospe. RNA in extracellular vesicles. *Wiley Interdiscip Rev RNA.* 2017;8(4):1-20. doi:10.1002/wrna.1413
183. Buschmann D, Kirchner B, Hermann S, et al. Evaluation of serum extracellular vesicle isolation methods for profiling miRNAs by next-generation sequencing. *J Extracell vesicles.* 2018;7(1). doi:10.1080/20013078.2018.1481321
184. Coenen-Stass AML, Magen I, Brooks T, et al. Evaluation of methodologies for microRNA biomarker detection by next generation sequencing. *RNA Biol.* 2018;15(8):1133-1145. doi:10.1080/15476286.2018.1514236
185. Witwer KW, Buzás EI, Bemis LT, et al. Standardization of sample collection, isolation and analysis methods in extracellular vesicle research. *J Extracell Vesicles.* 2013;2(1). doi:10.3402/jev.v2i0.20360
186. Mitchell DL, Vickers KC. Lipoprotein carriers of microRNAs. *Biochim Biophys Acta - Mol Cell Biol Lipids.* 2016;1861(12):2069-2074. doi:10.1016/j.bbalip.2016.01.011
187. Anel A, Gallego-Lleyda A, de Miguel D, Naval J, Martínez-Lostao L. Role of exosomes in the regulation of t-cell mediated immune responses and

- in autoimmune disease. *Cells*. 2019;8(2). doi:10.3390/cells8020154
188. Valenti R, Huber V, Iero M, Filipazzi P, Parmiani G, Rivoltini L. Tumor-released microvesicles as vehicles of immunosuppression. *Cancer Res*. 2007;67(7):2912-2915. doi:10.1158/0008-5472.CAN-07-0520
189. Li C, Donninger H, Eaton J, Yaddanapudi K. Regulatory Role of Immune Cell-Derived Extracellular Vesicles in Cancer: The Message Is in the Envelope. *Front Immunol*. 2020;11(July):1-18. doi:10.3389/fimmu.2020.01525
190. Théry C, Duban L, Segura E, Væron P, Lantz O, Amigorena S. Indirect activation of naïve CD4+ T cells by dendritic cell-derived exosomes. *Nat Immunol*. 2002;3(12):1156-1162. doi:10.1038/ni854
191. Montecalvo A, Shufesky WJ, Beer Stolz D, et al. Exosomes As a Short-Range Mechanism to Spread Alloantigen between Dendritic Cells during T Cell Allorecognition. *J Immunol*. 2008;180(5):3081-3090. doi:10.4049/jimmunol.180.5.3081
192. Mittelbrunn M, Gutiérrez-Vázquez C, Villarroya-Beltri C, et al. Unidirectional transfer of microRNA-loaded exosomes from T cells to antigen-presenting cells. *Nat Commun*. 2011;2(1). doi:10.1038/ncomms1285
193. Admyre C, Johansson SM, Paulie S, Gabrielsson S. Direct exosome stimulation of peripheral human T cells detected by ELISPOT. *Eur J Immunol*. 2006;36(7):1772-1781. doi:10.1002/eji.200535615
194. Schorey JS, Cheng Y, Singh PP, Smith VL. Exosomes and other extracellular vesicles in host-pathogen interactions. *EMBO Rep*. 2015;16(1):24-43. doi:10.15252/embr.201439363
195. Yin C, Han Q, Xu D, Zheng B, Zhao X, Zhang J. SALL4-mediated

- upregulation of exosomal miR-146a-5p drives T-cell exhaustion by M2 tumor-associated macrophages in HCC. *Oncoimmunology*. 2019;8(7):1-13. doi:10.1080/2162402X.2019.1601479
196. Wang X, Shen H, Zhangyuan G, et al. 14-3-3 ζ delivered by hepatocellular carcinoma-derived exosomes impaired anti-tumor function of tumor-infiltrating T lymphocytes article. *Cell Death Dis*. 2018;9(2). doi:10.1038/s41419-017-0180-7
197. Wang JF, Zhao XH, Wang YB, et al. circRNA-002178 act as a ceRNA to promote PDL1/PD1 expression in lung adenocarcinoma. *Cell Death Dis*. 2020;11(1). doi:10.1038/s41419-020-2230-9
198. Wang X, Shen H, He Q, Tian W, Xia A, Lu XJ. Exosomes derived from exhausted CD8⁺ T cells impaired the anticancer function of normal CD8⁺ T cells. *J Med Genet*. 2019;56(1):29-31. doi:10.1136/jmedgenet-2018-105439
199. Kim JH, Lee CH, Lee SW. Exosomal Transmission of MicroRNA from HCV Replicating Cells Stimulates Transdifferentiation in Hepatic Stellate Cells. *Mol Ther - Nucleic Acids*. 2019;14(March):483-497. doi:10.1016/j.omtn.2019.01.006
200. Devhare PB, Sasaki R, Shrivastava S, Bisceglie AM Di, Ray R, Ray RB. Exosome-Mediated Intercellular Communication between Hepatitis C Virus-Infected Hepatocytes and Hepatic Stellate. 2017;91(6):e02225-16. doi:10.1128/JVI.02225-16
201. Bukong TN, Momen-Heravi F, Kodys K, Bala S, Szabo G. Exosomes from Hepatitis C Infected Patients Transmit HCV Infection and Contain Replication Competent Viral RNA in Complex with Ago2-miR122-HSP90. *PLoS Pathog*. 2014;10(10). doi:10.1371/journal.ppat.1004424

202. Giannessi F, Aiello A, Franchi F, Percario ZA, Affabris E. The role of extracellular vesicles as allies of HIV, HCV and SARS viruses. *Viruses*. 2020;12(5). doi:10.3390/v12050571
203. Garcia-Retortillo M, Xavier F, Feliu A, et al. Hepatitis C virus kinetics during and immediately after liver transplantation. *Hepatology*. 2002;35(3):680-687. doi:10.1053/jhep.2002.31773
204. Domingo E. *Virus as Populations. Composition, Complexity, Dynamics and Biological Implications*. Elsevier.; 2019. doi:10.1016/C2017-0-04115-0
205. Pérez-Del-Pulgar S, Gregori J, Rodríguez-Frías F, et al. Quasispecies dynamics in hepatitis C liver transplant recipients receiving grafts from hepatitis C virus infected donors. *J Gen Virol*. 2015;96(12):3493-3498. doi:10.1099/jgv.0.000289
206. Farci P, Shimoda a, Coiana a, et al. The Outcome of Acute Hepatitis C Predicted by the Evolution of the Viral Quasispecies. *Science (80-)*. 2000;288(2000):339-344. doi:10.1126/science.288.5464.339
207. Gambato M, Gregori J, Quer J, et al. Hepatitis C virus intrinsic molecular determinants may contribute to the development of cholestatic hepatitis after liver transplantation. *J Gen Virol*. 2019;100(1):63-68. doi:10.1099/jgv.0.001175
208. Crespo G, Trota N, Londoño MC, et al. The efficacy of direct anti-HCV drugs improves early post-liver transplant survival and induces significant changes in waiting list composition. *J Hepatol*. 2018;69(1):11-17. doi:10.1016/j.jhep.2018.02.012
209. Farci P, Strazzer R, Alter HJ, et al. Early changes in hepatitis C viral quasispecies during interferon therapy predict the therapeutic outcome.

- Proc Natl Acad Sci U S A.* 2002;99(5):3081-3086. doi:10.1073/pnas.052712599
210. Perales C. Quasispecies dynamics and clinical significance of hepatitis C virus (HCV) antiviral resistance. *Int J Antimicrob Agents.* 2020;56(1). doi:10.1016/j.ijantimicag.2018.10.005
211. Pawlotsky JM. Hepatitis C virus population dynamics during infection. *Curr Top Microbiol Immunol.* 2006;299:261-284. doi:10.1007/3-540-26397-7_9
212. Massagué A, Ramírez S, Carrión J a, González P, Sánchez-Tapias JM, Forns X. Evolution of the NS3 and NS5B regions of the hepatitis C virus during disease recurrence after liver transplantation. *Am J Transplant.* 2007;7:2172-2179. doi:10.1111/j.1600-6143.2007.01894.x
213. Belli LS, Berenguer M, Cortesi PA, et al. Delisting of liver transplant candidates with chronic hepatitis C after viral eradication: A European study. *J Hepatol.* 2016;65(3):524-531. doi:10.1016/j.jhep.2016.05.010
214. Reig M, Mariño Z, Perelló C, et al. Unexpected high rate of early tumor recurrence in patients with HCV-related HCC undergoing interferon-free therapy. *J Hepatol.* 2016;65(4):719-726. doi:10.1016/j.jhep.2016.04.008
215. Kanwal F, Kramer J, Asch SM, Chayanupatkul M, Cao Y, El-Serag HB. Risk of Hepatocellular Cancer in HCV Patients Treated With Direct-Acting Antiviral Agents. *Gastroenterology.* 2017;153(4):996-1005.e1. doi:10.1053/j.gastro.2017.06.012
216. Watanabe T, Tokumoto Y, Joko K, et al. Predictors of hepatocellular carcinoma occurrence after direct-acting antiviral therapy in patients with hepatitis C virus infection. *Hepatol Res.* 2019;49(2):136-146. doi:10.1111/hepr.13278

217. Peleg N, Issachar A, Sneh Arbib O, et al. Liver steatosis is a major predictor of poor outcomes in chronic hepatitis C patients with sustained virological response. *J Viral Hepat.* 2019;26(11):1257-1265. doi:10.1111/jvh.13167
218. Fujiwara N, Friedman SL, Goossens N, Hoshida Y. Risk factors and prevention of hepatocellular carcinoma in the era of precision medicine. *J Hepatol.* 2018;68(3):526-549. doi:10.1016/j.jhep.2017.09.016
219. Sachdeva M, Chawla YK, Arora SK. Immunology of hepatocellular carcinoma. *World J Hepatol.* 2015;7(17):2080-2090. doi:10.4254/wjh.v7.i17.2080
220. E. John Wherry, Joseph N. Blattman, Kaja Murali-Krishna, Robbert van der Most and RA. Viral Persistence Alters CD8 T-Cell Immunodominance and Tissue Distribution and Results in Distinct Stages of Functional Impairment. *J Virol.* 2003;77(8):4911–4927. doi:10.1128/JVI.77.8.4911–4927.2003
221. Yi JS, Cox MA, Zajac AJ. T-cell exhaustion: Characteristics, causes and conversion. *Immunology.* 2010;129(4):474-481. doi:10.1111/j.1365-2567.2010.03255.x
222. Kahan SM, Wherry EJ, Zajac AJ. T cell exhaustion during persistent viral infections. *Virology.* 2015;479-480:180-193. doi:10.1016/j.virol.2014.12.033
223. Zhang C, Hua R, Cui Y, et al. Comprehensive mapping of antigen specific T cell responses in hepatitis C virus infected patients with or without spontaneous viral clearance. *PLoS One.* 2017;12(2):1-16. doi:10.1371/journal.pone.0171217
224. Corado J, Toro F, Rivera H, Bianco NE, Deibis L, De Sanctis JB. Impairment

- of natural killer (NK) cytotoxic activity in hepatitis C virus (HCV) infection. *Clin Exp Immunol.* 1997;109(3):451-457. doi:10.1046/j.1365-2249.1997.4581355.x
225. Pereira GL, Tarragô AM, Neves WLL, et al. Immunological Dynamics Associated with Direct-Acting Antiviral Therapies in Naive and Experimented HCV Chronic-Infected Patients. *Mediators Inflamm.* 2019;2019. doi:10.1155/2019/4738237
226. Sasaki R, Meyer K, Moriyama M, et al. Rapid hepatitis C virus clearance by antivirals correlates with immune status of infected patients. *J Med Virol.* 2019;91(3):411-418. doi:10.1002/jmv.25310
227. Hengst J, Falk CS, Schlaphoff V, et al. Direct-acting antiviral-induced hepatitis c virus clearance does not completely restore the altered cytokine and chemokine milieu in patients with chronic hepatitis c. *J Infect Dis.* 2016;214(12):1965-1974. doi:10.1093/infdis/jiw457
228. Ji Won Han, Pil Soo Sung, Kyung Hwan Kim, Seon-Hui Hong, Eui-Cheol Shin MJSS-HP. Dynamic Changes in Ex Vivo T-Cell Function after Viral Clearance in Chronic HCV Infection. 2018:1-39. doi:10.1093/infdis/jiz291
229. Pereira RM, Hogan PG, Rao A, Martinez GJ. Transcriptional and epigenetic regulation of T cell hyporesponsiveness. *J Leukoc Biol.* 2017;102(3):601-615. doi:10.1189/jlb.2RI0317-097R
230. Fuller MJ, Khanolkar A, Tebo AE, Zajac AJ. Maintenance, Loss, and Resurgence of T Cell Responses During Acute, Protracted, and Chronic Viral Infections. *J Immunol.* 2004;172(7):4204-4214. doi:10.4049/jimmunol.172.7.4204
231. Perez S, Kaspi A, Domovitz T, et al. Hepatitis C virus leaves an epigenetic signature post cure of infection by direct-acting antivirals. *PLoS Genet.*

- 2019;15(6):1-28. doi:10.1371/journal.pgen.1008181
232. Hamdane N, Jühling F, Crouchet E, et al. HCV-Induced Epigenetic Changes Associated With Liver Cancer Risk Persist After Sustained Virologic Response. *Gastroenterology*. 2019;156(8):2313-2329.e7. doi:10.1053/j.gastro.2019.02.038
233. Lange CM, Roomp K, Dragan A, et al. HLA class i allele associations with HCV genetic variants in patients with chronic HCV genotypes 1a or 1b infection. *J Hepatol*. 2010;53(6):1022-1028. doi:10.1016/j.jhep.2010.06.011
234. Sugimoto K, Kaplan DE, Ikeda F, et al. Strain-Specific T-Cell Suppression and Protective Immunity in Patients with Chronic Hepatitis C Virus Infection. *J Virol*. 2005;79(11):6976-6983. doi:10.1128/jvi.79.11.6976-6983.2005
235. Doumba PP, Serti E, Boutsikou M, Konstadoulakis MM, Georgopoulou U, Koskinas J. Phenotypic and functional alterations of primary human PBMCs induced by HCV non-enveloped capsid-like particles uptake. *Cell Mol Life Sci*. 2013;70(18):3463-3474. doi:10.1007/s00018-013-1344-y
236. Zhai N, Chi X, Li T, et al. Hepatitis C virus core protein triggers expansion and activation of CD4+CD25+regulatory T cells in chronic hepatitis C patients. *Cell Mol Immunol*. 2015;12(6):743-749. doi:10.1038/cmi.2014.119
237. Bes M, Sauleda S, Casamitjana N, et al. Reversal of nonstructural protein 3-specific CD4 + T cell dysfunction in patients with persistent hepatitis C virus infection. *J Viral Hepat*. 2012;19(4):283-294. doi:10.1111/j.1365-2893.2011.01549.x
238. Smyk-Pearson S, Tester IA, Lezotte D, Sasaki AW, Lewinsohn DM, Rosen

- HR. Differential antigenic hierarchy associated with spontaneous recovery from hepatitis C virus infection: Implications for vaccine design. *J Infect Dis.* 2006;194(4):454-463. doi:10.1086/505714
239. Diepolder HM, Zachoval R, Hoffmann RM, et al. Possible mechanism involving T-lymphocyte response to non-structural protein 3 in viral clearance in acute hepatitis C virus infection. *Lancet.* 1995;346(8981):1006-1007. doi:10.1016/S0140-6736(95)91691-1
240. Loaeza-del-Castillo A, Paz-Pineda F, Oviedo-Cárdenas E, Sánchez-Ávila F, Vargas-Voráčková F. AST to platelet ratio index (APRI) for the noninvasive evaluation of liver fibrosis. *Ann Hepatol.* 2008;7(4):350-357. doi:10.1016/s1665-2681(19)31836-8
241. Negro F. Natural History of Hepatic and Extrahepatic Hepatitis C Virus Diseases and Impact of Interferon-Free HCV Therapy. *Cold Spring Harb Perspect Med.* 2019;10(4):a036921. doi:10.1101/cshperspect.a036921
242. Aitken CK, Lewis J, Tracy SL, et al. High incidence of hepatitis C virus reinfection in a cohort of injecting drug users. *Hepatology.* 2008;48(6):1746-1752. doi:10.1002/hep.22534
243. Scott N, Wilson DP, Thompson AJ, et al. The case for a universal hepatitis C vaccine to achieve hepatitis C elimination. *BMC Med.* 2019;17(1):1-12. doi:10.1186/s12916-019-1411-9
244. El-Serag HB, Marrero JA, Rudolph L, Reddy KR. Diagnosis and Treatment of Hepatocellular Carcinoma. *Gastroenterology.* 2008;134(6):1752-1763. doi:10.1053/j.gastro.2008.02.090
245. Brennan K, Martin K, FitzGerald SP, et al. A comparison of methods for the isolation and separation of extracellular vesicles from protein and lipid particles in human serum. *Sci Rep.* 2020;10(1):1-13.

- doi:10.1038/s41598-020-57497-7
246. Baldrich P, Tamim S, Mathioni S, Meyers B. Ligation bias is a major contributor to nonstoichiometric abundances of secondary siRNAs and impacts analyses of microRNAs. *bioRxiv*. 2020:1-44. doi:10.1101/2020.09.14.296616
247. Dard-Dascot C, Naquin D, d'Aubenton-Carafa Y, Alix K, Thermes C, van Dijk E. Systematic comparison of small RNA library preparation protocols for next-generation sequencing. *BMC Genomics*. 2018;19(1):1-16. doi:10.1186/s12864-018-4491-6
248. Buschmann D, Kirchner B, Hermann S, et al. Evaluation of serum extracellular vesicle isolation methods for profiling miRNAs by next-generation sequencing. *J Extracell Vesicles*. 2018;7(1481321):1-18. doi:10.1080/20013078.2018.1481321
249. Ravi S, Axley P, Jones DA, et al. Unusually High Rates of Hepatocellular Carcinoma After Treatment With Direct-Acting Antiviral Therapy for Hepatitis C Related Cirrhosis. *Gastroenterology*. 2017;152(4):911-912. doi:10.1053/j.gastro.2016.12.021
250. Reig M, Mariño Z, Perelló C, et al. Unexpected high rate of early tumor recurrence in patients with HCV-related HCC undergoing interferon-free therapy. *J Hepatol*. 2016;65(4):719-726. doi:10.1016/j.jhep.2016.04.008
251. Domovitz T, Gal-Tanamy M. Tracking down the epigenetic footprint of hcv-induced hepatocarcinogenesis. *J Clin Med*. 2021;10(3):1-16. doi:10.3390/jcm10030551
252. Nishida N, Nagasaka T, Nishimura T, Ikai I, Boland CR, Goel A. Aberrant Methylation of Multiple Tumor Suppressor Genes in Aging Liver, Chronic Hepatitis, and Hepatocellular Carcinoma. *Hepatology*. 2008;47(3):908-

918. doi:10.1002/hep.22110
253. Jühling F, Hamdane N, Crouchet E, et al. Targeting clinical epigenetic reprogramming for chemoprevention of metabolic and viral hepatocellular carcinoma. *Gut*. 2021;70(1):157-169. doi:10.1136/gutjnl-2019-318918
254. Hoffmann MJ, Schulz WA. Causes and consequences of DNA hypomethylation in human cancer. *Biochem Cell Biol*. 2005;83(3):296-321. doi:10.1139/o05-036
255. Lee YA, Friedman SL. Reversal, maintenance or progression: What happens to the liver after a virologic cure of hepatitis C? *Antiviral Res*. 2014;107(1):23-30. doi:10.1016/j.antiviral.2014.03.012

VI. ANNEX

VI.I Isolation methods

Apart from the EVs isolation-methods mentioned in the third article, lipid nanoprobe, precipitation and magnetic bead-based methods, were also tested and discarded for miRNA sequencing.

VI.I.I Lipid nanoprobe

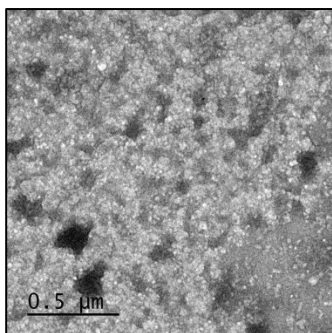
- DSPE-PEG-Biotin MW2000 nanoprobe (Nanocs, Cat#PG2-BNDS-2k) with streptavidin-magnetic beads (Thermo Scientific™, Cat#88817) was used directly in purified EVs to test its effectivity. 100 µl of purified EVs diluted in 500 µl of PBS 1X were tested against 50, 100 and 200 nmols of biotin- DSPE-PEG. Sample was incubated with lipid-nanoprobe for 10 min, at 4°C and 300 r.p.m. In parallel, sample was incubated overnight, at 4°C in rotation to test in which conditions lipid-nanoprobe works better. Magnetic beads were then added to the solution and incubated 30 min or 1 h at room temperature in rotation. Beads coated to the nanoprobe “containing EVs” were then washed, captured and resuspended in 100 µl of PBS 1X, therefore recovering 100 µl of concentrated EVs.
- DSPE-PEG-Desthiobiotin MW5000 (Nanocs, Cat# PG2-DSDSB-5k) with Sera-Mag SpeedBeads™ Neutravidin-Magnetic Beads (Thermo Scientific™, Cat#GE78152104010350), 100 µl of purified EVs diluted in 500 µl of PBS 1X were tested the same way than with Biotin-tagged DSPE-PEG. Beads were separated from EVs by adding biotin (Thermo Scientific, Cat#29129) to the sample, whom compete with desthiobiotin letting EVs release from lipid-nanoprobe and coated-beads and recovering 100 µl of concentrated EVs.

No EVs recovery was detected in beads phase for any of the two lipid-nanoprobes, indicating that this method was not specifically working so both were discarded for further experiments.

VI.I.II Precipitation-based method

- Total exosome isolation kit (Invitrogen™, Cat#4484450) was tested for plasma samples. After the two previously centrifugations specified in the third article, 300 µl of Invitrogen solution were added to 1 ml of sample, incubated 30 minutes at 4°C and centrifuged at 10,000 g for 5 minutes at room temperature, recovering 100ul of concentrated EVs.

After total precipitation, $8.39 \times 10^{12} \pm 2.54 \times 10^{11}$ particles/ml with a mean size of 95 ± 2.4 nm were recovered.



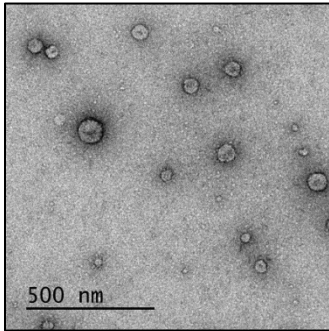
However, TEM images showed a heterogeneous and cloudy solution (Figure 19), demonstrating that this method was not pure enough and hence was not suitable for our purpose. Consequently, was discarded for further experiments.

Figure 19. TEM images of EV's concentrate extracted by precipitation-based method

VI.I.III Magnetic bead-based method

- MagCapture™ Exosome Isolation Kit PS (FUJIFILM Wako Chemicals U.S.A Corporation, Cat#293-77601) was tested for serum samples. After the two previously centrifugations mentioned in the third article, 60 µl of suspended streptavidin magnetic beads were added to 1 ml of sample. 500 µl of exosome capture immobilizing buffer and 10 µl of biotin-labeled exosome capture were added and incubated 10 minutes at 4°C in rotation. 1:500 of exosome binding enhancer was added afterwards and incubated for 3 hours

at 4°C in rotation. Then, beads were washed and eluted with 100 µl of exosome elution buffer, recovering 100 µl of concentrated EVs.



By magnetic capturing, $1.01 \times 10^{10} \pm 4.3 \times 10^8$ particles/ml with a mean size of 155 ± 4.8 nm were recovered. Moreover, TEM images, as seen in Figure 20, shown a pure and clean solution with vesicles that agree in size with those measured by NTA.

Figure 20. TEM images of EV's concentrate extracted by magnetic beads-based method

Once confirmed a good balance between quantity and pureness, total RNA was extracted but without giving favourable results. Thereupon, as RNA quantity and quality were not good enough, magnetic beads-based method was discarded for miRNA sequencing.

VI.II Articles in which the thesis candidate has collaborated

- Costafreda MI, Sauleda S, Riveiro-Barciela M, Rico A, **Llorens-Revull M**, Guix S, Pintó RM, Bosch A, Rodríguez-Frías F, Rando A, Piron M, Bes M. Specific Plasma MicroRNA Signatures Underlying the Clinical Outcomes of Hepatitis E Virus Infection. *Microbiol Spectr*. 2023;25:e0466422. [PMID: 36695578 DOI: 10.1128/spectrum.04664-22]
- Soria ME, García-Crespo C, Martínez-González B, Vázquez-Sirvent L, Lobo-Vega R, de Ávila AI, Gallego I, Chen Q, García-Cehic D, **Llorens-Revull M**, Briones C, Gómez J, Ferrer-Orta C, Verdaguer N, Gregori J, Rodríguez-Frías F, Buti M, Esteban JI, Domingo E, Quer J, Perales C. Amino acid substitutions associated with treatment failure for Hepatitis C virus infection. *J Clin Microbiol* 2020;58:1–16 [PMID: 32999010 DOI: 10.1128/JCM.01985-20]
- Chen Q, Perales C, Soria ME, García-Cehic D, Gregori J, Rodríguez-Frías F, Buti M, Crespo J, Calleja JL, Taberner D, Vila M, Lázaro F, Rando-Segura A, Nieto-Aponte L, **Llorens-Revull M**, Cortese MF, Fernandez-Alonso I, Castellote J, Niubó J, Imaz A, Xiol X, Castells L, Riveiro-Barciela M, Llaneras J, Navarro J, Vargas-Blasco V, Augustin S, Conde I, Rubín Á, Prieto M, Torras X, Margall N, Forn X, Mariño Z, Lens S, Bonacci M, Pérez-del-Pulgar S, Londoño MC, García-Buey ML, Sanz-Cameno P, Morillas R, Martró E, Saludes V, Masnou-Ridaura H, Salmerón J, Quíles R, Carrión JA, Forné M, Rosinach M, Fernández I, García-Samaniego J, Madejón A, Castillo-Grau P, López-Núñez C, Ferri MJ, Durández R, Sáez-Royuela F, Diago M, Gimeno C, Medina R, Buenestado J, Bernet A, Turnes J, Trigo-Daporta M, Hernández-Guerra M, Delgado-Blanco M, Cañizares A, Arenas JI, Gomez-Alonso MJ, Rodríguez M, Deig E, Olivé G, Río OD, Cabezas J, Quiñones I, Roget M, Montoliu S, García-Costa J, Force L, Blanch S, Miralbés M, López-de-Goicochea MJ, García-

Flores A, Saumoy M, Casanovas T, Baliellas C, Gilabert P, Martin-Cardona A, Roca R, Barenys M, Villaverde J, Salord S, Camps B, Silvan di Yacovo M, Ocaña I, Sauleda S, Bes M, Carbonell J, Vargas-Accarino E, Ruzo SP, Guerrero-Murillo M, Von Massow G, Costafreda MI, López RM, González-Moreno L, Real Y, Acero-Fernández D, Viroles S, Pamplona X, Cairó M, Ocete MD, Macías-Sánchez JF, Estébanez A, Quer JC, Mena-de-Cea Á, Otero A, Castro-Iglesias Á, Suárez F, Vázquez Á, Vieito D, López-Calvo S, Vázquez-Rodríguez P, Martínez-Cerezo FJ, Rodríguez R, Macenlle R, Cachero A, Mereish G, Mora-Moruny C, Fábregas S, Sacristán B, Albillos A, Sánchez-Ruano JJ, Baluja-Pino R, Fernández-Fernández J, González-Portela C, García-Martin C, Sánchez-Antolín G, Andrade RJ, Simón MA, Pascasio JM, Romero-Gómez M, Antonio del-Campo J, Domingo E, Esteban R, Esteban JI, Quer J. Deep-sequencing reveals broad subtype-specific HCV resistance mutations associated with treatment failure. *Antiviral Res* 2020;174 [PMID: 31857134 DOI: 10.1016/j.antiviral.2019.104694]

- Perales C, Chen Q, Soria ME, Gregori J, Garcia-Cehic D, Nieto-Aponte L, Castells L, Imaz A, **Llorens-Revull M**, Domingo E, Buti M, Esteban JI, Rodriguez-Frias F, Quer J. Baseline hepatitis C virus resistance-associated substitutions present at frequencies lower than 15% may be clinically significant. *Infect Drug Resist* 2018;11:2207–10 [PMID: 30519058 DOI: 10.2147/IDR.S172226]
- Soria ME, Gregori J, Chen Q, Garcia-Cehic D, **Llorens M**, de Avila AI, Beach NM, Domingo E, Rodriguez-Frias F, Buti M, Esteban R, Esteban JI, Quer J, Perales C. Pipeline for specific subtype amplification and drug resistance detection in hepatitis C virus. *BMC Infect Dis* 2018;18:446 [PMID: 30176817 DOI: 10.1186/s12879-018-3356-6]

- Riveiro-Barciela M, Bes M, Quer J, Valcarcel D, Piriz S, Gregori J, **Llorens M**, Salcedo MT, Piron M, Esteban R, Buti M, Sauleda S. Thrombotic thrombocytopenic purpura relapse induced by acute hepatitis E transmitted by cryosupernatant plasma and successfully controlled with ribavirin. *Transfusion* 2018;58:2501–5 [PMID: 30284732 DOI: 10.1111/trf.14831]
- Ordeig L, Garcia-Cehic D, Gregori J, Soria ME, Nieto-Aponte L, Perales C, **Llorens M**, Chen Q, Riveiro-Barciela M, Buti M, Esteban R, Esteban JI, Rodriguez-Frias F, Quer J. New hepatitis C virus genotype 1 subtype naturally harbouring resistance-associated mutations to NS5A inhibitors. *J Gen Virol* 2018;99:97–102 [PMID: 29239718 DOI: 10.1099/jgv.0.000996]
- Rodriguez-Frias F, Nieto-Aponte L, Gregori J, Garcia-Cehic D, Casillas R, Tabernero D, Homs M, Blasi M, Vila M, Chen Q, Vargas V, Castells L, Viladomiu L, Genesca J, Minguez B, Augustin S, Riveiro-Barciela M, Carbonell J, Perales C, Soria ME, Asensio M, **Llorens M**, Ordeig L, Godoy C, Buti M, Esteban R, Pumarola T, Esteban JI, Quer J. High HCV subtype heterogeneity in a chronically infected general population revealed by high-resolution hepatitis C virus subtyping. *Clin Microbiol Infect* 2017;23 [PMID: 28192235 DOI: 10.1016/j.cmi.2017.02.007]
- Nieto-Aponte L, Quer J, Ruiz-Ripa A, Tabernero D, Gonzalez C, Gregori J, Vila M, Asensio M, Garcia-Cehic D, Ruiz G, Chen Q, Ordeig L, **Llorens M**, Saez M, Esteban JI, Esteban R, Buti M, Pumarola T, Rodriguez-Frias F. Assessment of a novel automatic real-time PCR assay on the cobas 4800 analyzer as a screening platform for Hepatitis C virus genotyping in clinical practice: Comparison with massive sequencing. *J Clin Microbiol* 2017;55:504–9 [PMID: 27927921 DOI: 10.1128/JCM.01960-16]

- Chen Q, Belmonte I, Buti M, Nieto L, Garcia-Cehic D, Gregori J, Perales C, Ordeig L, **Llorens M**, Soria ME, Esteban R, Esteban JI, Rodriguez-Frias F, Quer J. New real-time-PCR method to identify single point mutations in hepatitis C virus. *World J Gastroenterol* 2016;22 [PMID: 27920481 DOI: 10.3748/wjg.v22.i43.9604]

